



DISSERTATION

Titel der Dissertation

„Participation of a Cyclopropane Ring within Foiled
Carbenes: Probing the Selectivity and Extent of
Stabilization“

Verfasserin

Ingrid Malene Apeland

angestrebter akademischer Grad

Doktorin der Naturwissenschaften (Dr. rer. nat.)

Wien, 2013

Studienkennzahl lt. Studienblatt:

A 791 419

Dissertationsgebiet lt. Studienblatt:

Chemie

Betreuer:

o. Univ.-Prof. Dr. Udo H. Brinker

To my grandfather, Owe, and my father, Terje

Acknowledgements

This work has been carried out under the supervision of Prof. Udo H. Brinker at the Institute of Chemistry, University of Vienna. First of all, I would like to thank him for giving me the opportunity to work in the field of reactive intermediate chemistry, for his guidance, and for all the interesting discussions we have had.

Furthermore, I would like to thank my former colleagues in the Brinker group, especially Mirjana Pacar, for their help and for making a pleasant working atmosphere.

I am grateful to Ass.-Prof. Hanspeter Kählig and Assoz.-Prof. Lothar Brecker (Institute of Organic Chemistry, University of Vienna) for helpful NMR interpretations. I would like to thank ao. Univ.-Prof. Vladimir Arion, Alexander Roller (Institute of Inorganic Chemistry, University of Vienna), and Dr. Jürgen Graf (Incoatec, Geesthacht, Germany) for single-crystal X-ray analyses. I also appreciate the fruitful discussions I have had about GC-MS measurements with ao. Univ.-Prof. Eberhard Lorbeer (Institute of Organic Chemistry, University of Vienna). Moreover, I wish to thank Ass.-Prof. Daniel Krois (Institute of Organic Chemistry, University of Vienna) and Dr. Murray G. Rosenberg (The State University at Binghamton) for helpful discussions. I would like to thank Dr. Hans Peter Reisenauer (Institute of Organic Chemistry, Justus-Liebig University, Giessen) for carrying out matrix isolation studies.

I want to express my gratitude to my friends and family for their support. I especially want to thank Federica Cappa for all the good moments we have shared over the last years at the University of Vienna, and Hjørdis Skår for essential moral support. Last, but not least, I want to thank my parents, Marit and Terje, who have encouraged me throughout my studies.

Ingrid Malene Apeland

Wien, 2013

Abbreviations

^{13}C	Carbon-13 nucleus
^1H	Hydrogen-1 nucleus
ATR	Attenuated Total Reflection
bp.	boiling point
CDCl_3	Deuterated Chloroform
COSY	Correlated Spectroscopy
DFT	Density Functional Theory
dr	diastereomeric ratio
EtOH	Ethanol
GC-MS	Gas Chromatography-Mass Spectrometry
h	hour
HMBC	Heteronuclear Multiple Bond Correlation
HMQC	Heteronuclear Multiple Quantum Coherence
HOMO	Highest Occupied Molecular Orbital
HRMS	High Resolution Mass Spectrometry
HTP	Hydride Transfer Potential
IR	Infrared
LUMO	Lowest Unoccupied Molecular Orbital
MeOAc	Methyl Acetate
MeOH	Methanol
min	minute
mp.	melting point
MS	Mass Spectrometry
NMR	Nuclear Magnetic Resonance
NOE	Nuclear Overhauser Enhancement
NOESY	Nuclear Overhauser Enhancement Spectroscopy
Ph	Phenyl
ppm	parts per million
rt	room temperature
rxn	reaction
SE	Stabilization Energy

<i>t</i> -BuOH	<i>tert</i> -Butyl alcohol
THF	Tetrahydrofuran
TLC	Thin-Layer Chromatography
TMS	Tetramethylsilane
TS	Transition State
<i>p</i> -TsOH	<i>para</i> -Toluenesulfonic acid
UV	Ultraviolet
UV-VIS	Ultraviolet Visible

Abstract (Deutsch)

Dieses Forschungsprojekt befasst sich mit dem Studium der Chemie des *endo*-Tricyclo[3.2.1.0^{2,4}]octan-8-ylidens, das im Endergebnis als ein „foiled carbene“ klassifiziert werden konnte. Obwohl die Umlagerungsreaktionen dieses Carbens bereits vorher untersucht worden waren, sollte seine Klassifizierung als ein „foiled carbene“ nun gründlicher durch Überprüfung seiner Stereoselektivität in *intermolekularen* Reaktionen bestimmt werden. Die besetzten Walshorbitale des *endo*-verknüpften Dreirings geben Elektronen in das leere p-Orbital des Carbenzentrums. Dies bewirkt dass die Brücke, die den divalenten Kohlenstoff enthält, sich zum Cyclopropanring hinneigt. Es wurde erwartet, dass die verwendeten Substrate sich dem Dreiring von der *anti*-Seite nähern sollten, wo aufgrund der Neigung der Brücke mehr Platz zur Verfügung steht.

Eine Oxadiazolin Carbovorstufe wurde synthetisiert und die nachfolgende Erzeugung des entsprechenden Carbens durch Thermolyse oder Photolyse induziert. *endo*-Tricyclo[3.2.1.0^{2,4}]octan-8-yliden wurde stereoselektiv mit Acrylnitril, Diethylamin, Benzaldehyd und Acetophenon abgefangen. Bei Durchführung der Reaktionen in Cyclohexan und Cyclohexen wurden jedoch Isomerisierungsreaktionen des Carbens favorisiert. Die Reaktionsträgheit mit der elektronenreichen Doppelbindung des Cyclohexens spricht für die Nucleophilie des *endo*-Tricyclo[3.2.1.0^{2,4}]octan-8-ylidens. Darüberhinaus reagierte das Carben nicht mit Alkanen wie Cyclohexan und Pentan, was auf seine Stabilität hinweist.

Zu Vergleichszwecken wurde auch die Stereoselektivität des Bicyclo[3.2.1]octan-8-ylidens in *intermolekularen* Reaktionen untersucht. Nach DFT-Rechnungen ist dieses Carben durch Hyperkonjugation stabilisiert, aber zu einem geringeren Ausmaß als die zuvor erwähnte Stabilisierung im *endo*-Tricyclo[3.2.1.0^{2,4}]octan-8-yliden durch Wechselwirkung mit den Walshorbitalen. Bicyclo[3.2.1]octan-8-yliden reagierte stereoselektiv mit Acrylnitril und Diethylamin. In Cyclohexan war wiederum die Umlagerung des Carbens favorisiert.

DFT-Rechnungen (B3LYP/6-31G^{*}) wurden durchgeführt, um die Stabilisierungsenergie einiger strukturell verwandter Carbene zu erforschen. Die Rechnungen deuten darauf hin, dass ein *exo*-verknüpfter Dreiring im Vergleich zu den *endo*-verknüpften Spezies nur einen geringen Stabilisierungseffekt auf den divalenten Kohlenstoff ausübt. Im Gegensatz dazu scheint die Kombination einer Doppelbindung *und* eines *endo*-verknüpften Dreirings zu noch weiter stabilisierten „foiled carbenes“ zu führen.

Abstract (English)

This research project set out to study the chemistry of *endo*-tricyclo[3.2.1.0^{2,4}]octan-8-ylidene, which as a concluding result is classified as a foiled carbene. Although rearrangement reactions of this carbene had previously been studied, its classification as a foiled carbene could be more thoroughly assessed by examining its stereoselectivity in *intermolecular* reactions. The occupied Walsh orbitals of the *endo*-fused three-membered ring donate electrons into the empty p orbital of the carbenic center. As a consequence, the bridge containing the divalent carbon leans towards the cyclopropane ring. The substrates employed were expected to approach the carbenic center *anti* to the three-membered ring, where more space is available due to the bending of the bridge.

An oxadiazoline carbene precursor was synthesized and the subsequent generation of the corresponding carbene was induced by thermolysis or photolysis. *endo*-Tricyclo[3.2.1.0^{2,4}]octan-8-ylidene was trapped stereoselectively with acrylonitrile, diethylamine, benzaldehyde, and acetophenone. When reactions were carried out in cyclohexane and cyclohexene, however, isomerization reactions of the carbene were favored. The lack of reactivity with the electron-rich double bond of cyclohexene reflects the nucleophilicity of *endo*-tricyclo[3.2.1.0^{2,4}]octan-8-ylidene. Moreover, the carbene did not react with alkanes, *i.e.*, cyclohexane and pentane, which indicates its stabilization.

For comparison, the stereoselectivity of bicyclo[3.2.1]octan-8-ylidene in *intermolecular* reactions was also studied. DFT calculations suggest that this carbene is stabilized by hyperconjugation, but to a lower extent than the aforementioned stabilization in *endo*-tricyclo[3.2.1.0^{2,4}]octan-8-ylidene through Walsh orbital interaction. Bicyclo[3.2.1]octan-8-ylidene reacted stereoselectively with acrylonitrile and diethylamine. Again, in cyclohexane, rearrangement of the carbene was favored.

DFT calculations at the B3LYP/6-31G* level of theory were performed in order to investigate the stabilization energy of some structurally related carbenes. The calculations indicated that an *exo*-fused three-membered ring provides little stabilizing effect on the divalent carbon in comparison to the corresponding *endo*-fused species. In contrast, the presence of a combination of double bond *and* *endo*-fused three-membered ring appears to even further stabilize foiled carbenes.

Publication

Reproduced in part with permission from:

“Probing the Nature and Extent of Stabilization within Foiled Carbenes: Homoallylic Participation by a Neighboring Cyclopropane Ring” Apeland, I. M.; Kählig, H.; Lorbeer, E.; Brinker, U. H. *J. Org. Chem.* **2013**, 78, 4879-4885.

© American Chemical Society.

This publication is attached at the back of the thesis. Some parts and phrases from the publication have been used directly in this thesis in chapters 3.1, 3.2, 4.1, 4.2, 4.3, 4.4, 7.2.1, and 7.2.2.

The majority of the work of the publication (ca. 90%) was carried out by the first author (IMA), which includes the written and the experimental work. Ass.-Prof. Hanspeter Kählig contributed with the interpretation of 2D NMR spectra and the recording of the diffusion-edited NMR spectra. Ao. Univ.-Prof. Eberhard Lorbeer acted as a consultant for the GC-MS experiments. Their combined contributions to the publication amount to a maximum of 10%.

Conferences

Parts of this thesis have been presented at the following conferences:

- Poster Presentation: “Stereoselectivity of Foiled Carbenes in Intermolecular Reactions” Apeland, I. M.; Brinker, U. H. 12th Tetrahedron Symposium, June 21 – 24, 2011, Sitges, Spain.
- Poster Presentation: “Stereoselectivity of Foiled Carbenes in Intermolecular Reactions” Apeland, I. M.; Brinker, U. H. 14th Austrian Chemistry Days, September 26 – 29, 2011, Linz, Austria.
- Oral “Flash” Presentation and Poster Presentation: “The Stereoselectivity of *endo*-Tricyclo[3.4.1.0^{2,4}]octan-8-ylidene in Intermolecular Reactions: Further Evidence of a Foiled Carbene” Apeland, I. M.; Brinker, U. H. 21st IUPAC International Conference of Physical Organic Chemistry, September 9 – 13, 2012, Durham, United Kingdom.

Table of Contents

1. Theory and Background	1
1.1 Carbenes: Structure and Reactivity.....	1
1.1.1 Singlet versus Triplet Ground State of Carbenes.....	1
1.1.2 Substituent Effects on Carbene Multiplicity.....	2
1.1.3 Reactions of Carbenes.....	4
1.1.4 Classification of Carbenes	8
1.2 Carbene Precursors: Oxadiazolines	10
1.2.1 Diazo Compounds.....	10
1.2.2 Thermolysis of Oxadiazolines	12
1.2.3 Photolysis of Oxadiazolines.....	13
1.3 Foiled Carbenes	14
1.3.1 1,2-Vinyl Shifts of Foiled Carbenes	14
1.3.2 Intermolecular Reactions of Foiled Carbenes.....	17
1.3.3 Cyclopropane versus Double Bond in Foiled Carbenes	21
1.4 Aim of the Study.....	26
2. Calculations of Geometries and Stabilization of <i>endo</i>-Tricyclo[3.2.1.0^{2,4}]octan-8-ylidene (14) and Related Carbenes	29
2.1 Computational Methodology for Determination of Geometry and Energy of Molecules.....	29
2.2 Results and Discussion	31
3. Preparation of Oxadiazoline Carbene Precursors	39
3.1 Synthesis of Oxadiazoline Carbene Precursor 29 for <i>endo</i> -Tricyclo[3.2.1.0 ^{2,4}]octan-8-ylidene (14)	39
3.2 Kinetic Measurements of Thermolytic Decomposition of Oxadiazoline Precursors 29a and 29b	43
3.3 Synthesis of Oxadiazoline Carbene Precursor 39 for Bicyclo[3.2.1]octan-8-ylidene (16)	47
4. Reactions of <i>endo</i>-Tricyclo[3.2.1.0^{2,4}]octan-8-ylidene (14)	51
4.1 Reaction in Cyclohexane and Cyclohexene: Rearrangements of Carbene 14 ...51	
4.2 Reaction in Methanol: Formal Insertion Into the O-H bond.....	64

4.3 Reaction in Acrylonitrile: Addition to the Double Bond.....	70
4.4 Reaction in Diethylamine: Insertion Into the N-H Bond.....	78
4.5 Reaction in Benzaldehyde and Acetophenone: Attack of the C-O Double Bond	80
5. Reactions of Bicyclo[3.2.1]octan-8-ylidene (16)	91
5.1 Reaction in Cyclohexane and Cyclohexene: Rearrangement of Carbene 16	91
5.2 Reaction in Acrylonitrile: Addition to the Double Bond.....	93
5.3 Reaction in Diethylamine: Insertion Into the N-H Bond.....	96
6. Conclusions	99
7. Experimental	107
7.1 Equipment and Methods	107
7.2 Procedures and Analytical Data.....	110
7.2.1 Preparation of Oxadiazoline Carbene Precursors	110
7.2.2 Reactions of <i>endo</i> -Tricyclo[3.2.1.0 ^{2,4}]octan-8-ylidene (14).....	119
7.2.3 Reactions of Bicyclo[3.2.1]octan-8-ylidene (16).....	127
References	129
Appendix	135
X-ray Analyses.....	137
Supplementary Data for Kinetic Measurements	149
NMR Spectra	151

1. Theory and Background

1.1 Carbenes: Structure and Reactivity

1.1.1 Singlet versus Triplet Ground State of Carbenes

Carbenes are species containing a neutral, divalent carbon with six electrons in its valence shell.¹ Hence, the shell is not full, and as a consequence they are generated as reactive intermediates. Four of the valence electrons are involved in two covalent bonds to the carbene's substituents, whereas the other two are nonbonding electrons. The nonbonding electrons can be arranged in several ways: for singlet states the two electrons have antiparallel spins, whereas for triplet states they have parallel spins.² The ground-state electronic configurations for triplet and singlet carbenes are shown in Figure 1.1.³

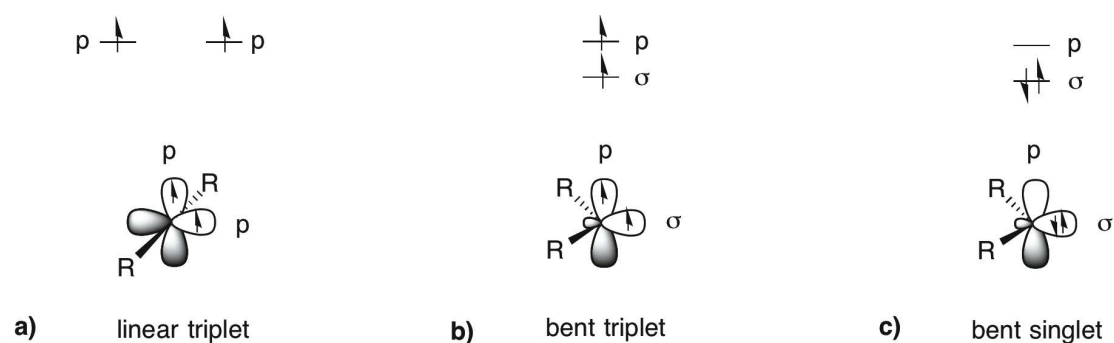


Figure 1.1: The ground-state electronic configuration of triplet and singlet carbenes.

Carbenes with a linear geometry comprise an sp -hybridized divalent carbon with two degenerate p orbitals (Figure 1.1a).¹ Thus, Hund's rule predicts a triplet ground state for which the nonbonding electrons occupy one p orbital each and have parallel spins. Most carbenes, however, are bent, and the degeneracy of the orbitals is broken.¹ One of the orbitals is stabilized by gaining s character and is denoted as σ , whereas the other remains unchanged. The result is an sp^2 -type hybridized divalent carbon.¹ In this case, the most stable configuration can either be triplet, with one electron in the σ and one in the p orbital (Figure 1.1b), or singlet, with the two electrons paired in the σ

orbital (Figure 1.1c). The triplet state is energetically favored by relief of Coulomb repulsion present between the paired electrons of the singlet state.⁴ However, it requires energy to promote an electron from the σ to the p orbital, and so the singlet state is favored by a large σ -p separation. Hoffmann suggested that a spacing of 2 eV is necessary for a singlet ground state, whereas a value below 1.5 eV leads to a triplet ground state.⁵ The relative energy of the two configurations can be expressed as the singlet-triplet gap ($\Delta G_{ST} = E_S - E_T$), where a large value indicates a more stable triplet state.

1.1.2 Substituent Effects on Carbene Multiplicity

Both electronic and steric effects influence the σ -p spacing.³ Hence, the multiplicity of a carbene is dependent on its substituents. Inductively, σ -electron-withdrawing groups stabilize the σ orbital of the carbene by increasing its *s* character.¹ This leads to a larger σ -p gap, which favors the singlet state. σ -Electron-donating substituents, on the other hand, favor the triplet state.¹ For example, when a divalent carbon has two electropositive lithium substituents attached, the triplet state is favored by 23 kcal/mol.⁶ When these are exchanged by two hydrogen atoms, the triplet state is still favored, but by 11 kcal/mol. With two electronegative fluorine substituents, however, the singlet state is favored by 45 kcal/mol. In the latter case, though, some of the stabilization is due to mesomeric effects, also called resonance effects.¹

Indeed, such mesomeric effects are in general more potent than inductive effects, due to a more efficient overlapping of the p or π orbitals of the substituent with the 2p orbital of the divalent carbon than for their respective σ orbitals.³ Substituents that donate electrons into the p orbital, such as -F, -Cl, -Br, -I, -OR, -SR, -NR₂, and -PR₂, raise the energy of the orbital, thus increasing the σ -p separation.⁷ In this case the singlet ground state is favored (Figure 1.2a). On the contrary, p-electron acceptors, such as -COR, -SOR, -SO₂R, -NO, and -NO₂, and conjugating groups, such as alkenes, alkynes or aryl groups, either decrease the σ -p gap or leave it more or less unchanged, and so the triplet ground state is anticipated (Figure 1.2b and Figure 1.2c).³

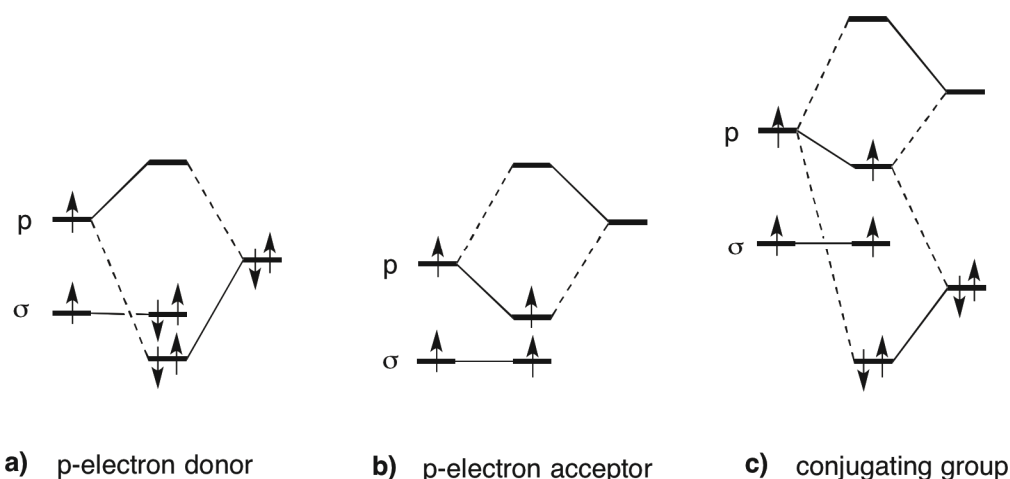


Figure 1.2: Mesomeric effects of substituents interacting with the carbene center.

Alkyl groups can stabilize the singlet state through hyperconjugative interaction, where electrons of one of its sigma bonds, usually a C-H or C-C bond, are donated into the empty p orbital of the divalent carbon.⁴ In the same way that carbocations are much more stabilized by hyperconjugation than radicals, singlet carbenes are more stabilized than triplet carbenes. Indeed, singlet carbenes are isoelectronic with carbocations, whereas triplet carbenes can be seen as diradicals.⁴

A way to stabilize triplet carbenes is to force them to be linear by introducing bulky substituents.⁴ Steric repulsion requires a widening of the R-C-R angle. As previously mentioned, linear carbenes have degenerate p orbitals that lead to a triplet ground state. For example, diadamantylcarbene (**1**),⁸ with an angle of 152°, and di(*tert*-butyl)carbene (**2**),⁹ with an angle of 143°, both have triplet ground states (Figure 1.3). Dimethylcarbene (**3**),¹⁰ on the other hand, with an angle of 111°, has a singlet ground state (Figure 1.3). Due to the geometric constraints, cyclopentylidene (**4**)¹¹ and cyclopropenylidene (**5**)¹² have singlet ground states as well, though in the latter case, aromatic effects are important too. However, steric effects only dictate the ground-state spin multiplicity, when electronic effects are negligible, which is seldom the case.¹³

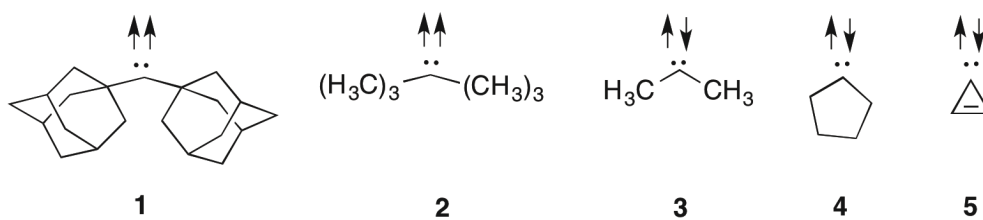


Figure 1.3: Influence of bond angle of carbenic carbon on ground-state spin multiplicity.

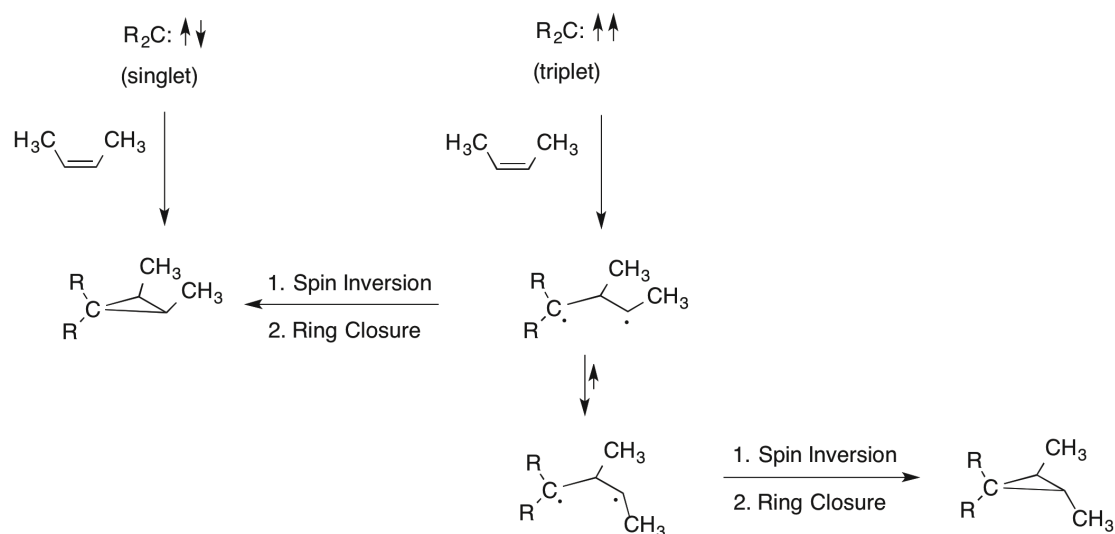
When the singlet and triplet states are close in energy, the solvent can influence the ground state multiplicity of the carbene. Since the singlet state is more polar than the triplet, it may be stabilized in polar solvents, *i.e.*, the singlet-triplet gap decreases as the solvent polarity increases.⁴

1.1.3 Reactions of Carbenes

It is important to note that it is not necessarily the ground-state multiplicity that is involved in the reaction of a reactive species.² Most molecules are ground-state singlets, and as a consequence, singlet carbenes are formed initially due to conservation of spin. Spin inversion to the triplet state may or may not occur depending on how fast the carbene reacts with a suitable acceptor.¹⁴ Furthermore, when the singlet and triplet state are close in energy, an equilibration may occur, and both spin states are involved in the reaction simultaneously. The singlet state has an advantage over the triplet; due to the possibility of forming *two* new bonds in one step, their reactions are often very exothermic.² Thus, if the singlet state is close in energy with the triplet, it is often the reacting state.

The spin state plays an important role for the carbene's reactivity. As a result of the unpaired nonbonding electrons, triplet carbenes exhibit a radical-like reactivity, whereas singlet carbenes, with their lone pair electrons and vacant p orbital, undergo in general concerted reactions.² This is well demonstrated by carbene addition reactions to double bonds to form cyclopropane derivatives (Scheme 1.1).²

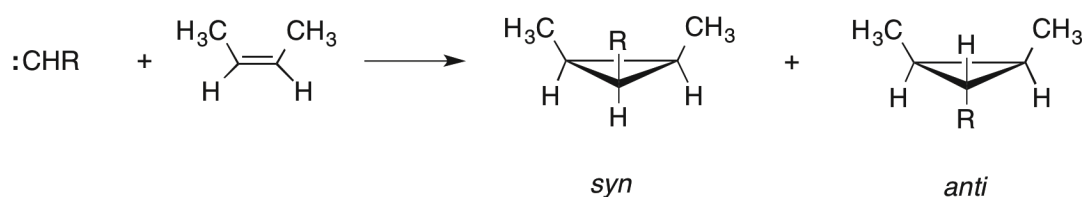
Scheme 1.1: Concerted versus Stepwise Addition of Carbenes to Alkenes



Triplet carbenes add in a stepwise manner to the double bond. For the initially formed diradical intermediate, a spin inversion is necessary prior to ring closure.² This inversion is slow enough for rotation about the C-C bonds to occur, leading to a mixture of products.² Singlet carbenes, on the other hand, add to the double bond through a stereospecific [1 + 2] cycloaddition, thereby preserving the *cis* or *trans* stereochemistry of the alkene.

If a singlet carbene has two different substituents and is adding to an alkene lacking both a center of symmetry and a twofold symmetry axis along the double bond (*e.g.* *cis*-2-butene), two different products can be formed (Scheme 1.2).¹⁴ The isomeric products are designated as *syn* and *anti*, where the *syn* configuration has the highest prioritized substituent of the carbene and highest prioritized substituent of the alkene on the same side of the resulting cyclopropane. The ability to discriminate between the two possible additions is referred to as the stereoselectivity of a carbene.¹⁴

Scheme 1.2: *Syn* and *Anti* Addition of Singlet Carbenes to Alkenes



Another important property of carbenes in their addition to double bonds is their philicity.² Electrophilic carbenes, such as CBr_2 and CCl_2 ,¹⁵ react preferentially with highly alkylated alkenes, where the interaction of the p (LUMO) orbital of the carbene with the π (HOMO) orbital of the double bond are dominating (Figure 1.4a).² On the other hand, nucleophilic carbenes, such as CH_3OCCH_3 ,¹⁶ show selectivity towards electron-poor alkenes, where the σ (HOMO) orbital interaction of the carbene with the π^* (LUMO) orbital of the double bond prevails (Figure 1.4b).²



Figure 1.4: Electrophilic and nucleophilic character of carbenes in their addition to alkenes.

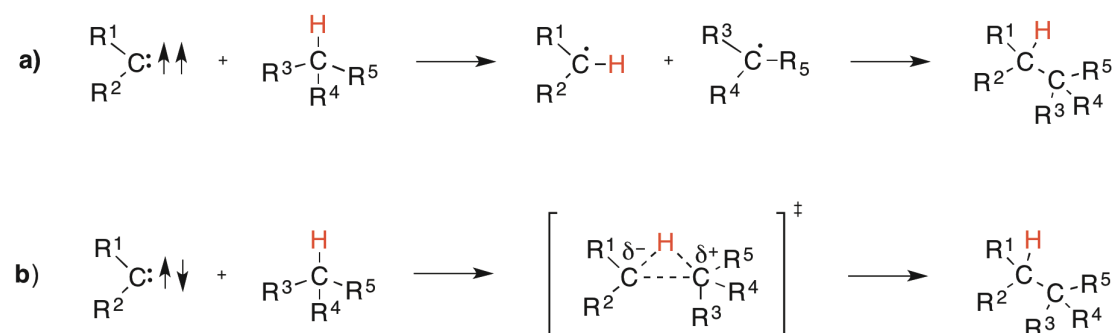
Some carbenes, such as CH_3OCCl and $\text{C}_6\text{H}_5\text{OCCH}_3$, are ambiphilic, which means that they can act *both* as electrophiles and nucleophiles, *i.e.*, both p - π and σ - π^* interactions are important.¹⁷ Their reactivity is high towards electron-rich and electron-poor alkenes, but low towards electronically moderate alkenes.²

Carbenes add to other multiple bonds as well, *e.g.*, to those of alkynes to give cyclopropene derivatives and to arenes.¹⁴ In the reaction with carbonyl double bonds, the carbene may either attack the carbon (nucleophilic carbenes) or the oxygen (electrophilic carbenes), thus forming a zwitterionic intermediate, or it may add to the double bond to give an epoxide.¹⁸

Insertion reactions are also common for carbenes. The insertion into unpolarized C-H bonds has been widely studied. Again, the mechanism of the reaction is dependent on the multiplicity of the carbene. Triplet carbenes abstract a hydrogen atom from the alkane, giving two radicals that subsequently recombine to form the insertion product

(Scheme 1.3a),¹⁹ whereas most singlet carbenes insert into the alkane in a one step process involving a three-center cyclic transition state (TS) (Scheme 1.3b).²⁰

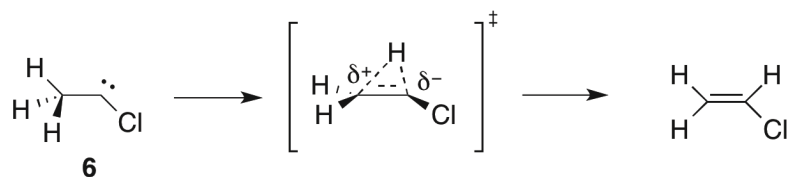
Scheme 1.3: Insertion of Singlet and Triplet Carbenes into C-H Bonds



The simplest carbene, methylene (CH₂), has been demonstrated to react almost indiscriminately with hydrocarbons.²¹ More stabilized carbenes, however, can differentiate between C-H bonds. The reactivity order is tertiary C-H bonds > secondary C-H bonds > primary C-H bonds. For instance, CCl₂ inserts selectively into tertiary bonds of methylcyclohexane and 2-methylhexane.²² The C-H bonds can also be activated by C-C hyperconjugative stabilization of the developed δ⁺ of the transition state. For example, the C-H bond at the C₄ position of 1-*tert*-butyl-4-methylcyclohexane is six times more reactive towards CCl₂, when it is in the equatorial position instead of the axial.²³

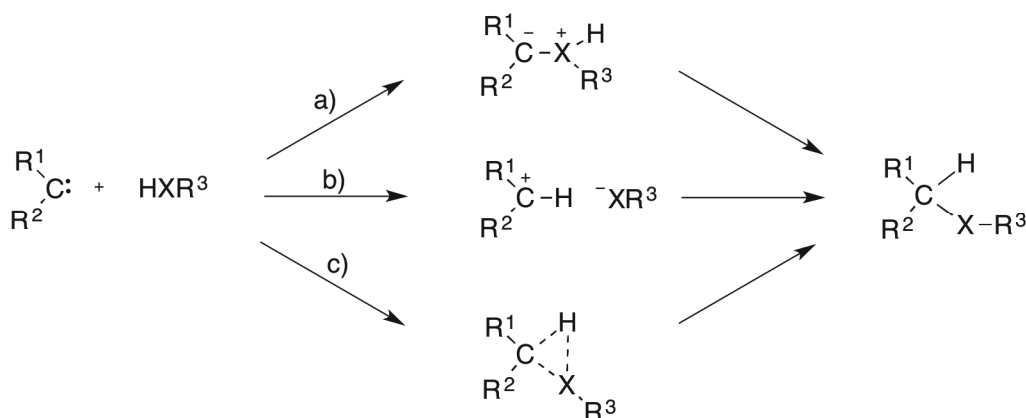
Singlet carbenes can undergo intramolecular insertion reactions, which may give access to highly strained compounds that are otherwise difficult to obtain.² A typical reaction of this kind is the insertion into β-C-H bonds to give alkenes, *i.e.*, 1,2-H shifts. One example of such a rearrangement is observed for chloromethylcarbene (**6**) (Scheme 1.4).² A three-centered transition state can be drawn, which bears resemblance to the TS for intermolecular C-H insertion (Scheme 1.3). Furthermore, singlet carbenes may insert into the γ-C-H bonds to give cyclopropane products.¹⁴ Other groups can undergo 1,2 shifts as well, and for alkylcarbenes the relative migratory aptitude is H > C₆H₅ > CH₃.²⁴ Alkyl migration is promoted by ring strain, and leads to reorganization of the structural framework.¹⁴

Scheme 1.4: 1,2-H Shift of Chloromethylcarbene (6)



Singlet carbenes may insert into polarized X-H bonds, such as O-H (alcohols), N-H (amines), S-H (thiols), and Si-H (silanes). Three different mechanisms are conceivable, as shown in Scheme 1.5.¹⁸ The carbene may insert through an ylidic mechanism, in which it attacks the heteroatom with a subsequent proton transfer (Scheme 1.5a).²⁵ Alternatively, the carbene may be initially protonated to give a carbenium ion, followed by an ion pair recombination (Scheme 1.5b).²⁶ Finally, there is the option of a concerted mechanism (Scheme 1.5c).

Scheme 1.5: Mechanisms for Carbene Insertion into Polarized X-H Bonds



1.1.4 Classification of Carbenes

The most common way to classify carbenes is according to their philicity.²⁷ Moss developed a carbene selectivity scale based on competition experiments in cyclopropanation reactions with alkenes.^{17,28} Carbenes are divided accordingly into three groups: electrophiles, ambiphiles, and nucleophiles. Such classification can also be viewed in terms of HOMO and LUMO orbitals.²⁹ However, this one-dimensional system does not take into account differences in reactivity. Consequently, stabilized and reactive electrophiles are placed into the same group, for example.

Therefore, a two-dimensional depiction was proposed, which takes into account both stability *and* philicity of singlet carbenes. This classification has been termed the Carbene Reactivity Surface.³⁰ It is based on the different reactivities of carbenes in insertion reactions into the C-H bond of acetonitrile and isobutene, which are calculated *in silico*. The carbenes are divided correspondingly into six groups: reactive electrophiles, stabilized electrophiles, stable electrophiles, reactive nucleophiles, stabilized nucleophiles, and stable nucleophiles (Figure 1.5).

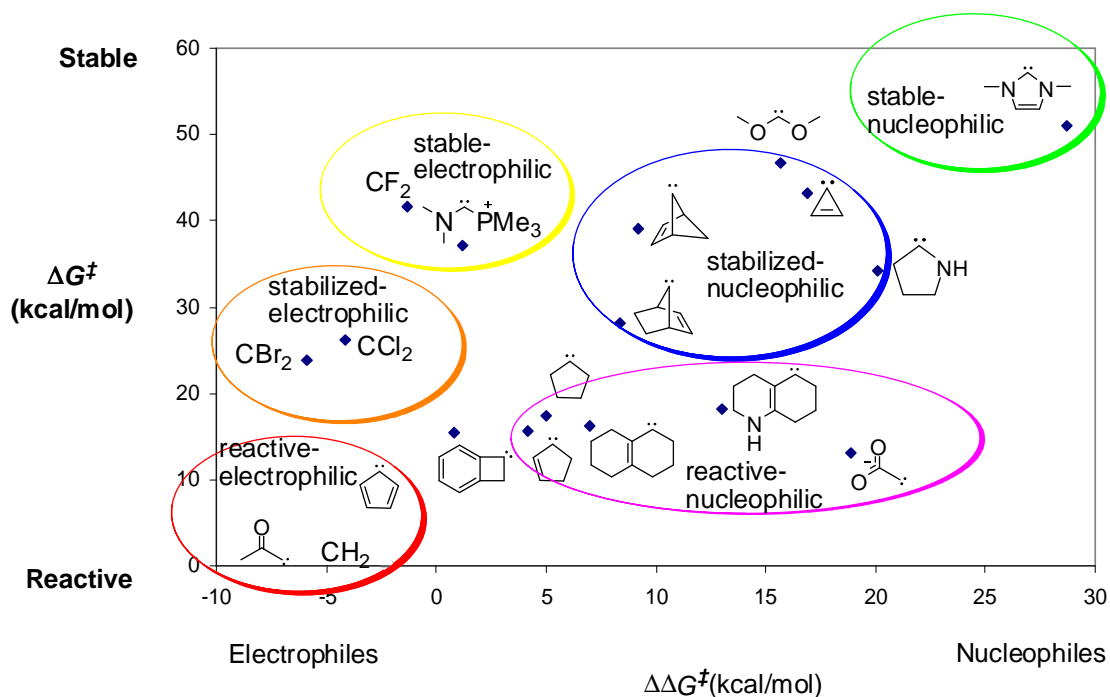


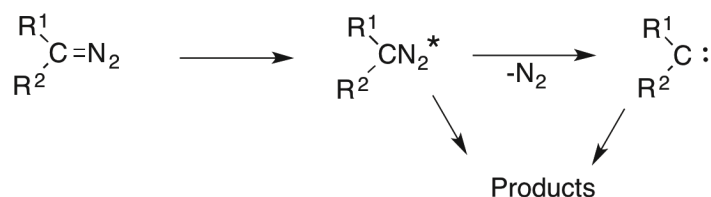
Figure 1.5: The Carbene Reactivity Surface.³⁰

1.2 Carbene Precursors: Oxadiazolines

1.2.1 Diazo Compounds

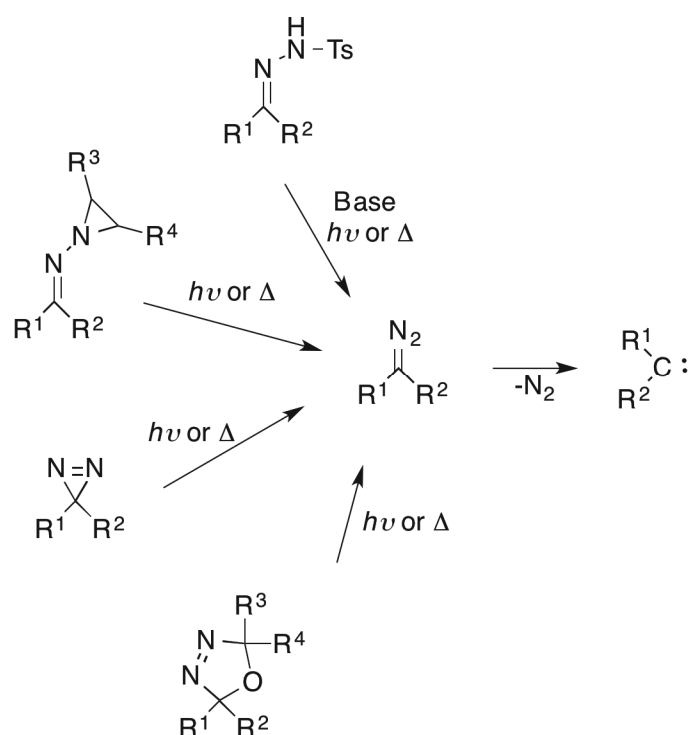
There are many ways to generate carbenes. The classical precursors are the diazo compounds of the general formula $R_2C=N_2$. The carbene is formed by extrusion of nitrogen by either photolysis, thermolysis, or transition-metal catalysis.¹⁴ In general, these compounds are considered a rather clean source of carbenes. By photochemical decomposition, however, it has been proven that in some cases excited diazo compounds, $R_2C=N_2^*$, may carry out so-called precursor chemistry, which closely mimics that of carbenes (Figure 1.6).^{2,14,31}

Scheme 1.6: Photolytic Decomposition of Diazo Compounds



Most diazo compounds are unstable and dangerous to handle, hence they have to be generated *in situ*. Several carbene precursors, such as tosylhydrazone salts, *N*-aziridinylimines, diazirines, and oxadiazolines, are believed to decompose, at least partly, through nonisolable diazo compounds (Scheme 1.7).²

Scheme 1.7: Decomposition of Some Carbene Precursors through Diazo Compounds



Tosylhydrazones decompose by base-catalyzed thermolysis or photolysis to the corresponding carbene. This is known as the Bamford-Stevens reaction.^{14,32} *p*-Toluenesulfinate is initially cleaved off to liberate the intermediate diazo compound, followed by loss of molecular nitrogen. The application of this method has its limitations, however, for example for base-sensitive substrates. Furthermore, the precursors cannot be used under acidic conditions, and they are poorly soluble in some organic solvents. Eschenmoser's *N*-aziridinylimines, on the other hand, are compatible with nonpolar solvents.³³ They also form diazo compounds upon photolysis or thermolysis with concomitant elimination of alkenes.

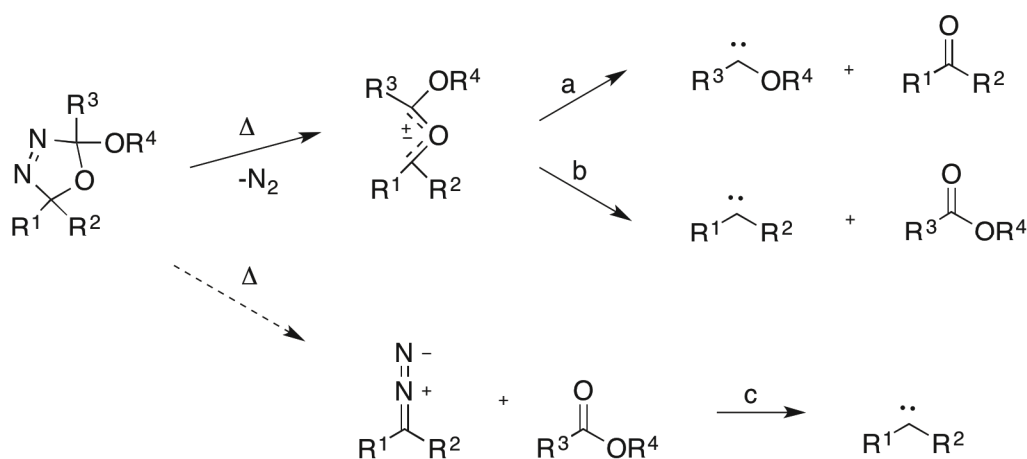
Diazirines are cyclic isomers of diazo compounds, but they are thermally more stable, making them quite ideal precursors. They are considered useful for mechanistic studies as they often, at least partly, generate the corresponding carbenes directly.^{14,34} However, diazirines can also carry out carbene-like chemistry in their excited state when photolyzed.³⁵

Δ^3 -1,3,4-Oxadiazolines (IUPAC name: 2,5-dihydro-1,3,4-oxadiazoles) are versatile and popular carbene precursors. Depending on their substituents and reaction condition, they decompose by different pathways to give a variety of reactive intermediates.³⁶ Two of the most common precursors are the 2,2-dialkoxy-5,5-dialkyl- Δ^3 -1,3,4-oxadiazolines and the 2-alkyl-2-alkoxy-5,5-dialkyl- Δ^3 -1,3,4-oxadiazolines. Their corresponding carbenes can be generated either by thermolysis or photolysis.

1.2.2 Thermolysis of Oxadiazolines

By thermolysis, the oxadiazolines decompose in most cases by a concerted, 1,3-dipolar cycloreversion to yield a carbonyl ylide and molecular nitrogen (Scheme 1.8).³⁷ In case of 2,2-dialkoxy-5,5-dialkyl- Δ^3 -1,3,4-oxadiazolines ($R^3 =$ alkoxy), the resulting ylide is cleaved selectively to give a dialkoxy-substituted carbene and a dialkylketone (Scheme 1.8, route a).³⁸ For instance, the thermolysis of 2,2-dimethoxy-5,5-dimethyl- Δ^3 -1,3,4-oxadiazoline is considered a convenient source to generate dimethoxycarbene.^{38a} In case of 2-alkyl-2-alkoxy-5,5-dialkyl- Δ^3 -1,3,4-oxadiazolines ($R^3 =$ alkyl), however, the carbonyl ylide may fragment in two different ways to give both alkoxyalkylcarbenes and dialkylcarbenes (Scheme 1.8, route a and b).³⁷

Scheme 1.8: Thermolysis of Δ^3 -1,3,4-Oxadiazolines



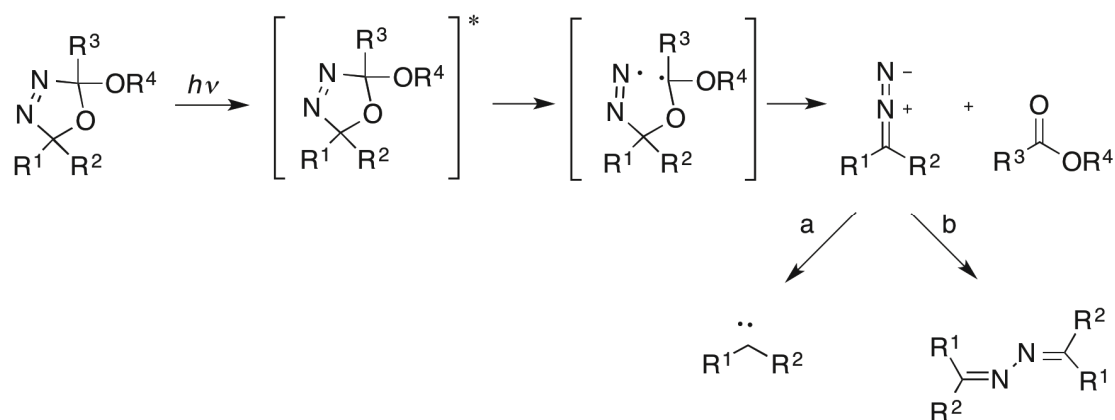
In some cases it has been possible to provide evidence of a carbonyl ylide intermediate, either by trapping experiments using substances such as methanol, acetone, norbornadiene, and dimethyl acetylenedicarboxylate,^{37,39} or by formation of

products deriving from cyclization of the ylide.⁴⁰ In most cases, however, it is not easy to trap them, which means they fragment rapidly to the corresponding carbenes. Moreover, for some oxadiazolines, competitive thermal cleavage to yield diazo alkanes as intermediates has been observed (Scheme 1.8, route c), *e.g.*, for 2-acetoxy-2-methoxy-5,5-dimethyl- Δ^3 -1,3,4-oxadiazoline.⁴¹

1.2.3 Photolysis of Oxadiazolines

The first photolysis of a Δ^3 -1,3,4-oxadiazoline was reported by Hoffmann and Luthardt in 1968.^{39a} In contrast to thermolysis, when oxadiazolines are photolyzed, they usually decompose through diazo compounds as intermediates. For both 2,2-dialkoxy-5,5-dialkyl- Δ^3 -1,3,4-oxadiazolines ($R^3 = \text{alkoxy}$) and 2-alkyl-2-alkoxy-5,5-dialkyl- Δ^3 -1,3,4-oxadiazolines ($R^3 = \text{alkyl}$) the dialkyl diazo compound is selectively formed (Scheme 1.9).⁴² At first, the oxadiazoline is excited to the $n \rightarrow \pi^*$ singlet state at about 300 nm, followed by intersystem crossing to the triplet state.³⁶ Thereafter, one of the C-N bonds is cleaved to generate a diazenyl diradical intermediate, which subsequently undergoes β -scission to form the diazo compound and a carbonyl compound.³⁶ The diazo intermediate decomposes subsequently to the corresponding carbene (Scheme 1.9, route a). Evidence of diazo intermediates have been provided by trapping them with 1,3-dipolarophiles^{42a,b} and by formation of azines^{42c-e} (Scheme 1.9, route b).

Scheme 1.9: Photolysis of Δ^3 -1,3,4-Oxadiazolines



1.3 Foiled Carbenes

In 1968, Gleiter and Hoffmann coined the term “foiled carbenes” for a particular case of stabilized singlet carbenes.⁴³ The classic example is norbornen-7-ylidene (**7**) (Figure 1.6a).⁴⁴ These reactive species have an ideally positioned double bond incorporated into the system that donates electrons from the π bond into the empty p orbital of the divalent carbon. A consecutive addition is foiled, as it would lead to an impossibly strained product (Figure 1.6c). Instead, there is a formation of a two-electron, three-center bond with a charge-delocalized arrangement (Figure 1.6b), also found in certain analogous carbonium ions.⁴⁵

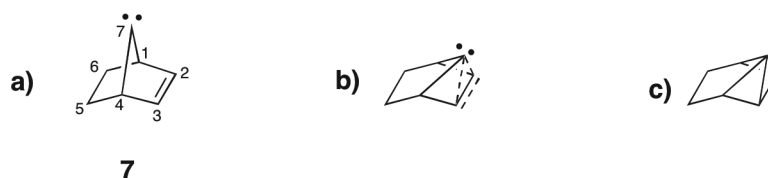


Figure 1.6: Stabilization of norbornen-7-ylidene (**7**) by electron donation from the π bond into the empty p orbital of the divalent carbon.

Furthermore, Gleiter and Hoffmann predicted the following:

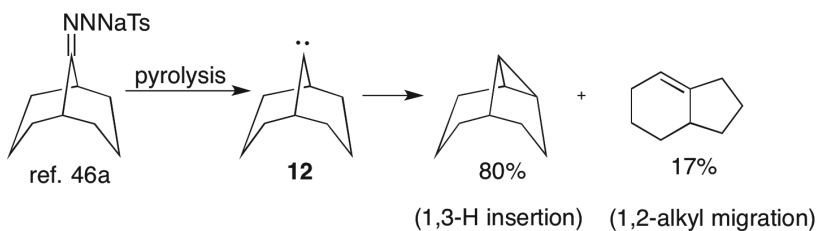
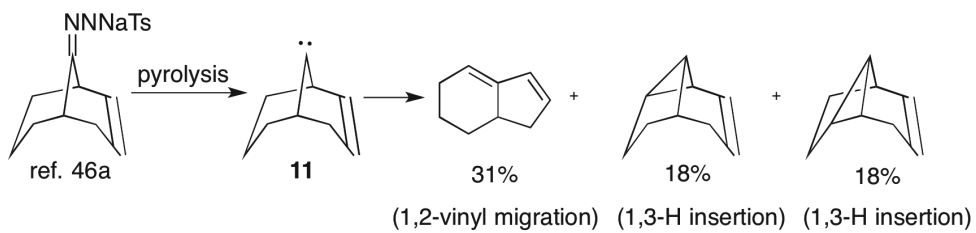
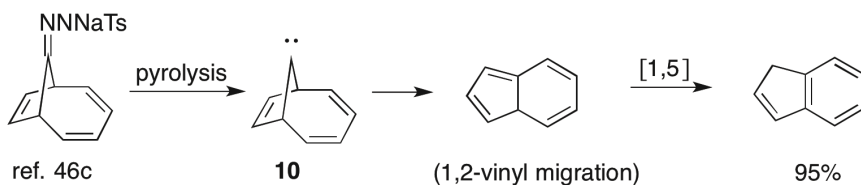
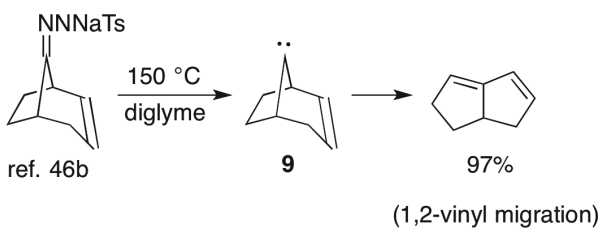
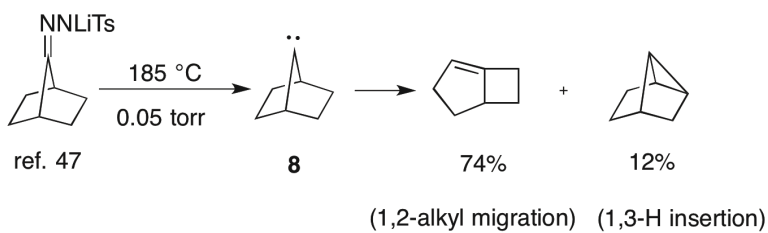
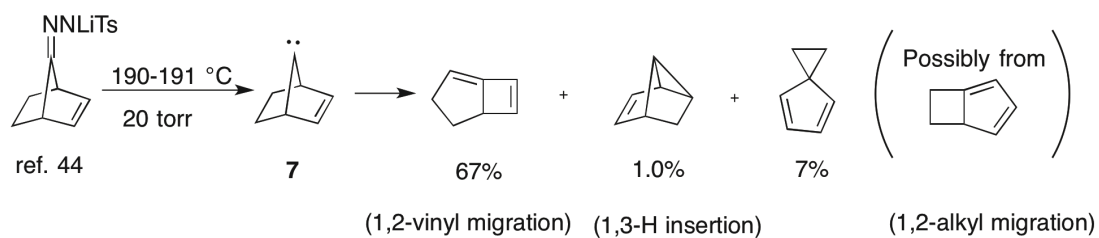
- the stabilization should lead to a large σ -p gap favoring the singlet state
- the bridge containing the divalent carbon should lean towards the double bond
- there should be an increased nucleophilicity of the carbene due to the electron donation from the double bond into the carbenic center

1.3.1 1,2-Vinyl Shifts of Foiled Carbenes

These predictions inspired a great deal of research to prove such an interaction. The obtained results were, however, mainly limited to rearrangement reactions of the foiled carbenes.^{44,46} The predominant rearrangement for thermally generated foiled carbenes is the 1,2-vinyl migration. 1,3-H insertions and 1,2-alkyl shifts, which are typical for their alkane analogues, are less frequent. This is demonstrated in Scheme

1.10 for carbenes **7-12**, where yields are given in relative yields.^{44,46a-c,47} 1,2-H insertions, which are common for singlet carbenes, are impeded due to poor overlapping of the p orbital of divalent carbon with the σ orbital of the neighboring C-H bond.

Scheme 1.10: Rearrangements of Some Foiled Carbenes and Some of Their Alkane Analogues



Even though 1,2-vinyl shifts are typical for foiled carbenes, this is not adequate evidence for a special p- π interaction. Vinyl migrations are in any case facile for thermally generated allyl carbenes.⁴⁸ Furthermore, recent calculations predicted that some species, which have been claimed to be foiled carbenes, actually are bent away from the double bond. For example, bicyclo[3.3.1]non-2-en-9-ylidene (**11**) represents such a case.⁴⁹

1.3.2 Intermolecular Reactions of Foiled Carbenes

It was proposed that the p- π interaction should be reflected in the stereoselectivity of foiled carbenes in intermolecular reactions. Reactions of singlet carbenes are often exceptionally exothermic, and Hammond's Postulate states that the TS resembles that of the reactants under such conditions.⁵⁰ For a reaction involving a carbene intermediate (Figure 1.7), the TS of the product formation is close in structure to the carbene. Thus, the nature and variety of the products are good measures of the intermediate structure. Due to the bending of the bridge towards the double bond in foiled carbenes, it is anticipated that the reactant should approach the carbenic carbon more easily *anti* to the double bond, where more space should be available.⁴³ For example, the bridge of norbornen-7-ylidene (**7**) is predicted by DFT calculations to lean towards the double bond by $\omega = 37^\circ$ when compared to norbornene.^{49,51}

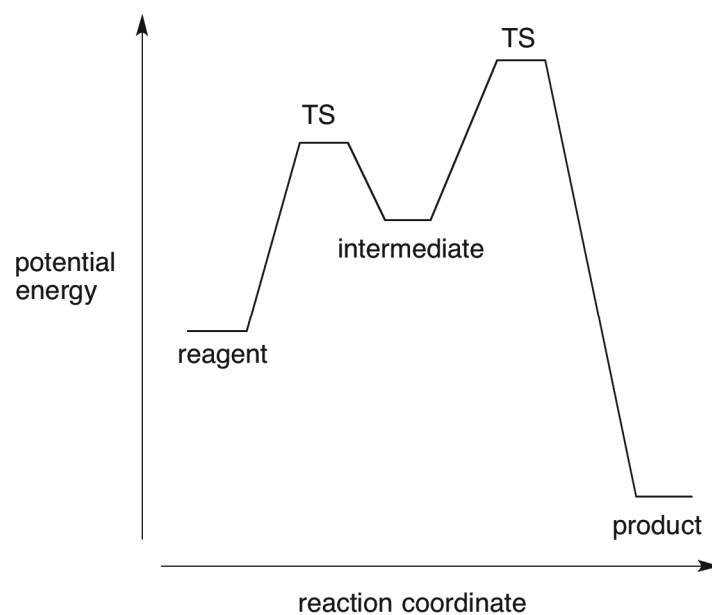
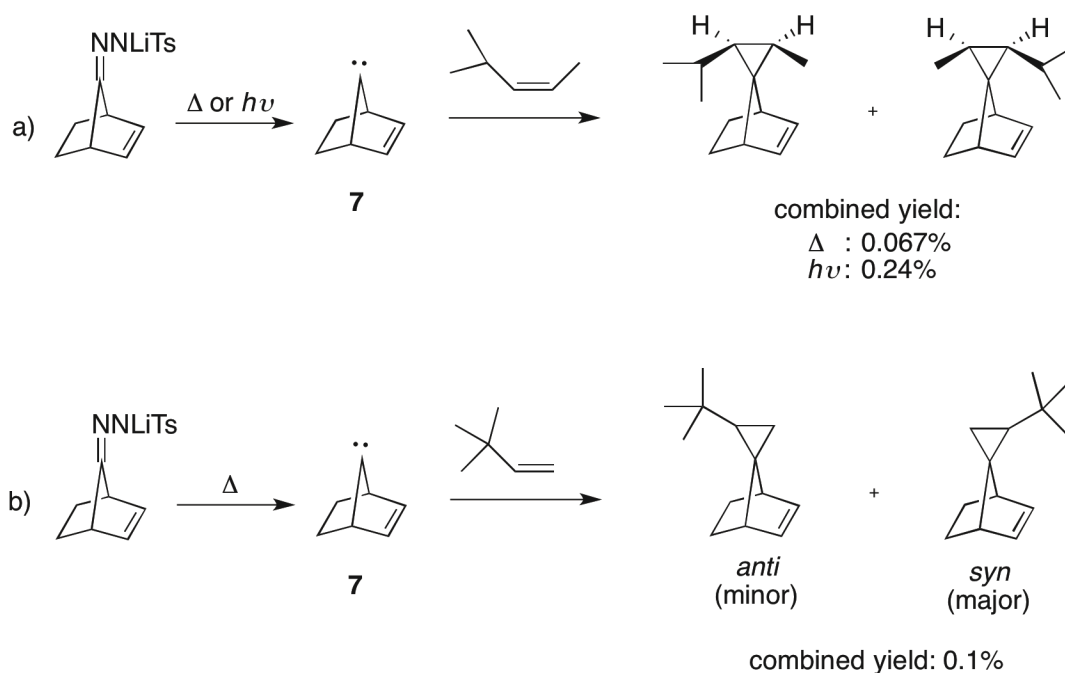


Figure 1.7: Energy profile of an exothermic reaction involving an intermediate.

In 1972, Moss and Dolling reported the first alkene addition to a foiled carbene. The Bamford-Stevens precursor of carbene **7** was thermolyzed or photolyzed in *cis*-4-methylpent-2-en, and in both cases, a mixture of *syn* and *anti* products were detected (Scheme 1.11a).⁵² The ratio of the products was not provided and no conclusion regarding the stereoselectivity of **7** can be drawn. However, the reaction was found to be stereospecific, *i.e.*, the *cis* stereochemistry of the alkene was preserved in both addition products, which is expected for singlet carbenes. Furthermore, the low yields obtained by addition to the electron-rich double bond (0.067% by thermolysis and 0.24% by photolysis) indicated a nucleophilic behavior of carbene **7**. For comparison, norbornan-7-ylidene (**8**) added to the same alkene in yields of 23% by thermolysis and 8.4% by photolysis.⁵²

Scheme 1.11: Intermolecular Addition Reactions of Norbornen-7-ylidene (7)



Then, Moss and Ho carried out a thermolysis by addition of *tert*-butylethylene (3,3-dimethylbut-1-ene) to **7** (Scheme 1.11b).⁵³ Two products were obtained wherein the *tert*-butyl group was oriented *syn* or *anti* to the double bond in a ratio of 7:1. The major product was of the opposite stereochemistry than what had been anticipated. Nevertheless, these results did not rule out the possibility of bending, but indicated that the stereoselectivity of the addition is more complex.

Years later, the reaction mechanism was investigated by computational chemistry.⁵⁴ The most stable TS was found for *tert*-butylethylene approaching the divalent carbon *anti* to the double bond, with the bulky *tert*-butyl substituent directed head-on to avoid steric interaction with the *exo* hydrogens at the C₅ and C₆ of **7** (Figure 1.8). This would lead to the *syn* product, which was indeed the major product obtained experimentally. Thus, for addition reactions, one has to take into consideration both from which face the alkene is approaching *and* the orientation of its substituents.

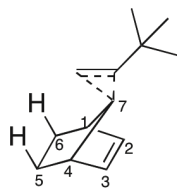
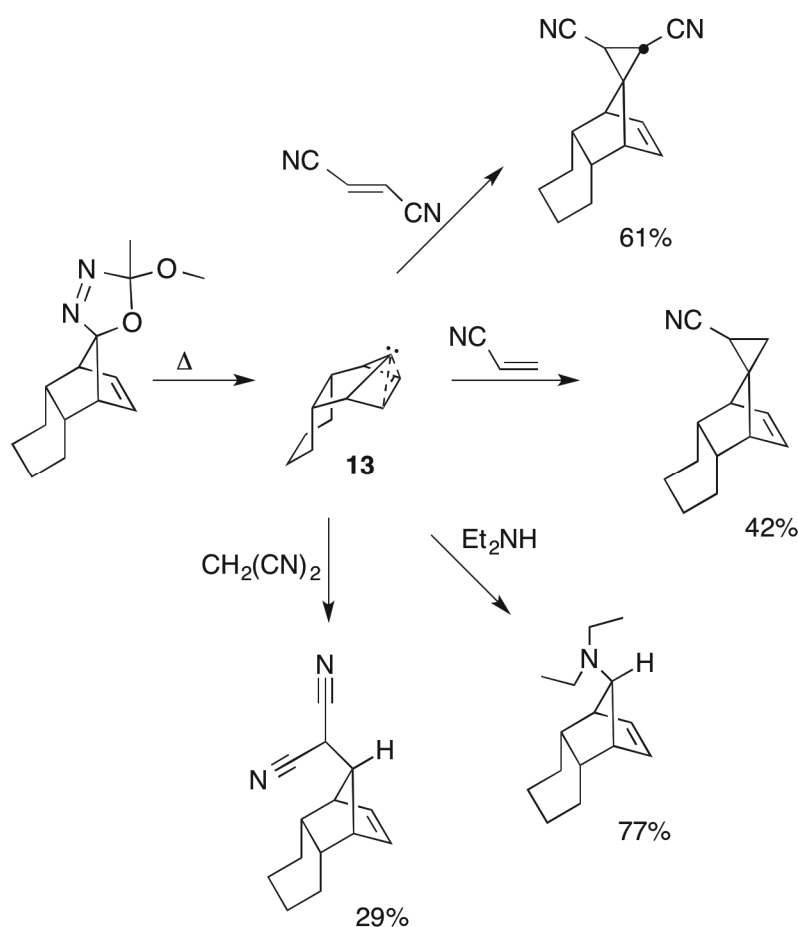


Figure 1.8: Transition state for the addition of *tert*-butylethylene to **7**.

In order to obtain intermolecular products in reasonable yields, it was important to take into account the predominantly nucleophilic behavior of foiled carbenes. Carbene **7** is classified as a stabilized nucleophile according to the Carbene Reactivity Surface.³⁰ *endo*-Tricyclo[6.2.1.0^{2,7}]undec-9-en-11-ylidene (**13**), comprising **7** as a subunit, was generated by thermal decomposition of an oxadiazoline precursor in the presence of electron-poor alkenes, *i.e.*, fumaronitrile and acrylonitrile.⁵⁴ The addition products were obtained in yields of 61% and 42%, respectively (Scheme 1.12). For the unsymmetric acrylonitrile, the *anti* addition product was obtained exclusively. DFT calculations suggested the product to be formed by the substrate nearing the carbenic center *anti* to the double bond of carbene **13**. Additionally, **13** could be trapped with diethylamine (77%)⁵⁵ and malononitrile (29%),⁵⁶ in each case also by *anti* approach of the substrates (Scheme 1.12).

Scheme 1.12: Intermolecular Reactions of *endo*-Tricyclo[6.2.1.0^{2,7}]undec-9-en-11-ylidene (13)



1.3.3 Cyclopropane versus Double Bond in Foiled Carbenes

Cyclopropanes are known to resemble alkenes more than their higher cycloalkane homologs. The three-membered ring has a high angle strain due to the C-C-C angles being forced to be 60°. To release some of this strain, the C-C bonds are bent outwards to so-called “banana bonds”, and the density of the bonding electrons is highest off the straight C-C connecting line. Thus, the C-C single bonds of cyclopropane have a higher p character than normal ones.

There are two different models to describe this bonding situation, *i.e.*, the molecular orbital (MO) model of Walsh (Figure 1.9a) and the valence bond (VB) model of Coulson and Moffitt (Figure 1.9b).⁵⁷ According to the MO model, the three occupied molecular orbitals determine the properties of the C-C bonds in cyclopropane, which

consist of one lower-lying σ orbital and two equal-energy “quasi π ” orbitals. In contrast, the VB model describes the C-C bonds as a result of sp^5 -hybridized orbitals. For both models, the resemblance to C-C double bonds is demonstrated (Figure 1.9).

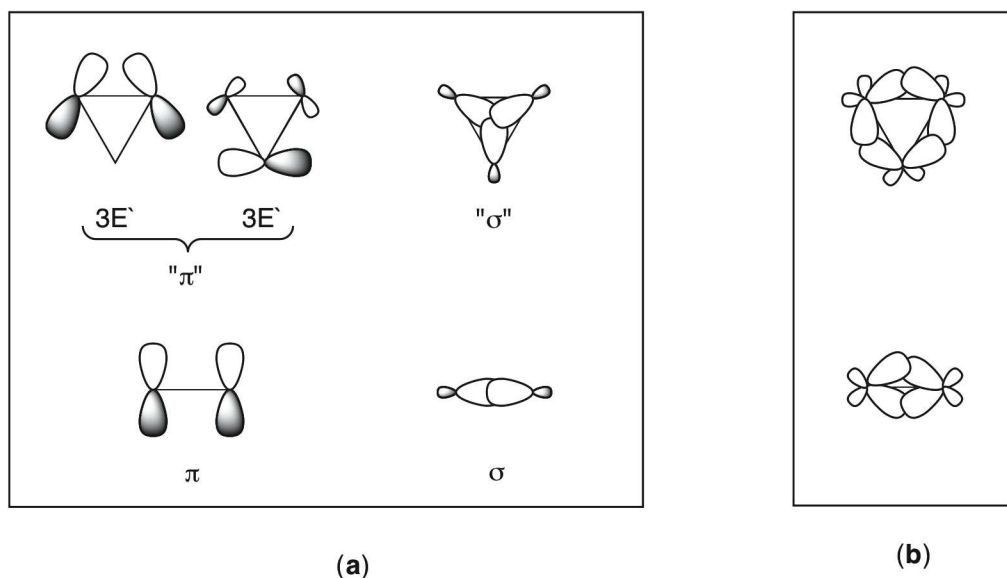


Figure 1.9: (a): Molecular orbital (MO) model of bonding in cyclopropane and ethylene. (b): Valence bonds (VB) model of cyclopropane and ethylene.

Computational calculations indicate that the three-membered ring of *endo*-tricyclo[3.2.1.0^{2,4}]octan-8-ylidene (**14**) stabilizes the divalent carbon in a way similar as the double bond does in norbornen-7-ylidene (**7**) (Figure 1.10).⁵⁸ The Walsh orbitals in carbene **14** mimic that of the π -MO in carbene **7**, and they are able to establish a two-electron, three-center delocalized bond with the carbene's p-AO. It is crucial for the cyclopropane ring to be *endo*-fused in order for the Walsh orbitals to be able to interact with the divalent carbon. Therefore, the corresponding *exo*-tricyclo[3.2.1.0^{2,4}]octan-8-ylidene (**15**) is not expected to experience such stabilization, as the Walsh orbitals are not beneficially oriented to enable such an interaction (Figure 1.10).

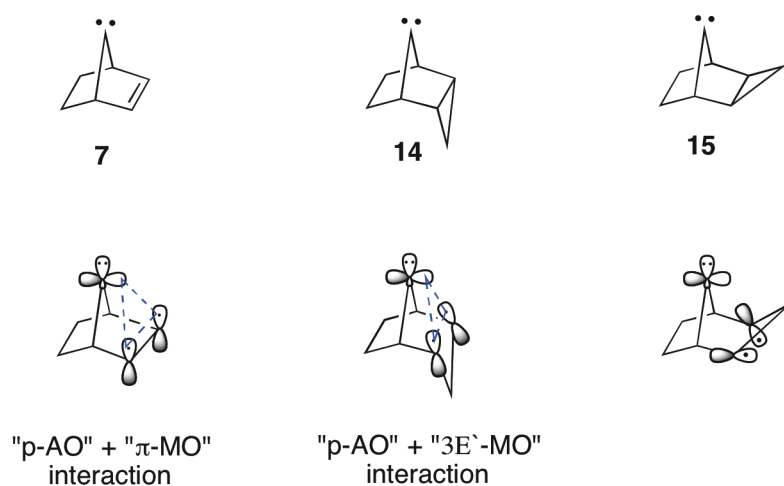


Figure 1.10: Spatial orientation of π and Walsh orbitals in carbenes **7**, **14**, and **15**.

Foiled carbenes were defined by Gleiter and Hoffmann to be “systems where a stabilization is obtained by the inception of a facile carbene reaction which is foiled by the impossibility of attaining the final product geometry”.⁴³ This definition also applies to the lack of insertion into C-H bonds, and consequently carbene **14** belongs to this class by the impossibility of undergoing a 1,3-H insertion at the C₂ and C₄ positions. Such reactions would lead to a product featuring an inverted carbon atom C₂ or C₄ with all four bonds pointed in one hemisphere (Figure 1.11c).

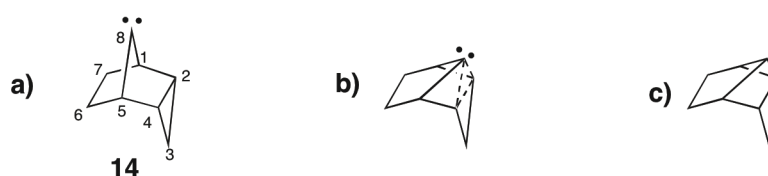
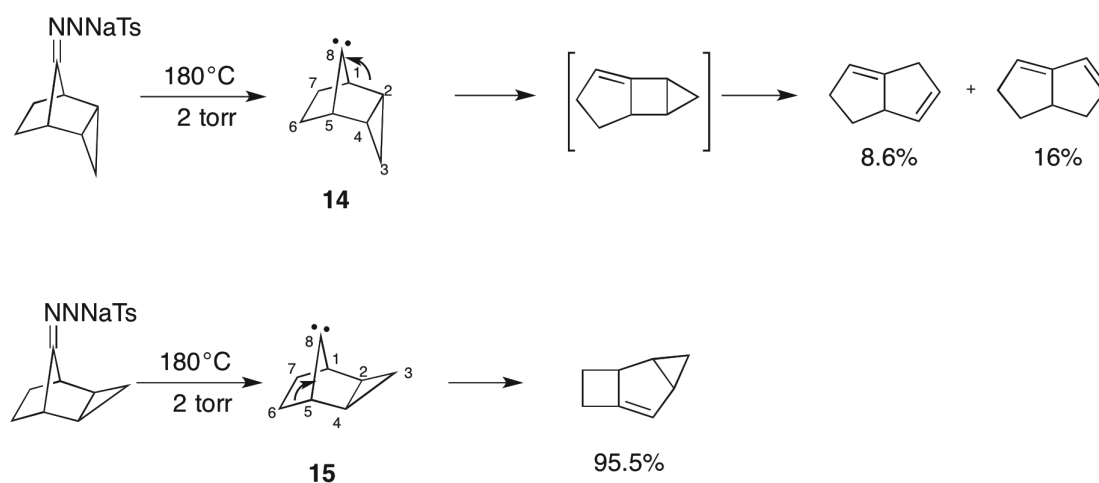


Figure 1.11: Stabilization of *endo*-tricyclo[3.2.1.0^{2,4}]octan-8-ylidene (**14**) by electron donation from the Walsh orbitals into the empty p orbital of the divalent carbon.

Only few experiments have been carried out to prove any interaction of the Walsh orbitals with the empty p orbital of the divalent carbon in **14**. Murahashi and co-workers studied the rearrangement of carbene **14** and **15** from vacuum pyrolysis of their Bamford-Stevens precursors as shown in Scheme 1.13 (yields are given in relative yields) (Scheme 1.13).⁵⁹ For the *endo*-fused analogue **14**, the rearrangement products were argued to derive from cleavage of the C₁-C₂ or C₄-C₅ bond,

respectively, adjacent to the three-membered ring. This can be compared to the 1,2-vinyl shift of carbene **7**.⁴⁴ No products were formed by 1,2-alkyl migration from cleavage of the C₁-C₇ or the C₅-C₆ bond. The relatively low isolated amount of rearrangement products seems to be due to the competing formation of C₇H₁₀ products, which are thought to derive from expulsion of atomic carbon from carbene **14**. The rearrangement products obtained from the *exo*-fused analogue **15**, on the other hand, seem to be formed exclusively from 1,2-alkyl migration by cleavage of the C₁-C₇ or C₅-C₆ bond, respectively. However, since different rearrangement mechanisms may be proposed for the formation of product from **14** and **15**, a Walsh-orbital interaction in **14** is not sufficiently proven.

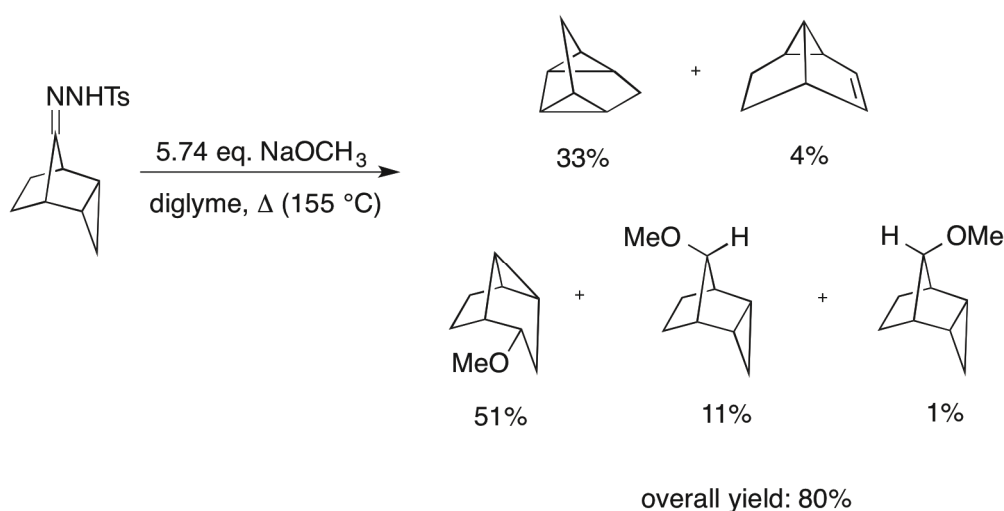
Scheme 1.13: Pyrolysis of Bamford-Stevens Precursor of *endo*-Tricyclo[3.2.1.0^{2,4}]octan-8-ylidene (14**) and *exo*-Tricyclo[3.2.1.0^{2,4}]octan-8-ylidene (**15**)**



Freeman *et al.* carried out thermolyses of the tosylhydrazone of **14** in diglyme (*i.e.*, 2,5,8-trioxanonane) in the presence of sodium methoxide.⁶⁰ The rearrangement products from these experiments, however, are different from those obtained by vacuum pyrolysis (Scheme 1.14). Mechanistic studies were performed using deuterated substrates, and there was a strong support for an intermolecular carbene-to-carbene rearrangement, with the solvent acting as a proton-transfer agent (*vide infra*: Chapter 4.1).^{60b} The absence of solvent in the experiments of Murahashi *et al.* may therefore be responsible for the different outcome. The rearrangement products

obtained by Freeman *et al.* is best explained to occur through a mechanism involving interaction of the divalent carbon and the Walsh orbitals, thus supporting the proposed bending of **14**. There were also some intermolecular products isolated resulting from a reaction of **14** with methanol, which is formed in the reaction of the tosylhydrazone and sodium methoxide. However, these products are thought to derive from carbonium ion pathways by initial protonation of carbene **14**, and therefore provide no evidence of any carbene-cyclopropane interaction.

Scheme 1.14: Thermolysis of Bamford-Stevens Precursor of *endo*-Tricyclo[3.2.1.0^{2,4}]octan-8-ylidene (14**) in Diglyme**



To this author's knowledge, no additional experiments have been carried out for *endo*-tricyclo[3.2.1.0^{2,4}]octan-8-ylidene (**14**).

1.4 Aim of the Study

The aim of this research was to advance the knowledge of the chemistry of foiled carbenes. These carbenes, stabilized by an intramolecular double bond, had already been quite thoroughly studied. In contrast, examination of such species stabilized by an incorporated cyclopropane ring was rather incomplete, especially regarding experimental results. Thus far, almost exclusively the rearrangements of *endo*-tricyclo[3.2.1.0^{2,4}]octan-8-ylidene (**14**) had been investigated.

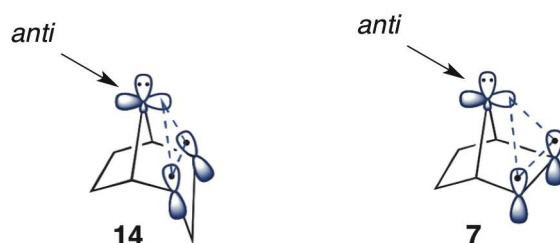


Figure 4.1: Comparison of stabilization of carbene **14** and **7** by interaction of each carbene's empty p orbital with the Walsh orbitals and double bond π orbitals, respectively.

It was anticipated that the classification of **14** as a foiled carbene could be more comprehensively assessed by studying its *intermolecular* reactions. Interaction of the Walsh orbitals of the three-membered ring with the p orbital of the divalent carbene should result in a bending of the bridge towards the stabilizing moiety. As a result, the substrate is expected to approach the face of the carbenic center *anti* to the cyclopropane ring, in the same manner as for foiled carbenes stabilized by a double bond (Figure 4.1). In other words, carbene **14** should react stereoselectively. Moreover, such donation of electrons into the p orbital of the divalent carbon should lead to a nucleophilic behavior of the carbene. Thus, it was important to study the reactions of **14** with both electron-poor and electron-rich alkenes.

Furthermore, it was of interest to compare the reactive behavior of **14** to a structurally related carbene that does not belong to the group of foiled carbenes, *e.g.*, bicyclo[3.2.1]octan-8-ylidene (**16**), to probe the importance of the appropriately oriented Walsh orbitals.

Moreover, DFT calculations of stabilization energies were going to be performed for *endo*-tricyclo[3.2.1.0^{2,4}]octan-8-ylidene (**14**) and some structurally related carbenes to compliment the experimental findings.

To sum it up, this thesis will consist of:

1. Synthesis of appropriate carbene precursors
2. Intermolecular reactions with the corresponding carbenes
3. DFT calculations of stabilizing energies of relevant carbenes

2. Calculations of Geometries and Stabilization of *endo*-Tricyclo[3.2.1.0^{2,4}]octan-8-ylidene (14) and Related Carbenes

2.1 Computational Methodology for Determination of Geometry and Energy of Molecules

Computational chemistry is an important tool for obtaining information about structure, energy, reactivity, and physical properties of molecules. The calculations are based on quantum and molecular mechanics.⁶¹ There are several methods for carrying out the calculations.⁶² By molecular mechanics methods, the molecule is viewed as a collection of balls held together by springs and can be used for geometry optimizations. The minimum-energy geometry of a molecule is found by expressing the energy as a function of its resistance towards bending and stretching of the bonds. It is mainly used to calculate energies for small to medium-sized molecules. The advantage of using this method is that the calculations are fast and undemanding. One of its weaknesses, however, is that it ignores the electrons of a molecule and it can only provide parameters like dipole moments by analogy.

Ab initio calculations give the molecule's energy and wavefunction based on approximations of the Schrödinger equation, *e.g.*, the Born-Oppenheimer approximation.⁶² The necessary approximation determines the level of the calculation. The main uses are calculating geometries, energies, vibrational frequencies, spectra (IR, UV, NMR), ionization potentials, electron affinities, dipole moments, and other properties related to electron distribution. Such calculations are in general quite reliable, but they are rather slow compared to other methods. The simplest type of *ab initio* calculations is the Hartree-Fock method.

Semiempirical calculations are also based on the Schrödinger equation, but they are combined with experimental quantities.⁶² More approximations are employed as well, and so these computations are fast compared to *ab initio*. Examples of such

calculations are the simple and the extended Hückel methods. Semiempirical methods are usually adequate for finding geometries of normal molecules and transition states. A weakness is that some experimental parameters that might be needed for the molecule of interest may not be available. Furthermore, errors are less systematic and therefore more difficult to correct.

For density functional theory (DFT) calculations, the electron probability density function is used, rather than a wavefunction.⁶² The method is based on the probability of finding an electron within a given volume, and is therefore a function of only three variables (x , y , z). DFT computations may be applied for finding geometries, energies, frequencies, and properties arising from electron distribution, such as dipole moments, charges, and bond orders. The main advantage of this method is that rather high quality calculations can be obtained relative to the time needed. It is not as accurate as the highest level of *ab initio* methods, but it can handle much bigger molecules. Furthermore, the method can be improved by combining it with the Hartree-Fock exchange term: a so-called hybrid DFT functional.

2.2 Results and Discussion

DFT calculations were performed in order to investigate the stabilization energies of the singlet state of *endo*-tricyclo[3.2.1.0^{2,4}]octan-8-ylidene (**14**) and some structurally related carbenes (Figure 2.1). The degree of bending of the bridge containing the divalent carbon was estimated as well. The aim was to get a better understanding of how relatively small structural changes of **14** would influence its behavior. It was of interest to compare the stabilization obtained by interaction of the carbenic center with a double bond to that of a three-membered ring (both *endo*- and *exo*-fused), and to see how the presence of both these moieties would affect the reactive species.

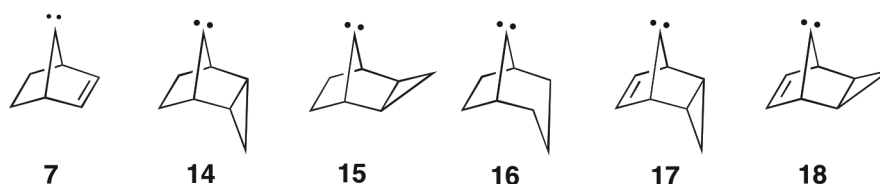


Figure 2.1: Stabilization energies and degree of bending were estimated for some structural related carbenes by DFT calculations using B3LYP/6-31G(d) methodology.

The calculations were carried out using the Spartan '04 quantum chemistry program.⁶³ The optimized geometries of the carbenes were obtained by employing Becke's three-parameter hybrid method⁶⁴ and the correlation-energy functional of Lee, Yang, and Parr (B3LYP).⁶⁵ The B3LYP/6-31G(d) level of theory was applied. The geometries were confirmed by vibrational analysis, and for all calculations the number of imaginary frequencies (NImag) was zero.

Mieusset and Brinker had previously calculated the bending of the bridge in **7**,^{49,51} and Freeman *et al.* had computed the stabilization energies for **7** and **14**.⁵⁸ However, since different programs were used, *i.e.*, Gaussian '04 and Gaussian '94, respectively, and in some cases a different level of theory was applied, these values were recalculated with Spartan '04 in order to compare them directly with the additional results obtained. However, the re-examined values did not change by any significant extent.

First, the optimized geometries were analyzed to determine the bending of the bridge containing the divalent carbon. This bending was measured in relation to that of the corresponding alkanes of the carbenes, *i.e.*, the compounds obtained by a formal hydrogenation of the carbenic center. For example, carbene **14** was compared with *endo*-tricyclo[3.2.1.0^{2,4}]octane. The angle between the C_B-C_A-C_E plane (Figure 2.2a) and C_B-C_C-C_D-C_E plane (Figure 2.2b) was determined for the carbene. Thereafter, this angle was established for the corresponding alkane as well. The degree of bending was defined as the difference between those two angles. For instance, this angle was found to be 89.5° for carbene **14** and 122.2° for *endo*-tricyclo[3.2.1.0^{2,4}]octane. Thus, the bridge of carbene **14** is bent by about 32.7°. Additionally, the distance between the divalent carbon and one of the carbons of the stabilizing bond was determined (C_A-C_C) (Figure 2.2c).

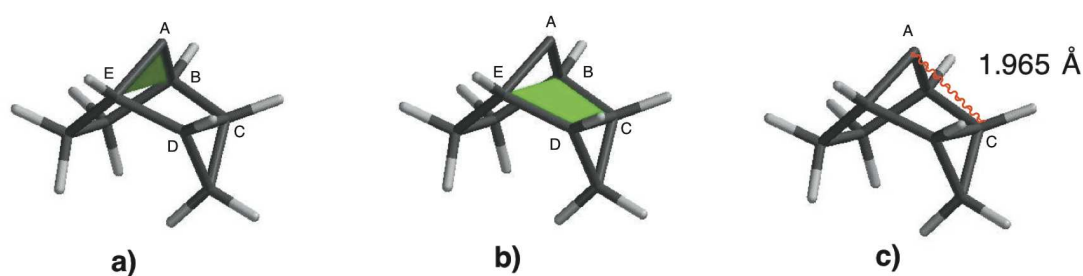


Figure 2.2: Illustrations of planes and distances used for analyzing the bending of the bridge containing the divalent carbon.

All results are given in Table 2.1, where the optimized geometries of the carbenes are shown as well. For some carbenes, two energy minima were found with the bridge bending to one or the other side. In order to find more than one minimum, the bridge was “forced” in both directions prior to optimization of the geometries.

Table 2.1: Optimized Geometries and Bending for Carbenes 7 and 14-18

intermediate	optimized geometry	angle carbene ^a	angle alkane ^a	relative bending alkane-carbene	C _A -C _C distance ^b (Å)
7a (π stabilized)		90.1°	127.4°	37.3°	1.893
7b (σ stabilized)		104.8°	120.6°	15.8°	2.202
14 (Walsh stabilized)		89.5°	122.2°	32.7°	1.965
15 (σ stabilized)		105.1°	121.5°	16.4°	2.182
16a (σ stabilized)		100.8°	115.8°	15.0°	2.354
16b (σ stabilized)		100.8°	115.8°	15.0°	2.378
17a (π stabilized)		87.8°	125.1°	37.3°	1.874
17b (Walsh stabilized)		84.9°	119.1°	34.2°	1.925
18 (π stabilized)		87.6°	124.4°	36.8°	1.860

^a The angle is defined as the angle between the plane of C_B-C_A-C_E and the plane of C_B-C_C-C_D-C_E (Figure 2.2). ^b The distance is measured between the divalent carbon C_A and one of the carbon of the stabilizing C_C-C_D bond.

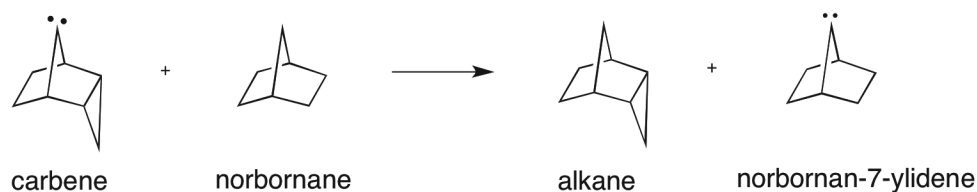
The results given in Table 2.1 demonstrate a comparable degree of bending when an *endo*-fused three-membered ring stabilizes the carbene as when it is stabilized by a double bond. For **14** and **17b**, the degree of bending is $\omega = 32.7^\circ$ and 34.2° , respectively, whereas for **7a**, **17a**, and **18**, it lies between 36.8 - 37.3° . When the three-membered ring is *exo*-fused, however, *i.e.*, for carbene **15**, the carbene “prefers” the σ stabilization on the other side of the bridge, thus leaning in the opposite direction of the three-membered ring by $\omega = 16.4^\circ$. Also in other cases of σ stabilization, *e.g.*, for **7b**, **16a**, and **16b**, the bending was found to be in the range of 15.0 - 15.8° . The C_A - C_C distances were consistent with the bending of the carbenes.

Next, the stabilization energies were calculated by calibrating the Hartree energies of the carbenes against that of nobornan-7-ylidene (**8**). The isodesmic equation shown in Scheme 2.1 was applied, and the stabilization energy is then given as

$$SE = E_{\text{alkane}} + E_{\text{nornornan-7-ylidene}} - E_{\text{carbene}} - E_{\text{nornornane}}$$

Thus, a positive SE value means that the calculated carbene is more stable than **8**, whereas a negative SE value means that it is less stable.

Scheme 2.1: Isodesmic Reaction Used for the Calculation of Stabilization Energies



The results are presented in Table 2.2, where the Hartree energies are given in kcal/mol.

Table 2.2: Stabilization Energies of Carbenes 7 and 14-18^a

intermediate	carbene (kcal/mol)	norbornane (kcal/mol)	alkane (kcal/mol)	norbornan-7- ylidene (kcal/mol)	SE ^b (kcal/mol)
7a	-170307.9		-171139.2		15.9
7b	-170294.2		-171139.2		2.2
14	-194966.4		-195799.3		14.3
15	-194959.6		-195804.5		2.3
16a	-195750.4	-171917.9	-196593.3	-171070.7	4.3
16b	-195742.4		-196593.3		-3.7
17a	-194191.6		-195020.3		18.5
17b	-194191.3		-195020.3		18.2
18	-194197.6		-195022.2		22.6

^aEnergies of the species are calculated at the B3LYP/6-31G(d) level (NImag = 0 in each case) in Hartrees. ^bThe stabilization energies were calculated using $SE = E_{\text{alkane}} + E_{\text{norbornan-7-ylidene}} - E_{\text{carbene}} - E_{\text{norbornane}}$, using the isodesmic equation shown in Scheme 2.1.

Thus, the computational analyses indicate that the *endo*-fused three-membered ring stabilizes the carbene in a similar way as a double bond. The stabilization energies of **7a** and **14** were found to be 15.9 and 14.3 kcal/mol, respectively. In contrast to **14**, a second energy minimum was found for carbene **7**, where it is stabilized by σ interactions with SE = 2.2 kcal/mol. This stabilization is, however, much smaller.

Furthermore, it is demonstrated that an *exo*-fused three-membered ring has little stabilizing effect on the carbenic center in comparison with an *endo*-fused. Carbene **15** has a stabilization energy of 2.3 kcal/mol, obtained by σ stabilization at the opposite side of the cyclopropane unit. Thus, the Walsh orbitals of the three-membered ring are not beneficially oriented for stabilizing carbene **15**.

It was of interest to compare carbene **14** with **16**, which is structurally very similar, but misses the bond between C_C and C_D, which is the crucial bond for stabilization of carbene **14**. Removal of this bond makes the structure of **16** more flexible, and as a consequence, two conformers were found for this species, *i.e.* a chair-like conformer (**16a**) and a boat-like conformer (**16b**). **16a** is more stabilized than **16b**, presumably

due to a more beneficial hyperconjugative interaction with the C-H bonds at C_C and C_D. It has a stabilization of 4.3 kcal/mol, which is higher than that of **15**, but still much lower than the values found for the foiled carbenes in Table 2.2. Carbene **16b** has a negative stabilization energy of -3.7 kcal/mol.

The presence of both a double bond *and* an *endo*-fused three-membered ring in **17** appears to further stabilize foiled carbenes. There are two energy minima, one for which the carbenic center is interacting with the cyclopropane ring, with SE = 18.2 kcal/mol, and one for which it is interacting with the double bond, with SE = 18.5 kcal/mol. Thus, the latter conformer is slightly more stable. Hoffmann and Gleiter carried out extended Hückel calculations, for which the potential energy curve of **17** was found.⁴³ In contrast to DFT calculations, these results predicted a deeper minimum by interaction with the cyclopropane ring than with the double bond. In any case, the energy difference between the two competing interactions is minor.

The most stabilized carbene, however, is carbene **18**, comprising both a double bond and an *exo*-fused cyclopropane. Only one energy minimum was found, for which the carbenic center is interacting with the double bond. The stabilization energy was found to be 22.6 kcal/mol.

Table 2.3 shows the correlation between the stabilization energies, the bending of the carbenes, and the C_A-C_C distances. The more stabilized carbenes have a higher degree of bending. The bending, however, seems to be determined only by which moiety the divalent carbon is interacting with. For example, when the carbene is stabilized by a double bond, the bridge bending is about 37° in all cases. For Walsh stabilization by an *endo*-fused cyclopropane, the bridge is bent by about 32.7-34.2°. In contrast, by σ stabilization the bridge is tilted by only 15.0-16.4°. For the stabilization energies, the situation is more complex. For instance, both carbenes **7** and **18** are stabilized by a double bond, but the stabilization energies differ by 6.6 kcal/mol. However, the stabilization seems to concur with the distance between the divalent carbon and the stabilizing bond (C_A-C_C). The order of increasing stability is nearly the same as the order of decreasing bond length, *i.e.*, the closer the distance, the higher the SE.

Table 2.3: Comparison of Stabilization Energies and Bending for Carbenes 7 and 14-18

intermediate	relative bending carbene-alkane	distance (Å)	SE (kcal/mol)
7a	37.3°	1.893	15.9
7b	15.8°	2.202	2.2
14	32.7°	1.965	14.3
15	16.4°	2.182	2.3
16a	15.0°	2.354	4.3
16b	15.0°	2.378	-3.7
17a	37.3°	1.874	18.5
17b	34.2°	1.925	18.2
18	36.8°	1.860	22.6

The calculations show that foiled carbenes **7**, **14**, **17**, and **18** distinguish themselves quite clearly from norbornan-7-ylidene (**8**) and carbenes **15** and **16**. The stabilization energies obtained for carbene **7** and **14** were similar to those obtained by Freeman (15.56 and 14.06 kcal/mol, respectively).^{58a}

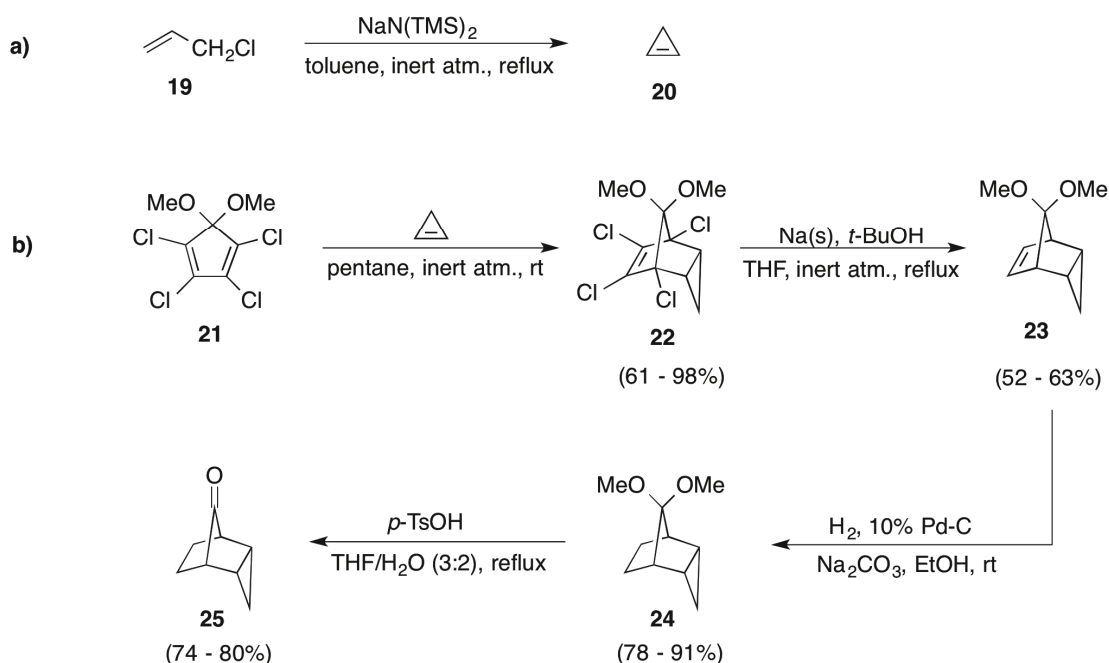
These results were encouraging for carrying on experimentally to prove the bending and stabilization of carbene **14**. Furthermore, it would also be of interest to examine an additional carbene for comparison purposes, in particular a less stable one, like **15** or **16**, or the higher stabilized carbenes **17** or **18**.

3. Preparation of Oxadiazoline Carbene Precursors

3.1 Synthesis of Oxadiazoline Carbene Precursor **29** for *endo*-Tricyclo[3.2.1.0^{2,4}]octan-8-ylidene (**14**)

A convenient precursor had to be found for *endo*-tricyclo[3.2.1.0^{2,4}]octan-8-ylidene (**14**). It should be obtainable in high yields, and the decomposition to carbene **14** should be fairly clean. First, *endo*-tricyclo[3.2.1.0^{2,4}]octan-8-one (**25**) needed to be synthesized in four steps from 5,5-dimethoxy-1,2,3,4-tetrachlorocyclopentadiene (**21**) in a similar way to published procedures (Scheme 3.1).⁶⁶

Scheme 3.1: Synthesis of *endo*-Tricyclo[3.2.1.0^{2,4}]octan-8-one (**25**)



Cyclopropene (**20**) was generated *in situ* by treating a solution of allyl chloride (**19**) in toluene at reflux with sodium bis(trimethylsilyl)amide (Scheme 3.1a). The allyl chloride undergoes dehydrohalogenation to a vinyl carbene, which by intramolecular rearrangement generates cyclopropene. It had been shown that using bis(trimethylsilyl)amide instead of sodium amide increases the yield of **20** from about

10 to 40%.^{66b-d} The resulting cyclopropene gas was carried by a stream of argon into a solution of the substituted cyclopentadiene **21** in pentane. Subsequent Diels-Alder cycloaddition led to the tricyclic compound **22**, with exclusive formation of the *endo* configuration. At first, the reaction was carried out keeping the pentane solution at $-80\text{ }^{\circ}\text{C}$, and allowing the mixture to reach room temperature only after completed addition of cyclopropene (Table 3.1, entry 1). However, yields could be improved when the solution was kept at room temperature during the addition (Table 3.1, entry 2). A larger excess of allyl chloride (**19**) increased the yield further (Table 3.1, entry 3). The room temperature needed for the reaction is in striking contrast to the elevated temperatures necessary for addition of ethylene to cyclopentadiene (ca. $190\text{ }^{\circ}\text{C}$).⁶⁷ Obviously, the double bond of highly strained cyclopropene undergoes the Diels-Alder reaction much faster. Subsequent dechlorination, hydrogenation of the double bond, and deketalization of **22** gave the desired ketone **25**.

Table 3.1: Different Conditions Applied for Synthesis of Compound 22

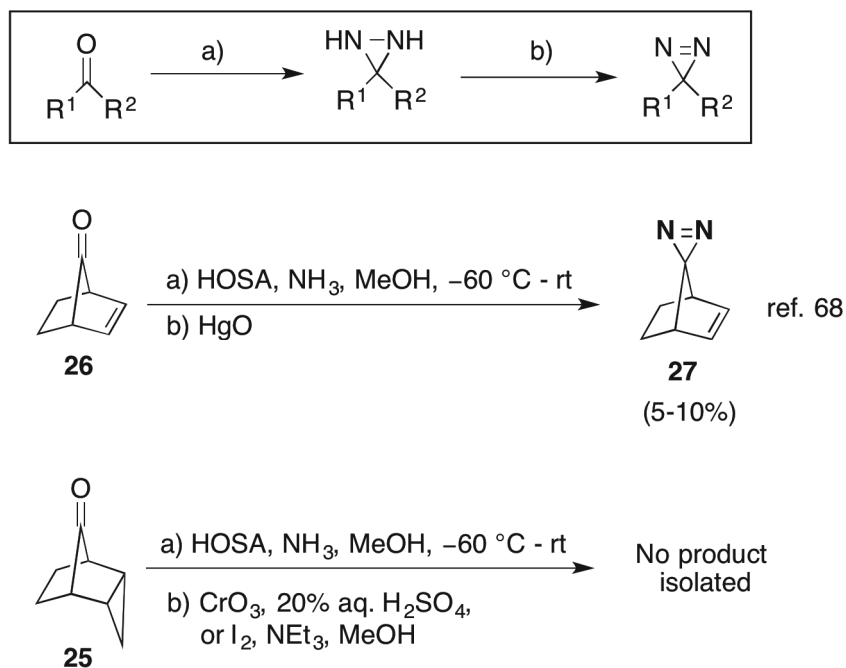
entry	19 ^a (mol)	NaN(TMS) ₂ (mol)	21 (mol)	temp. ^b ($^{\circ}\text{C}$)	yield of 22 ^c (%)
1	0.144	0.160	0.057	-80 - rt	22
2	0.147	0.164	0.057	rt	61
3	0.295	0.330	0.074	rt	98

^aAllyl chloride was added in excess of 2.5-4.0 mol equivalents compared to **21**. ^bTemperature of the solution of **21** in pentane. ^cYield based on percent of **21** converted to **22**.

Initially, an attempt was made to prepare the corresponding diazirine of *endo*-tricyclo[3.2.1.0^{2,4}]octan-8-ylidene (**14**). Diazirines are known to be a rather clean source for carbenes and therefore useful for mechanistic studies.^{14,34} Only a small amount decomposes through a diazo compound, whereas for the majority, the carbene is generated directly. For instance, the product distribution obtained by irradiation of spiro[bicyclo[2.2.1]heptene-7,3'-diazirine] (**27**), shown in Scheme 3.2, in methanol suggest participation of only 4-6% of the corresponding diazo compound.⁶⁸ However, obtaining satisfying yields of diazirines from strained compounds has been proven rather difficult. For instance, **27** was obtained in a yield of only 5-10% from ketone **26** (Scheme 3.2).⁶⁸ Conversion of ketone **25** to the corresponding diazirine turned out not

to be so straightforward either. Under the conditions applied (Scheme 3.2), the ketone remained mainly unreacted. The oxidation step was carried out both with chromium trioxide and iodine, respectively, since the latter had worked well for other strained ketones.⁶⁹ In neither case, however, could the desired diazirine be isolated.

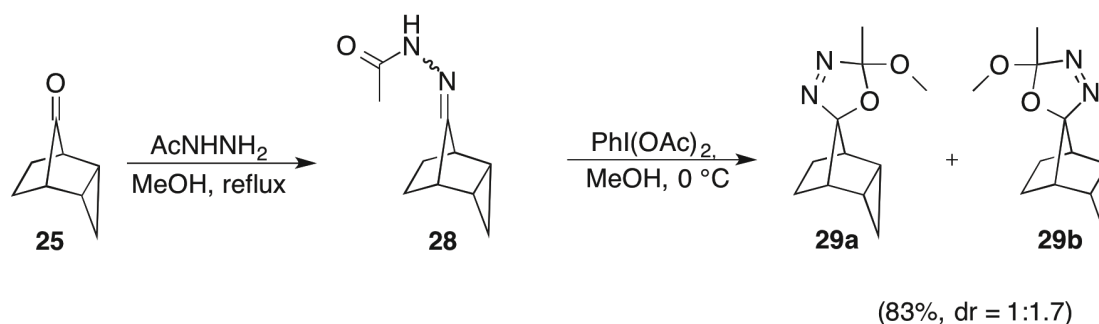
Scheme 3.2: Attempt of Synthesizing the Diazirine Precursor from Ketone 25



These experiments were not encouraging, as the diazirine would be needed in larger quantities. Therefore, no further efforts were made of synthesizing such a precursor. On the other hand, oxadiazolines had been proven both easy to synthesize and useful precursors of related carbenes, *e.g.*, for *endo*-tricyclo[6.2.1.0^{2,7}]undec-9-en-11-ylidene (**13**).^{54-56,70} Thus, they were the next choice. These precursors decompose both by photolysis and thermolysis. The corresponding carbenes, however, are not produced directly from oxadiazolines, but through either carbonyl ylides or diazo intermediates (*vide supra*: Chapter 1.2.2 and 1.2.3). Hence, the generation is less clean than the one from diazirine precursors.³⁶⁻⁴² The necessary oxadiazoline for generating carbene **14**, *i.e.*, (1'*R*,2'*R*,4'*S*,5'*S*)-5-methoxy-5-methylspiro[2,5-dihydro-1,3,4-oxadiazole-2,8'-tricyclo[3.2.1.0^{2,4}]octane] (**29**), could be easily obtained in two steps from ketone **25** through hydrazide **28** (Scheme 3.3).⁷¹ A mixture of two diastereomers was formed in an overall yield of 83% (dr = 1:1.7).

Scheme 3.3: Synthesis of Oxadiazolines 29a and 29b Used to Generate Carbene

14



Isomers **29a** and **29b** were separated by column chromatography, and the absolute configuration of each pseudoasymmetric spirocyclic C atom (*i.e.*, *r/syn* vs *s/anti*) was determined by X-ray crystallography (Figure 3.1).

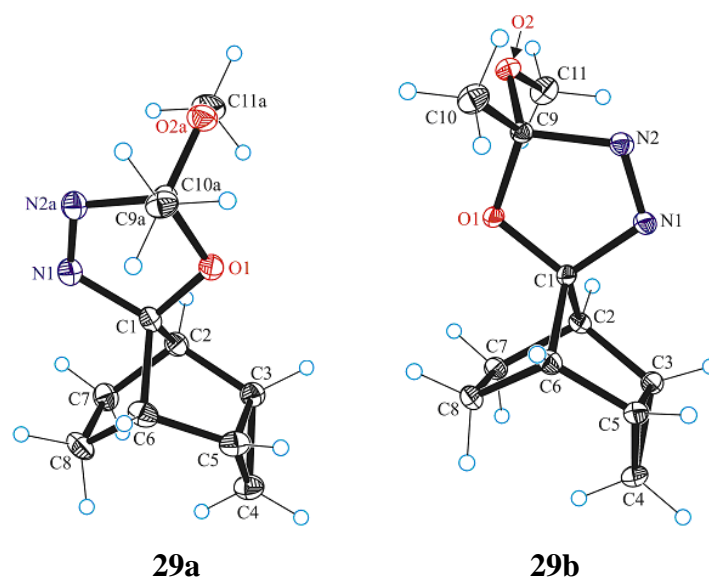


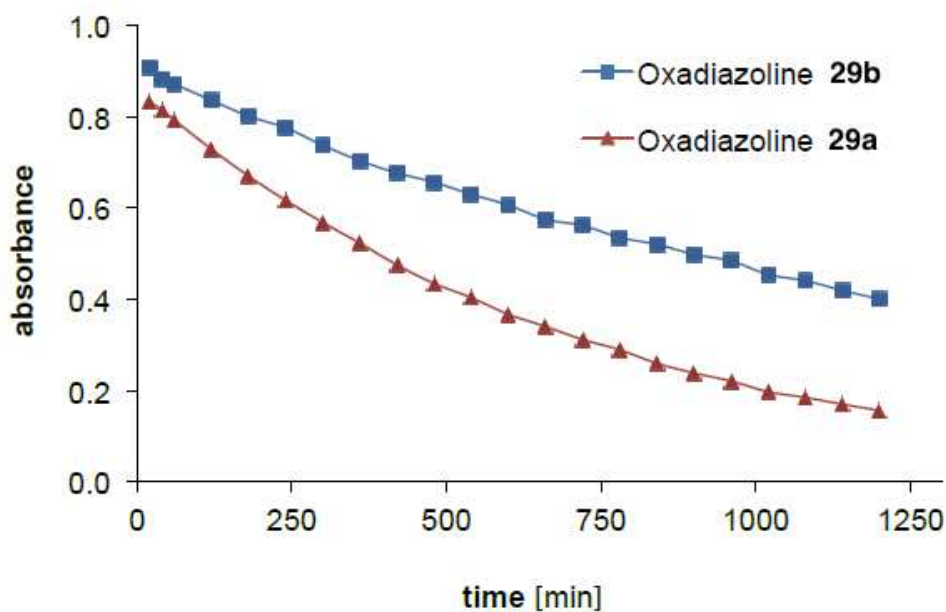
Figure 3.1: Single-crystal X-ray diffraction was used to elucidate the structures *rel*-(1'*R*,2*r*,2'*R*,4'*S*,5*R*,5'*S*)-5-methoxy-5-methylspiro[2,5-dihydro-1,3,4-oxadiazole-2,8'-tricyclo[3.2.1.0^{2,4}]octane] (**29a**) and *rel*-(1'*R*,2*s*,2'*R*,4'*S*,5*R*,5'*S*)-5-methoxy-5-methylspiro[2,5-dihydro-1,3,4-oxadiazole-2,8'-tricyclo[3.2.1.0^{2,4}]octane] (**29b**).

3.2 Kinetic Measurements of Thermolytic Decomposition of Oxadiazoline Precursors **29a** and **29b**

One method to compare the diastereomers of oxadiazoline **29**, to see if they differ significantly when decomposing to carbene **14**, was to study their kinetics. By thermolysis, oxadiazolines normally decompose by initial expulsion of molecular nitrogen to give an ylide intermediate.³⁷⁻³⁸ The rate of thermolysis of **29a** and **29b** was measured at 116 °C and monitored by UV spectroscopy. A solution of the oxadiazoline in decane (1 mg/mL) was prepared for each diastereomer. The Beer-Lambert law states that the UV absorption is dependent on the concentration of the solute ($A = \epsilon cl$, where ϵ = molar absorptivity, c = concentration of solute, and l = length of sample cell).⁷² Thus, the kinetics could be measured by observing the decay of the absorption maxima of the oxadiazoline groups of **29a** and **29b** at $\lambda_{\max} = 338$ and 333 nm, respectively (Figure 3.2). The decay was found to follow a first-order rate law in both cases, which is expected for unimolecular reactions, *i.e.*, a reaction where the rate depends only on the concentration of one molecule. The half-lives ($\tau_{1/2}$) of the oxadiazolines were 8.3 and 16.5 h, respectively. Thus, by applying the rate law for first-order reactions,

$$k = \ln 2 / \tau_{1/2},$$

the rate constants were found to be $k = 2.3 \times 10^{-5} \text{ s}^{-1}$ and $k = 1.2 \times 10^{-5} \text{ s}^{-1}$ in each case. These values are typical for the decomposition of oxadiazolines.^{38a,42f}



Oxadiazoline **29a**:

$$\lambda_{\max} = 338 \text{ nm}$$

$$A = 0.8697 \cdot \exp(-0.0014 t)$$

$$k(116 \text{ }^\circ\text{C})_{\text{decane}} = 2.33 \times 10^{-5} \text{ s}^{-1}$$

Oxadiazoline **29b**:

$$\lambda_{\max} = 333 \text{ nm}$$

$$A = 0.9074 \cdot \exp(-0.0007 t)$$

$$k(116 \text{ }^\circ\text{C})_{\text{decane}} = 1.17 \times 10^{-5} \text{ s}^{-1}$$

Figure 3.2: Decay of oxadiazolines **29a** and **29b** at 116 °C monitored using their UV absorption maxima and found to be first-order.

Diastereomer **29a** decomposes twice as fast as **29b**, because its configuration ostensibly allows the cyclopropane ring to anchimerically assist with the expulsion of molecular nitrogen. Such an interpretation is supported by results from solvolysis experiments with tricyclo[3.2.1.0^{2,4}]octan-8-ol derivatives, which have shown that the relative orientation of the cyclopropane subunit and the leaving group at C₈ is decisive when considering the rates of solvolysis (Figure 3.3).^{57e,66f,g} The order of observed reactivity is *endo,anti* >> *exo,syn* > *endo,syn* > *exo,anti* with ratios of 10¹²:10⁴:10:1.*

* Here, the position of the cyclopropane ring is expressed as *endo* or *exo*, and the substituent at the bridgehead is *anti*- or *syn*-positioned relative to the cyclopropane ring.

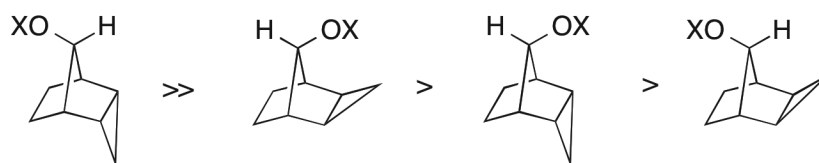
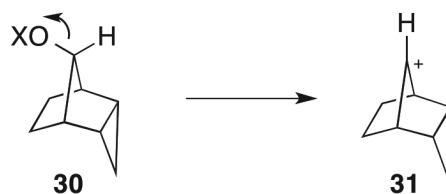


Figure 3.3: Relative rate of solvolysis for tricyclo[3.2.1.0^{2,4}]octan-8-ol derivatives.

The immensely increased rate for the *endo,anti* analogue **30** is resulting from stabilization of the developing positive charge at C₈ by backside participation of the *endo*-fused cyclopropane ring (Scheme 3.4).

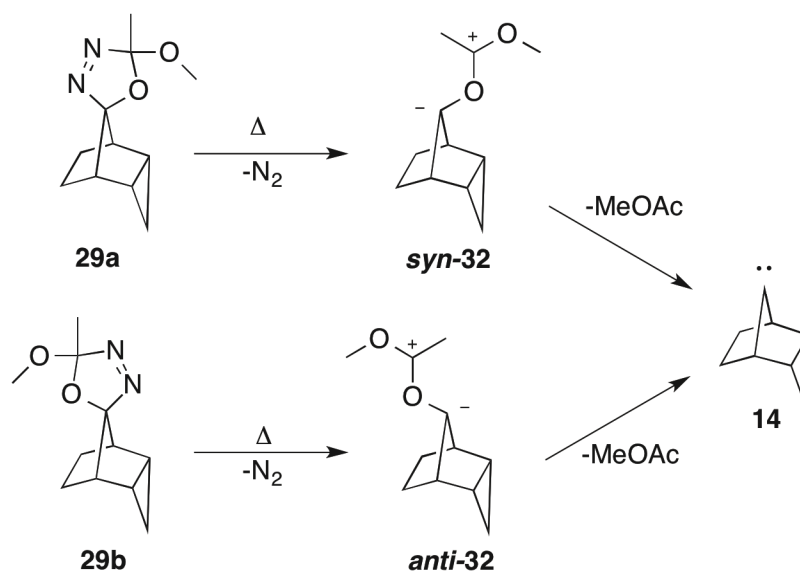
Scheme 3.4: Backside Participation by Cyclopropyl Group During Solvolysis



Therefore, due to the *endo,anti* relationship between the nitrogen atoms and three-membered ring of **29a**, a similar anchimeric assistance might take place for expulsion of molecular nitrogen. Oxadiazoline **29b**, on the other hand, comprises an *endo,syn* relationship and decomposes slower. In contrast to the solvolysis reactions for tricyclo[3.2.1.0^{2,4}]octan-8-ol derivatives, a negative charge is developing at C₈, and consequently the nature of the anchimeric interaction must be different. For instance, the filled Walsh orbital of the cyclopropane moiety of **29a** might interact with an antibonding MO, resulting in the loss of N₂.

An alternative explanation is that the ylide intermediate *anti*-**32** generated from **29b** is less stable than carbonyl ylide intermediate *syn*-**32** generated from **29a** (Scheme 3.5). The electron lone pair of the carbanionic center of *anti*-**32** is oriented in such a way that it may experience destabilizing interaction with the Walsh orbitals. Consequently, ylide *anti*-**32** should be higher in energy than *syn*-**32** and therefore slower to generate.

Scheme 3.5: Possible Destabilization of Carbonyl Ylide Intermediate *anti*-32 by Cyclopropyl Participation



In any case, the 2-fold rate increase is modest compared to the 10^{11} increase for the solvolysis experiments, thus the steric or electronic effects causing **29a** to decompose faster than **29b** are less potent.

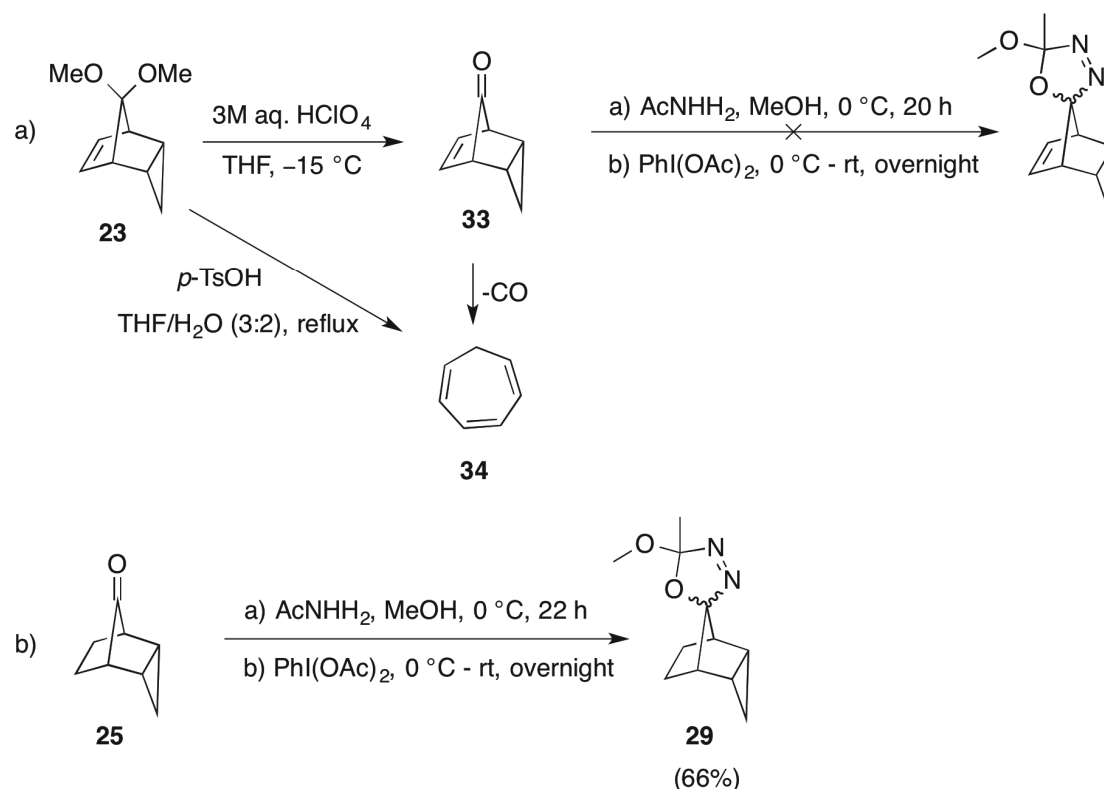
3.3 Synthesis of Oxadiazoline Carbene Precursor **39** for Bicyclo[3.2.1]octan-8-ylidene (**16**)

It was of interest to synthesize an oxadiazoline precursor for one of the other carbenes that had been studied by calculations as well, in order to compare its stereoselectivity in intermolecular reactions with that of carbene **14**. *endo*-Tricyclo[3.2.1.0^{2,4}]oct-6-en-8-ylidene (**17**) was an intriguing candidate for such a study. Since **17** comprises both a double bond *and* an *endo*-fused cyclopropyl group, the DFT computations carried out revealed two energy minima; one where the bridge is bending towards the double bond, and one where it is tilted toward the three-membered ring. The calculations predicted the carbene to be slightly more stable when stabilized by the double bond (*vide supra*). Thus, by studying the intermolecular reactions of **17**, it should be possible to find out if one interaction would control the stereoselectivity more than the other.

endo-Tricyclo[3.2.1.0^{2,4}]oct-6-en-8-one (**33**), needed for synthesizing the appropriate oxadiazoline precursor of carbene **17**, could be obtained by hydrolysis of ketal **23** (Scheme 3.6a). An initial attempt to hydrolyze **23** by refluxing it with *p*-toluenesulfonic acid resulted in the formation of cyclohepta-1,3,5-triene (**34**). This could have been predicted, as ketone **33** is known to readily undergo decarbonylation.^{66e,66h,73} At 36 °C ketone **33** has a half-life of approximately 130 min.^{73b} In cyclohexane solution at 30 °C, the half-life is reduced to 10 min.^{66h} However, **33** could be isolated when the temperature was kept at 0 °C.^{66h} The first step of any oxadiazoline synthesis, *i.e.*, condensation of a ketone with acetyl hydrazide, is usually carried out under reflux, which would not be appropriate in this case, as the conditions would be too harsh for ketone **33**. Thus, some preliminary experiments were carried out with ketone **25** to see if milder conditions could be applied. When the conditions of the first step were kept at 0 °C for 3 hours, oxadiazoline **29** could be obtained in a yield of 15%. Increasing the reaction time to 22 hours raised the yield to 66% (dr = 1:1.7) (Scheme 3.6b). Carrying out the reaction at lower temperatures did not change the ratio of the diastereomers **29a** and **29b**. By applying the same conditions for ketone **33**, however, not even a trace of the

oxadiazoline product could be detected (Scheme 3.6). Instead, the ketone remained unreacted.

Scheme 3.6: Attempt of Preparing the Oxadiazoline Precursor for Carbene 17



The tosylhydrazone precursor of carbene **17** had previously been prepared,^{59c} but using a different precursor was not desirable as the comparison to carbene **14** should be as close as possible. Instead, bicyclo[3.2.1]octan-8-ylidene (**16**) was chosen for the studies. This is also an interesting carbene to use for comparison, as it comprises a similar structure to **14**, but lacks the *endo*-fused cyclopropyl group with its stabilizing Walsh orbitals (Figure 3.4). Thus, by examining carbenes **14** and **16**, one can get a better idea of the importance of the interaction of the Walsh orbitals with the empty p orbital of the carbenic center in regard to reactivity and stereoselectivity.

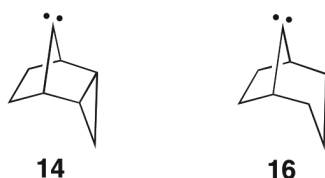
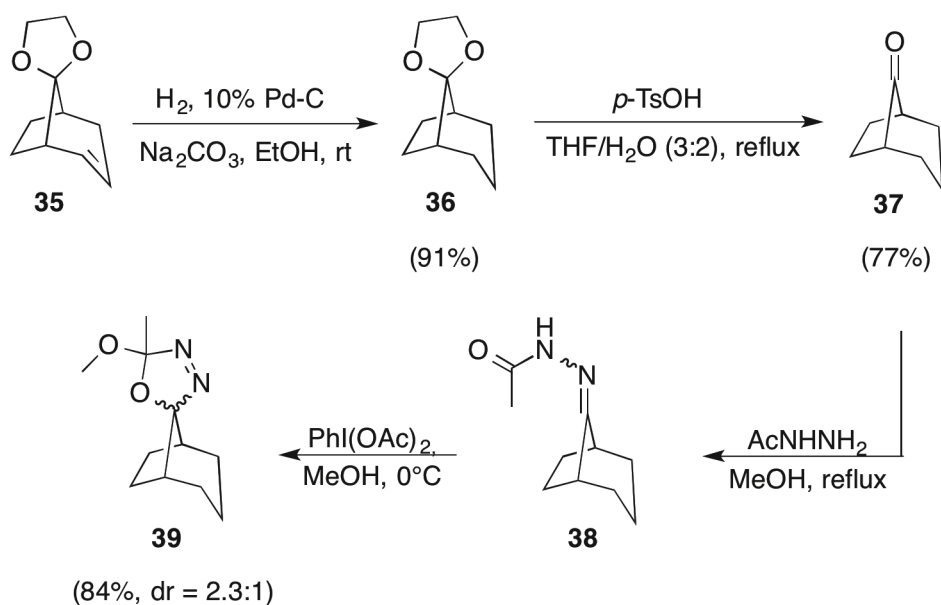


Figure 3.4: Carbene **14** and **16** used for experimental research.

Initially, the required ketone bicyclo[3.2.1]octane-8-one (**37**) was synthesized from spiro[bicyclo[3.2.1]oct-2-ene-8,2'-[1.3]dioxolane] (**35**) in two steps (Scheme 3.7). Subsequently, the novel oxadiazoline precursor of carbene **16**, *i.e.*, *rac*-(1*R*,5*S*)-5'-methoxy-5'-methylspiro[bicyclo[3.2.1]octane-8,2'-2,5-dihydro-1,3,4-oxadiazole] (**39**), could be easily prepared from ketone **37** through hydrazone **38** (Scheme 3.7).⁷¹ Oxadiazoline **39** was obtained as a diastereomeric mixture in a combined yield of 84% (dr = 2.3:1).

Scheme 3.7: Synthesis of Oxadiazoline **39** Used to Generate Carbene **16**



Thus, one could proceed to study the intermolecular reactions of carbene **14** and **16**.

4. Reactions of *endo*-Tricyclo[3.2.1.0^{2,4}]octan-8-ylidene (**14**)

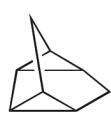
4.1 Reaction in Cyclohexane and Cyclohexene: Rearrangements of Carbene **14**

Carbene **14** could be generated from oxadiazoline **29**, both by thermolysis (165 °C) and photolysis ($\lambda > 200$ nm, water bath, rt). All experiments were conducted by dissolving either precursor **29a** or **29b** in the neat substrate under investigation. For photolysis, a medium pressure mercury lamp doped with iron(II) iodide with maximum wavelength of $\lambda = 370$ nm was utilized. It was placed in a water-cooling jacket made out of quartz, thus filtering out wavelengths below 200 nm. For thermolysis, a pressure tube was applied.

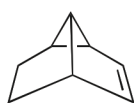
First, the chemistry of **14** in cyclohexane and cyclohexene was studied under conditions given in Table 4.1. The resulting solutions were subjected to GC-MS analysis, and yields were determined by using camphor as internal standard. The main products formed are shown in Figure 4.1. In some cases small peaks could be detected in the chromatograms that might derive from compounds formed by intermolecular reactions of carbene **14** with cyclohexane (M^+ ; $m/z = 190$) or cyclohexene (M^+ ; $m/z = 188$) (Table 4.1). With cyclohexane the carbene could insert into one of the C-H bonds, whereas for cyclohexene it may add to the double bond as well. However, the estimated yields were low (ca. 2-8 %). This lack of reactivity may indicate a stabilization of carbene **14**, but it could also simply mean that other competing reactions are faster. Moreover, the slow addition to the electron-rich double bond of cyclohexene suggests that **14** acts as a nucleophilic carbene as gauged by the philicity scale of carbenes in carbene-alkene addition reactions.^{17,28}

Table 4.1: GC-MS Analysis of Product Distribution Obtained by Thermolysis and Photolysis of Oxadiazolines 29a and 29b in Cyclohexane and Cyclohexene

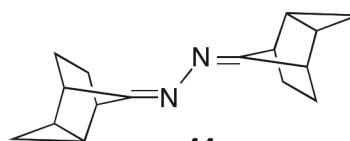
precursor	substrate	concn (mg/mL)	cond	yields of intermol. products (%)	yield of rearrang. product 41 (%)	yield of rearrang. product 42 (%)	yield of azine 44 (%)
29a	cyclohexane	10	Δ	3	55	3	—
29b		10	Δ	4	17	1	31
29a		6	$h\nu$	—	23	2	31
29a		10	$h\nu$	—	27	2	47
29b		5	$h\nu$	—	20	1	38
29b		11	$h\nu$	—	44	3	31
29a	cyclohexene	10	Δ	5	71	10	—
29b		10	Δ	4	71	10	—
29a		6	$h\nu$	8	20	2	35
29a		10	$h\nu$	6	15	1	40
29b		5	$h\nu$	3	25	2	17
29b		12	$h\nu$	2	12	1	25



41



42



44

Figure 4.1: Main products formed by thermolysis and photolysis of oxadiazolines **29a** and **29b** in cyclohexane and cyclohexene.

One of the GC-MS chromatograms is shown in Figure 4.2 for illustration. It depicts the product mixture obtained by thermolysis of **29b** in cyclohexane.

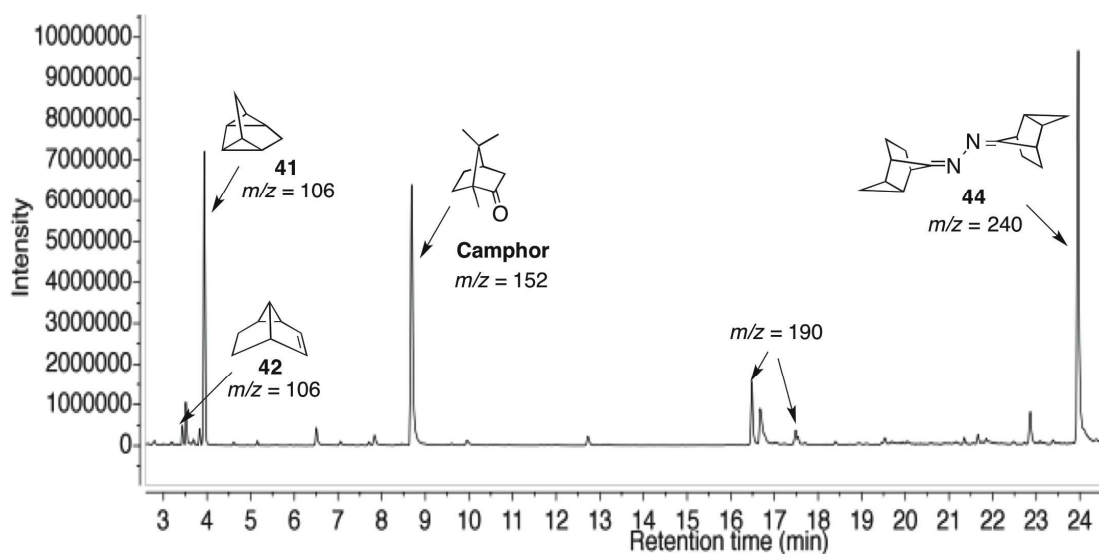


Figure 4.2: GC-MS chromatogram of product mixture obtained by thermolysis of **29b** in cyclohexane, using camphor as internal standard.

In all experiments there was significant formation of a product presumably resulting from rearrangement of **14** (M^+ ; $m/z = 106$) (Table 4.1). In order to identify this compound, a scaled-up thermolysis of **29b** was carried out in pentane, and after careful concentration, the resulting product mixture was subjected to diffusion-edited NMR.⁷⁴ Two spectra with attenuated signals were obtained after conducting two pulsed-field-gradient spin-echo experiments: one with a low gradient amplitude of 3% and one with a much higher one of 73%. A pure trace of tetracyclo[3.3.0.0.^{2,8}0^{4,6}]octane (**41**) was computed by subtracting these spectra from each other after the vertical scale was adjusted to the peaks of the undesired background (Figure 4.3). Both the ^1H NMR and ^{13}C NMR signals were in accordance with the values for compound **41** found in the literature (Figure A.21 and A.22, Appendix).⁷⁵

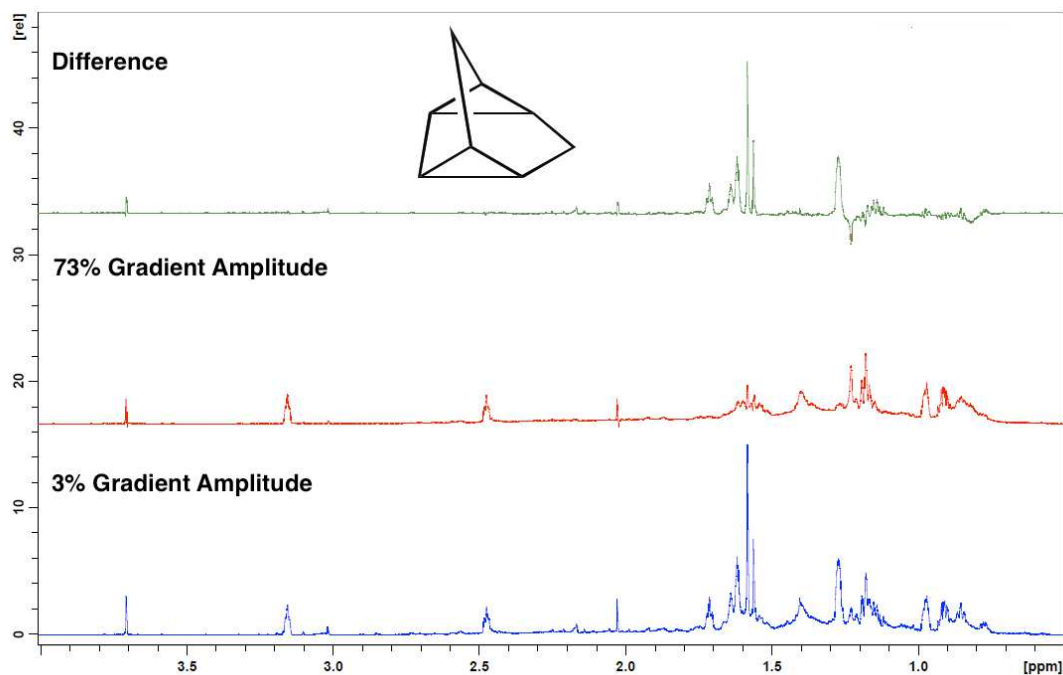


Figure 4.3: Diffusion-edited NMR was carried out for tetracyclo[3.3.0.0^{2,8}.0^{4,6}]octane (**41**), where one spectrum was recorded with 3% gradient amplitude and one with 73%.

There was also minor formation of another product with the same mass as **41**, which is thought to be tricyclo[3.3.0.0^{4,6}]oct-2-ene (dihydrosemibullvalene) (**42**). This is based on the characteristic ¹H NMR pattern of the alkenyl hydrogens, which could be observed when **29b** was thermolyzed in cyclohexane-*d*₁₂ (Figure 4.4).^{42f,76} The ¹H spectrum also shows formation of **41**, the main rearrangement product, methyl acetate deriving from oxadiazoline decomposition, and azine **44**. The rearrangement products **41** and **42** were obtained in ratios of 7:1-20:1, depending on the conditions applied (Table 4.1).

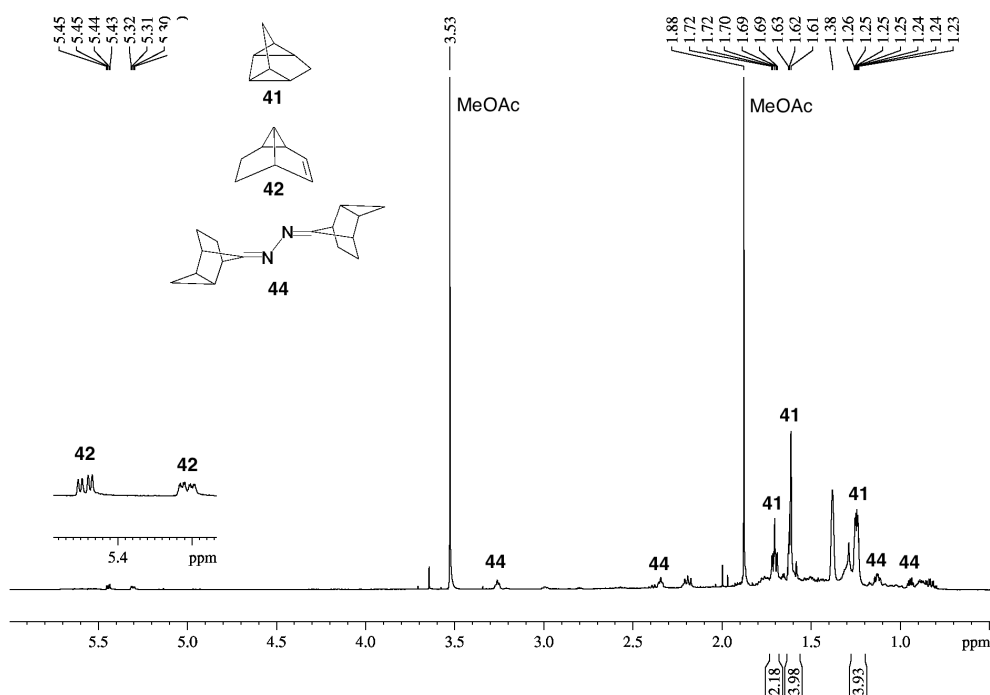
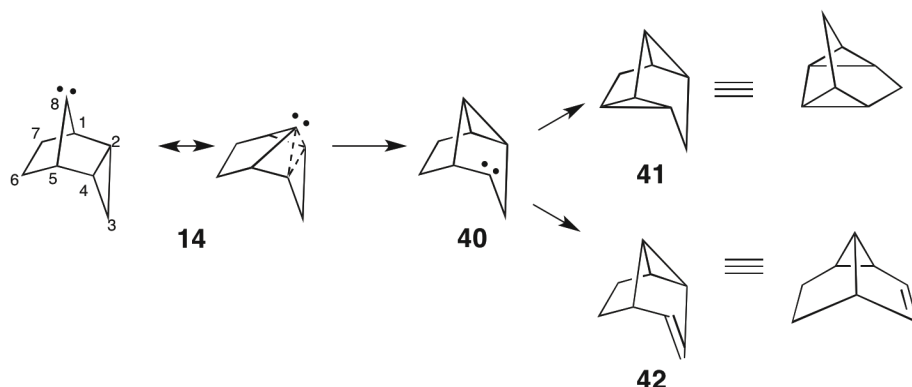


Figure 4.4: ¹H NMR spectrum of product mixture obtained after thermolysis of **29b** in cyclohexane-*d*₁₂ (400.13 MHz).

Compounds **41** and **42** are the same rearrangement products obtained by Freeman *et al.* by thermolysis of the tosylhydrazone precursor of **14** in diglyme, in the presence of sodium methoxide (*vide supra*: Chapter 1.3.3).⁶⁰ A mechanism for the formation of **41** and **42** was proposed to involve conversion of carbene **14** into carbene **40**, as shown in Scheme 4.1. This was deduced by studying the products obtained when labeling the tosylhydrazone precursor.^{60b} The findings supported an *intermolecular* carbene-to-carbene rearrangement of **14** → **40**, with the solvent acting as a proton-transfer agent.

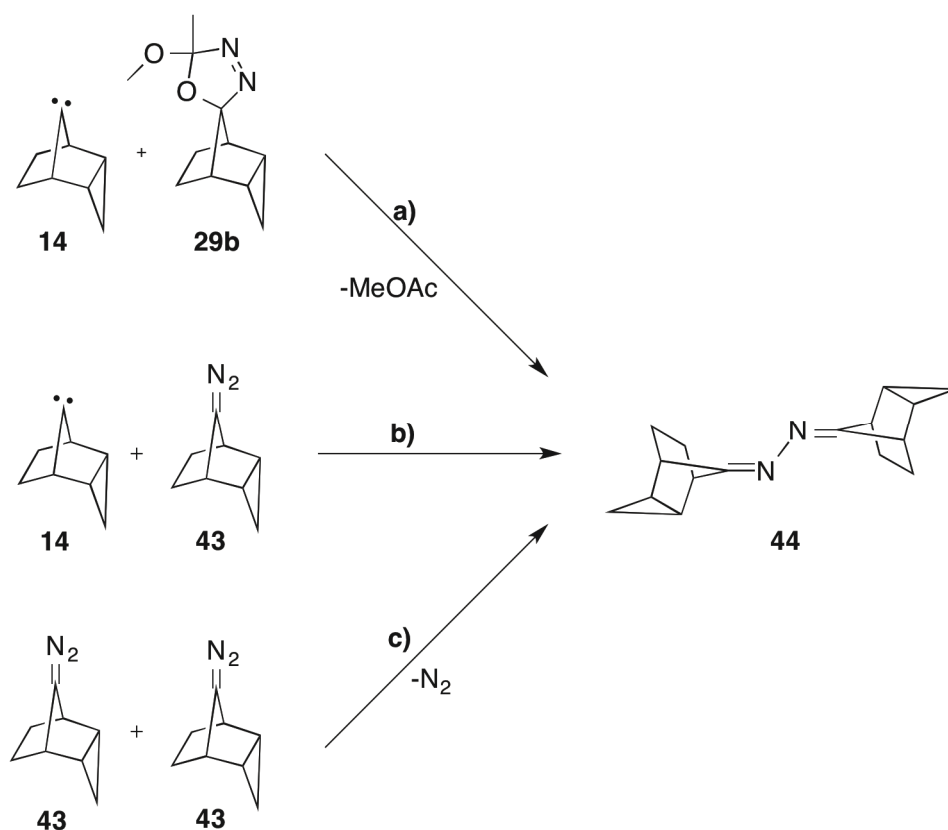
Scheme 4.1: Intermolecular Carbene-to-Carbene Rearrangement of **14**



In an initial attempt to identify rearrangement products **41** and **42**, pyrolysis of neat oxadiazoline **29b** was carried out at 200 °C and 0.6 torr. The volatile products were collected in a cooling trap. The chromatogram obtained by GC-MS measurements showed the formation of two rearrangement products (M^+ ; $m/z = 106$) with different retention times as those obtained by thermolysis of **29** in cyclohexane and cyclohexene. Furthermore, the ^1H NMR spectrum displayed a number of signals in the double bond area. This could mean that the products were similar to those obtained by Murahashi *et al.* from pyrolysis of the tosylhydrazone precursor of **14** (*vide supra*: Chapter 1.3.3).^{59a,b} Thus, rearrangements of **14** proceed differently with and without a solvent. The identification of these additional rearrangement products was not further pursued, as it was the chemistry of **14** in solution that was of interest.

In addition to rearrangement products **41** and **42**, in most experiments formation of *endo*-tricyclo[3.2.1.0^{2,4}]octan-8-one azine (**44**) was observed (Table 4.1). The compound could be isolated in a yield of 11% by scaling up the thermolysis of **29b** in pentane. At least three different possible mechanisms for the formation of azine **44** can be discussed (Scheme 4.2).^{42c,77} Carbene **14** may attack the remote N atom of its precursor **29**, where subsequent loss of methyl acetate will afford **44** (Scheme 4.2a). Alternatively, the carbene could attack diazo intermediate **43**, which is generated by loss of methyl acetate from oxadiazoline **29** (Scheme 4.2b). Finally, diazo compound **43** may undergo a cycloaddition with itself followed by loss of N_2 (Scheme 4.2c).

Scheme 4.2: Mechanisms for Formation of Azine 44



These processes may occur simultaneously, of which the dominant one depends on the concentration of the solution. In dilute solution, the carbene attack of the diazo alkane usually dominates (route b), whereas at higher concentrations, the cycloaddition might be the operating (route c).^{77b} One argument favoring route c, is that carbene **14** might prefer to undergo fast rearrangements rather than attacking the diazo compound or the oxadiazoline precursor. Thus, the mechanism is likely to involve diazo intermediate **43**. Therefore, to prove the formation of **43**, oxadiazolines **29a** and **29b** were submitted to matrix isolation studies. The IR spectra acquired for **29a** are given in Figure 4.5.

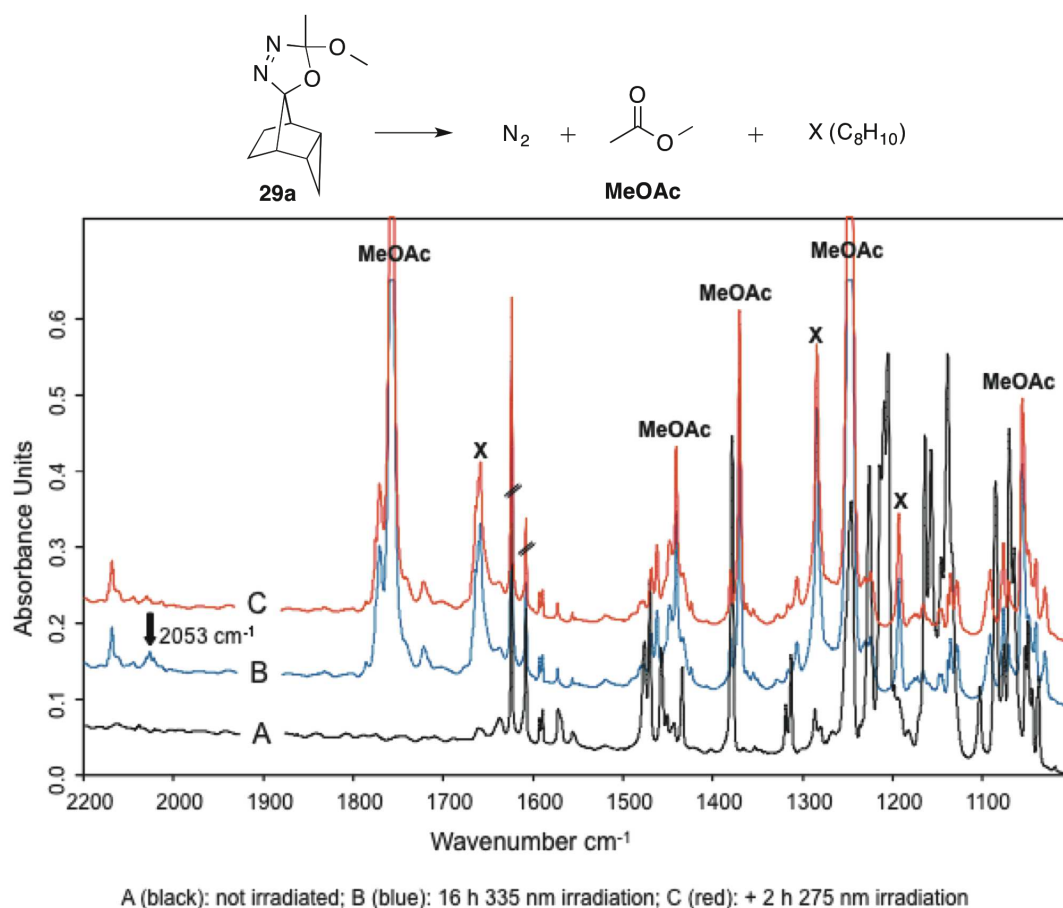


Figure 4.5: IR spectra acquired under matrix isolation conditions of oxadiazoline **29a** (Ar, 10 K).

By irradiation at 335 nm for 16 hours, oxadiazoline **29a** slowly decomposes and a weak signal at 2053 cm^{-1} is appearing (Figure 4.5, spectrum B). This band is typical for the N–N-stretching vibration of diazo compounds. Thus, the experiments provide strong evidence that **43** is formed during photolysis. Subsequent irradiation for 2 hours at the shorter wavelength of 275 nm leads to a bleaching of this signal (Figure 4.5, spectrum C). Also by irradiation of oxadiazoline **29b** at 335 nm, the same IR band (2053 cm^{-1}) is formed.

Furthermore, the IR spectra recorded demonstrate the formation of methyl acetate, which is cleaved off during decomposition of the oxadiazolines. No spectral indications were observed for carbene **14**, however. This is not surprising since its electronic absorption most likely falls into the region of the excitation wavelength range of the photolysis, and therefore the carbene is expected to undergo a light-

induced rearrangement.^{42f} Indeed, a compound of the general formula C₈H₁₀ is observed, which should be an olefin according to the characteristic band at 1658 cm⁻¹, and probably is formed by an intramolecular rearrangement of **14**. The compound is marked with an X in Figure 4.5. The band found between 2141 and 2135 cm⁻¹, which is quite broad, almost certainly derives from small amounts of carbon monoxide developed during irradiation (pure CO and argon give rise to a band at 2138 cm⁻¹). Moreover, the band in question stays when irradiation is continued at 275 nm.

The decomposition of **29a** and **29b** in cyclohexane and cyclohexene, shows that azine **44** in general is formed more frequently during photolysis than thermolysis (Table 4.1). A lack of azine production might suggest that the oxadiazoline decomposes by a different route, thus avoiding formation of diazo compound **43**. Oxadiazolines **29a** and **29b** may also decompose by initial loss of N₂, yielding carbonyl ylides *syn*-**32** and *anti*-**32**, respectively, which further collapses to carbene **14**.

It was suspected that formation of **44** is dependent on the concentration of the oxadiazoline in the reaction mixture, which would make a bimolecular reaction of their decomposition intermediates more likely (Scheme 4.2). Therefore, **29a** and **29b** were thermolyzed in pentane at different concentrations (Table 4.2). At 4 mg/mL no formation of azine **44** was detected, whereas at 15 mg/mL and higher, **44** always occurred. By photolysis, on the other hand, the azine was found also when the reaction is carried out at lower concentrations of 5-6 mg/mL (Table 4.1). One explanation for this might be that by photolysis, the oxadiazoline decomposes mainly through diazo compound **43**. As a consequence, **43** is always abundant, making the formation of **44** more likely. In contrast, by thermolysis, the oxadiazoline might decompose through *both* **43** and ylide intermediate **32**, and as a result higher concentrations of the oxadiazoline are needed to obtain the same amount of **43** as by photolysis.

Table 4.2: Formation of Azine 44 Dependence on Concentration of Oxadiazolines 29a and 29b

precursor	substrate	concn (mg/mL)	cond	formation of 44
29a	pentane	4	Δ	no
29b		4	Δ	no
29a		15	Δ	yes
29b		16	Δ	yes
29b		20	Δ	yes
29b		53	Δ	yes
29b		85	Δ	yes

The ^{13}C NMR spectrum of **44** displays two sets of signals in a 1:1 ratio, for which all signals are consistently paired. After evaporation of the solvent, the sample was redissolved and allowed to stand for 3 hours before subjected to another analysis. The spectrum now revealed one major and one minor set of signals. However, the original 1:1 ratio was reestablished over time (24 h) after equilibration of the two compounds (Figure 4.6).

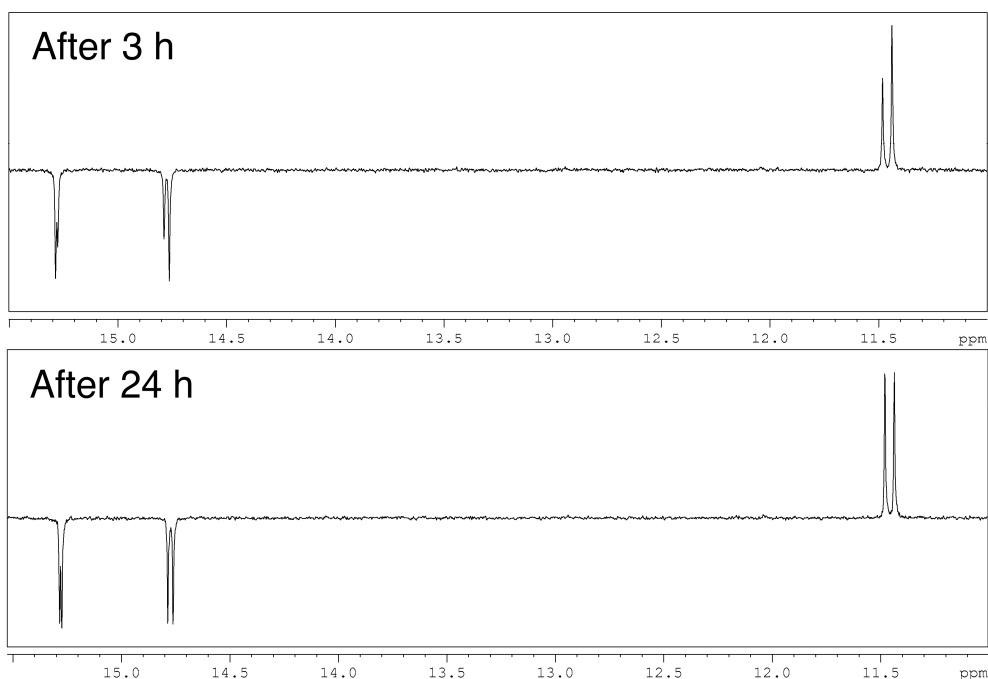


Figure 4.6: A detail of the ^{13}C NMR spectrum demonstrating the equilibration of **44**.

The changing intensities of the two signal sets should be a result of an isomerization process in solution. Three different conformational isomers are possible, *i.e.*, *s-trans*, *s-cis*, and *s-gauche* (Figure 4.7). The *s-cis* form is destabilized due to interaction of the vicinal electron lone pairs and steric repulsion between the substituents, whereas the *s-gauche* form is usually destabilized by alkyl substitution.⁷⁸ Thus, the *s-trans* form usually is the only conformer detected by spectroscopic methods, and the two signal sets should be a result of a different kind of isomerization.

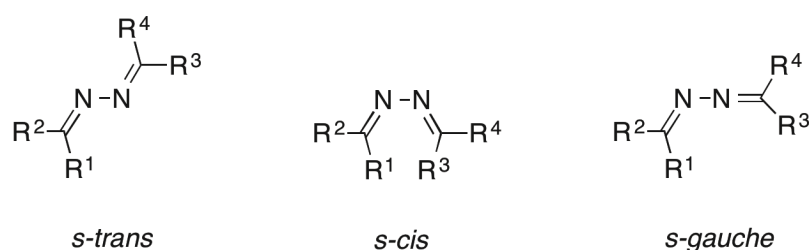


Figure 4.7: Three conformational isomers of azines are possible.

Three different configurational isomers are possible, due to *cis* and *trans* isomerism of the C-N double bond (Figure 4.8). The *Z,E* and *E,Z* isomers represent the same meso compound. To be able to define the *Z* and *E* stereochemistry in **44**, the *R* stereochemistry of bridgehead carbon C₁ is given priority over *S* stereochemistry of C₅.

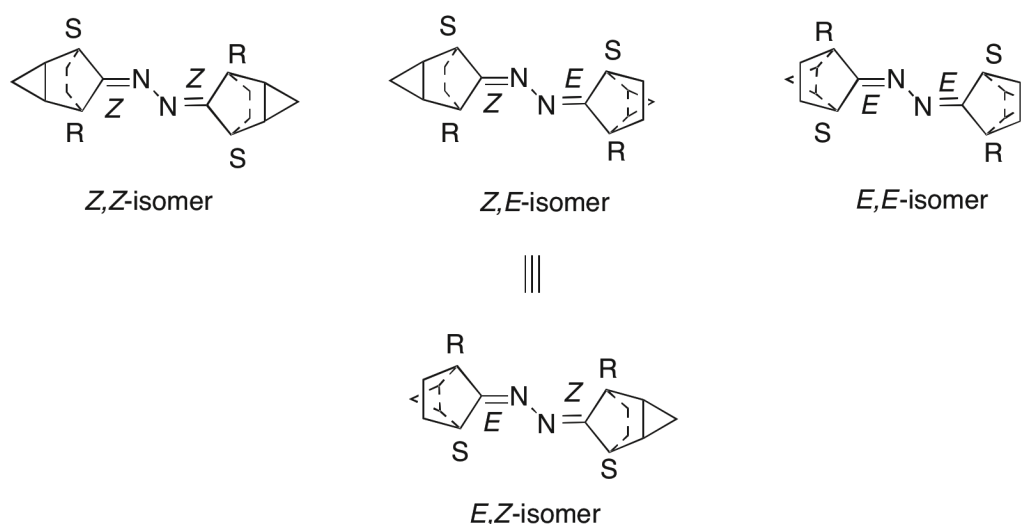


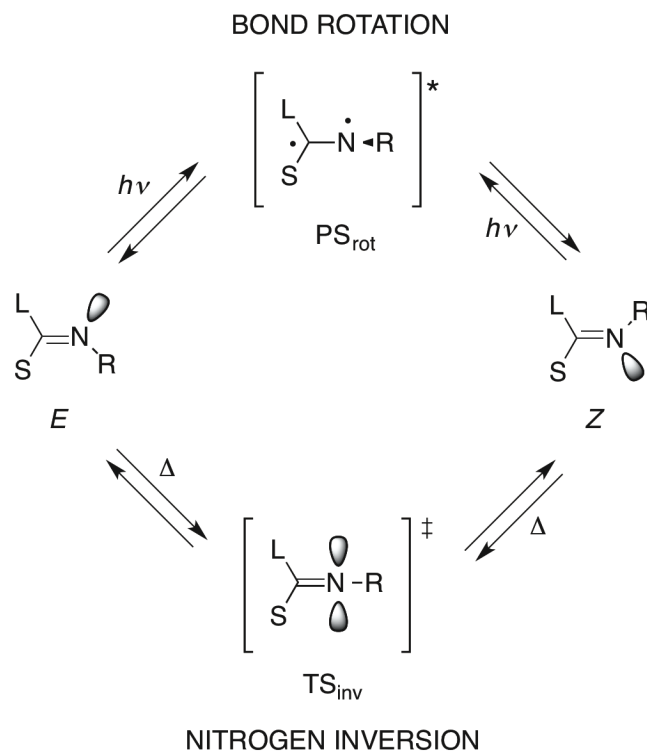
Figure 4.8: Possible stereoisomers of azine **44**.

In solution, *cis-trans* isomerization of the C-N double bond may occur, and the ratio of the resulting isomers depends on the polarity of the solvent.^{78a,79} The *Z,Z* and *E,E* isomers are enantiomers and should give rise to one of the signal sets, whereas the *Z,E* meso compound should give rise to the other. The energy barrier for transformation of the *Z,E* isomer to either the *Z,Z* or the *E,E* isomer should be the same. Thus, all three structures shown in Figure 4.8 are probably present in solution. Apparently, this equilibration process is reversible by removal of solvent.

Two different processes for isomerization of the C-N double bond of imine derivatives have been proposed, *i.e.*, either rotation by photolysis or inversion by thermolysis (Scheme 4.3).⁸⁰ The photolytic process occurs by an out-of-plane rotation via an excited state, whereas the thermal interconversion transpires at the ground state through a linear transition state. There are some indications that the thermal conversion for azines has a mixed rotation/inversion mechanism.^{80a,81} As the

equilibration is occurring with the sample tube inside the magnet of the NMR instrument where it is dark, a thermal process seems more likely.

Scheme 4.3: Rotation Processes of the C-N Double Bond in Imine Derivatives



Although such isomerizations have not been proven, they are the most plausible explanation for the two equilibrating signal sets in the ^{13}C NMR spectrum.

4.2 Reaction in Methanol: Formal Insertion Into the O-H bond

In the previously mentioned experiment by Freeman *et al.*, the tosylhydrazone precursor of **14** was thermolyzed in diglyme in the presence of sodium methoxide.⁶⁰ In addition to formation of rearrangement products **41** and **42**, three methyl ethers were obtained resulting from reaction of **14** with methanol (*vide supra*: Chapter 1.3.3).⁶⁰ These compounds are believed to form through a carbonium ion pathway in which the carbene is protonated. The methanol needed for this process arises from reaction of the tosylhydrazone precursor with sodium methoxide. By varying the conditions, it was possible to shut off either the carbonium ion route leading to methyl ethers or the carbene route affording rearrangement products.

Here, with an oxadiazoline, a different carbene precursor was used, which was directly dissolved in neat methanol. In addition, the reactions were carried out under *both* thermolytic and photolytic conditions. This could lead to a different outcome. In these experiments, carbene **14** afforded exclusively methyl ether products, probably due to the large amount of methanol available. Under all conditions, the GC-MS of the product mixture showed the formation of one main compound, which was isolated by column chromatography and identified as *rac*-(1*R*,2*S*,4*S*,5*R*,6*R*)-2-methoxytricyclo[3.3.0.0^{4,6}]octane (**48**). Compound **48** is spectroscopically identical with the main methyl ether obtained by the reported Bamford–Stevens reaction.⁶⁰ Reaction conditions and isolated yields are given in Table 4.3.

Table 4.3: Isolated Yields of Products 48 and 46 Obtained by Thermolysis and Photolysis of Oxadiazolines 29a and 29b in Methanol

precursor	substrate	concn (mg/mL)	cond	rxn time (h)	yield of product 48 (%)	yield of product 46 (%)
29a	methanol	19	Δ	4	28 (35) ^a	26 (48) ^a
29b		19	Δ	4	44 (76) ^a	—
29a		20	<i>hν</i>	7	33 (80) ^a	—
29b		20	<i>hν</i>	7	47 (77) ^a	—

^a Crude Product

The yields of **48** were considerably lower after chromatography (Table 4.3). Since the crude products were quite pure according to ¹H NMR analysis, it is possible that **48** decomposes on the silica adsorbent. Thus, the yields were also determined by GC-MS analysis using camphor as internal standard, and indeed they were somewhat higher than the isolated ones (Table 4.4). The combined yields of additionally formed methyl ethers could be determined as well (<9%).

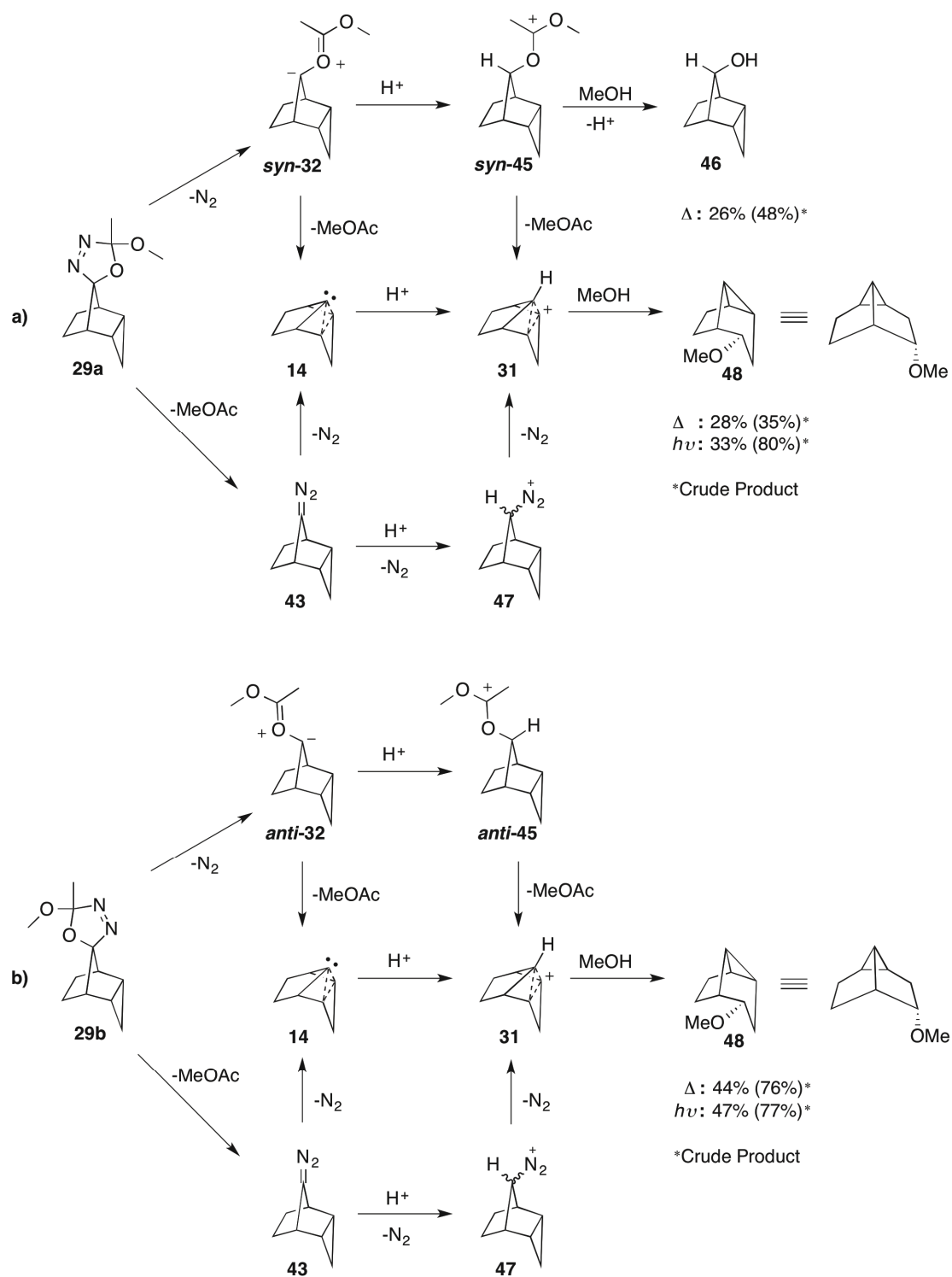
Table 4.4: GC-MS Analysis of Product Distribution Obtained from Thermolysis and Photolysis of Oxadiazolines 29a and 29b in Methanol

precursor	substrate	concn (mg/mL)	cond	yield of product 48 (%)	yield of other methyl ethers (%)	yield of product 46 (%)
29a	methanol	10	Δ	41	1	31
29b		10	Δ	67	2	—
29a		10	<i>hν</i>	63	9	—
29b		11	<i>hν</i>	55	8	—

Product **49** is best explained to form by reaction of carbonium ion **31** with methanol. There are several possible routes from precursors **29a** and **29b** to **31** (Scheme

4.4).^{26,68,70,82} The oxadiazolines may either decompose through diazo compound **43** or carbonyl ylide **32** to generate carbene **14**, which is subsequently protonated. Alternatively, either the diazo compound or the carbonyl ylide may be protonated first, where subsequent loss of N₂ or methyl acetate, respectively, gives **31** directly. In the latter case, the formation of **14** is avoided.

Scheme 4.4: Thermolysis and Photolysis of Oxadiazolines 29a and 29b in the Presence of Methanol



The positive charge in **31** is delocalized among C₂, C₄, and C₈.^{57e,66f,g,73b,83} Product **48** is formed by an attack of methanol at C₂ or C₄, which indicates that the charge is concentrated largely at these identical carbon atoms. The participation of the nonclassical ion is supported by the exclusive formation of *endo* product, for which the delocalized charge in **31** shields it from an attack by methanol at the less sterically hindered *exo* positions of C₂ and C₄. Consequently, formation of the corresponding *exo* methyl ether of **48** is prevented. The *endo* stereochemistry was confirmed by two-dimensional NMR analysis.

No product resulting from attack of methanol at C₈ was isolated. Some of the additional methyl ethers observed by the GC-MS analysis of the product distribution may derive from such a reaction, but should not amount to more than about 9% (Table 4.4). This is interesting when compared to the reaction of norbornen-7-ylidene (**7**) in methanol. Protonation of **7** is also predicted to give a nonclassical ion, *i.e.*, carbonium ion **49**, with a three-center, delocalized charge between the bridge carbon and the two former double bond carbons (Figure 4.9).^{45b,c,84} By photolysis of the diazirine precursor of **7** in methanol, 93% of the products derive from an *anti* attack by methanol at the C₇ bridge carbon of **49** to give *anti*-7-methoxybicyclo[2.2.1]hept-2-ene (**50**) (Figure 4.9).⁶⁸ Only 4.7% of the products resulted from attack at the double bond C₂ and C₃ carbons, which are analogue to the C₂ and C₄ carbons of carbonium ion **31**. This may be due to different distribution of the positive charge in the two delocalized systems. Indeed, calculations have indicated greater stabilization of the carbocationic center by interaction with a cyclopropane ring than with a double bond.⁸⁵ Thus, one possible explanation is that carbons C₂ and C₄ in protonated **14**, *i.e.*, **31**, carry greater net charges than carbons C₂ and C₃ in protonated **7**, *i.e.*, **49**.

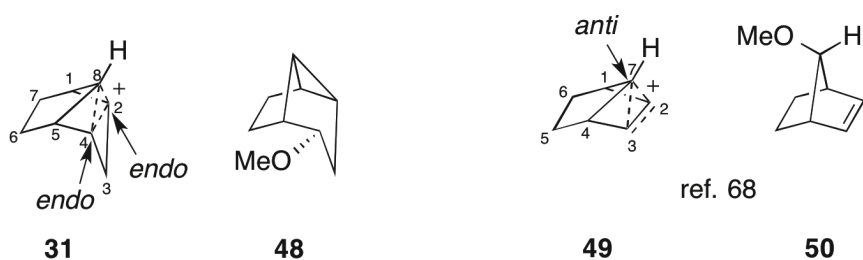


Figure 4.9: Positions for main attack by methanol at carbonium ions **31** and **49**, and the respective main products **48** and **50**.

In addition to methyl ether **48**, *endo,syn*-tricyclo[3.2.1.0^{2,4}]octan-8-ol (**46**) was formed in a yield of 26% by thermolysis of **29a** in methanol (Scheme 4.4a). The formation of alcohol **46** is best explained by protonation of the proximal ylide intermediate *syn*-**32** to afford *syn*-**45**, thereby locking in the stereoconfiguration at C₈. Subsequent methanolysis of *syn*-**45** gives product **46**. A similar reaction sequence was observed for the oxadiazoline precursor of carbene **13**.⁷⁰ In contrast, the distal ylide intermediate *anti*-**32**, formed from thermolysis of **29b**, might collapse before being trapped by a proton due to destabilization of the negative charge by the cyclopropyl group (Scheme 4.4). However, proton transfer rates to a negatively charged C atom are extremely fast. Hence, an alternative explanation could be that *anti*-**32** is first protonated to *anti*-**45**, but instead of methanolysis to yield an alcohol, as for *syn*-**45**, anchimeric assistance in *anti*-**45** allows methyl acetate to leave, resulting in carbonium ion **31**. Since **46** is not formed during photolysis, it can be assumed that the oxadiazoline decomposes through diazo intermediate **43** rather than the carbonyl ylide.

4.3 Reaction in Acrylonitrile: Addition to the Double Bond

It is important to note that the stereochemistry of methyl ether **48** is not decided by the geometry of the carbene **14**, but rather by the structure of carbonium ion **31**. Thus, different conditions were needed where **14** could be directly trapped with an added substrate. Since foiled carbenes in general are nucleophilic, trapping them with an electron-deficient double bond has been proven to be successful.⁵⁴ When **29a** and **29b** were thermolyzed in acrylonitrile under the conditions given in Table 4.5, *rel*-(1*s*,1'*R*,2'*R*,4'*S*,5'*S*)-spiro[cyclopropane-1,8'-tricyclo[3.2.1.0^{2,4}]octane]-2-carbonitrile (**51**) was formed in yields of 76% and 81%, respectively. These yields are considerably higher than those obtained for carbene **13**.⁵⁴

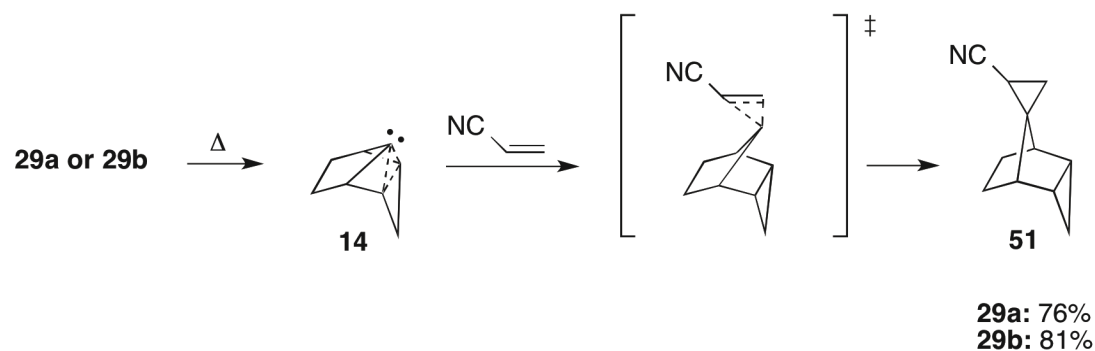
Table 4.5: Isolated Yields of Product 51 Obtained by Thermolysis of Oxadiazolines 29a and 29b in Acrylonitrile

precursor	substrate	concn (mg/mL)	cond	rxn time (h)	yield of product 51 (%)
29a	acrylonitrile	20	Δ	4	76
29b	acrylonitrile	21	Δ	4	81

The stereochemistry of product **51** was assigned with the help of two-dimensional NMR experiments. Because the reaction occurs stereoselectively, with the cyano group *anti* to the cyclopropane ring, it can be assumed that the product is formed through a concerted mechanism, which is expected for singlet carbenes.² The assumed TS, shown in Scheme 4.5, is expected to be similar to the calculated TS for the reaction of the related carbene **13** with the same substrate.⁵⁴ Previous DFT calculations suggest that the *anti* product is formed with electron-poor alkenes, whereas the *syn* product is preferred in reactions with electron-rich alkenes.⁵⁴ In both cases, the alkene approaches the divalent carbon *anti* to the stabilizing moiety, *i.e.*, double bond or cyclopropane ring, respectively. However, subsequent stereoelectronic

effects determine how the substituents of the alkene are oriented in the in the approach. Both the nucleophilic behavior and the diastereoselectivity in this reaction provide strong evidence for a foiled carbene **14**.

Scheme 4.5: Thermolysis of Oxadiazolines **29a and **29b** in the Presence of Acrylonitrile**



The GC-MS chromatograms obtained after completed reactions show that *anti* product **51** was formed exclusively from both **29a** and **29b**, *i.e.*, the reaction occurred completely stereoselectively. This is demonstrated for **29b** in Figure 4.10. Furthermore, no rearrangement products could be detected.

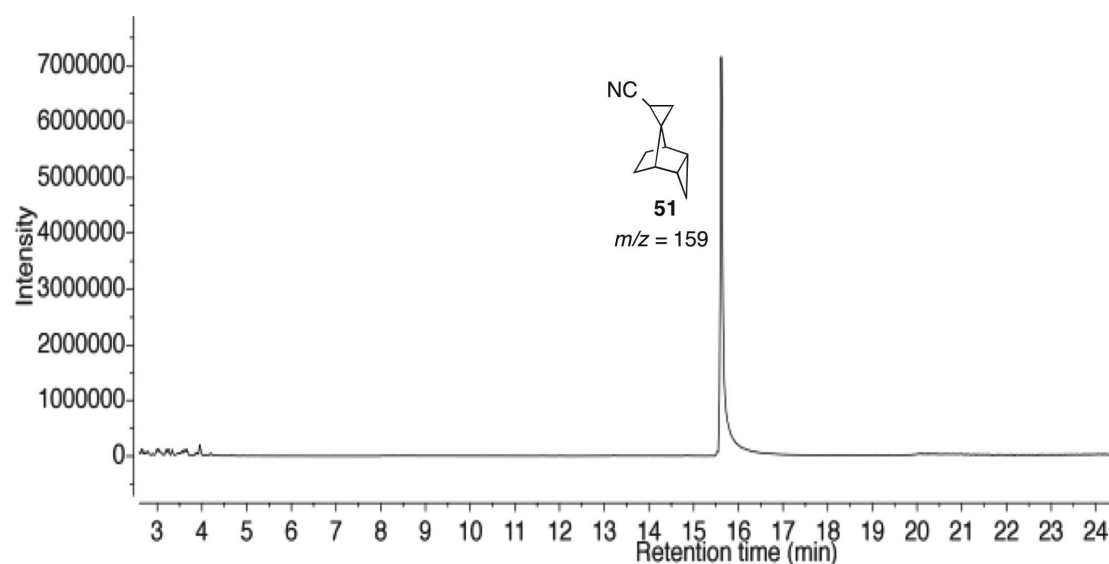


Figure 4.10: GC-MS chromatogram of product distribution obtained by thermolysis of **29b** in acrylonitrile.

For the thermolysis of **29a**, the chromatogram also revealed minor formation of compounds that probably derive from trapping of carbonyl ylide *syn-32* with acrylonitrile (M^+ ; $m/z = 233$) (Figure 4.11).

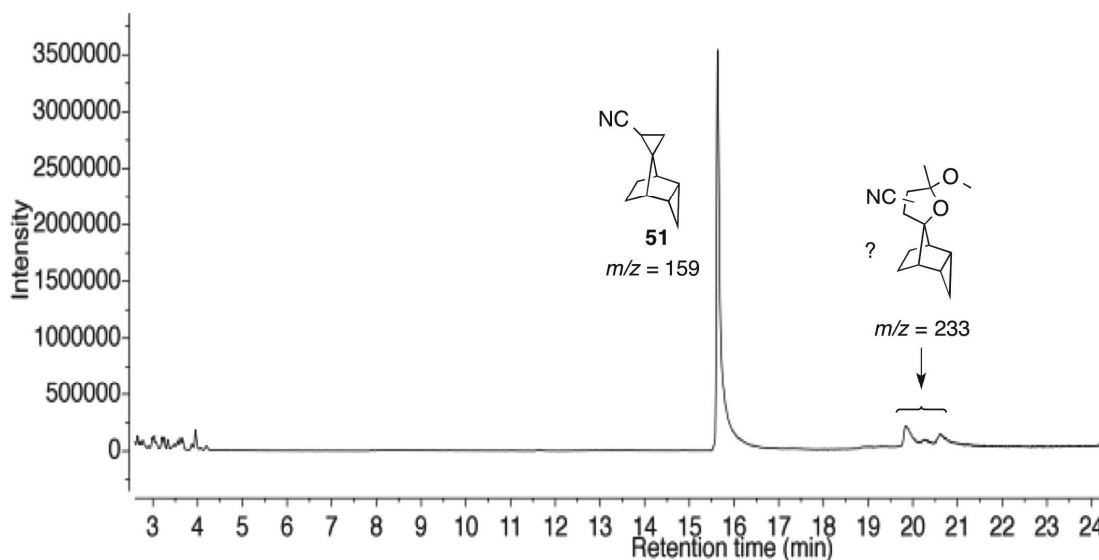
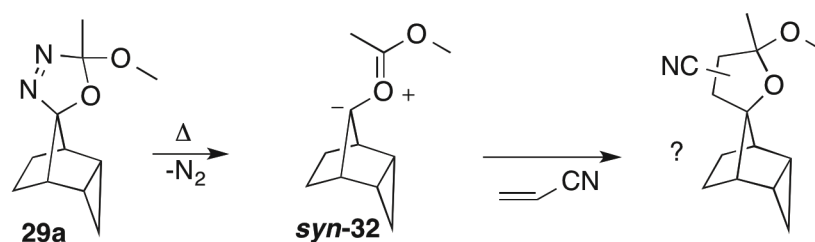


Figure 4.11: GC-MS chromatogram of product distribution obtained by thermolysis of **29a** in acrylonitrile

Indeed, dipolarophiles are known to be able to capture carbonyl ylides through [3 + 2] cycloaddition reactions to give tetrahydrofuran derivatives (Scheme 4.6).^{39b,86} These products were isolated as a mixture in a combined yield of 3%. The ^1H NMR spectrum of the mixture shows signals for methyl and methoxy groups, which provides further evidence of such a reaction (Figure A.50, Appendix). The fact that the carbonyl ylide formed by thermolysis of **29b**, *i.e.*, *anti-32*, was not trapped, again indicates that this intermediate is less stable than *syn-32*.

Scheme 4.6: Possible Trapping of Carbonyl Ylide *syn*-32 With Acrylonitrile



The first time the reaction was carried out, acrylonitrile had not been adequately dried. In this case, the obtained yields of **51** were rather low, *i.e.*, 12% and 11% from **29a** and **29b**, respectively (Table 4.6). Additionally, *rac*-(1*R*,2*S*,4*S*,5*R*,6*R*)-2-hydroxytricyclo[3.3.0.0^{4,6}]octane (**52**) was isolated in yields of 9% and 11%, respectively.

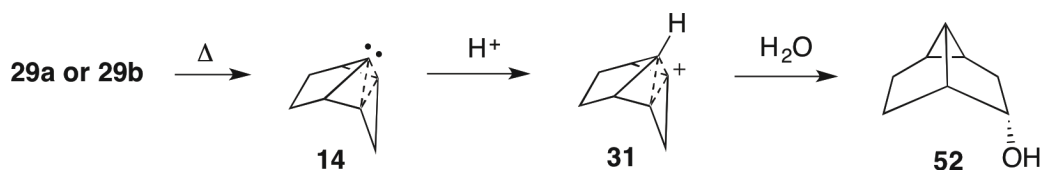
Table 4.6: Isolated Yields of Products **51 and **52** Obtained by Thermolysis of Oxadiazolines **29a** and **29b** in Acrylonitrile Containing Traces of Water**

precursor	substrate	concn (mg/mL)	cond	rxn time (h)	yield of product 51 (%)	yield of product 52 (%)
29a	acrylonitrile (undried)	21	Δ	4	12	9
29b	acrylonitrile (undried)	21	Δ	4	11	11

Product **52** is most likely formed by a mechanism similar to that of reaction of **14** with methanol (Scheme 4.7). Indeed water and methanol have comparable pK_a values of 15.7 and 15.5 (in water), respectively.⁸⁷ Thus, the carbene is initially protonated to the nonclassical carbonium ion **31**, comprising a delocalized charge between C₂, C₄, and C₈. The water molecule attacks either at C₂ or C₄ from the *endo* direction, consequently resulting in product **52**. Whether the alcohol group is oriented *endo* or

exo could not be determined by two-dimensional NMR spectroscopy, but the spectroscopic data and melting point of **52** were in agreement with the literature values for the *endo* analogue.^{66g,88}

Scheme 4.7: Formation of Alcohol 52 by Thermolysis of Oxadiazoline 29b in Acrylonitrile Containing Traces of Water



The GC-MS chromatogram of the product mixture obtained by thermolysis of **29b** in acrylonitrile containing traces of water shows that considerable formation of rearrangement products **41** and **42** had taken place (Figure 4.12). One possible explanation for this, is that traces of water might be facilitating the carbene-to-carbene rearrangement **14** \rightarrow **40** by assisting the proton-transfer step of the intermolecular rearrangement mechanism (*vide supra*: Chapter 4.1). Furthermore, there was formation of one additional product with the same mass as **51** (M^+ ; $m/z = 159$) in a ratio of 4:1. This product may derive from addition of acrylonitrile to the rearranged carbene **40**. It could also be the diastereomer of product **51**, with the cyano group directed *syn* to the cyclopropane ring, instead of *anti*. It is, however, unlikely that the presence of water should influence the stereoselectivity of the reaction. Finally, the GC-MS chromatogram revealed three peaks resulting from compounds with molecular ion peaks of $m/z = 163$. These products have been observed under different conditions too, *e.g.*, by photolysis of **29a** or **29b** in cyclohexane, but again only when the solvents had not been sufficiently dried. Thus, since the only common factors are the presence of the respective oxadiazoline and wet solvents, these compounds should result from side reactions of the precursor in the presence of water. Note, however, that unless otherwise stated, only results using properly dried solvents are presented.

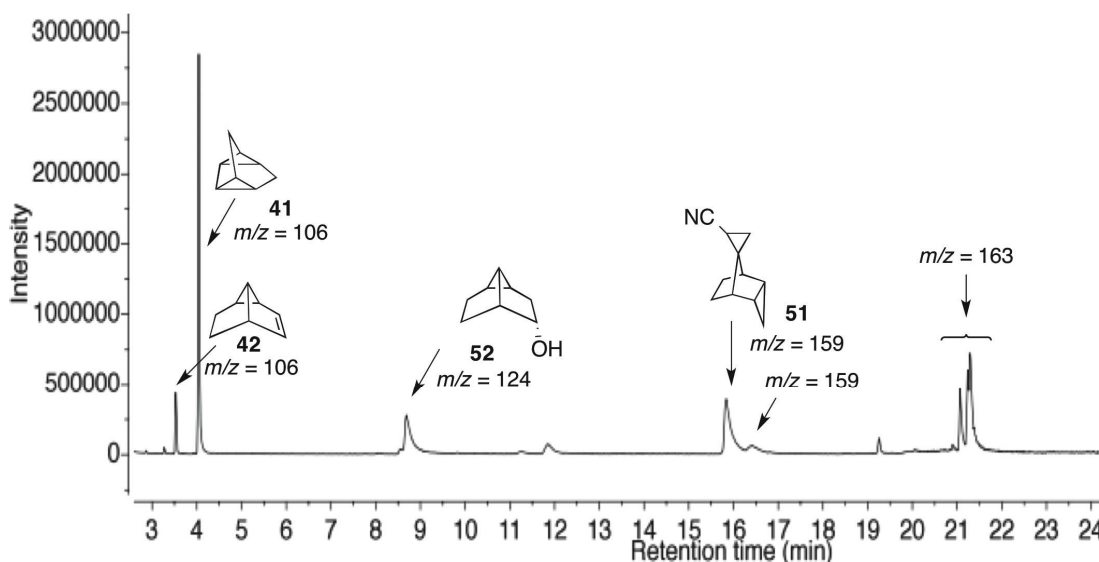


Figure 4.12: GC-MS chromatogram of product distribution obtained by thermolysis of **29b** in acrylonitrile containing traces of water.

To verify the influence of water in the reaction, thermolysis of **29b** was carried out with 0.3% H_2O (v/v) added to properly dried acrylonitrile. This resulted in a GC-MS chromatogram similar to that obtained when insufficiently dried acrylonitrile was applied; products **51** and **52** were formed, as well as rearrangement products **41** and **42** (Figure 4.13). Thus, when compared to the reaction in carefully dried acrylonitrile (Figure 4.10 and 4.11), a relatively low concentration of water is sufficient to prevent the addition reaction of carbene **14** to acrylonitrile.

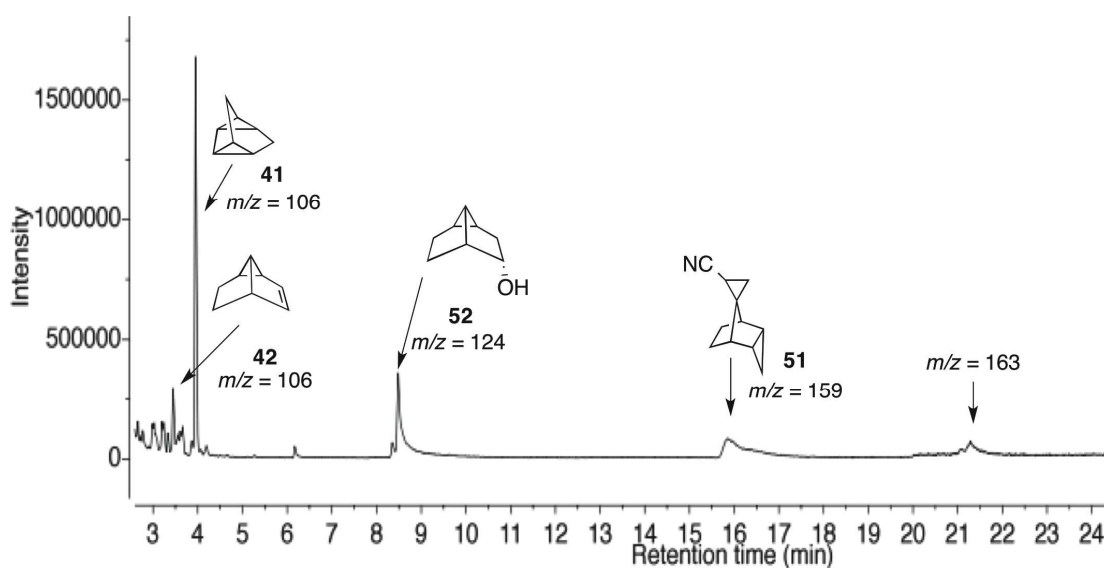


Figure 4.13: GC-MS chromatogram of product distribution obtained by thermolysis of **29b** in 0.3% H₂O (v/v) in acrylonitrile.

Furthermore, when the amount of water was raised to 10% (v/v) in acrylonitrile, product **52** was formed almost exclusively (Figure 4.14). No traces of product **51** could be detected. Thus, the rate of reaction of carbene **14** with H₂O prevents any addition to acrylonitrile or rearrangement of the carbene. Product **52** was isolated in a yield of 66%. There was a minor peak that gave a mass spectrum with a fragmentation pattern almost identical to that of alcohol **46**, but with a slightly different retention time.

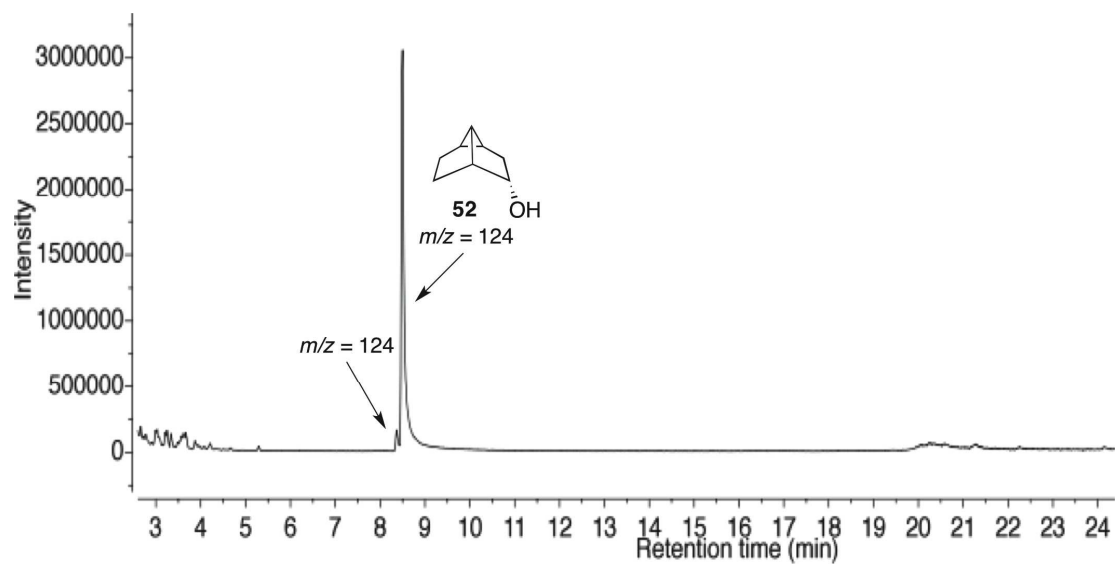


Figure 4.14: GC-MS chromatogram of product distribution obtained by thermolysis of **29b** in 10% H₂O (v/v) in acrylonitrile.

4.4 Reaction in Diethylamine: Insertion Into the N-H Bond

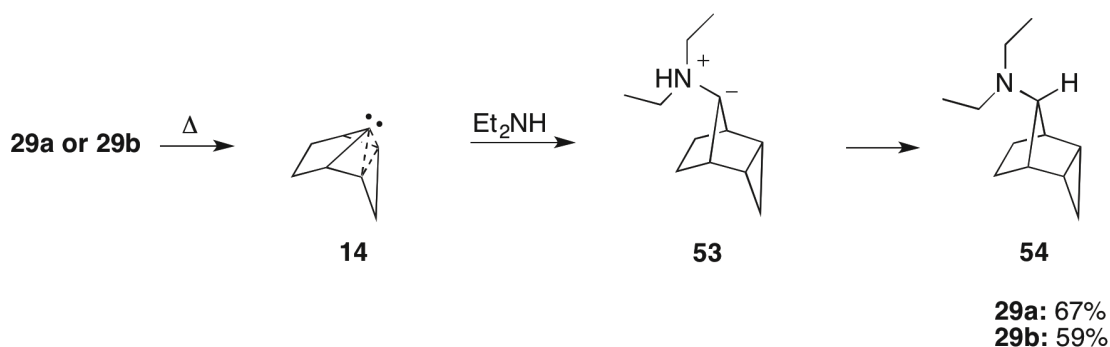
Foiled carbenes also exhibit ambiphilic behavior. For instance, carbene **13** was trapped with diethylamine in relatively high yields.⁵⁵ Other examples of insertion of both electrophilic and nucleophilic carbenes into N-H bonds of amines are known.⁸⁹ Therefore, thermolyses were carried out for **29a** and **29b** in neat diethylamine under conditions given in Table 4.7. One main product was obtained, *i.e.*, *endo,anti-N,N*-diethyltricyclo[3.2.1.0^{2,4}]octan-8-amine (**54**), in yields of 67% and 59%, respectively. The stereochemistry of **54** was determined by two-dimensional NMR spectroscopy.

Table 4.7: Isolated Yields of Product 54 Obtained by Thermolysis of Oxadiazolines 29a and 29b in Diethylamine

precursor	substrate	concn (mg/mL)	cond	rxn time (h)	yield of product 54 (%)
29a	diethylamine	20	Δ	4	67
29b	diethylamine	20	Δ	4	59

The reaction of **14** → **54** is assumed to proceed through ylide intermediate **53** (Scheme 4.8).^{25,55} For some carbenes, stable nitrogen ylides has been isolated.⁹⁰ The trigonal pyramidal geometry of the carbanionic center preserves the diastereoselectivity of step **14** → **53**. Hence, the stereochemistry suggests an *anti* approach of diethylamine. In any case, even if the mechanism would involve a concerted insertion of carbene **14** into the N-H bond, an *anti* approach is necessary to obtain **54**. Therefore, this reaction also suggests a foiled carbene **14** as an intermediate.

Scheme 4.8: Thermolysis of Oxadiazolines **29a** and **29b** in the Presence of Diethylamine



The GC-MS chromatograms of the product mixtures obtained, reveals small amounts of an additional compound with the same mass as **54** (M^+ ; $m/z = 179$) in ratios of 30:1 and 58:1 from **29a** and **29b**, respectively. The minor product could be the *syn* analog of **54**, or it could result from a reaction of diethylamine with rearranged carbene **40**. The product mixture obtained from thermolysis of **29b** in diethylamine is shown in Figure 4.15.

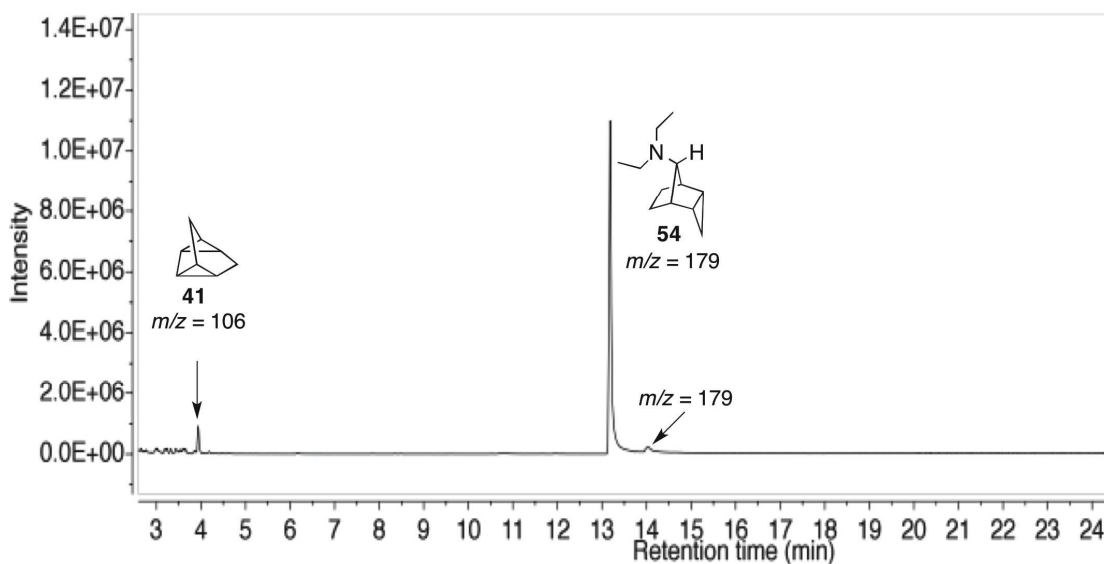


Figure 4.15: GC-MS chromatogram of product distribution obtained by thermolysis of **29b** in diethylamine.

4.5 Reaction in Benzaldehyde and Acetophenone: Attack of the C-O Double Bond

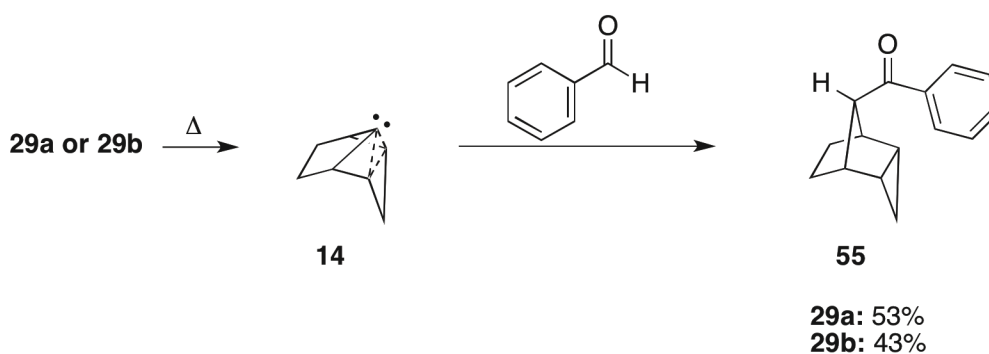
When **29a** and **29b** were thermolyzed in benzaldehyde under the conditions given in Table 4.8, phenyl((1*R*,2*R*,4*S*,5*S*,8*r*)-tricyclo[3.2.1.0^{2,4}]octan-8-yl)methanone (**55**) was isolated in yields of 53% and 43%, respectively.

Table 4.8: Isolated Yields of Product 55 Obtained by Thermolysis of Oxadiazolines 29a and 29b in Benzaldehyde

precursor	substrate	concn (mg/mL)	cond	rxn time (h)	yield of product 55 (%)
29a	benzaldehyde	22	Δ	6	53
29b	benzaldehyde	30	Δ	4	43

The observed stereochemistry of product **55** was unexpected (Scheme 4.9). The reaction seems to have proceeded through an insertion of carbene **14** into the C-H bond of the aldehyde group, with a benzaldehyde molecule approaching *syn* to the carbenic center.

Scheme 4.9: Thermolysis of Oxadiazolines 29a and 29b in the Presence of Benzaldehyde



Predominantly electrophilic carbenes insert into C-H bonds of compounds with a high hydride transfer potential (HTP),⁹¹ *i.e.*, compounds with neighboring atoms that efficiently stabilize the partial positive charge buildup of the transition state. Such activated C-H bonds are found for instance in secondary ethers and tertiary hydrocarbons.⁹² Nucleophilic carbenes, on the other hand, have been shown to insert into compounds with an acidic C-H bond, for which the developing negative charge is stabilized.^{56,93} For example, the reaction of carbene **13** with malononitrile (*vide supra*: Chapter 1.3.2) is calculated to occur by a formal insertion into the acidic C-H bond (pKa = 11.8 in water⁹⁴) with an initial protonation of the carbene, followed by an ion-pair recombination.⁵⁶ This is the same mechanism described previously for the reaction of foiled carbenes with methanol. Benzaldehyde has a pKa value of 14.9 in water,^{87b} similar to that of methanol (pKa = 15.5 in water^{87a}). Thus, one could imagine that carbene **14** would formally insert into the C-H bond of benzaldehyde in a similar manner as into the O-H bond of methanol. However, the determined stereochemistry of product **55** suggests a different reaction pathway. The structure of **55** was confirmed by single-crystal X-ray diffraction (Figure 4.16).

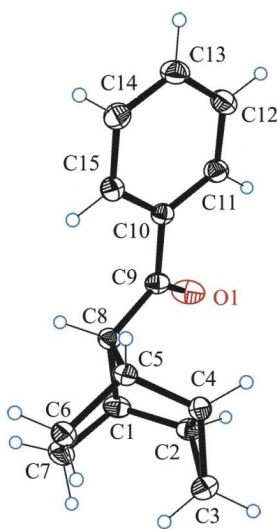


Figure 4.16: Single-crystal X-ray diffraction was used to elucidate the structure of phenyl((1*R*,2*R*,4*S*,5*S*,8*r*)-tricyclo[3.2.1.0^{2,4}]octan-8-yl)methanone (**55**).

Furthermore, the GC-MS of the product mixture revealed considerable formation of an additional product with the same mass as **55** (M^+ ; $m/z = 212$) (Figure 4.17). These

two products were formed in a ratio of 2:3, both from **29a** and **29b**, with **55** as the major isomer. The fragmentation pattern of the mass spectra of the two isomers are too different for the minor product to be the diastereomer of **55** that differs at C₈, *i.e.*, the product that would arise by insertion of carbene **14** into benzaldehyde by an *anti* approach. Benzoyl groups are easily detectable in mass spectra, with a strong peak at $m/z = 105$ due to a stable C₆H₅CO⁺ fragment ion. This is indeed the base peak of compound **55**. However, there is only a weak peak at $m/z = 105$ for the minor compound, and it is therefore unlikely to comprise a benzoyl group. Moreover, the minor product turned out to be unstable, and it could neither be isolated by column chromatography or by Kugelrohr distillation.

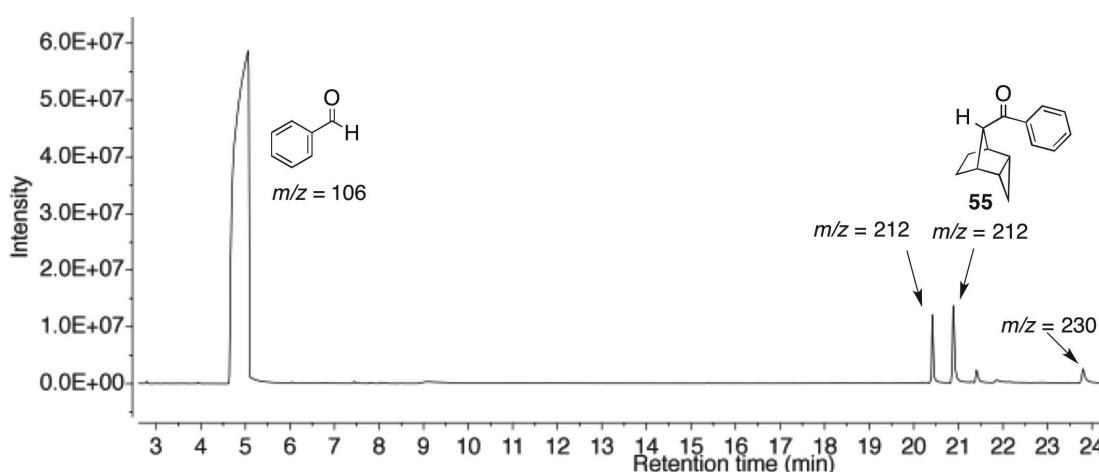


Figure 4.17: GC-MS chromatogram of product distribution obtained by thermolysis of **29a** in benzaldehyde.

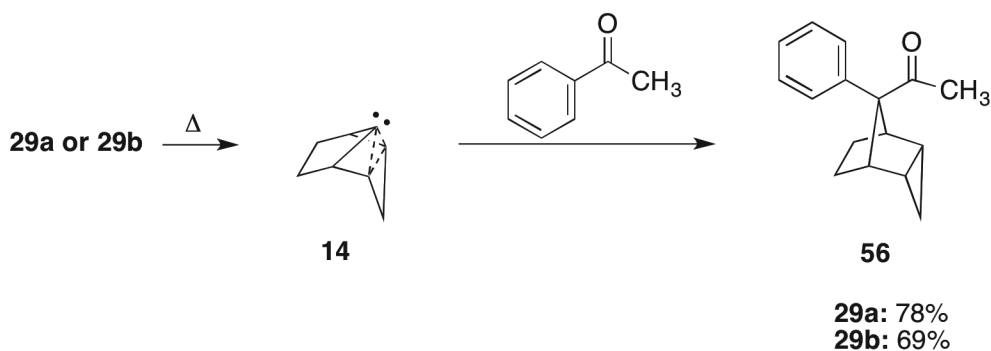
Thus, to better understand the outcome of the reaction with benzaldehyde, the chemistry of **14** in acetophenone was studied. The ketone resembles benzaldehyde, but obviously does not have a hydrogen atom attached to the carbonyl carbon. As a consequence, no C-H insertion is possible at this position, and any resulting product must be formed by a different mechanism. When **29a** and **29b** were thermolyzed in acetophenone under the conditions given in Table 4.9, 1-((1*R*,2*R*,4*S*,5*S*,8*r*)-8-phenyltricyclo[3.2.1.0^{2,4}]octan-8-yl)ethan-1-one (**56**) was isolated in yields of 78% and 69%, respectively.

Table 4.9: Isolated Yields of Product 56 Obtained by Thermolysis of Oxadiazolines 29a and 29b in Acetophenone

precursor	substrate	concn (mg/mL)	cond	rxn time (h)	yield of product 56 (%)
29a	acetophenone	21	Δ	4	78
29b	acetophenone	21	Δ	4	69

Product **56** is the result of a formal insertion of carbene **14** into the C-C bond between the carbonyl and the phenyl group (Scheme 4.10). However, a mechanism involving a direct insertion into a C-C bond is highly unlikely, and another reaction path should take place.

Scheme 4.10: Thermolysis of Oxadiazolines 29a and 29b in the Presence of Acetophenone



The structure of **56** was confirmed by single-crystal X-ray diffraction as well (Figure 4.18).

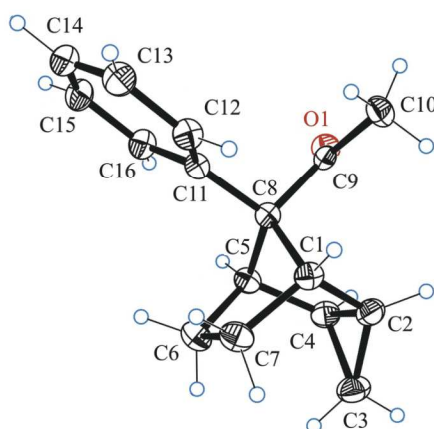


Figure 4.18: Single-crystal X-ray diffraction was used to elucidate the structure of 1-((1*R*,2*R*,4*S*,5*S*,8*r*)-8-phenyltricyclo[3.2.1.0^{2,4}]octan-8-yl)ethan-1-one (**56**).

The GC-MS chromatogram of the product mixture showed only small formation of an additional product with the same mass as **56** (M^+ ; $m/z = 226$), which was obtained in a ratio of 14:1 from both **29a** and **29b** (Figure 4.19).

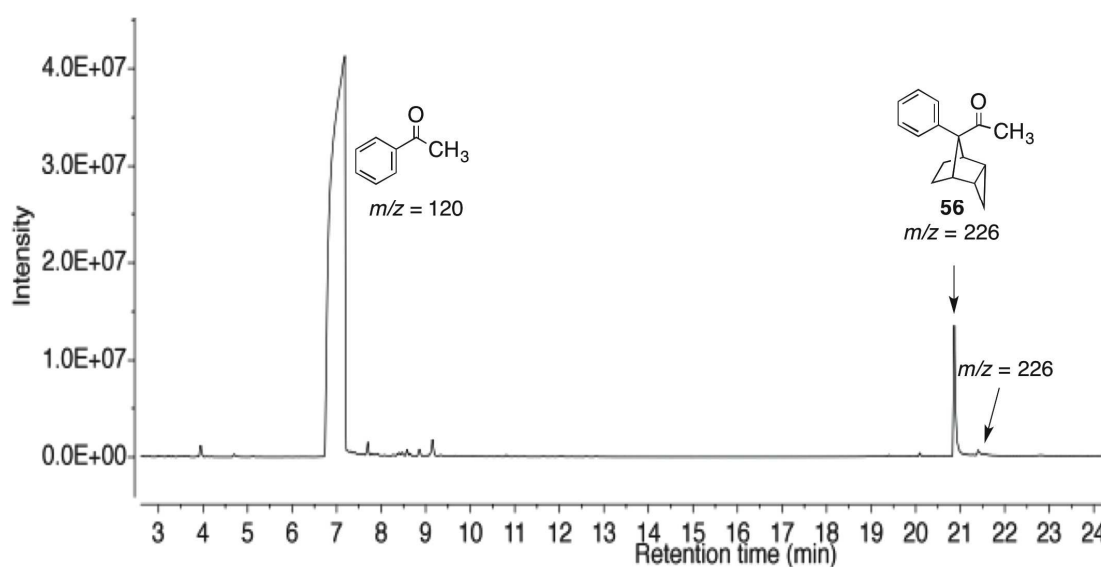
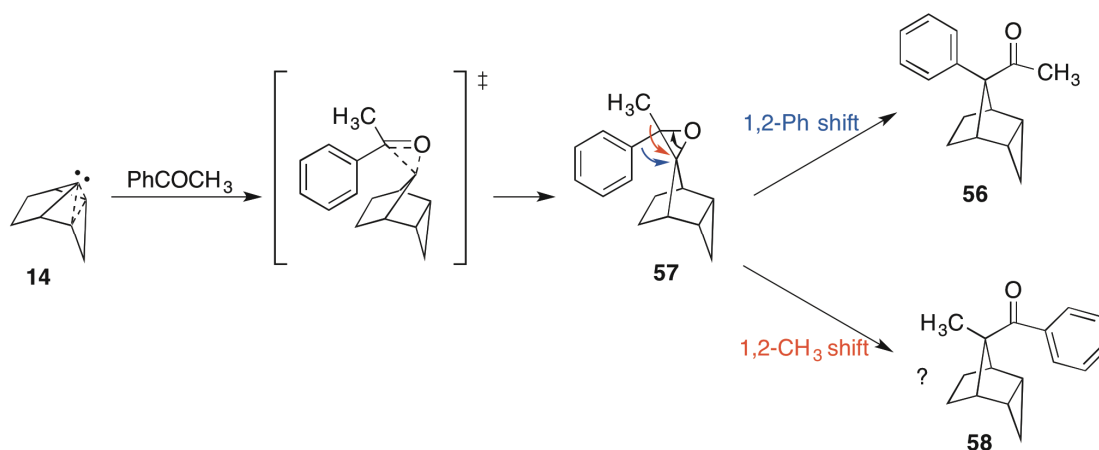


Figure 4.19: GC-MS chromatogram of product distribution obtained by thermolysis of **29a** in acetophenone.

A possible reaction path to product **56** consist of addition of carbene **14** to the carbonyl double bond to form an epoxide, followed by a thermal opening of the epoxide (Scheme 4.11). The carbene would then add to the C-O double bond in a concerted [2 + 1] cycloaddition, with the acetophenone approaching the carbenic center face *anti* to the cyclopropane ring. Thus, epoxide **57** is obtained, with its ring oxygen directed *syn* to the three-membered ring. Also in other cases, nucleophilic carbenes are believed to react with carbonyl groups by a concerted addition.^{38e,95} In a subsequent concerted, nucleophilic 1,2-phenyl shift, the phenyl group migrates to the C₈ bridge carbon from the *anti* face. This is the shortest possible migration route, leading to the formation of **56**. Consequently, the migration-terminus carbon is inverted in an S_N2-like manner.⁹⁶ Thermal ring opening of epoxides by 1,2 shifts are known from the literature.^{38e,39a,96-97}

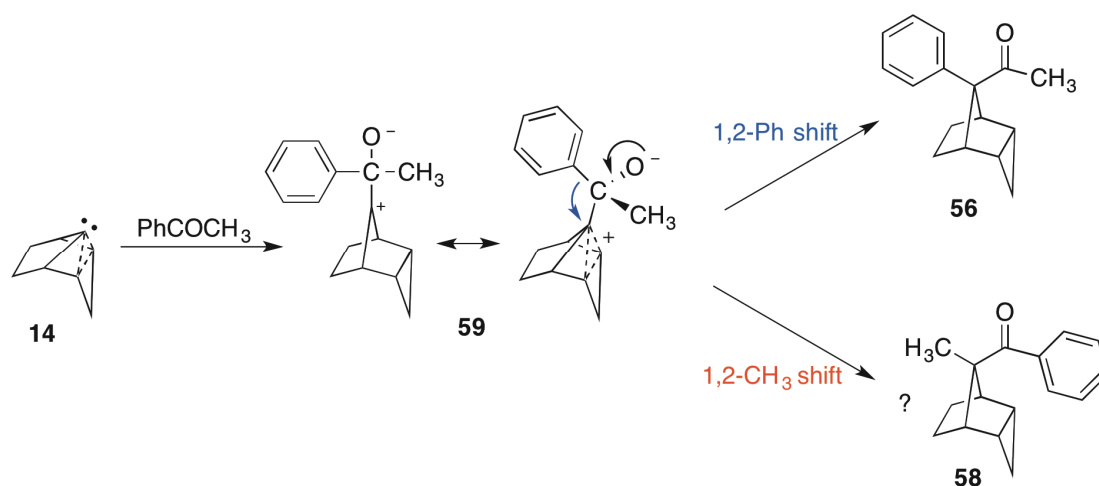
Scheme 4.11: Proposed Mechanism for Formation of Products 56 and 58 Through Epoxide 57



Alternatively, nucleophilic carbenes may attack electron-poor carbonyl carbons.⁹⁸ Thus, attack of carbene **14** at the carbonyl carbon of acetophenone would lead to ylide **59** shown in Scheme 4.12. The carbocationic center is likely to experience a delocalization of the positive charge in a similar manner as in nonclassical carbonium ion **31**.^{45,97c,99} In the nonclassical intermediate **59**, rotation around the C₈-C₉ bond can lead to a conformation that will allow the migrating phenyl group to attack the migration terminus from the preferred *anti* side, while the *syn* side is shielded by the

delocalized positive charge. Consequently, the reaction occurs stereospecifically, also yielding product **56**. However, it is also possible that a combination of the two proposed mechanisms occurs, *i.e.*, initially formed epoxide **57** rearranges to intermediate **59**.

Scheme 4.12: Proposed Mechanism for Formation of Products 56 and 58 Through Nonclassical Intermediate 59

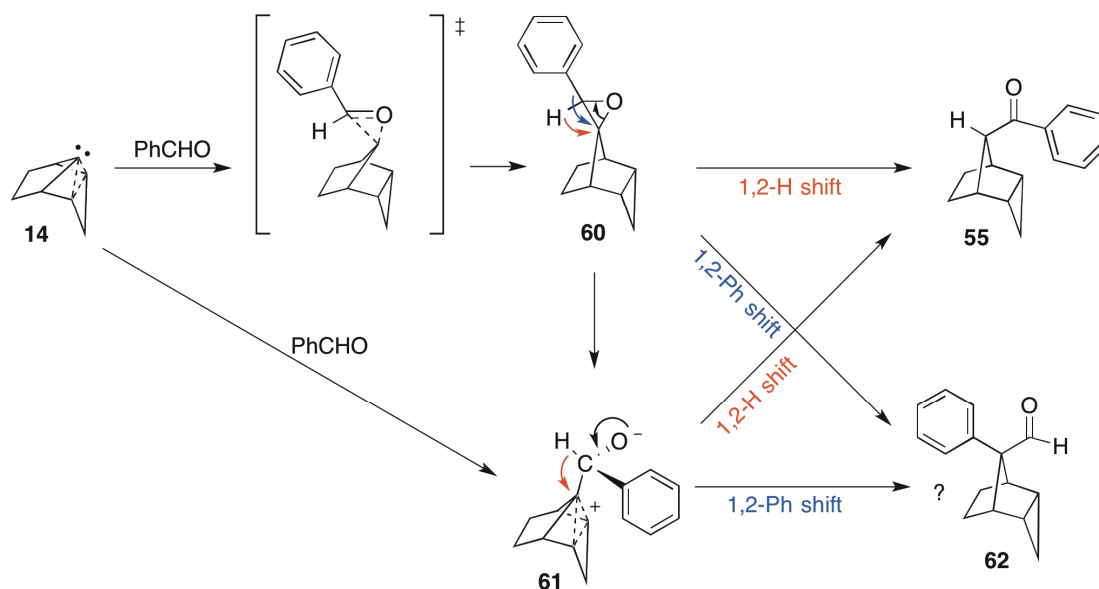


The mass spectrum of the minor product **58** shows a base peak at $m/z = 105$ and is therefore likely to comprise a benzoyl group. Compound **58** would be expected to result from a competitive 1,2-methyl shift for the ring opening of epoxide **57** or rearrangement of intermediate **59** (Scheme 4.11 and Scheme 4.12). By competing migrations, the group that can stabilize the developing positive charge at the migration origin usually stays behind. This would explain the lower aptitude of the methyl group.¹⁰⁰ Product **58** was not isolated and properly identified, however, and other structures can be discussed.

Similar mechanisms may be applied for the reaction of carbene **14** with benzaldehyde (Scheme 4.13). Product **55** can be formed from a concerted [2 + 1] addition of carbene **14** to the aldehyde function to give epoxide **60**. As discussed before, benzaldehyde is approaching the divalent carbon of **14** from the *anti* side. Subsequent thermal rearrangement to yield product **55** occurs by a nucleophilic 1,2-hydrogen shift. Alternatively, attack of **14** at the carbonyl carbon gives the nonclassical

intermediate **61**, for which a 1,2-hydrogen shift by *anti* attack at the migration terminus leads to product **55**.

Scheme 4.13: Proposed Mechanisms for Formation of Products 55 and 62



Since the phenyl group in intermediates **60** and **61** should also have a high migratory aptitude, considerable product formation as a result of a 1,2-phenyl migration should take place.^{97a,100} This would lead to aldehyde **62**, shown in Scheme 4.13. However, such aldehydes are easily oxidized to their corresponding carboxylic acids.^{97c} This would explain the considerable formation of a product that was not isolated (Figure 4.17). As the possible oxidation of **62** was not considered at the time, no special care was taken to collect the resulting carboxylic acid. Furthermore, the purification by chromatography and distillation were complicated by the excess of benzaldehyde and its oxidation to benzoic acid.

Neither the structure of product **58**, nor the structure of product **62**, has been proven yet. However, the mass spectra of the products provide some support for the interpretation. Compound **58**, the minor product formed by reaction of carbene **14** with acetophenone, has a base peak of $m/z = 105$ and a fragmentation pattern similar to that of **55**, the main product obtained from the reaction of carbene **14** with benzaldehyde (Figure 4.20). These structures are expected to result from 1,2-methyl and 1,2-hydrogen shifts, respectively. Compound **62**, the minor product formed by

reaction of carbene **14** with benzaldehyde, has a base peak of $m/z = 144$ and a fragmentation pattern similar to that of **56**, the main product obtained from reaction of carbene **14** with acetophenone (Figure 4.20). Both products are believed to result from 1,2-phenyl shifts. Thus, these experiments suggest the overall relative migratory aptitude in this kind of reactions to be $H > C_6H_5 \gg CH_3$.

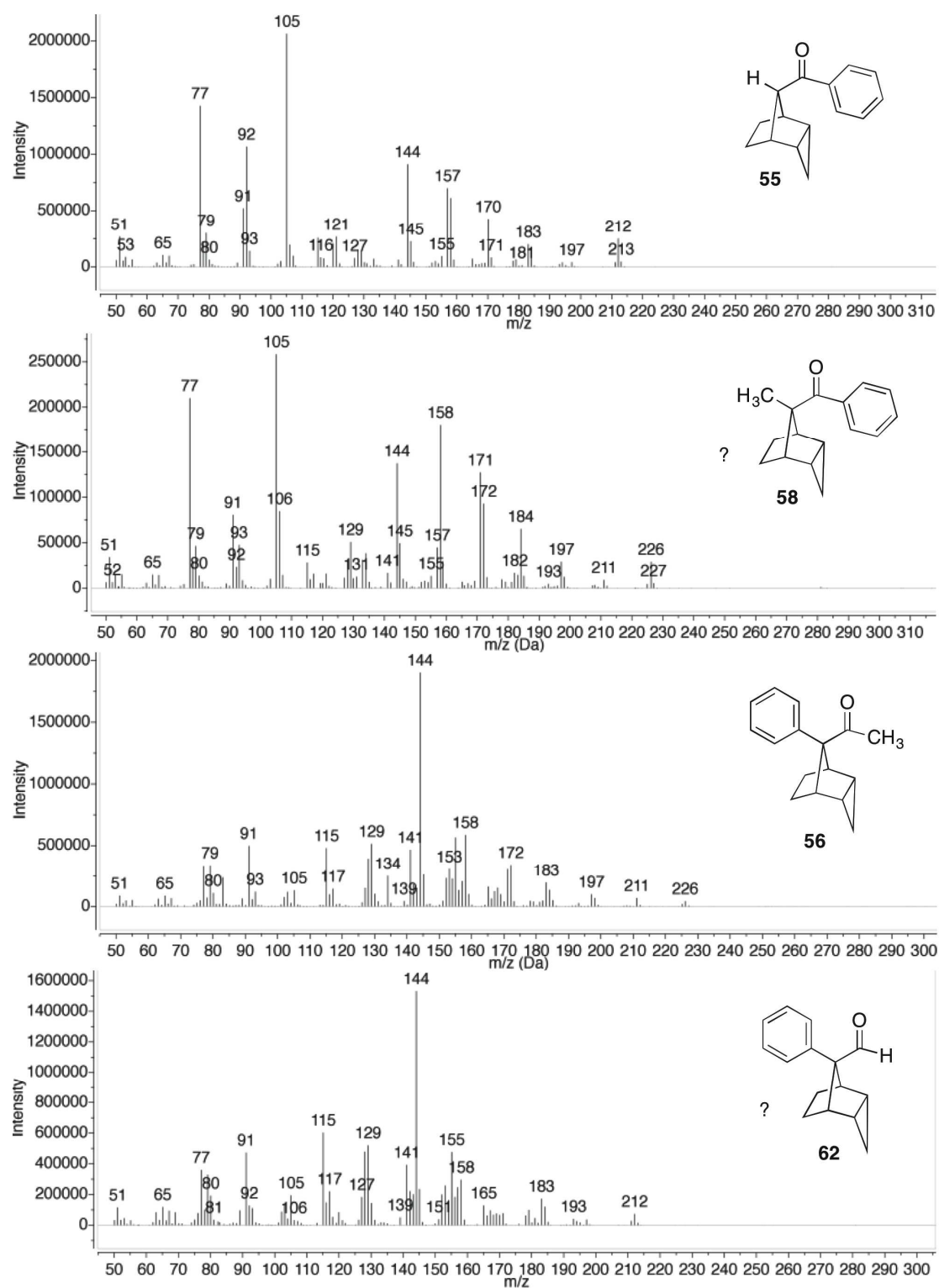


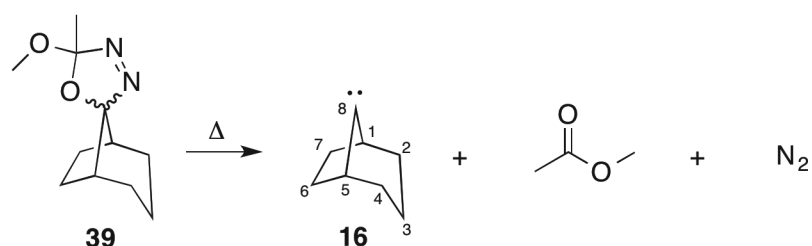
Figure 4.20: Comparison of the mass spectra of unknown compounds **58** and **62** with the mass spectra of known compounds **55** and **56**.

5. Reactions of Bicyclo[3.2.1]octan-8-ylidene (16)

5.1 Reaction in Cyclohexane and Cyclohexene: Rearrangement of Carbene 16

Next, the chemistry of carbene **14** was compared to that of bicyclo[3.2.1]octan-8-ylidene (**16**). According to calculations in this study, carbene **16** has a stabilization energy of 4.3 kcal/mol in its chair-like conformer, which is much less than the SE of **14** (14.3 kcal/mol). The stabilization is believed to result from hyperconjugative interactions with the C-H bonds at the equivalent C₂ and C₄ positions. Indeed, carbenic centers can also bend towards σ bonds due to such stabilization, thus affecting the geometry of the reactive species.^{49,101} Oxadiazoline **39** was used as precursor for the generation of carbene **16** (Scheme 5.1). Since the diastereomers of oxadiazoline **29** showed almost identical reactivities, precursor **39** was applied as a diastereomeric mixture (dr = 2.3:1). The experiments were carried out by thermolysis at 165 °C in a pressure tube, for which **39** was dissolved in the neat substrate under investigation.

Scheme 5.1: Thermolysis of Oxadiazoline 39 to Yield Carbene 16



First, **39** was thermolyzed in cyclohexane and cyclohexene and the resulting reaction mixtures were subjected to GC-MS analysis. The yields of the product distributions were determined by using camphor as internal standard (Table 5.1). Some small peaks were detected in the chromatograms that might derive from compounds formed by intermolecular reactions of carbene **16** with cyclohexane (M^+ ; $m/z = 192$) or cyclohexene (M^+ ; $m/z = 190$) in combined yields of 2 and 17%, respectively. As in the

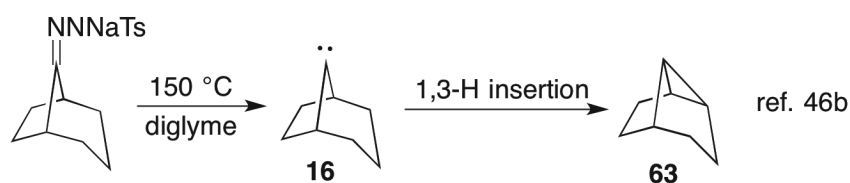
case of carbene **14**, this reluctant reactivity may indicate a stabilization of **16**, but it could also simply mean that competing reactions occur faster. Moreover, the slow addition to the electron-rich double bond of cyclohexene suggests that **16** is like **14** a nucleophilic carbene.^{17,28} The estimated yields of addition products are, however, slightly higher than those of carbene **14**.

Table 5.1: GC-MS Analysis of Product Distribution Obtained from Thermolysis and Photolysis of Oxadiazoline **39 in Cyclohexane and Cyclohexene**

precursor	substrate	concn (mg/mL)	cond	yields of intermol. products (%)	yield of rearrang. product (%)
39	cyclohexane	10	Δ	2	71
39	cyclohexene	10	Δ	17	43

In both cyclohexane and cyclohexene, isomerization of carbene **16** was favored, giving a rearrangement product (M^+ ; $m/z = 108$) in yields of 71% and 43%, respectively. It is likely to be the same 1,3-hydrogen insertion product obtained by thermolysis of the tosylhydrazone precursor of **16** in a solution of sodium methoxide and dry diglyme, *i.e.*, tricyclo[3.3.0.0^{2,8}]octane (**63**) (Scheme 5.2).^{46b}

Scheme 5.2: Intramolecular 1,3-H Insertion of Carbene **16 to Give Product **63****



No azine formation could be detected, and so there was no evidence of a diazo intermediate.

5.2 Reaction in Acrylonitrile: Addition to the Double Bond

When oxadiazoline **39** was thermolyzed in acrylonitrile under the conditions given in Table 5.2, spiro[bicyclo[3.2.1]octane-8,1'-cyclopropane]-2'-carbonitrile (**64**) was obtained in yields of 14-18%. Thus, the yields were considerably lower than those obtained from the reaction of carbene **14** with acrylonitrile.

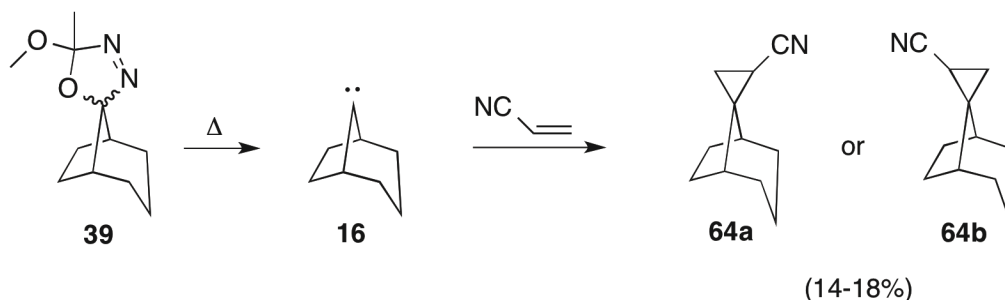
Table 5.2: Isolated Yields of Product 64 Obtained by Thermolysis of Oxadiazoline 39 in Acrylonitrile

precursor	substrate	concn (mg/mL)	cond	rxn time (h)	yield of product 64 (%)
39	acrylonitrile	19	Δ	4	14
39		18	Δ	4	18

The reaction occurred stereoselectively. It was, however, difficult to determine the stereochemistry of **64** by two-dimensional NMR spectroscopy due to very close signals in the ^1H NMR spectrum. Moreover, the quality of the crystals was not good enough to carry out single-crystal X-ray analysis, although several attempts of recrystallization were made. Thus, product **64** either has *syn* (**64a**) or *anti* (**64b**) stereochemistry (Scheme 5.3).[†] Nevertheless, the reaction shows that the space available on the *syn* and *anti* sides of the divalent carbon of **16** is different enough for a stereoselective reaction to take place. This may be due to both geometric and stereoelectronic effects.

[†] Here, the substituent at the bridgehead is *anti*- or *syn*-positioned relative to the larger ring of the bicyclo[3.2.1]octanyl moiety of the structure.

Scheme 5.3: Thermolysis of Oxadiazolines **39** in the Presence of Acrylonitrile



The GC-MS chromatogram of the product distribution revealed two other minor products with the same molecular mass as **64** (M^+ ; $m/z = 161$) (Figure 5.1). Both compounds were formed in a ratio of 6:1. One of them may be the diastereomer of **64** with the cyano group directed in the opposite direction. The other product might derive from addition to the cyano group instead of the double bond of acrylonitrile to afford a substituted *2H*-azirine product.¹⁰²

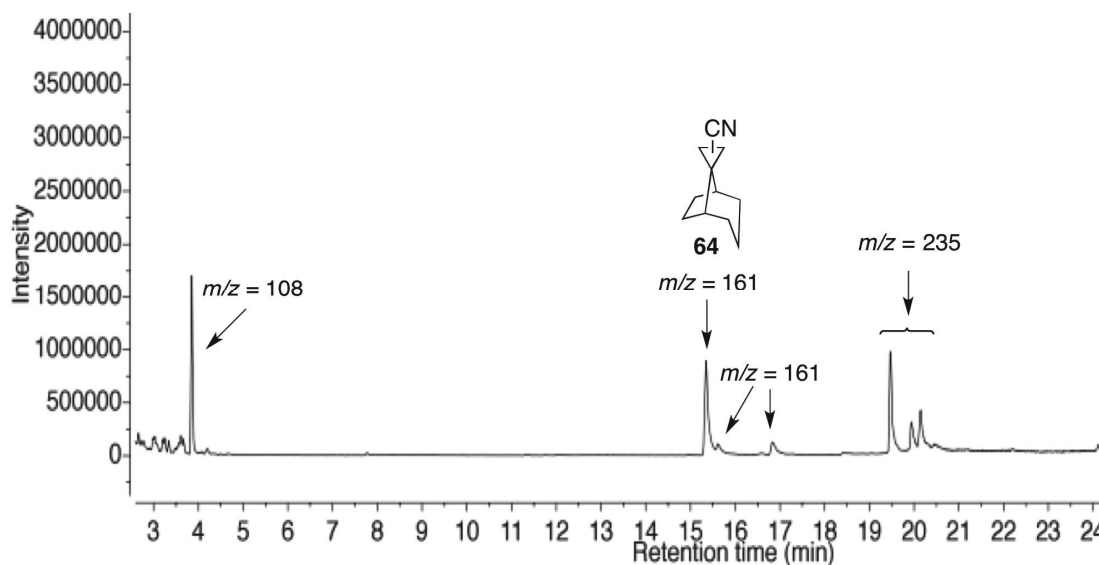
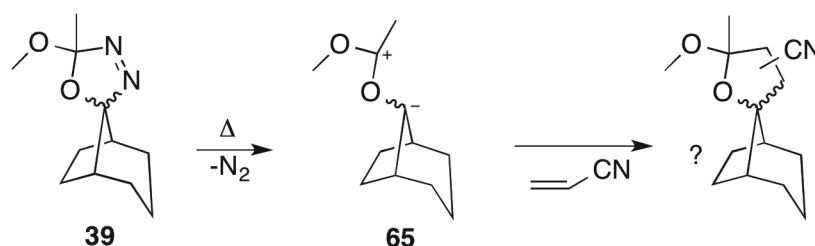


Figure 5.1: GC-MS chromatogram of product distribution obtained by thermolysis of **39** in acrylonitrile.

In addition, the chromatogram displays some formation of the same rearrangement product found by thermolysis of **39** in cyclohexane and cyclohexene (M^+ ; $m/z = 108$) and some products with a molecular ion peak of $m/z = 235$. The latter compounds

most likely result from trapping of carbonyl ylide **65** with acrylonitrile by a [3 + 2] cycloaddition, thus yielding tetrahydrofuran derivatives (Scheme 5.4).^{39b,86} A similar result was observed for thermolysis of oxadiazoline **29a** (*vide supra*: Chapter 4.3). Such a formation is supported by methoxy and methyl group signals in the ¹H NMR spectrum of the mixture of these products (Figure A.81, Appendix). Intermediate ylide **65** may be generated by loss of molecular nitrogen from oxadiazoline **39**.

Scheme 5.4: Possible Trapping of Carbonyl Ylide **65** With Acrylonitrile



The yields of the products were determined by GC-MS analysis, using camphor as internal standard (Table 5.3). The yield of **64** was estimated to be 23%, similar to the isolated ones (14-18%). The two minor addition products were formed in about 3 and 4%, respectively. Furthermore, ca. 35% of the rearrangement product was obtained. By comparison, only traces of rearrangement products are formed from the reaction of carbene **14** in acrylonitrile. The products obtained by possible trapping of carbonyl ylide **65** with acrylonitrile were found in a combined yield of 17%.

Table 5.3: GC-MS Analysis of Product Distribution Obtained from Thermolysis of Oxadiazoline **39 in Acrylonitrile**

precursor	substrate	concn (mg/mL)	yield of	yield of	yields of other	yields of
			rearrang. product (%)	product 64 (%)	products with M^+ ; $m/z = 161$ (%)	products with M^+ ; $m/z = 235$ (%)
39	acrylonitrile	10	35	23	3+4	9+2+6

5.3 Reaction in Diethylamine: Insertion Into the N-H Bond

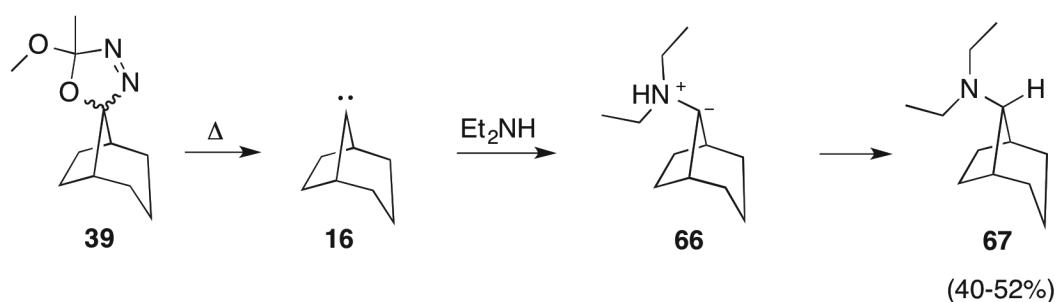
Finally, the reaction of **16** in diethylamine was studied. Under the conditions listed in Table 5.4, *rel*-(1*R*,5*S*,8*r*)-*N,N*-diethylbicyclo[3.2.1]octan-8-amine (**67**) was obtained in yields of 40-52%, which are only slightly lower than those isolated for carbene **14**. The stereochemistry was determined by two-dimensional NMR spectroscopy.

Table 5.4: Isolated Yields of Product 67 Obtained by Thermolysis of Oxadiazoline 39 in Diethylamine

precursor	substrate	concn (mg/mL)	cond	rxn time (h)	yield of product 67 (%)
39	diethylamine	20	Δ	4	40-52

The reaction is suspected to occur through ylide intermediate **66**, followed by a proton transfer to give product **67** (Scheme 5.5). To acquire the obtained stereochemistry of **67**, diethylamine should approach the divalent carbon of **16** from the *anti* side. Thus, **16** displays the same stereoselectivity as carbene **14**. It seems like the calculated bending of only 15° for carbene **16** versus the 33° computed for carbene **14** is sufficient to control the stereoselectivity.

Scheme 5.5: Thermolysis of Oxadiazoline 39 in the Presence of Diethylamine



The GC-MS chromatogram of the product distribution shows that the reaction occurred completely stereoselectively, *i.e.*, only product **67** (Figure 5.2). Some rearrangement product of **16** is observed as well.

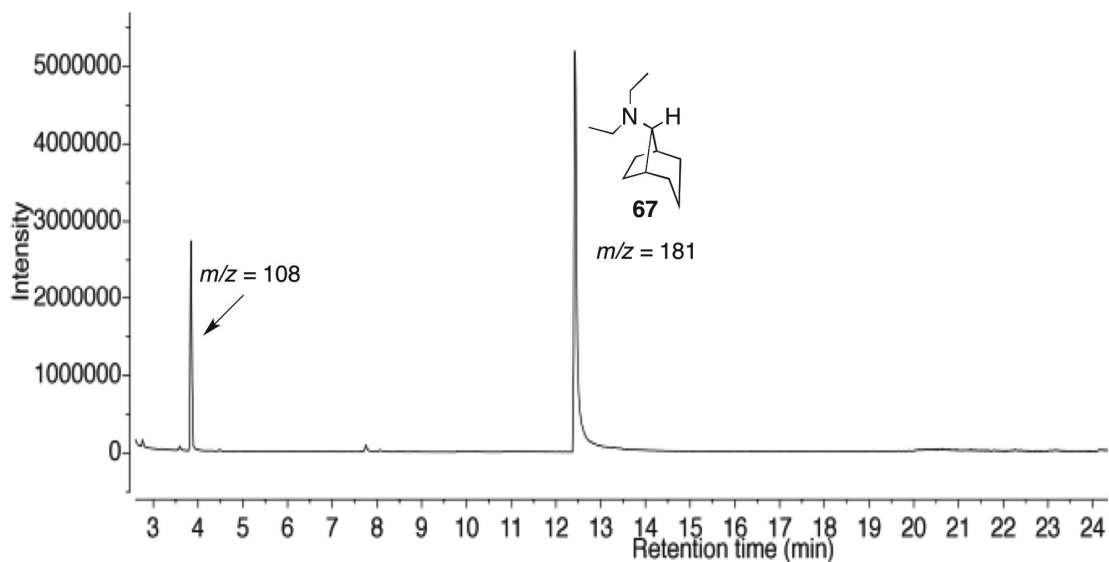


Figure 5.2: GC-MS chromatogram of product distribution obtained by thermolysis of **39** in diethylamine.

Again, the yields were determined by GC-MS analysis (Table 5.4). The yield of the rearrangement product was found to be 20%. Product **67** was estimated to form in a yield of about 70%, somewhat higher than the isolated yield.

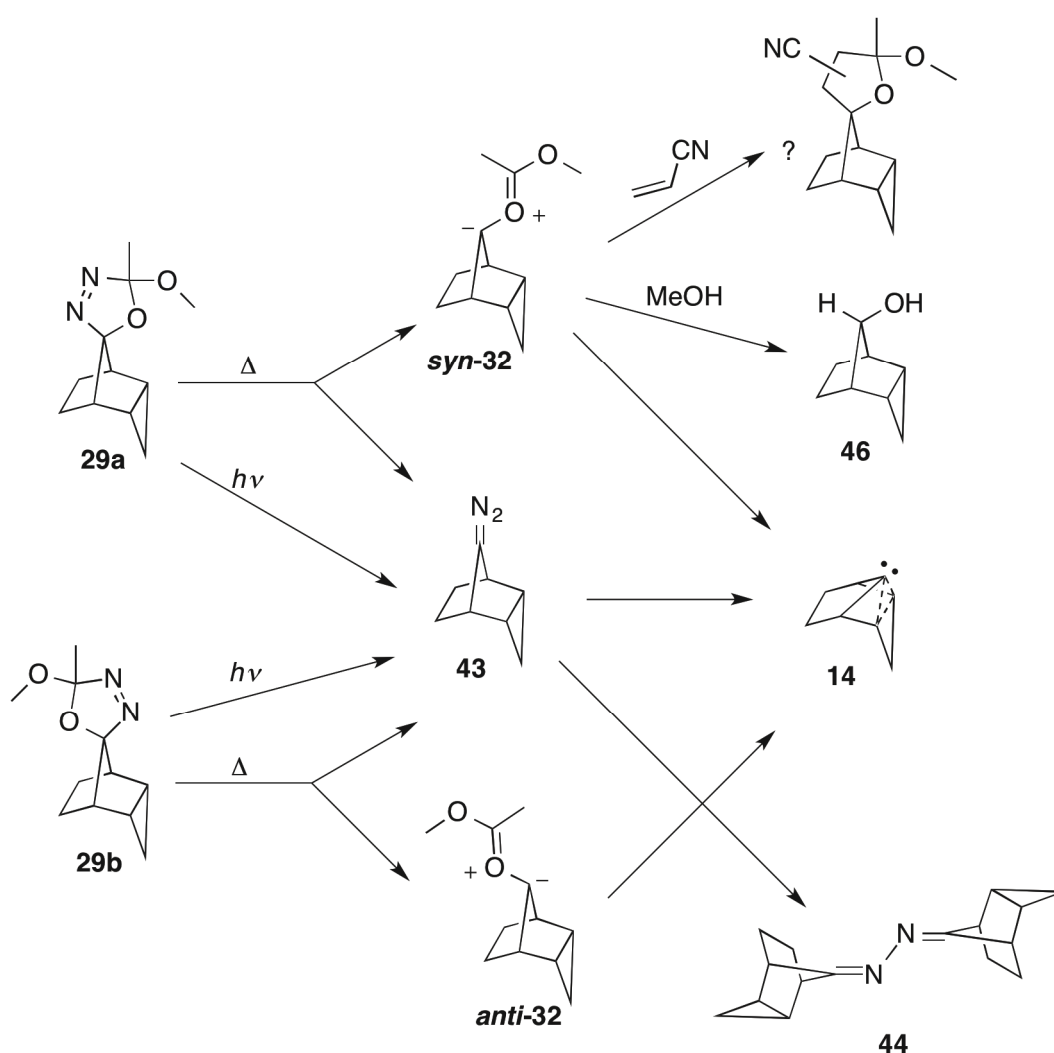
Table 5.4: GC-MS Analysis of Product Distribution Obtained by Thermolysis of Oxadiazoline 39 in Diethylamine

precursor	substrate	concn (mg/mL)	yield of product 67 (%)	yield of rearrang. product (%).
39	diethylamine	11	70	20

6. Conclusions

Oxadiazolines **29a** and **29b** are useful precursors for *endo*-tricyclo[3.2.1.0^{2,4}]octan-8-ylidene (**14**) (Scheme 6.1). They may generate carbene **14** through carbonyl ylides *syn*-**32** and *anti*-**32**, respectively, by initial loss of molecular nitrogen. Alternatively, they can decompose through diazo compound **43** by initial loss of methyl acetate.

Scheme 6.1: Decomposition of **29a** and **29b** by Thermolysis and Photolysis



From thermolysis of **29a**, intermediate *syn*-**32** could be trapped with methanol to give tricyclic alcohol **46**. There are also indications of capture of *syn*-**32** with acrylonitrile. The corresponding carbonyl ylide *anti*-**32** obtained from **29b**, on the other hand, was not trapped under the same conditions. Thus, *anti*-**32** seems to be more labile,

possibly due to destabilization of its negative charge at C₈ by electron donation from the three-membered ring. Furthermore, **29a** decomposes about twice as fast as **29b** at 116 °C. This may be explained by a higher activation energy required for **29b** to form the less stable *anti*-**32** than for **29a** to form *syn*-**32**. An alternative interpretation is that the three-membered ring in **29a** anchimerically assists in the expulsion of molecular nitrogen, due to the *endo,anti* relationship. Otherwise, the two diastereomers **29a** and **29b** show almost identical reactivities.

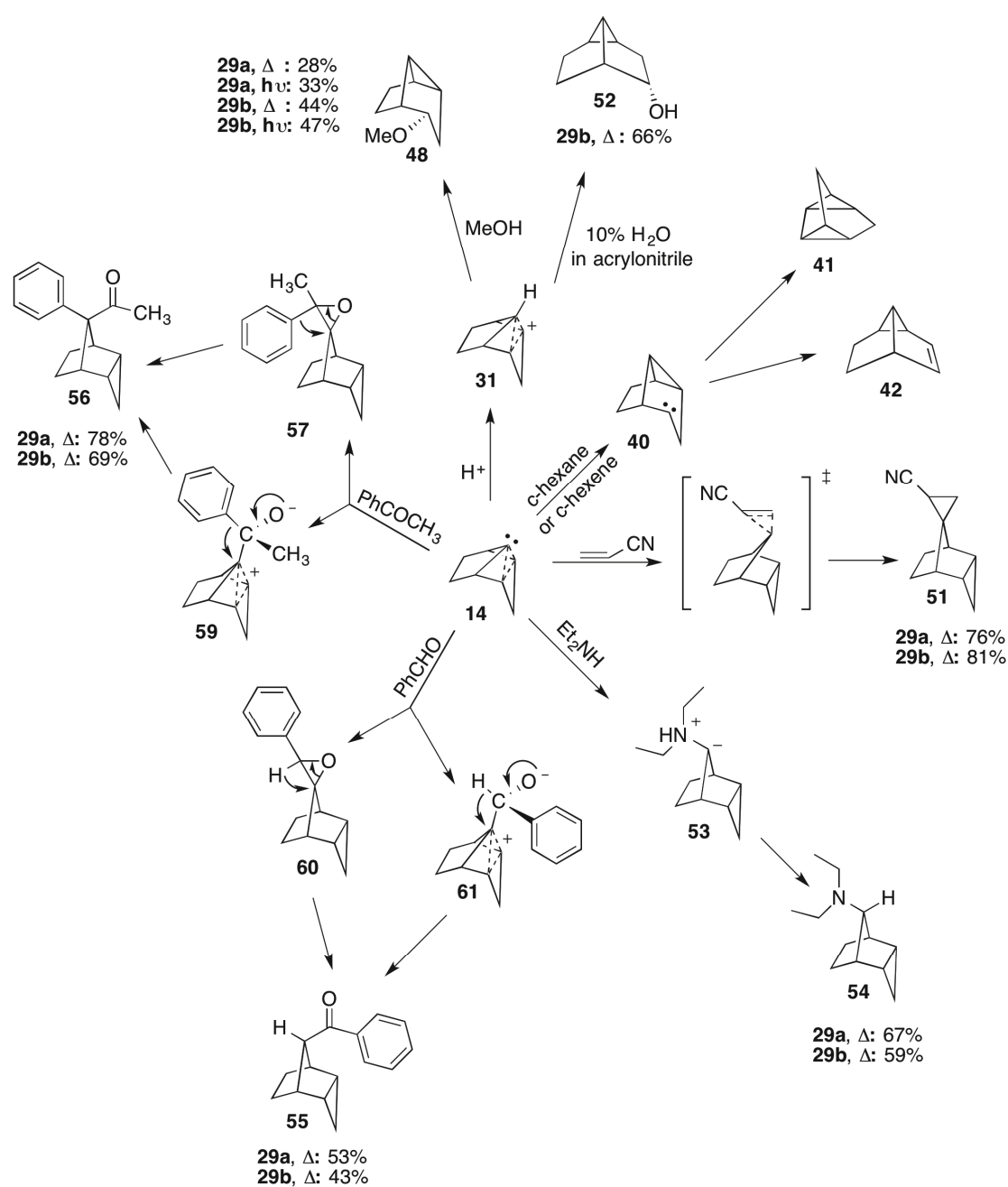
By photolysis, oxadiazolines **29a** and **29b** seem to mainly decompose through diazo compound **43**. This is deduced from the frequent formation of azine **44** in cyclohexane and cyclohexene, which is believed to derive either from a reaction of carbene **14** with **43**, or by cycloaddition of **43** with itself. Intermediate **43** could also be detected under matrix isolation conditions by irradiation at 335 nm, and was identified by an IR band at 2053 cm⁻¹ typical of the N–N-stretching vibration of diazo compounds. The carbonyl intermediates *syn*-**32** and *anti*-**32**, on the other hand, were not observed or trapped during any photolysis experiments (Scheme 6.1).

The reactions carried out in this study support a stabilization of carbene **14**, for which the occupied Walsh orbitals of the three-membered ring donate electron density into the empty p orbital of the divalent carbon. Carbene **14** reacts with a number of different substrates, for which the resulting products and their isolated yields are summarized in Scheme 6.2. Stabilization of **14** is expressed by its sluggish reaction with cyclohexane and cyclohexene. Instead, rearrangement reactions to form products **41** and **42** are preferred. The reluctant addition of **14** to the double bond of cyclohexene and the successful addition to acrylonitrile classify the carbene as a nucleophile.

Due to the donation of electrons from the three-membered ring to the carbenic center of **14**, the bridge containing the divalent carbon bends towards the cyclopropane ring, as in the case for the related norbornen-7-ylidene (**7**). This bending is reflected in intermolecular reactions with acrylonitrile, to give product **51**, and diethylamine, to afford product **54**. In both cases, the substrate approaches the divalent carbon *anti* to the three-membered ring, where more space is available. In the presence of water and

methanol, carbene **14** is protonated, thus giving the nonclassical carbonium ion **31**, for which the positive charge is delocalized between C₂, C₄, and C₈. Subsequent attack by methanol or water at one of the identical C₂ or C₄ atoms yields products **48** and **52**, respectively. In both cases, the substrate is shown to attack from the *endo* direction, as the *exo* face is shielded due to the delocalized, positive charge.

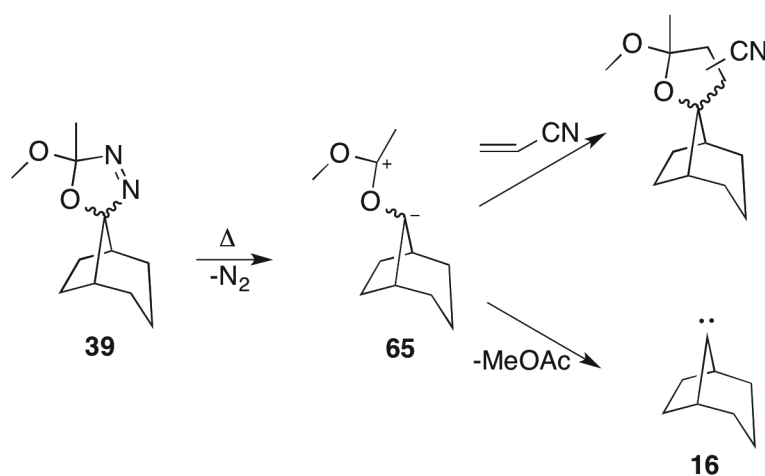
Scheme 6.2: Reactions of Carbene 14 in Cyclohexane, Cyclohexene, Acrylonitrile, Diethylamine, Benzaldehyde, Acetophenone, Methanol, and 10% H₂O in Acrylonitrile



Carbene **14** also reacts with the carbonyl group of benzaldehyde and acetophenone, respectively. In the reaction with benzaldehyde, two products are formed in a ratio of 3:2, for which the major product was identified by single-crystal X-ray analysis as compound **55**. With acetophenone, the reaction occurred more selective with the formation of two products in a ratio of 14:1. The major product was identified as compound **56**. Two possible mechanisms have been suggested. Either the reaction occurs by a [2 + 1] cycloaddition of carbene **14** to the carbonyl group with formation of an epoxide, for which the substrate is approaching the divalent carbon from the *anti* face. This would support a bending of the bridge in carbene **14**. A stereoselective S_N2-like opening of the epoxides through a nucleophilic rearrangement would afford **55** and **56**, respectively. Alternatively carbene **14** may attack the carbonyl carbon to give the corresponding ylides **59** and **61**, respectively. Nonclassical stabilization of the positive charge causes the migrating groups to attack the migration terminus C₈ from the *anti* side. The stereochemistry of the product would then be determined by a nonclassical carbonium ion, instead of a nonclassical carbene. The minor products formed in the reactions are expected to result from competing migrations. Thus, both mechanisms suggested would support a relative migratory aptitude of H > C₆H₅ >> CH₃.

Oxadiazoline **39** was a convenient source for generating carbene **16** by thermolysis. It was employed as a diastereomeric mixture (Scheme 6.3). There were indications of capture of carbonyl ylide intermediate **65** with acrylonitrile. No azine formation could be detected, and thus evidence for the generation of a diazo intermediate was not found.

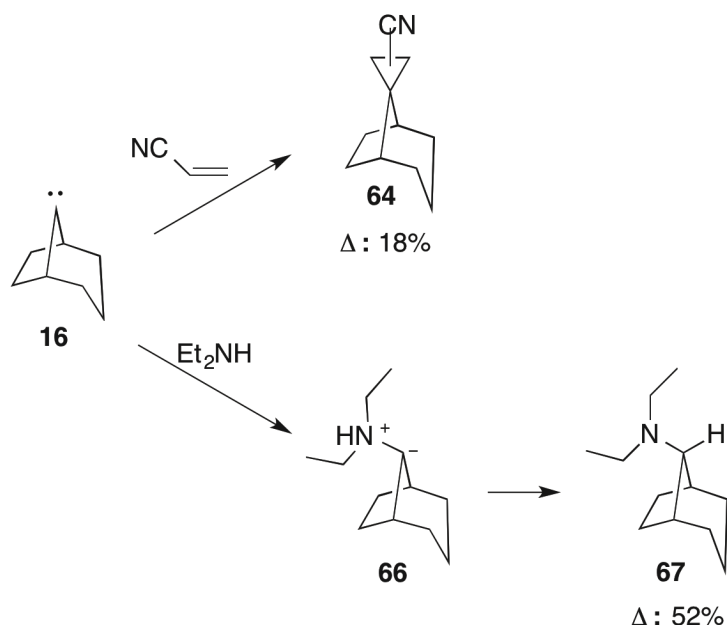
Scheme 6.3: Decomposition of **39** by Thermolysis



In cyclohexane and cyclohexene, carbene **16** undergoes a rearrangement reaction, most likely by an intramolecular 1,3-H insertion. The reluctance to undergo an intermolecular reaction with cyclohexane indicates stabilization for this carbene. However, it may also simply mean that the isomerization reaction is more competitive. The stabilization of **16** is probably resulting from hyperconjugative interaction of the empty p orbital of the divalent carbon with the C-H bonds at C_2 and C_4 . The products detected by GC-MS analysis, which possibly derive from addition reaction of **16** to the double bond of cyclohexene, are obtained in slightly higher yields than those for carbene **14**. Furthermore, carbene **16** adds to acrylonitrile in much lower yields than **14** (Scheme 6.4). This might suggest **16** to be less nucleophilic than **14**, although judging philicity based on yields is not really appropriate. The addition of **16** to acrylonitrile occurred stereoselectively. However, the stereochemistry of the resulting product **64** is not known.

In the reaction with diethylamine, **67** is formed in relatively high yields as the only intermolecular product (Scheme 6.4). Thus, the reaction occurs completely stereoselectively. The stereochemistry of the product suggests diethylamine to approach the carbenic center of **16** from the *anti* face. Hence, the bending of the bridge in **16** seems to be sufficient to secure stereoselectivity.

Scheme 6.4: Reactions of Carbene **16** in Acrylonitrile and Diethylamine



In many ways, carbene **16** behaves similar to carbene **14**. The higher SE calculated for **14** of 14.3 kcal/mol seems to be reflected mainly by a higher nucleophilicity than for carbene **16** (SE = 4.3 kcal/mol). Therefore, the electron donation from the Walsh orbitals in **14** should be more potent than the electron donation by hyperconjugation in **16**. Even if **14** is calculated to bend towards its stabilizing moiety to a higher degree than **16**, *i.e.*, 32.7° and 15.0°, respectively, both carbenes react stereoselectively in intermolecular reactions.

Although carbene **16** exhibits a similar chemistry as carbene **14**, it is not a foiled carbene by definition. In contrast to the group of foiled carbenes, it may react with its stabilizing moiety, *i.e.*, it may insert into the C-H bonds at C₂ and C₄. The difference of reactivity seems to be mainly expressed by more competitive rearrangement reactions for **16** and a seemingly lower degree of nucleophilicity.

Replacing the CH=CH unit in norbornen-7-ylidene (**7**) with an *endo*-fused cyclopropane ring, as in carbene **14**, leads to a comparable reactive behavior. Thus, on the basis of the experiments outlined in this study, carbene **14** rightfully belongs to the family of foiled carbenes.

Further research on this project should involve mechanistic studies for the reactions of carbene **14** with benzaldehyde and acetophenone, for instance by DFT calculations of the corresponding transition states and by isolation of the minor products formed. Furthermore, additional reactions should be carried out to better distinguish between the reactivity of carbenes **14** and **16** to underline why one is a foiled carbene and the other is not. There are still a number of experiments that should be carried out to map the reactive behavior of foiled carbenes. This is interesting especially from a mechanistic aspect, but also, from a synthetic one. These reactions seem to give access to otherwise difficult to achieve products, proceeding with a high diastereoselectivity.

7. Experimental

7.1 Equipment and Methods

Melting point

Melting points were measured on a melting point microscope and are uncorrected.

Spectroscopy

The NMR spectra were obtained on either a DRX 400 WB instrument, operating at a frequency of 400.13 MHz for ^1H and 100.62 MHz for ^{13}C , or a DRX 600 at a frequency of 600.13 MHz for ^1H and 150.92 for ^{13}C . Routine measurements were carried out with an AV400 instrument, operating at a frequency of 400.27 MHz for ^1H and 100.66 MHz for ^{13}C . The chemical shifts are given in ppm with respect to TMS. For the ^1H NMR spectra, the residual peak of CDCl_3 ($\delta_{\text{H}} = 7.26$ ppm) or cyclohexane- d_{12} ($\delta_{\text{H}} = 1.38$ ppm) was used as an internal standard. The coupling constants are reported in Hertz (Hz). Multiplicities are written as (s) for singlet, (d) for doublet, (t) for triplet, (q) for quartet, and (m) for multiplet. For the ^{13}C NMR spectra, the central peak of the CDCl_3 triplet ($\delta_{\text{C}} = 77.16$ ppm) was used as an internal standard. Conventional gradient-enhanced two-dimensional COSY, NOESY, HMBC, and HMQC spectra were used to derive proton and carbon assignments. The diffusion edited NMR experiments were done on the DRX 600 instrument, where a longitudinal eddy current delay sequence with 1 ms smoothed square bipolar gradient pulse pairs¹⁰³ was used, with a diffusion delay set to 100 ms. Two spectra were recorded, one with 3% and the second with 73% gradient amplitude. The resulting ^1H NMR spectra were subtracted by scaling the signal intensity of the background signals to equal heights.

Infrared spectra were measured with an ATR attachment, and the absorptions are given in wavenumbers (cm^{-1}). The intensities are given as (s) for strong, (m) for medium, (w) for weak, and (br) for broad.

UV spectra were obtained on an UV-VIS spectrometer with a double-grid monochromator and a wavelength range from 190 to 900 nm.

Spectrometry

GC-MS data were obtained using an instrument equipped with a mass selective detector (70 eV) on a 30 m × 0.25 mm HP-5MS poly(methylphenylsiloxane) (95% dimethyl and 5% diphenyl, 0.25 μm film-thickness) capillary column using helium as carrier gas. The spectra are reported as m/z (% relative intensity).

General Settings for GC-MS Analysis:

Method 1: Pressure: 0.416 bar. Flow: 0.7 mL/min. Average velocity: 32 cm/s. Injection volume: 1.0 μL. Split ratio: 25:1. Injection temperature: 270 °C. Starting temperature: 80 °C for 2 min. Ramp: 5 °C/min up to 145 °C. Ramp: 15 °C/min up to 220 °C. Isotherm: 220 °C for 3 min. Ramp: 15 °C/min up to 270 °C. Isotherm: 270 °C for 3 min.

Method 2: Pressure: 0.417 bar. Flow: 0.7 mL/min. Average velocity: 32 cm/s. Injection volume: 1.0 μL. Split ratio: 100:1. Injection temperature: 160 °C. Starting temperature: 80 °C for 2 min. Ramp: 5 °C/min up to 145 °C. Ramp: 15 °C/min up to 220 °C. Isotherm: 220 °C for 3 min. Ramp: 15 °C/min up to 270 °C. Isotherm: 270 °C for 3 min.

Method 3: Pressure: 0.423 bar. Flow: 0.7 mL/min. Average velocity: 32 cm/s. Injection volume: 1.0 μL. Split ratio: 100:1. Injection temperature: 270 °C. Starting temperature: 80 °C for 2 min. Ramp: 5 °C/min up to 145 °C. Ramp: 15 °C/min up to 220 °C. Isotherm: 220 °C for 3 min. Ramp: 15 °C/min up to 270 °C. Isotherm: 270 °C for 3 min.

HRMS was performed either on a mass spectrometer outfitted with a Time-of-Flight (TOF) analyzer using ESI techniques, or a double-focusing sector field analyzer using EI (70 eV) techniques.

Elemental analysis

The elemental analyses were carried out at the Microanalytical Laboratory at the University of Vienna.

X-ray crystallography

Single-crystal X-ray analyses were obtained on an X8 APEXII CCD diffractometer equipped with an M86-E00034 Kryo-Flex Low Temperature Device (temperature range: 90-300 K).

Photolysis

Photolysis experiments were carried out using a medium pressure mercury lamp doped with FeI_2 (700 W, $\lambda_{\text{max}} = 370$ nm), which was placed in a water-cooled jacket made of quartz.

Chromatography

Analytical TLC were performed on aluminum plates with silica gel 60 F₂₅₄, and detection was obtained with an iodine chamber or a UV lamp at $\lambda = 254$ nm. Flash chromatography was conducted using silica gel 60 (230-400 mesh) as stationary phase with hexane, ethyl acetate, and dichloromethane in different ratios as mobile phase.

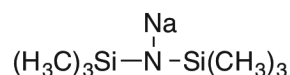
Chemicals

Dry toluene and pentane was obtained by distillation from calcium hydride. Dry THF was obtained by distillation from sodium. Cyclohexane, cyclohexene, acrylonitrile, diethylamine, methanol, and benzaldehyde were distilled and dried over molecular sieves (3 Å or 4 Å) before use. Commercially available compounds were used without further purification. Argon was used for inert atmosphere.

7.2 Procedures and Analytical Data

7.2.1 Preparation of Oxadiazoline Carbene Precursors

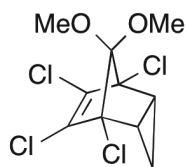
Sodium bis(trimethylsilyl)amide.



Sodium amide (25.6 g, 0.656 mol), hexamethyldisilazane (150 mL, 0.719 mol, 1.1 mol equiv), and dry toluene (150 mL) were added to a 500-mL, three-necked flask under argon equipped with a septum, a mechanical stirrer, and a condenser. The reaction mixture was heated to reflux and stirred for 24 h. The toluene was removed by distillation using a water-vacuum pump, bp. 40 °C at 58 mmHg (lit. bp. 111 °C/760 mmHg).¹⁰⁴ The product was dried overnight using a vacuum pump (0.05 mmHg) to give the title compound (105.6 g, 88%) as a white solid. Spectroscopic data were in agreement with the IR spectrum found in the Integrated Spectral Database System of Organic Compounds (National Institute of Advanced Industrial Science and Technology, Japan).

IR: ν 2948 (m, br), 2324 (w), 2249 (w), 1981 (w), 1608 (w), 1440 (m), 1244 (m), 1180 (w), 1025 (m), 930 (m), 877 (m), 821 (s), 678 (m) cm^{-1} .

endo-8,8-Dimethoxy-1,5,6,7-tetrachlorotricyclo[3.2.1.0^{2,4}]oct-6-ene (22).

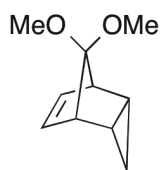


Sodium bis(trimethylsilyl)amide (60.5 g, 0.330 mol) and dry toluene (150 mL) were mixed in a 250-mL, three-necked flask under argon equipped with a septum, a stopper, and a cooler. The mixture was heated to 145 °C to give a vigorous reflux.

Allyl chloride (24.0 mL, 0.295 mol, 0.9 mol equiv) was added dropwise over a period of 1.5 h and the mixture was left boiling for another 30 min. At the top of the cooler was an outlet tube that led the formed cyclopropene into a 50-mL, two-necked flask charged with 5,5-dimethoxy-1,2,3,4-tetrachlorocyclopentadiene (19.5 g, 0.074 mol) and dry pentane (30 mL). The two-necked flask was held at room temperature and was equipped with a cold trap held at -78 °C by a mixture of dry ice and acetone. After completion of the reaction, the pentane was removed on a rotary evaporator. The product was further dried on a vacuum pump (0.05 mmHg) to give the title compound (22.0 g, 98%) as a white solid. Spectroscopic data were in agreement with the literature.^{66e-h}

¹H NMR (400.27 MHz, CDCl₃): δ 3.64 (s, 3H), 3.52 (s, 3H), 1.84-1.80 (dd, *J* = 7.1 Hz (d), 3.5 Hz (d), 2H), 0.96-0.90 (dt, *J* = 7.6 Hz (d), 7.1 Hz (t), 1H), 0.47-0.42 (td, *J* = 3.5 Hz (t), 7.6 Hz (d), 1H) ppm. ¹³C NMR (100.66 MHz, CDCl₃): δ 127.0 (2xC), 121.4 (C), 75.0 (2xC) 52.2 (2xCH₃), 20.0 (2xCH), 14.0 (CH₂) ppm. IR: ν 2951 (w), 2845 (w), 1599 (m), 1316 (w), 1275 (m), 1183 (s), 1153 (s), 1118 (s), 1058 (m), 1024 (m), 1002 (s), 980 (s), 929 (m), 890 (w), 848 (m), 791 (s), 758 (s), 696 (m), 665 (m), 627 (w) cm⁻¹. MS (EI, 70 eV): *m/z* 304 [M]⁺ (<1), 269 (89), 267 (91), 254 (9), 232 (20), 220 (100), 207 (26), 193 (49), 171 (52), 159 (31), 123 (33), 109 (11), 97 (11), 87 (11), 73 (11), 59 (24).

***endo*-8,8-Dimethoxytricyclo[3.2.1.0^{2,4}]oct-6-ene (23).**

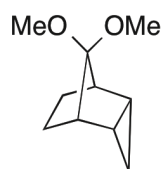


endo-8,8-Dimethoxy-1,5,6,7-tetrachlorotricyclo[3.2.1.0^{2,4}]oct-6-ene (**22**) (14.4 g, 47.4 mmol), *tert*-butyl alcohol (38.0 g, 0.513 mol, 11 mol equiv), and dry tetrahydrofuran (200 mL) were added to a 250-mL, three-necked flask equipped with a septum, a mechanical stirrer, and a condenser. Argon gas was used for an inert atmosphere. Finely cut sodium (24 g) was added, and the reaction mixture was refluxed for 4 h. The mixture was cooled to 0 °C and methanol (100 mL) was added to destroy excess

sodium. The reaction mixture was transferred to a separation funnel using water (400 mL) and dichloromethane (400 mL). The two phases were separated, followed by extraction of the aqueous phase with dichloromethane (3 x 200 mL). The combined organic extracts were dried (MgSO₄), filtered, and concentrated. The product was isolated by flash chromatography using hexane/ethyl acetate (8:2) to give the title compound (4.95 g, 63%) as a yellow liquid. Spectroscopic data were in agreement with the literature.^{66e-h}

¹H NMR (400.27 MHz, CDCl₃): δ 5.73 (m, 2H), 3.25 (s, 3H), 3.11 (s, 3H), 2.88-2.84 (m, 2H), 1.27-1.22 (m, 2H), 0.57-0.51 (m, 1H), 0.41-0.37 (m, 1H) ppm. ¹³C NMR (100.66 MHz, CDCl₃): δ 129.5 (C), 127.8 (2xCH), 52.2 (CH₃), 50.4 (CH₃), 45.3 (2xCH), 12.0 (CH₂), 7.2 (2xCH) ppm. IR: ν 3063 (w), 2981 (m), 2948 (m), 2828 (m), 1453 (w), 1434 (w), 1334 (w), 1262 (s), 1211 (m), 1166 (m), 1106 (s), 1067 (s), 1021 (m), 898 (m), 864 (w), 809 (m), 755 (m), 714 (m), 666 (m), 554 (m) cm⁻¹. MS (EI, 70 eV): *m/z* 166 [M]⁺ (5), 165 (27), 135 (5), 119 (40), 105 (11), 91 (100), 77 (12), 65 (18), 59 (19). HRMS (ESI) *m/z*: [M + Na]⁺ calcd for C₁₀H₁₄O₂Na 189.0891; found 189.0884.

***endo*-8,8-Dimethoxytricyclo[3.2.1.0^{2,4}]octane (24).**



endo-8,8-Dimethoxytricyclo[3.2.1.0^{2,4}]oct-6-ene (**23**) (7.69 g, 46.3 mmol), sodium carbonate (3.40 g), and 10% palladium on charcoal (0.680 g) were dissolved in dry ethanol (150 mL). Hydrogenation was carried out at room temperature for 5 h. After the completion of the reaction, argon was bubbled into the mixture. The reaction mixture was transferred to a separation funnel using water (200 mL) and dichloromethane (200 mL). The two phases were separated, followed by extraction of the aqueous phase with dichloromethane (4 x 100 mL). The combined organic extracts were dried (MgSO₄), filtered, and concentrated. The title compound (7.12 g,

91%) was obtained as a colorless liquid. Spectroscopic data were in agreement with the literature.^{66e-h}

¹H NMR (400.27 MHz, CDCl₃): δ 3.33 (s, 3H), 3.22 (s, 3H), 2.15-2.10 (m, 2H), 1.63-1.57 (m, 2H), 1.33-1.27 (m, 2H), 1.03-0.98 (m, 2H), 0.97-0.93 (m, 1H), 0.77-0.71 (m, 1H) ppm. ¹³C NMR (100.66 MHz, CDCl₃): δ 124.7 (C), 51.3 (CH₃), 50.6 (CH₃), 38.0 (2xCH), 24.7 (2xCH₂), 17.4 (2xCH), 13.1 (CH₂) ppm. IR: ν 2963 (m), 2828 (w), 1473 (w), 1450 (w), 1312 (w), 1284 (m), 1212 (m), 1178 (w), 1142 (s), 1124 (m), 1100 (s), 1062 (s), 1021 (s), 982 (m), 925 (m), 842 (w), 789 (m), 765 (m) cm⁻¹. MS (EI, 70 eV): *m/z* 168 [M]⁺ (<1), 137 (5), 114 (9), 109, (3), 101 (100), 91 (7), 77 (9), 55 (19).

***endo*-Tricyclo[3.2.1.0^{2,4}]octan-8-one (25).**

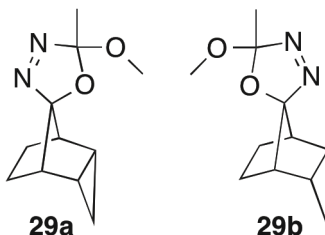


endo-8,8-Dimethoxytricyclo[3.2.1.0^{2,4}]octane (**24**) (4.71 g, 28.0 mmol), *p*-toluenesulfonic acid (0.53 g, 2.8 mmol, 10 mol %) and tetrahydrofuran-water (200 mL, 3:2) were mixed and refluxed overnight. Tetrahydrofuran was removed on a rotary evaporator. The reaction mixture was transferred to a separation funnel using water (50 mL) and dichloromethane (100 mL). The two phases were separated, followed by extraction of the aqueous phase with dichloromethane (2 x 100 mL). The combined organic phases were dried (MgSO₄), filtered, and concentrated. The product was isolated by flash chromatography using hexane/ethyl acetate (8:2) to give the title compound (2.73 g, 80%) as a yellow liquid. Spectroscopic data were in agreement with the literature.^{66f-h}

¹H NMR (400.27 MHz, CDCl₃): δ 2.21-2.10 (m, 2H), 1.70-1.59 (m, 2H), 1.33-1.24 (m, 2H), 1.18-1.08 (m, 2H), 1.02-0.92 (m, 1H), 0.79-0.72 (m, 1H) ppm. ¹³C NMR (100.66 MHz, CDCl₃): δ 204.2 (C), 38.1 (2xCH), 20.9 (2xCH₂), 8.6 (2xCH), 6.3 (CH₂) ppm. IR: ν 2997 (w), 2958 (w), 2879 (w), 1826 (w), 1755 (s), 1475 (w), 1434

(w), 1304 (w), 1182 (w), 1119 (m), 1037 (m), 946 (w), 933 (w), 837 (w), 796 (w), 749 (m), 730 (m) cm^{-1} . MS (EI, 70 eV): m/z 122 $[\text{M}]^+$ (6), 94 (90), 91 (44), 79, (100), 66 (59), 55 (39), 51 (18).

***rac*-(1'*R*,2'*R*,4'*S*,5'*S*)-5-Methoxy-5-methylspiro[2,5-dihydro-1,3,4-oxadiazole-2,8'-tricyclo[3.2.1.0^{2,4}]octane] (29).**



Method 1: *endo*-Tricyclo[3.2.1.0^{2,4}]octan-8-one (**25**) (1.830 g, 14.98 mmol) and acetyl hydrazide (1.225 g, 16.54 mmol, 1.1 mol equiv) were dissolved in dry methanol (100 mL) and refluxed for 3 h. The reaction mixture was cooled to 0 °C and (diacetoxyiodo)benzene (5.308 g, 16.48 mmol, 1.1 mol equiv) was added over a period of 5 min. The mixture was left stirring overnight as the ice bath melted. The solvent was removed on a rotary evaporator and the product was isolated as a diastereomeric mixture (dr = 1:1.7) by column chromatography using hexane/ethyl acetate (4:1) as eluant to give **29** (2.594 g, 83%). The two diastereomers were separated by column chromatography using hexane/dichloromethane (2:3) as eluant affording **29a** and **29b** as white solids.

Method 2: *endo*-Tricyclo[3.2.1.0^{2,4}]octan-8-one (**25**) (0.100 g, 0.819 mmol) and acetyl hydrazide (0.066 g, 0.891 mmol, 1.1 mol equiv) were dissolved in dry methanol (12 mL) and stirred on an ice bath for 22 h. (Diacetoxyiodo)benzene (0.263 g, 0.817 mmol) was added over a period of 5 min. The solvent was removed on a rotary evaporator and the product was isolated as a diastereomeric mixture (dr = 1:1.7) by column chromatography using hexane/ethyl acetate (4:1) as eluant to give **29** (0.112 g, 66%).

rel-(1'*R*,2'*r*,2'*R*,4'*S*,5'*R*,5'*S*)-5-Methoxy-5-methylspiro[2,5-dihydro-1,3,4-oxadiazole-2,8'-tricyclo[3.2.1.0^{2,4}]octane] (**29a**): mp: 35–39 °C. ¹H NMR (400.13 MHz, CDCl₃): δ 3.09 (s, 3H), 2.38-2.16 (m, 3H), 2.03-1.97 (m, 1H), 1.68-1.59 (m, 2H), 1.63 (s, 3H), 1.44–1.34 (m, 3H), 1.06-1.01 (dt, *J* = 7.4 Hz (t), 6.5 Hz (d), 1H) ppm. ¹³C NMR (100.62 MHz, CDCl₃): δ 142.3 (C), 130.2 (C), 50.2 (CH₃), 45.0 (CH), 43.7 (CH), 24.3 (CH₂), 24.1 (CH₂), 23.1 (CH₃), 20.7 (CH), 20.6 (CH), 16.7 (CH₂) ppm. IR: ν 3069 (w), 2964 (m), 2880 (w), 1568 (w), 1477 (w), 1446 (w), 1377 (m), 1309 (w), 1240 (m), 1203 (s), 1131 (s), 1081 (m), 1045 (s), 987 (w), 927 (s), 907 (s), 872 (s), 787 (w), 760 (m) cm⁻¹. MS (EI, 70 eV): *m/z* 208 [M]⁺ (<1), 177 (7), 153 (4), 115 (6), 105 (38), 91 (100), 78 (48), 65 (10), 51 (7). HRMS (ESI) *m/z*: [M + H]⁺ calcd for C₁₁H₁₇N₂O₂ 209.1290; found 209.1289. Anal. Calcd for C₁₁H₁₆N₂O₂: C, 63.44; H, 7.74; N, 13.45; O, 15.37. Found: C, 63.76; H, 7.61; N, 13.34; O, 15.21.

rel-(1'*R*,2'*s*,2'*R*,4'*S*,5'*R*,5'*S*)-5-Methoxy-5-methylspiro[2,5-dihydro-1,3,4-oxadiazole-2,8'-tricyclo[3.2.1.0^{2,4}]octane] (**29b**): mp: 54–58 °C. ¹H NMR (400.13 MHz, CDCl₃): δ 3.05 (s, 3H), 2.26-2.21 (m, 1H), 2.05-1.99 (m, 1H), 1.83-1.73 (m, 3H), 1.72-1.64 (m, 1H), 1.58 (s, 3H), 1.39-1.24 (m, 2H), 1.17-1.11 (m, 1H), 0.95-0.88 (m, 1H) ppm. ¹³C NMR (100.62 MHz, CDCl₃): δ 141.1 (C), 131.8 (C), 50.1 (CH₃), 44.7 (CH), 43.4 (CH), 25.8 (CH₂), 25.7 (CH₂), 23.0 (CH₃), 16.9 (CH), 16.6 (CH), 12.2 (CH₂) ppm. IR: ν 3024 (w), 2966 (m), 2877 (w), 1560 (w), 1472 (w), 1448 (w), 1376 (m), 1313 (w), 1238 (m), 1201 (s), 1138 (s), 1083 (m), 1051 (s), 977 (w), 913 (s), 869 (m), 791 (m), 761 (m) cm⁻¹. MS (EI, 70 eV): *m/z* 208 [M]⁺ (<1), 177 (9), 153 (5), 115 (6), 105 (38), 91 (100), 78 (45), 65 (8), 51 (6). HRMS (EI, 70 eV) *m/z*: [M]⁺ calcd for C₁₁H₁₆N₂O₂ 208.1212; found 208.1215. Anal. Calcd for C₁₁H₁₆N₂O₂: C, 63.44; H, 7.74; N, 13.45; O, 15.37. Found: C, 63.65; H, 7.63; N, 13.31; O, 14.93.

***endo*-Tricyclo[3.2.1.0^{2,4}]oct-6-en-8-one (33).**



Aqueous perchloric acid (3M, 2 mL) and tetrahydrofuran (3 mL) were cooled to -10 °C. *endo*-8,8-Dimethoxytricyclo[3.2.1.0^{2,4}]oct-6-ene (**23**) (0.231 g, 1.39 mmol) dissolved in tetrahydrofuran (1 mL) was added dropwise. The bath was cooled to -15 °C, and the mixture was stirred for 4 h. After neutralization with solid sodium bicarbonate and addition of water (10 mL), the mixture was extracted with diethyl ether (2 x 15 mL). The combined organic phases were washed with saturated, aqueous sodium carbonate (5 mL), dried (MgSO₄), filtered, and concentrated under reduced pressure at 0 °C, giving the title compound as a liquid. Spectroscopic data were in agreement with the literature.^{66e,73b,105}

¹H NMR (400.27 MHz, CDCl₃): δ 6.00-5.91 (m, 2H), 3.15-3.06 (m, 2H), 1.47-1.37 (m, 2H), 0.73-0.64 (m, 1H), 0.16-0.05 (m, 1H) ppm. ¹³C NMR (100.66 MHz, CDCl₃): δ 184.3 (C), 126.6 (2xCH), 46.0 (2xCH), 3.5 (2xCH), 2.2 (CH₂) ppm.

Hydrolysis of *endo*-8,8-Dimethoxytricyclo[3.2.1.0^{2,4}]oct-6-ene (23**).**

endo-8,8-Dimethoxytricyclo[3.2.1.0^{2,4}]oct-6-ene (**23**) (2.173 g, 13.07 mmol), *p*-toluenesulfonic acid (0.018 g, 0.094 mmol, 1 mol %) and tetrahydrofuran-water (10 mL, 3:2) were mixed and refluxed for 2 h. Tetrahydrofuran was removed on a rotary evaporator. The reaction mixture was transferred to a separation funnel using water and dichloromethane. The two phases were separated, followed by extraction of the aqueous phase with dichloromethane. The combined organic phases were dried (MgSO₄), filtered, and concentrated, giving cyclohepta-1,3,5-triene (**34**) (0.385 g, 32%) as a liquid. Spectroscopic data were in agreement with the ¹H NMR spectrum found in the Integrated Spectral Database System of Organic Compounds (National Institute of Advanced Industrial Science and Technology, Japan).

¹H NMR (400.27 MHz, CDCl₃): δ 6.65-6.96 (m, 2H), 6.25-6.16 (m, 2H), 5.44-5.34 (m, 2H), 2.32-2.23 (m, 2H) ppm.

Spiro[bicyclo[3.2.1]octane-8,2'-[1.3]dioxolane (36).



Spiro[bicyclo[3.2.1]oct-2-ene-8,2'-[1.3]dioxolane] (**35**) (2.53 g, 15.2 mmol), sodium carbonate (1.13 g), and 10% palladium on charcoal (0.232 g) were dissolved in dry ethanol (60 mL). Hydrogenation was carried out at room temperature for 4 h. After completion of the reaction, argon was bubbled into the mixture. The reaction mixture was transferred to a separation funnel using water (200 mL) and dichloromethane (200 mL). The two phases were separated, followed by extraction of the aqueous phase with dichloromethane (3 x 100 mL). The combined organic extracts were dried (MgSO_4), filtered, and concentrated. The title compound (2.33 g, 91%) was obtained as a colorless liquid. Spectroscopic data were in agreement with the literature.¹⁰⁶

^1H NMR (400.27 MHz, CDCl_3): δ 3.29-3.88 (m, 4H), 1.89-1.75 (m, 6H), 1.48-1.32 (m, 6H) ppm. ^{13}C NMR (100.66 MHz, CDCl_3): δ 117.2 (C), 64.8 (CH_2), 63.6 (CH_2), 839.4 (2xCH), 29.4 (2x CH_2), 25.2 (2x CH_2) 16.7 (CH_2) ppm. MS (EI, 70 eV): m/z 168 $[\text{M}]^+$ (68), 153 (8), 139 (35), 125, (100), 113 (24), 99 (65), 80 (20), 67 (14), 55 (33).

Bicyclo[3.2.1]octane-8-one (37).

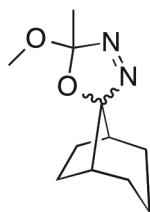


Spiro[bicyclo[3.2.1]octane-8,2'-[1.3]dioxolane (**36**) (2.30 g, 13.7 mmol), *p*-toluenesulfonic acid (0.266 g, 1.40 mmol, 10 mol %), and tetrahydrofuran-water (100 mL, 3:2) were mixed and refluxed overnight. Tetrahydrofuran was removed on a rotary evaporator. The reaction mixture was transferred to a separation funnel using dichloromethane (100 mL). The two phases were separated, followed by extraction of

the aqueous phase with dichloromethane (3 x 100 mL). The combined organic phases were dried (MgSO₄), filtered, and concentrated, giving the title compound (1.31 g, 77 %) as a yellow white solid. Spectroscopic data were in agreement with the literature.¹⁰⁶⁻¹⁰⁷

¹H NMR (400.27 MHz, CDCl₃): δ 2.28-2.20 (m, 2H), 2.02-1.80 (m, 7H), 1.79-1.73 (m, 2H), 1.60-1.51 (m, 1H) ppm. ¹³C NMR (100.66 MHz, CDCl₃): δ 45.1 (2xCH), 37.2 (2xCH₂), 22.9 (2xCH₂), 17.6 (CH₂) ppm (signal of carbonyl carbon (222.9 ppm)¹⁰⁷ lies outside of the measured range, *i.e.* -20 to 220 ppm). IR: ν 2932 (m), 2873 (m), 2856 (m), 1738 (s), 1475 (w), 1452 (m), 1282 (m), 1235 (w), 1189 (m), 1076 (m), 1001 (m), 958 (m), 824 (w), 766 (w), 694 (w) cm⁻¹. MS (EI, 70 eV): *m/z* 124 [M]⁺ (95), 106 (14), 95 (24), 91, (13), 81 (93), 78 (62), 67 (100), 54 (92) 51 (6).

***rac*-(1*R*,5*S*)-5'-Methoxy-5'-methylspiro[bicyclo[3.2.1]octane-8,2'-2,5-dihydro-1,3,4-oxadiazole] (39).**



Bicyclo[3.2.1]octane-8-one (**37**) (1.272 g, 10.24 mmol) and acetyl hydrazide (0.843 g, 11.38 mmol) were dissolved in dry methanol (80 mL) and refluxed for 4 h. Methanol was removed on a rotary evaporator. The residue was dissolved in dry methanol (80 mL) and the mixture was cooled to 0 °C. (Diacetoxyiodo)benzene (3.430 g, 10.65 mmol) was added over a period of 5 min. The mixture was left stirring for 15 min. The solvent was removed on a rotary evaporator and the product was isolated as a diastereomeric mixture (dr = 2.3:1) by column chromatography using dichloromethane/ethyl acetate (3:2) as eluant to give the title compound (1.803 g, 84%) as a colorless liquid.

¹H NMR (400.13 MHz, CDCl₃): δ 3.05 and 3.04 (2s in a ratio of 2.3:1, 3H), 2.54-2.21 (m, 2H), 2.17-2.11 (m, 1H), 2.00-1.79 (m, 3H), 1.76-1.41 (m, 6H), 1.59 and 1.58 (2s

in a ratio of 1:2.3, 3H) ppm. ^{13}C NMR (100.62 MHz, CDCl_3): δ 132.0 and 130.9 (C), 129.6 and 129.6 (C), 50.2 and 50.1 (CH_3), 45.9 and 41.1 (CH), 43.9 and 39.8 (CH), 30.0 and 25.6 (CH_2), 29.9 and 25.3 (CH_2), 28.1 and 27.7 (CH_2), 27.8 and 27.6 (CH_2), 23.9 and 23.3 (CH_3), 17.4 and 16.7 (CH_2) ppm. IR: ν 2941 (m), 2834 (m), 1568 (w), 1453 (m), 1202 (m), 1155 (m), 1099 (m), 1070 (m), 1055 (m), 970 (w), 939 (m), 907 (s), 868 (m), 831 (w), 735 (w), 648 (w) cm^{-1} . MS (major diastereomer) (EI, 70 eV): m/z 179 [$\text{M} - \text{OMe}$] $^+$ (18), 167 (10), 139 (4), 125 (51), 109 (24), 93 (43), 79 (100), 67 (34), 55 (17). MS (minor diastereomer) (EI, 70 eV): m/z 179 [$\text{M} - \text{OMe}$] $^+$ (25), 167 (4), 139 (6), 125 (87), 109 (39), 93 (31), 79 (100), 67 (51), 55 (23). HRMS (ESI) m/z : [$\text{M} + \text{Na}$] $^+$ calcd for $\text{C}_{11}\text{H}_{18}\text{N}_2\text{O}_2\text{Na}$ 233.1266; found 233.1257. Anal. Calcd for $\text{C}_{11}\text{H}_{18}\text{N}_2\text{O}_2$: C, 62.83; H, 8.63; N, 13.32; O. Found: C, 63.20; H, 8.39; N, 12.93.

7.2.2 Reactions of *endo*-Tricyclo[3.2.1.0^{2,4}]octan-8-ylidene (14)

General Procedure for GC-MS Analysis of Thermolysis and Photolysis of Oxadiazoline 29a and 29b in Cyclohexane, Cyclohexene, and Methanol.

For thermolysis, the oxadiazoline was dissolved in cyclohexane, cyclohexene, or methanol and stirred in a pressure tube at 165 °C for 3-6 h. For photolysis, the oxadiazoline was dissolved in cyclohexane, cyclohexene, or methanol within a round-bottomed flask equipped with a rubber septum. The solution was degassed with argon and subjected to photolysis for 6-15 h. The temperature was controlled with a water bath. Prior to GC-MS analysis, camphor was added as an internal standard to the obtained reaction mixtures.

Tetracyclo[3.3.0.0.^{2,8}0^{4,6}]octane (41).



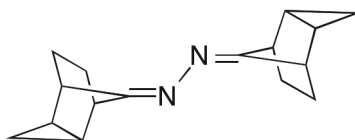
A solution of oxadiazoline **29b** (0.319 g, 1.53 mmol) in pentane (20 mL) was stirred in a pressure tube for 4 h at 165 °C. Pentane was carefully removed by Kugelrohr distillation and the residue was subjected to gradient NMR analysis. Spectroscopic data were in agreement with the literature.⁷⁵

^1H NMR (600.13 MHz, CDCl_3): δ 1.74-1.69 (m, 2H), 1.65-1.55 (m, 4H), 1.29-1.25 (m, 4H). ^{13}C NMR (150.92 MHz, CDCl_3): δ 25.7 (4xCH), 24.0 (2xCH₂), 21.8 (2xCH). MS (EI, 70 eV): m/z 106 [M]⁺ (42), 91 (100), 78 (79), 65 (10), 51 (14).

Thermolysis of **29b** in Cyclohexane- d_{12} .

A solution of oxadiazoline **29b** (0.030 g, 0.14 mmol) in cyclohexane- d_{12} (1 mL) was stirred in a pressure tube for 3 h at 165 °C. The reaction mixture was subjected to NMR analysis (see Figure 4.4 for ^1H NMR spectrum of the mixture).

endo-Tricyclo[3.2.1.0^{2,4}]octan-8-one Azine (**44**).



A solution of oxadiazoline **29b** (0.254 g, 1.22 mmol) in pentane (3 mL) was stirred in a pressure tube for 4 h at 165 °C. The reaction mixture was filtered and concentrated. The product was isolated by column chromatography using hexane/ethyl acetate (1:1) as eluant giving **44** (0.016 g, 11%) as a sticky white solid.

mp: 130–143 °C. ^1H NMR (600.13 MHz, CDCl_3): δ 3.21-3.14 (m, 2H), 2.54-2.46 (m, 2H), 1.69-1.51 (m, 4H), 1.47-1.36 (m, 4H), 1.28-1.16 (m, 4H), 1.03-0.97 (m, 2H), 0.97-0.90 (m, 2H) ppm. ^{13}C NMR (150.92 MHz, CDCl_3): δ 180.88 and 180.79 (2xC), 37.62 and 37.61 (2xCH), 32.44 and 32.42 (2xCH), 24.04 and 24.00 (2xCH₂), 23.44 and 23.42 (2xCH₂), 15.29 and 15.28 (2xCH), 14.79 and 14.76 (2xCH), 11.48 and 11.44 (2xCH₂) ppm. IR: ν 3029 (m), 2950 (m), 2873 (m), 1682 (s), 1523 (m), 1473 (m), 1311 (m), 1301 (m), 1180 (w), 1147 (m), 1108 (m), 1047 (m), 1030 (m), 928 (m), 789 (m), 757 (s), 719 (m) cm^{-1} . MS (EI, 70 eV): m/z 240 [M]⁺ (12), 174 (3), 120 (36), 93 (100), 77 (27), 65 (13), 54 (7). HRMS (ESI) m/z : [$\text{M} + \text{H}$]⁺ calcd for $\text{C}_{16}\text{H}_{21}\text{N}_2$ 241.1705; found 241.1696.

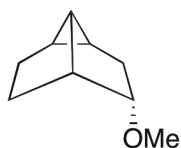
***endo,syn*-Tricyclo[3.2.1.0^{2,4}]octan-8-ol (**46**).**



See the procedure below for thermolysis of **29a** in methanol. **46** was isolated (0.022 g, 26%) as a white solid. Spectroscopic data were in agreement with the literature.^{66g,108}

¹H NMR (400.13 MHz, CDCl₃): δ 4.27-4.16 (m, 1H), 2.32-2.24 (m, 1H), 2.07-1.99 (m, 2H), 1.61-1.51 (m, 2H), 1.50-1.40 (m, 2H), 1.31-1.23 (m, 1H), 1.10-0.97 (m, 3H) ppm. ¹³C NMR (100.62 MHz, CDCl₃): δ 93.8 (CH), 41.0 (2xCH), 24.2 (2xCH₂), 19.8 (2xCH), 18.7 (CH₂) ppm. IR: ν 3279 (m, br), 3031 (w), 3006 (w), 2955 (m), 2877 (m), 1476 (m), 1351 (m), 1267 (m), 1189 (m), 1129 (s), 1061 (s), 987 (w), 932 (w), 781 (m), 755 (m), 724 (m) cm⁻¹. MS (EI, 70 eV): *m/z* 124 [M]⁺ (1), 109 (14), 106 (15), 91 (70), 78 (70), 70 (100), 68 (51), 57 (56).

***rac*-(1*R*,2*S*,4*S*,5*R*,6*R*)-2-Methoxytricyclo[3.3.0.0^{4,6}]octane (**48**).**



From thermolysis of **29a**: A solution of oxadiazoline **29a** (0.141 g, 0.677 mmol) in methanol (7.5 mL) was stirred in a pressure tube for 4 h at 165 °C. The reaction mixture was filtered and concentrated in vacuo. The crude product was subjected to column chromatography using hexane/ethyl acetate (9:1) as eluant giving **49** (0.026 g, 28%) as a yellow liquid.

From thermolysis of **29b**: A solution of oxadiazoline **29b** (0.143 g, 0.687 mmol) in methanol (7.5 mL) was stirred in a pressure tube for 4 h at 165 °C. The reaction mixture was filtered and concentrated in vacuo. The crude product was subjected to

column chromatography using hexane/ethyl acetate (9:1) as eluant giving **49** (0.042 g, 44%) as a yellow liquid.

From photolysis of **29a**: A solution of oxadiazoline **29a** (0.100 g, 0.480 mmol) in methanol (5 mL) was degassed with argon and photolyzed for 7 h, using a water bath for cooling. The reaction mixture was filtered and concentrated in vacuo. The crude product was subjected to column chromatography using hexane/ethyl acetate (9:1) as eluant giving **49** (0.022 g, 33%) as a yellow liquid.

From photolysis of **29b**: A solution of oxadiazoline **29b** (0.100 g, 0.480 mmol) in methanol (5 mL) was degassed with argon and photolyzed for 7 h, using a water bath for cooling. The reaction mixture was filtered and concentrated in vacuo. The crude product was subjected to column chromatography using hexane/ethyl acetate (9:1) giving **49** (0.031 g, 47%) as a yellow liquid. Spectroscopic data were in agreement with the literature.^{60b}

¹H NMR (400.13 MHz, CDCl₃): δ 3.80-3.72 (m, 1H), 3.22 (s, 3H), 2.60-2.51 (m, 1H), 2.25-2.12 (m, 1H), 1.99-1.88 (m, 1H), 1.83-1.69 (m, 2H), 1.69-1.57 (m, 1H), 1.49-1.39 (m, 2H), 1.16-1.05 (m, 2H) ppm. ¹³C NMR (100.62 MHz, CDCl₃): δ 88.1 (CH), 56.8 (CH₃), 43.6 (CH), 30.3 (CH₂), 27.3 (CH₂), 27.2 (CH), 26.0 (CH), 24.1 (CH₂), 19.2 (CH) ppm. IR: ν 3029 (m), 2943 (m), 2867 (m), 1736 (m), 1471 (m), 1450 (m), 1367 (m), 1349 (m), 1212 (m), 1177 (m), 1117 (s), 1098 (s), 975 (m) cm⁻¹. MS (EI, 70 eV): *m/z* 138 [M]⁺ (4), 123 (3), 106 (28), 91 (21), 84 (10), 79 (45), 71 (100), 67 (17), 53 (5). HRMS (EI, 70 eV) *m/z*: [M]⁺ calcd for C₉H₁₄O 138.1045; found 138.1044.

***rel*-(1*s*,1'*R*,2'*R*,4'*S*,5'*S*)-Spiro[cyclopropane-1,8'-tricyclo[3.2.1.0^{2,4}]octane]-2-carbonitrile (51).**

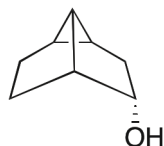


From thermolysis of **29a**: A solution of oxadiazoline **29a** (0.122 g, 0.586 mmol) in acrylonitrile (6 mL) was stirred in a pressure tube for 4 h at 165 °C. The reaction mixture was filtered and concentrated in vacuo. The product was isolated by column chromatography using hexane/ethyl acetate (4:1) as eluant giving **51** (0.071 g, 76%) as a white solid.

From thermolysis of **29b**: A solution of oxadiazoline **29b** (0.125 g, 0.600 mmol) in acrylonitrile (6 mL) was stirred in a pressure tube for 4 h at 165 °C. The reaction mixture was filtered and concentrated in vacuo. The product was isolated by column chromatography using hexane/ethyl acetate (4:1) as eluant giving **51** (0.077 g, 81%) as a white solid.

mp: 34-36 °C. ¹H NMR (400.13 MHz, CDCl₃): δ 2.02-1.94 (m, 1H), 1.84-1.70 (m, 1H), 1.68-1.48 (m, 4H), 1.42-1.19 (m, 5H), 1.14-1.08 (m, 1H), 0.88-0.83 (dt, *J* = 7.4 Hz (t), 6.3 Hz (d), 1H) ppm. ¹³C NMR (100.62 MHz, CDCl₃): δ 121.0 (C), 54.4 (C), 41.7 (CH), 40.7 (CH), 26.8 (CH₂), 26.4 (CH₂), 21.7 (CH), 21.2 (CH), 16.1 (CH₂), 14.6 (CH₂), 3.9 (CH) ppm. IR: ν 3028 (m), 2959 (s), 2877 (m), 2228 (s), 1474 (m), 1442 (m), 1386 (w), 1317 (m), 1302 (m), 1205 (w), 1173 (m), 1113 (m), 1097 (m), 1037 (m), 1010 (s), 963 (m), 928 (s), 837 (m), 786 (s), 732 (s) cm⁻¹. MS (EI, 70 eV): *m/z* 159 [M]⁺ (<1), 144 (4), 130 (15), 117 (15), 104 (21), 91 (50), 78 (100), 65 (10), 51 (9). HRMS (ESI) *m/z*: [M + Na]⁺ calcd for C₁₁H₁₃NNa 182.0946; found 182.0947.

***rac*-(1*R*,2*S*,4*S*,5*R*,6*R*)-2-Hydroxytricyclo[3.3.0.0^{4,6}]octane (52).**

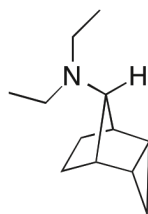


A solution of oxadiazoline **29b** (0.101 g, 0.485 mmol) in 10% water (v/v) in acrylonitrile (6 mL) was stirred in a pressure tube for 4 h at 165 °C. The reaction mixture was transferred to a separation funnel using dichloromethane (50 mL) and water (50 mL). The two phases were separated, followed by extraction of the aqueous phase with dichloromethane (3 x 50 mL). The combined organic phases were dried

(MgSO₄), filtered, and concentrated. The crude product was subjected to column chromatography using hexane/ethyl acetate (8:2) as eluant giving **52** (0.040 g, 66%) as a white solid. Spectroscopic data were in agreement with the literature.^{66g,88}

mp: 75–81 °C (lit. mp. 77-79.5 °C).^{66g} ¹H NMR (600.13 MHz, CDCl₃): δ 4.30-4.21 (m, 1H), 2.46-2.39 (m, 1H), 2.26-2.18 (m, 1H), 2.02-1.92 (m, 1H), 1.83-1.75 (m, 2H), 1.73–1.60 (m, 1H), 1.52-1.39 (m, 2H), 1.14-1.08 (m, 1H), 1.07-1.01 (m, 1H) ppm. ¹³C NMR (150.92 MHz, CDCl₃): δ 79.2 (CH), 46.7 (CH), 30.0 (CH₂), 29.9 (CH₂), 27.3 (CH), 25.6 (CH), 24.1 (CH₂), 19.2 (CH) ppm. IR: ν 3310 (m, br), 3030 (w), 2946 (m), 2868 (m), 1474 (w), 1452 (w), 1344 (w), 1313 (w), 1271 (w), 1158 (w), 1074 (s), 1052 (s), 1026 (m), 1002 (w), 982 (w), 915 (w), 882 (w), 845 (w), 781 (m), 761 (m), 693 (m), 651 (m) cm⁻¹. MS (EI, 70 eV): *m/z* 124 [M]⁺ (2), 106 (76), 95 (32), 91 (56), 80 (100), 67 (97), 57 (23).

***endo,anti-N,N*-Diethyltricyclo[3.2.1.0^{2,4}]octan-8-amine (54).**

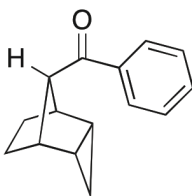


From thermolysis of **29a**: A solution of oxadiazoline **29a** (0.122 g, 0.586 mmol) in diethylamine (6 mL) was stirred in a pressure tube for 4 h at 165 °C. The reaction mixture was filtered and concentrated in vacuo. The product was isolated by column chromatography using ethyl acetate as eluant giving **54** (0.070 g, 67%) as a yellow liquid.

From thermolysis of **29b**: A solution of oxadiazoline **29b** (0.120 g, 0.576 mmol) in diethylamine (6 mL) was stirred in a pressure tube for 4 h at 165 °C. The reaction mixture was filtered and concentrated in vacuo. The product was isolated by column chromatography using ethyl acetate as eluant giving **54** (0.061 g, 59%) as a yellow liquid.

^1H NMR (400.13 MHz, CDCl_3): δ 2.94-2.91 (m, 1H), 2.59-2.50 (q, $J = 7.1$ Hz, 4H), 2.20-2.14 (m, 2H), 1.68-1.58 (m, 2H), 1.28-1.19 (m, 2H), 0.97-0.92 (t, $J = 7.1$, 6H), 0.92-0.85 (m, 3H), 0.56-0.49 (dt, $J = 7.4$ Hz (t), 6.0 Hz (d), 1H) ppm. ^{13}C NMR (100.62 MHz, CDCl_3): δ 83.2 (CH), 43.6 (2x CH_2), 38.4 (2xCH), 25.1 (2x CH_2), 19.1 (2xCH), 12.2 (CH_2), 10.8 (2x CH_3) ppm. IR: ν 3022 (m), 2964 (s), 2816 (m), 1469 (m), 1369 (m), 1209 (m), 1180 (m), 1121 (m), 1070 (m), 1038 (m), 988 (w), 791 (m), 740 (m) cm^{-1} . MS (EI, 70 eV): m/z 179 [$\text{M}]^+$ (2), 164 (4), 125 (5), 112 (100), 99 (13), 79 (11), 56 (15). HRMS (ESI) m/z : [$\text{M} + \text{H}]^+$ calcd for $\text{C}_{12}\text{H}_{22}\text{N}$ 180.1752; found 180.1746.

Phenyl((1*R*,2*R*,4*S*,5*S*,8*r*)-tricyclo[3.2.1.0^{2,4}]octan-8-yl)methanone (55).



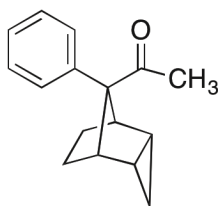
From thermolysis of **29a**: A solution of oxadiazoline **29a** (0.098 g, 0.471 mmol) in benzaldehyde (4.5 mL) was stirred in a pressure tube for 6 h at 165 °C. The product was isolated by column chromatography using hexane/ethyl acetate (4:1) as eluant giving **55** (0.053 g, 53%) as a white solid.

From thermolysis of **29b**: A solution of oxadiazoline **29b** (0.150 g, 0.720 mmol) in benzaldehyde (5 mL) was stirred in a pressure tube for 4 h at 165 °C. The product was isolated by column chromatography using hexane/ethyl acetate (4:1) as eluant giving **55** (0.065 g, 43%) as a white solid.

mp: 45–50 °C. ^1H NMR (400.13 MHz, CDCl_3): δ 7.96 (m, 2H), 7.57-7.51 (m, 1H), 7.48-7.43 (m, 2H), 3.58-3.54 (m, 1H), 2.72-2.66 (m, 2H), 1.69–1.61 (m, 2H), 1.52-1.50 (m, 2H), 1.30-1.23 (m, 2H), 1.15-1.11 (m, 1H), 0.86-0.79 (m, 1H) ppm. ^{13}C NMR (100.62 MHz, CDCl_3): δ 200.3 (C), 137.8 (C), 132.6 (CH), 128.5 (2xCH), 128.3 (2xCH), 74.5 (CH), 40.7 (2xCH), 27.1 (2x CH_2), 22.4 (2xCH), 17.4 (CH_2) ppm. IR: ν 3057 (w), 2964 (m), 2876 (w), 1718 (m), 1673 (s), 1596 (w), 1477 (w), 1446

(m), 1353 (m), 1312 (m), 1297 (m), 1271 (m), 1219 (s), 1122 (m), 1020 (m), 868 (m), 846 (m), 821 (m), 907 (s), 744 (m), 691 (s), 670 (m) cm^{-1} . MS (EI, 70 eV): m/z 212 $[\text{M}]^+$ (12), 197 (2), 183 (10), 115 (6), 170 (19), 157 (32), 144 (42), 129 (7), 121 (12), 115 (13), 105 (100), 92 (50), 77 (69), 65 (5), 51 (13). HRMS (ESI) m/z : $[\text{M} + \text{Na}]^+$ calcd for $\text{C}_{15}\text{H}_{16}\text{ONa}$ 235.1099; found 235.1093. Anal. Calcd for $\text{C}_{15}\text{H}_{16}\text{O}$: C, 84.87; H, 7.60; O, 7.54. Found: C, 84.46; H, 7.58; O, 7.66.

1-((1*R*,2*R*,4*S*,5*S*,8*r*)-8-Phenyltricyclo[3.2.1.0^{2,4}]octan-8-yl)ethan-1-one (56).



From thermolysis of **29a**: A solution of oxadiazoline **29a** (0.104 g, 0.499 mmol) in acetophenone (5 mL) was stirred in a pressure tube for 4 h at 165 °C. The product was isolated by column chromatography using hexane/ethyl acetate (4:1) as eluant giving **56** (0.088 g, 78%) as a white solid.

From thermolysis of **29b**: A solution of oxadiazoline **29b** (0.150 g, 0.720 mmol) in acetophenone (7 mL) was stirred in a pressure tube for 4 h at 165 °C. The product was isolated by column chromatography using hexane/ethyl acetate (4:1) as eluant giving **56** (0.113 g, 69%) as a white solid.

mp: 133–136 °C. ^1H NMR (600.13 MHz, CDCl_3): δ 7.36-7.33 (m, 2H), 7.31-7.27 (m, 2H), 7.23-7.19 (m, 1H), 3.05-3.02 (m, 2H), 2.17 (s, 3H), 1.60–1.56 (m, 2H), 1.44-1.39 (m, 2H), 1.22-1.18 (m, 1H), 1.13-1.08 (m, 2H), 0.84-0.79 (m, 1H) ppm. ^{13}C NMR (150.92 MHz, CDCl_3): δ 209.6 (C), 138.9 (C), 128.7 (2xCH), 128.7 (2xCH), 127.0 (CH), 90.8 (C), 41.7 (2xCH), 27.0 (CH_3), 24.8 (2x CH_2), 21.8 (2xCH), 16.8 (CH_2) ppm. IR: ν 3046 (w), 2931 (w), 1688 (s), 1597 (w), 1477 (w), 1454 (w), 1356 (m), 1312 (m), 1229 (m), 1124 (m), 1038 (m), 937 (w), 899 (w), 792 (m), 750 (m), 695 (s) cm^{-1} . MS (EI, 70 eV): m/z 226 $[\text{M}]^+$ (3), 211 (5), 197 (7), 183 (15), 172 (25), 158 (41), 144 (100), 129 (37), 115 (33), 105 (9), 91 (36), 79 (24), 65 (6), 51 (6). HRMS (ESI)

m/z : $[M + Na]^+$ calcd for $C_{16}H_{18}ONa$ 249.1255; found 249.1254. Anal. Calcd for $C_{16}H_{18}O$: C, 84.91; H, 8.02; N. Found: C, 84.71; H, 7.77.

7.2.3 Reactions of Bicyclo[3.2.1]octan-8-ylidene (16)

General Procedure for GC-MS Analysis of Thermolysis of Oxadiazoline 39 in Cyclohexane, Cyclohexene, Acrylonitrile, and Diethylamine.

For thermolysis, the oxadiazoline was dissolved in cyclohexane, cyclohexene, acrylonitrile, or diethylamine and stirred in a pressure tube at 165 °C for 4 h. Camphor was added as an internal standard to the resultant reaction mixtures prior to GC-MS analysis.

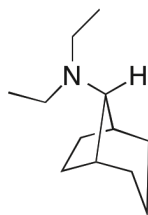
Spiro[bicyclo[3.2.1]octane-8,1'-cyclopropane]-2'-carbonitrile (64).



A solution of oxadiazoline **39** (0.088 g, 0.418 mmol) in acrylonitrile (5 mL) was stirred in a pressure tube for 4 h at 165 °C. The reaction mixture was filtered and concentrated in vacuo. The product was isolated by column chromatography using hexane/ethyl acetate (9:1) as eluant giving **64** (0.012 g, 18%) as a white solid.

mp: 39-46 °C. 1H NMR (600.13 MHz, $CDCl_3$): δ 2.03-1.95 (m, 1H), 1.92-1.83 (m, 2H), 1.70-1.47 (m, 8H), 1.41-1.37 (m, 1H), 1.27-1.23 (m, 1H), 1.22-1.16 (m, 2H) ppm. ^{13}C NMR (150.92 MHz, $CDCl_3$): δ 120.7 (C), 42.2 (CH), 41.1 (CH), 39.2 (CH), 31.4 (CH_2), 31.4 (CH_2), 28.2 (CH_2), 28.0 (CH_2), 18.0 (CH_2), 14.8 (CH_2), 9.8 (CH) ppm. IR: ν 3030 (m), 2929 (s), 2872 (m), 2853 (m), 2230 (s), 1478 (m), 1452 (m), 1297 (w), 1257 (w), 1188 (w), 1085 (m), 1049 (m), 1020 (m), 1011 (m), 976 (m), 935 (m), 895 (m), 843 (m), 804 (m), 770 (w), 755 (s) cm^{-1} . MS (EI, 70 eV): m/z 161 $[M]^+$ (3), 146 (4), 132 (14), 118 (8), 108 (85), 93 (31), 80 (100), 67 (23), 53 (7). HRMS (ESI) m/z : $[M + Na]^+$ calcd for $C_{11}H_{15}NNa$ 184.1102; found 184.1093.

***rel*-(1*R*,5*S*,8*r*)-*N,N*-Diethylbicyclo[3.2.1]octan-8-amine (67).**



A solution of oxadiazoline **39** (0.071 g, 0.338 mmol) in diethylamine (3.5 mL) was stirred in a pressure tube for 4 h at 165 °C. The reaction mixture was filtered and concentrated in vacuo. The product was isolated by column chromatography using ethyl acetate as eluant giving **67** (0.032 g, 52%) as a yellow liquid.

¹H NMR (400.13 MHz, CDCl₃): δ 2.64-2.56 (q, *J* = 7.1 Hz, 4H), 2.34-2.32 (m, 1H), 2.27-2.20 (m, 2H), 1.87-1.77 (m, 2H), 1.54-1.29 (m, 8H), 0.97-0.90 (t, *J* = 7.1 Hz, 6H) ppm. ¹³C NMR (100.62 MHz, CDCl₃): δ 72.8 (CH), 42.3 (2xCH₂), 38.3 (2xCH), 32.5 (2xCH₂), 27.4 (2xCH₂), 18.5 (CH₂), 11.2 (2xCH₃) ppm. IR: ν 2927 (s), 2852 (s), 2811 (m), 1568 (w), 1470 (m), 1450 (m), 1369 (m), 1337 (w), 1289 (w), 1222 (w), 1200 (w), 1183 (w), 1162 (m), 1057 (m), 1037 (w), 999 (w), 952 (w), 787 (w), 848 (w), 781 (m), 734 (w) cm⁻¹. MS (EI, 70 eV): *m/z* 181 [M]⁺ (34), 166 (100), 152 (38), 138 (30), 124 (30), 112 (35), 86 (14), 67 (14), 58 (26). HRMS (ESI) *m/z*: [M + H]⁺ calcd for C₁₂H₂₄N 182.1909; found 182.1905.

References

1. Bertrand, G. In *Reactive Intermediate Chemistry*; Moss, R. A.; Platz, M. S.; Jones, M., Jr., Eds.; Wiley: Hoboken, NJ, 2004; pp. 329-374.
2. Jones, M., Jr.; Moss, R. A. In *Reactive Intermediate Chemistry*; Moss, R. A.; Platz, M. S.; Jones, M., Jr., Eds.; Wiley: Hoboken, NJ, 2004; pp. 273-328.
3. Tomioka, H. In *Carbene Chemistry: From Fleeting Intermediates to Powerful Reagents*; Bertrand, G., Ed.; Fontis Media S.A: Lausanne, Switzerland, 2002; pp. 103-152.
4. Tomioka, H. In *Reactive Intermediate Chemistry*; Moss, R. A.; Platz, M. S.; Jones, M., Jr., Eds.; Wiley: Hoboken, NJ, 2004; pp. 375-462.
5. Hoffmann, R. *J. Am. Chem. Soc.* **1968**, *90*, 1475.
6. a) Harrison, J. F. *J. Am. Chem. Soc.* **1971**, *93*, 4112. b) Harrison, J. F.; Liedtke, R. C.; Liebman, J. F. *J. Am. Chem. Soc.* **1979**, *101*, 7162.
7. Fleming, I. *Frontier Orbitals and Organic Chemical Reactions*; Wiley: New York, 1976.
8. Myers, D. R.; Senthilnathan, V. P.; Platz, M. S.; Jones, M., Jr. *J. Am. Chem. Soc.* **1986**, *108*, 4232.
9. Gano, J. E.; Wettach, R. H.; Platz, M. S.; Senthilnathan, V. P. *J. Am. Chem. Soc.* **1982**, *104*, 2326.
10. a) Modarelli, D. A.; Morgan, S.; Platz, M. S. *J. Am. Chem. Soc.* **1992**, *114*, 7034. b) Richards, C. A., Jr.; Kim, S.-J.; Yamaguchi, Y.; Schaefer, H. F., III *J. Am. Chem. Soc.* **1995**, *117*, 10104.
11. Xu, G.; Chang, T.-M.; Zhou, J.; McKee, M. L.; Shevlin, P. B. *J. Am. Chem. Soc.* **1999**, *121*, 7150.
12. Reisenauer, H. P.; Maier, G.; Riemann, A.; Hoffmann, R. W. *Angew. Chem.* **1984**, *96*, 596.
13. Moss, R. A.; Platz, M. S.; Jones, M., Jr. *Reactive Intermediate Chemistry*; Wiley: Hoboken, NJ, 2004.
14. Kirmse, W. *Carbene Chemistry*; Academic: New York, 1971; Vol. 1.
15. a) Skell, P. S.; Garner, A. Y. *J. Am. Chem. Soc.* **1956**, *78*, 5430. b) Doering, W. v. E.; Henderson, W. A., Jr. *J. Am. Chem. Soc.* **1958**, *80*, 5274.
16. Sheridan, R. S.; Moss, R. A.; Wilk, B. K.; Shen, S.; Wlostowski, M.; Kesselmayr, M. A.; Subramanian, R.; Kmiecik-Lawryniewicz, G.; Krogh-Jespersen, K. *J. Am. Chem. Soc.* **1988**, *110*, 7563.
17. Moss, R. A. *Acc. Chem. Res.* **1980**, *13*, 58.
18. Bourissou, D.; Guerret, O.; Gabbaie, F. P.; Bertrand, G. *Chem. Rev.* **2000**, *100*, 39.
19. a) Closs, G. L.; Closs, L. E. *J. Am. Chem. Soc.* **1969**, *91*, 4549. b) Roth, H. D. *J. Am. Chem. Soc.* **1972**, *94*, 1761.
20. Doering, W. v. E.; Prinzbach, H. *Tetrahedron* **1959**, *6*, 24.
21. a) Doering, W. v. E.; Buttery, R. G.; Laughlin, R. G.; Chaudhuri, N. *J. Am. Chem. Soc.* **1956**, *78*, 3224. b) Richardson, D. B.; Simmons, M. C.; Dvoretzky, I. *J. Am. Chem. Soc.* **1960**, *82*, 5001.
22. Seyferth, D.; Burlitch, J. M.; Yamamoto, K.; Washburne, S. S.; Attridge, C. J. *J. Org. Chem.* **1970**, *35*, 1989.
23. Likhovotvorik, I. R.; Yuan, K.; Brown, D. W.; Krasutskii, P. A.; Smyth, N.; Jones, M., Jr. *Tetrahedron Lett.* **1992**, *33*, 911.

24. a) Evanseck, J. D.; Houk, K. N. *J. Phys. Chem.* **1990**, *94*, 5518. b) Nickon, A. *Acc. Chem. Res.* **1993**, *26*, 84.
25. Kirmse, W. *Eur. J. Org. Chem.* **2005**, 237.
26. Kirmse, W.; Meinert, T.; Modarelli, D. A.; Platz, M. S. *J. Am. Chem. Soc.* **1993**, *115*, 8918.
27. a) Schoeller, W. W.; Brinker, U. H. *Z. Naturforsch* **1980**, *35b*, 475. b) Schoeller, W. W. *Tetrahedron Lett.* **1980**, *21*, 1505. c) Soundararajan, N.; Platz, M. S.; Jackson, J. E.; Doyle, M. P.; Oon, S. M.; Liu, M. T. H.; Anand, S. M. *J. Am. Chem. Soc.* **1988**, *110*, 7143. d) Mendez, F.; Garcia-Garibay, M. A. *J. Org. Chem.* **1999**, *64*, 7061. e) Sander, W.; Kotting, C.; Hubert, R. *J. Phys. Org. Chem.* **2000**, *13*, 561.
28. Moss, R. A. *Acc. Chem. Res.* **1989**, *22*, 15.
29. a) Jones, W. M.; Brinker, U. H. In *Pericyclic Reactions*; Marchand, A. P.; Lehr, R. E., Eds.; Academic: New York, 1977; Vol. 1; pp. 109-198. b) Jones, W. M.; LaBar, R. A.; Brinker, U. H.; Gebert, P. H. *J. Am. Chem. Soc.* **1977**, *99*, 6379, footnote 27.
30. Miesusset, J.-L.; Brinker, U. H. *J. Org. Chem.* **2008**, *73*, 1553.
31. Chang, K.-T.; Shechter, H. *J. Am. Chem. Soc.* **1979**, *101*, 5082.
32. a) Bamford, W. R.; Stevens, T. S. *J. Chem. Soc.* **1952**, 4735. b) Dauben, W. G.; Willey, F. G. *J. Am. Chem. Soc.* **1962**, *84*, 1497.
33. a) Kirmse, W. *Eur. J. Org. Chem.* **1998**, 201. b) Eschenmoser, A.; Felix, D.; Ohloff, G. *Helv. Chim. Acta* **1967**, *50*, 708. c) Felix, D.; Müller, R. K.; Horn, U. J., R.; Schreiber, J.; Eschenmoser, A. *Helv. Chim. Acta* **1972**, *55*, 1276.
34. Bonneau, R.; Liu, M. T. H. *J. Am. Chem. Soc.* **1996**, *118*, 7229.
35. a) Frey, H. M. *Pure Appl. Chem.* **1964**, *9*, 527. b) Mansoor, A. M.; Stevens, I. D. R. *Tetrahedron Lett.* **1966**, 1733. c) Platz, M. S.; White, W. R. I.; Modarelli, D. A.; Celebi, S. *Res. Chem. Intermed.* **1994**, *20*, 175. d) Moss, R. A. *Pure Appl. Chem.* **1995**, *67*, 741.
36. Warkentin, J. *J. Chem. Soc., Perkin Trans. 1* **2000**, 2161.
37. a) Békhazi, M.; Warkentin, J. *J. Am. Chem. Soc.* **1981**, *103*, 2473. b) Békhazi, M.; Warkentin, J. *J. Am. Chem. Soc.* **1983**, *105*, 1289.
38. a) El-Saidi, M.; Kassam, K.; Pole, D. L.; Tadey, T.; Warkentin, J. *J. Am. Chem. Soc.* **1992**, *114*, 8751. b) Isaacs, L.; Diederich, F. *Helv. Chim. Acta* **1993**, *76*, 2454. c) Kassam, K.; Warkentin, J. *J. Org. Chem.* **1994**, *59*, 5071. d) Suh, D.; Pole, D. L.; Warkentin, J.; Terlouw, J. K. *Can. J. Chem.* **1996**, *74*, 544. e) Pole, D. L.; Warkentin, J. *J. Org. Chem.* **1997**, *62*, 4065. f) Kassam, K.; Pole, D. L.; El-Saidi, M.; Warkentin, J. *J. Am. Chem. Soc.* **1994**, *116*, 1161. g) Venneri, P. C.; Warkentin, J. *J. Am. Chem. Soc.* **1998**, *120*, 11182. h) Pezacki, J. P.; Loncke, P. G.; Ross, J. P.; Warkentin, J.; Gadosy, T. A. *Org. Lett.* **2000**, *2*, 2733. i) Plazuk, D.; Warkentin, J.; Werstiuk, N. H. *Tetrahedron* **2005**, *61*, 5788. j) Warkentin, J. *Acc. Chem. Res.* **2009**, *42*, 205.
39. a) Hoffmann, R. W.; Luthardt, H. *J. Chem. Ber.* **1968**, *101*, 3861. b) Sharma, P. K.; Warkentin, J. *Tetrahedron Lett.* **1995**, *36*, 7591.
40. Couture, P.; El-Said, M.; Warkentin, J. *Can. J. Chem.* **1997**, *75*, 326.
41. Czardybon, W.; Warkentin, J.; Werstiuk, N. H. *Can. J. Chem.* **2003**, *81*, 1438.
42. a) Majchrzak, M. W.; Békhazi, M.; Tse-Sheepy, I.; Warkentin, J. *J. Org. Chem.* **1989**, *54*, 1842. b) Jefferson, E. A.; Warkentin, J. *J. Org. Chem.* **1994**, *59*, 455. c) Pezacki, J. P.; Couture, P.; Dunn, J. A.; Warkentin, J.; Wood, P. D.; Lusztyk, J.; Ford, F.; Platz, M. S. *J. Org. Chem.* **1999**, *64*, 4456. d) Tae, E. L.; Zhu, Z.; Platz, M. S.; Pezacki, J. P.; Warkentin, J. *J. Phys. Chem. A* **1999**,

- 103, 5336. e) Snoonian, J. R.; Platz, M. S. *J. Phys. Chem. A* **2001**, *105*, 2106.
 f) Brinker, U. H.; Bespokojev, A. A.; Reisenauer, H. P.; Schreiner, P. R. *J. Org. Chem.* **2012**, *77*, 3800.
43. Gleiter, R.; Hoffmann, R. *J. Am. Chem. Soc.* **1968**, *90*, 5457.
44. Moss, R. A.; Dolling, U.-H.; Whittle, J. R. *Tetrahedron Lett.* **1971**, 931.
45. a) Winstein, S.; Trifan, D. S. *J. Am. Chem. Soc.* **1949**, *71*, 2953. b) Winstein, S.; Shatavsky, M.; Norton, C.; Woodward, R. B. *J. Am. Chem. Soc.* **1955**, *77*, 4183. c) Brookhart, M.; Diaz, A.; Winstein, S. *J. Am. Chem. Soc.* **1966**, *88*, 3135. d) Rzepa, H. S.; Allan, C. S. M. *J. Chem. Educ.* **2010**, *87*, 221. e) Bartlett, P. D. *Nonclassical Ions*; W. A. Benjamin: New York, 1965.
46. a) Fisch, M. H.; Pierce, H. D., Jr. *J. Chem. Soc., Chem. Commun.* **1970**, 503. b) Fickes, G. N.; Rose, C. B. *J. Org. Chem.* **1972**, *37*, 2898. c) Antkowiak, T. A.; Sanders, D. C.; Trimitsis, G. B.; Press, J. B.; Shechter, H. *J. Am. Chem. Soc.* **1972**, *94*, 5366. d) Moss, R. A.; Ho, C.-T. *Tetrahedron Lett.* **1976**, 3397. e) Brown, W. T.; Jones, W. M. *J. Org. Chem.* **1979**, *44*, 3090. f) Brinker, U. H.; König, L. *J. Am. Chem. Soc.* **1981**, *103*, 212. g) Brinker, U. H.; König, L. *Chem. Lett.* **1984**, 45. h) Rajan Babu, T. V.; Shechter, H. *J. Am. Chem. Soc.* **1976**, *98*, 8261. i) Brinker, U. H.; Ritzer, J. *J. Am. Chem. Soc.* **1981**, *103*, 2116.
47. Moss, R. A.; Whittle, J. R. *J. Chem. Soc., Chem. Commun.* **1969**, 341.
48. a) Zimmerman, H. E.; Sousa, L. R. *J. Am. Chem. Soc.* **1972**, *94*, 834. b) Schneider, M.; Csacsko, B. *Angew. Chem. Int. Ed. Engl.* **1977**, *16*, 867. c) Katz, T. J.; Wang, E. J.; Acton, N. *J. Am. Chem. Soc.* **1971**, *93*, 3782. d) Burger, U.; Mazonod, F. *Tetrahedron Lett.* **1976**, 2881. e) Closs, G. L.; Larrabee, R. B. *Tetrahedron Lett.* **1965**, 287.
49. Miesusset, J.-L.; Brinker, U. H. *J. Am. Chem. Soc.* **2007**, *72*, 263.
50. Hammond, G. S. *J. Am. Chem. Soc.* **1955**, *77*, 334.
51. Miesusset, J.-L.; Brinker, U. H. *J. Am. Chem. Soc.* **2006**, *128*, 15843.
52. Moss, R. A.; Dolling, U.-H. *Tetrahedron Lett.* **1972**, 5117.
53. Moss, R. A.; Ho, C.-T. *Tetrahedron Lett.* **1976**, 1651.
54. Miesusset, J.-L.; Abraham, M.; Brinker, U. H. *J. Am. Chem. Soc.* **2008**, *130*, 14634.
55. Miesusset, J.-L.; Bespokojev, A.; Pacar, M.; Abraham, M.; Arion, V. B.; Brinker, U. H. *J. Org. Chem.* **2008**, *73*, 6551.
56. Miesusset, J.-L.; Schrems, A.; Abraham, M.; Arion, V. B.; Brinker, U. H. *Tetrahedron* **2009**, *65*, 765.
57. a) Sugden, T. M. *Nature* **1947**, *160*, 367. b) Walsh, A. D. *Trans. Faraday. Soc.* **1949**, *45*, 179. c) Coulson, C. A.; Moffitt, W. E. *Phil. Mag.* **1949**, *40*, 1. d) Bernett, W. A. *J. Chem. Educ.* **1967**, *44*, 17. e) Haywood-Farmer, J. *Chem. Rev.* **1974**, *74*, 315. f) de Meijere, A. *Angew. Chem. Int. Ed. Engl.* **1979**, *18*, 809.
58. a) Freeman, P. K. *J. Am. Chem. Soc.* **1998**, *120*, 1619. b) Freeman, P. K.; Pugh, J. K. *J. Org. Chem.* **2000**, *65*, 6107. c) Freeman, P. K.; Dacres, J. E. *J. Org. Chem.* **2003**, *68*, 1386.
59. a) Murahashi, S.-I.; Okumura, K.; Kubota, T.; Moritani, I. *Tetrahedron Lett.* **1973**, 4197. b) Murahashi, S.-I.; Okumura, K.; Maeda, Y.; Sonoda, A.; Moritani, I. *Bull. Chem. Soc. Jap.* **1974**, *47*, 2420. c) Okumura, K.; Murahashi, S.-I. *Tetrahedron Lett.* **1977**, 3281.

60. a) Freeman, P. K.; Raghavan, R. S.; Kuper, D. G. *J. Am. Chem. Soc.* **1971**, *93*, 5288. b) Freeman, P. K.; Hardy, T. A.; Raghavan, R. S.; Kuper, D. G. *J. Org. Chem.* **1977**, *42*, 3882.
61. Grant, G. H.; Richards, W. G. *Computational Chemistry*; Oxford University Press: New York, 1995.
62. Lewars, E. *Computational Chemistry: Introduction to the Theory and Applications of Molecular and Quantum Mechanics*; Kluwer Academic Publishers: Dordrecht, 2003.
63. Kong, J.; White, C. A.; Krylov, A. I.; Sherrill, D.; Adamson, R. D.; Furlani, T. R.; Lee, M. S.; Lee, A. M.; Gwaltney, S. R.; Adams, T. R.; Ochsenfeld, C.; Gilbert, A. T. B.; Kedziora, G. S.; Rassolov, V. A.; Maurice, D. R.; Nair, N.; Shao, Y.; Besley, N. A.; Maslen, P. E.; Dombroski, J. P.; Daschel, H.; Zhang, W.; Korambath, P. P.; Baker, J. B., Edward F. C.; Van Voorhis, T.; Oumi, M.; Hirata, S.; Hsu, C.-P.; Ishikawa, N.; Florian, J.; Warshel, A.; Johnson, B. G.; Gill, P. M. W.; Head-Gordon, M.; Pople, J. A. *J. Computational Chem.* **2000**, *21*, 1532.
64. Becke, A. D. *J. Chem. Phys.* **1993**, *98*, 5648.
65. Lee, C.; Yang, W.; Parr, R. G. *Phys. Rev. B* **1988**, *37*, 785.
66. a) Wannagat, U.; Niederprüm, H. *Chem. Ber.* **1961**, *94*, 1540. b) Closs, G. L.; Krantz, K. D. *J. Org. Chem.* **1966**, *31*, 638. c) Binger, P.; Wedemann, P.; Goddard, R.; Brinker, U. H. *J. Org. Chem.* **1996**, *61*, 6462. d) Binger, P.; Wedemann, P.; Brinker, U. H. *Org. Synth.* **2000**, *77*, 254. e) Clarke, S. C.; Johnson, B. L. *Tetrahedron Lett.* **1967**, 617. f) Battiste, M. A.; Deyrup, C. L.; Pincock, R. E.; Haywood-Farmer, J. *J. Am. Chem. Soc.* **1967**, *89*, 1954. g) Haywood-Farmer, J. S.; Pincock, R. E. *J. Am. Chem. Soc.* **1969**, *91*, 3020. h) Clarke, S. C.; Frayne, K. J.; Johnson, B. L. *Tetrahedron* **1969**, *25*, 1265.
67. a) Wiberg, K. B.; Bartley, W. J. *J. Am. Chem. Soc.* **1960**, *82*, 6375. b) Joshel, L. M.; Butz, L. W. *J. Am. Chem. Soc.* **1941**, *63*, 3350. c) Hoch, P. E. *J. Org. Chem.* **1961**, *26*, 2066.
68. Kirmse, W.; Meinert, T. *J. Chem. Soc., Chem. Commun.* **1994**, 1065.
69. a) Mieusset, J.-L.; Wagner, G.; Su, K.-J.; Steurer, M.; Pacar, M.; Abraham, M.; Brinker, U. H. *Eur. J. Org. Chem.* **2009**, 5907. b) Krois, D.; Brinker, U. H. *Synthesis* **2001**, 379.
70. Mieusset, J.-L.; Billing, P.; Abraham, M.; Arion, V. B.; Brecker, L.; Brinker, U. H. *Eur. J. Org. Chem.* **2008**, 5336.
71. Yang, R.-Y.; Dai, L.-X. *J. Org. Chem.* **1993**, *58*, 3381.
72. Pavia, D. L.; Lampman, G. M.; Kriz, G. S. *Introduction to Spectroscopy*, 3rd ed.; Brooks/Cole, 2001.
73. a) Halton, B.; Battiste, M. A.; Rehberg, R.; Deyrup, C. L.; Brennan, M. E. *J. Am. Chem. Soc.* **1967**, *89*, 5964. b) Tanida, H.; Tsuji, T.; Irie, T. *J. Am. Chem. Soc.* **1967**, *89*, 1953. c) Clarke, S. C.; Johnson, B. L. *Tetrahedron* **1971**, *27*, 3555. d) Rubio, M.; Hernandez, A. G.; Daudey, J. P.; Cetina R., R.; Diaz, A. *J. Org. Chem.* **1980**, *45*, 150.
74. Kählig, H.; Dietrich, K.; Dorner, S. *Monatsh. Chem.* **2002**, *133*, 589.
75. a) LeBel, N. A.; Liesemer, R. N. *J. Am. Chem. Soc.* **1965**, *87*, 4301. b) Jefford, C. W.; De los Heros, V. *Bull. Soc. Chim. Belg.* **1979**, *88*, 969.
76. a) Chapman, O. L.; Borden, G. W.; King, R. W.; Winkler, B. *J. Am. Chem. Soc.* **1964**, *86*, 2660. b) Christl, M.; Herzog, C.; Kemmer, P. *Chem. Ber.* **1986**, *119*, 3045.

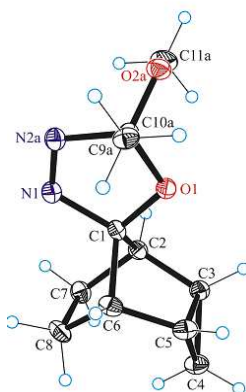
77. a) Regitz, M.; Maas, G. *Diazo Compounds: Properties and Synthesis*; Academic: New York, 1986. b) Abelt, C. J.; Pleier, J. M. *J. Am. Chem. Soc.* **1989**, *111*, 1795. c) Merkley, N.; El-Said, M.; Warkentin, J. *Can. J. Chem.* **2000**, *78*, 356.
78. a) Rutavichyus, A.; Valyulene, S.; Kuodis, Z. *Chem. Heterocycl. Compd.* **1997**, *33*, 118. b) Sanz, D.; Ponce, M. A.; Claramunt, R. M.; Fernandez-Castano, C.; Foces-Foces, C.; Elguero, J. *J. Phys. Org. Chem.* **1999**, *12*, 455. c) Pinto, J.; Silva, V. L. M.; Silva, A. M. S.; Claramunt, R. M.; Sanz, D.; Torralba, M. C.; Torres, M. R.; Reviriego, F.; Alkorta, I.; Elguero, J. *Magn. Reson. Chem.* **2013**, *51*, 203.
79. Dale, J.; Zechmeister, L. *J. Am. Chem. Soc.* **1953**, *75*, 2379.
80. a) Blanco, F.; Alkorta, I.; Elguero, J. *Croat. Chem. Acta* **2009**, *82*, 173. b) Lehn, J.-M. *Chem. Eur. J.* **2006**, *12*, 5910.
81. Blanco, F.; Alkorta, I.; Elguero, J. *J. Mol. Struct.* **2007**, *847*, 25.
82. a) Kirmse, W.; Chiem, P. V.; Henning, P. G. *J. Am. Chem. Soc.* **1983**, *105*, 1695. b) Kirmse, W. In *Advances in Carbene Chemistry*; Brinker, U. H., Ed.; JAI: Greenwich, CT, 1994; Vol. 1; pp. 1-57. c) Kirmse, W. In *Advances in Carbene Chemistry*; Brinker, U. H., Ed.; Elsevier: Amsterdam, 2001; Vol. 3; pp. 1-51.
83. Tanida, H. *Acc. Chem. Res.* **1968**, *1*, 239.
84. a) Diaz, A.; Brookhart, M.; Winstein, S. *J. Am. Chem. Soc.* **1966**, *88*, 3133. b) Lhomme, J.; Diaz, A.; Winstein, S. *J. Am. Chem. Soc.* **1969**, *91*, 1548. c) Laube, T. *J. Am. Chem. Soc.* **1989**, *111*, 9224.
85. Hoffmann, R. *Tetrahedron Lett.* **1965**, 3819.
86. a) Albin, A.; Arnold, D. R. *Can. J. Chem.* **1978**, *56*, 2985. b) Enssle, M.; Buck, S.; Werz, R.; Maas, G. *Beilstein J. Org. Chem.* **2012**, *8*, 433. c) Klukovich, H. M.; Kean, Z. S.; Ramirez, A. L. B.; Lenhardt, J. M.; Lin, J.; Hu, X.; Craig, S. L. *J. Am. Chem. Soc.* **2012**, *134*, 9577.
87. a) Ballinger, P.; Long, F. A. *J. Am. Chem. Soc.* **1960**, *82*, 795. b) Serjeant, E. P.; Dempsey, B. *Ionization Constants of Organic Acids in Aqueous Solution*; Pergamon: Oxford, 1979.
88. Buckeridge, R. G.; Frayne, K. J.; Johnson, B. L. *Aust. J. Chem.* **1975**, *28*, 1311.
89. a) Moody, C. J. *Angew. Chem. Int. Ed.* **2007**, *46*, 9148. b) Baumann, L. K.; Mbuvi, H. M.; Du, G.; Woo, L. K. *Organometallics* **2007**, *26*, 3995. c) Lee, E. C.; Fu, G. C. *J. Am. Chem. Soc.* **2007**, *129*, 12066. d) Frey, G. D.; Lavallo, V.; Donnadiou, B.; Schoeller, W. W.; Bertrand, G. *Science* **2007**, *316*, 439.
90. a) Zugravescu, I.; Rucinschi, E.; Surpateanu, G. *Tetrahedron Lett.* **1970**, 941. b) Speziale, A. J.; Tung, C. C.; Ratts, K. W.; Yao, A. *J. Am. Chem. Soc.* **1965**, *87*, 3460.
91. Miesusset, J.-L.; Brinker, U. H. *J. Org. Chem.* **2007**, *72*, 10211.
92. a) Yoshida, Z.; Tabushi, I.; Takahashi, N. *J. Am. Chem. Soc.* **1970**, *92*, 6670. b) Buxton, S. R.; Holm, K. H.; Skattebøl, L. *Tetrahedron Lett.* **1987**, *28*, 2167. c) Tverezovsky, V. V.; Baird, M. S.; Bolesov, I. G. *Tetrahedron* **1997**, *53*, 14773. d) Nadipuram, A. K.; Kerwin, S. M. *Tetrahedron Lett.* **2006**, *47*, 353. e) Godula, K.; Sames, D. *Science* **2006**, *312*, 67.
93. a) Arduengo, A. J., III; Calabrese, J. C.; Davidson, F.; Dias, H. V. R.; Goerlich, J. R.; Krafczyk, R.; Marshall, W. J.; Tamm, M.; Schmutzler, R. *Helv. Chim. Acta* **1999**, *82*, 2348. b) Wanzlick, H.-W.; Ahrens, H. *Chem. Ber.* **1964**, *97*, 2447.

94. Bell, R. P. *The Proton in Chemistry*; Cornell University Press: Ithaca, N.Y., 1959.
95. a) Igau, A.; Baceiredo, A.; Trinquier, C.; Bertrand, G. *Angew. Chem.* **1989**, *101*, 617. b) Illa, O.; Gornitzka, H.; Baceiredo, A.; Bertrand, G.; Branchadell, V.; Ortuno, R. M. *J. Org. Chem.* **2003**, *68*, 7707. c) Illa, O.; Gornitzka, H.; Branchadell, V.; Baceiredo, A.; Bertrand, G.; Ortuno, R. M. *Eur. J. Org. Chem.* **2003**, 3147.
96. Zhu, Y.; Shu, L.; Tu, Y.; Shi, Y. *J. Org. Chem.* **2001**, *66*, 1818.
97. a) Parker, R. E.; Isaacs, N. S. *Chem. Rev.* **1959**, *59*, 737. b) Williamson, K. L.; Johnson, W. S. *J. Org. Chem.* **1961**, *26*, 4653. c) Bly, R. K.; Bly, R. S. *J. Org. Chem.* **1963**, *28*, 3165. d) Johnson, C. K.; Dominy, B.; Reusch, W. *J. Am. Chem. Soc.* **1963**, *85*, 3894. e) Williamson, K. L.; Coburn, J. I.; Herr, M. F. *J. Org. Chem.* **1967**, *32*, 3934. f) Kretchmer, R. A.; Frazee, W. J. *J. Org. Chem.* **1971**, *36*, 2855. g) Williams, J. R.; Sarkisian, G. M.; Quigley, J.; Hasiuk, A.; VanderVennen, R. *J. Org. Chem.* **1974**, *39*, 1028.
98. a) Venneri, P. C.; Warkentin, J. *Can. J. Chem.* **2000**, *78*, 1194. b) Dawid, M.; Venneri, P. C.; Warkentin, J. *Can. J. Chem.* **2001**, *79*, 110. c) Dawid, M.; Warkentin, J. *Can. J. Chem.* **2003**, *81*, 598.
99. Scholz, F.; Himmel, D.; Heinemann, F. W.; Schleyer, P. v. R.; Meyer, K.; Krossing, I. *Science* **2013**, *341*, 62.
100. Smith, M. B.; March, J. *March's Advanced Organic Chemistry: Reactions, Mechanisms, and Structure*, 5th ed.; Wiley: New York, 2001.
101. a) Cieplak, A. S. *J. Am. Chem. Soc.* **1981**, *103*, 4540. b) Armstrong, B. M.; McKee, M. L.; Shevlin, P. B. *J. Am. Chem. Soc.* **1995**, *117*, 3685. c) Worthington, S. E.; Cramer, C. J. *J. Phys. Org. Chem.* **1997**, *10*, 755. d) Lambert, J. B.; Liu, X. *Tetrahedron* **1997**, *53*, 9989. e) Farlow, R. A.; Thamattoor, D. M.; Sunoj, R. B.; Hadad, C. M. *J. Org. Chem.* **2002**, *67*, 3257. f) Kaneno, D.; Tomoda, S. *Org. Lett.* **2003**, *5*, 2947. g) Knoll, W.; Kaneno, D.; Bobek, M. M.; Brecker, L.; Rosenberg, M. G.; Tomoda, S.; Brinker, U. H. *J. Org. Chem.* **2012**, *77*, 1340.
102. Knoll, W.; Mieusset, J.-L.; Arion, V. B.; Brecker, L.; Brinker, U. H. *Org. Lett.* **2010**, *12*.
103. Wu, D.; Chen, A.; Johnson, C. S., Jr. *J. Magn. Reson. A.* **1995**, *115*, 260.
104. Weast, R. C. *Handbook of Chemistry and Physics*, 52 ed.; The Chemical Rubber Company: Cleveland, Ohio, 1971.
105. Bicker, R.; Kessler, H.; Steigel, A.; Stohrer, W. D. *Chem. Ber.* **1975**, *108*, 2708.
106. Nelsen, S. F.; Kapp, D. L. *J. Am. Chem. Soc.* **1986**, *108*, 1265.
107. Heumann, A.; Kolshorn, H. *J. Org. Chem.* **1979**, *44*, 1575.
108. Haywood-Farmer, J.; Pincock, R. E.; Wells, J. I. *Tetrahedron* **1966**, *22*, 2007.

Appendix

X-ray Analyses

Crystallographic data for *rel*-(1'*R*,2*r*,2'*R*,4'*S*,5*R*,5'*S*)-5-methoxy-5-methylspiro[2,5-dihydro-1,3,4-oxadiazole-2,8'-tricyclo[3.2.1.0^{2,4}]octane] (29a)



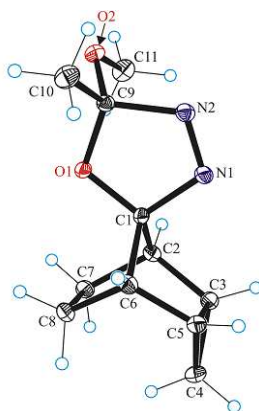
Empirical formula:	C ₁₁ H ₁₆ N ₂ O ₂
Formula weight:	208.26
Temperature	100(2) K
Wavelength	1.54178 Å
Crystal system, space group	orthorhombic, P212121
Unit cell dimensions	a = 6.5107(2) Å alpha = 90 deg. b = 9.4968(3) Å beta = 90 deg. c = 17.2373(5) Å gamma = 90 deg.
Volume	1065.80(6) Å ³
Z, Calculated density	4, 1.298 Mg/m ³
Absorption coefficient	0.733 mm ⁻¹
F(000)	448
Crystal size	0.22 x 0.04 x 0.03 mm
Theta range for data collection	5.13 to 69.70 deg.
Index ranges	-7 <= h <= 6, -10 <= k <= 11, -18 <= l <= 20
Reflections collected / unique	7437 / 1969 [R(int) = 0.0485]
Completeness to 2theta = 69.70	99.2%
Refinement method	Full-matrix least-squares on F ²
Data / restraints / parameters	1969 / 19 / 173
Goodness-of-fit on F ²	1.069
Final R indices [I > 2sigma(I)]	R1 = 0.0327, wR2 = 0.0865
R indices (all data)	R1 = 0.0348, wR2 = 0.0879
Absolute structure parameter	0.1(2)
Largest diff. peak and hole	0.172 and -0.163 e.Å ⁻³

Bond Lengths (Å) and Angles (deg) for 29a

N(1)-N(2A)	1.242(7)	C(3)-C(2)-C(1)	99.58(11)
N(1)-N(2)	1.255(3)	C(7)-C(2)-C(1)	100.81(10)
N(1)-C(1)	1.4738(18)	C(3)-C(2)-H(2)	114.3
C(2)-C(3)	1.5274(19)	C(7)-C(2)-H(2)	114.3
C(2)-C(7)	1.5353(19)	C(1)-C(2)-H(2)	114.3
C(2)-C(1)	1.5430(19)	C(4)-C(3)-C(5)	59.63(9)
C(2)-H(2)	1.0000	C(4)-C(3)-C(2)	120.59(12)
C(3)-C(4)	1.5095(19)	C(5)-C(3)-C(2)	104.36(11)
C(3)-C(5)	1.521(2)	C(4)-C(3)-H(3)	118.6
C(3)-H(3)	1.0000	C(5)-C(3)-H(3)	118.6
C(4)-C(5)	1.507(2)	C(2)-C(3)-H(3)	118.6
C(4)-H(4A)	0.9900	C(5)-C(4)-C(3)	60.57(9)
C(4)-H(4B)	0.9900	C(5)-C(4)-H(4A)	117.7
C(5)-C(6)	1.535(2)	C(3)-C(4)-H(4A)	117.7
C(5)-H(5)	1.0000	C(5)-C(4)-H(4B)	117.7
C(6)-C(8)	1.543(2)	C(3)-C(4)-H(4B)	117.7
C(6)-C(1)	1.5526(18)	H(4A)-C(4)-H(4B)	114.8
C(6)-H(6)	1.0000	C(4)-C(5)-C(3)	59.79(9)
C(1)-O(1A)	1.420(8)	C(4)-C(5)-C(6)	120.38(13)
C(1)-O(1)	1.420(3)	C(3)-C(5)-C(6)	103.66(10)
N(2)-C(9)	1.504(3)	C(4)-C(5)-H(5)	118.7
O(1)-C(9)	1.419(3)	C(3)-C(5)-H(5)	118.7
C(9)-O(2)	1.381(3)	C(6)-C(5)-H(5)	118.7
C(9)-C(10)	1.535(3)	C(5)-C(6)-C(8)	111.58(12)
O(2)-C(11)	1.410(2)	C(5)-C(6)-C(1)	99.54(10)
C(11)-H(11A)	0.9800	C(8)-C(6)-C(1)	100.27(11)
C(11)-H(11B)	0.9800	C(5)-C(6)-H(6)	114.5
C(11)-H(11C)	0.9800	C(8)-C(6)-H(6)	114.5
C(10)-H(10A)	0.9800	C(1)-C(6)-H(6)	114.5
C(10)-H(10B)	0.9800	O(1A)-C(1)-O(1)	12.1(7)
C(10)-H(10C)	0.9800	O(1A)-C(1)-N(1)	105.0(4)
N(2A)-C(9A)	1.499(7)	O(1)-C(1)-N(1)	105.10(17)
O(1A)-C(9A)	1.419(8)	O(1A)-C(1)-C(2)	107.7(5)
C(9A)-O(2A)	1.382(6)	O(1)-C(1)-C(2)	117.54(19)
C(7)-C(8)	1.554(2)	N(1)-C(1)-C(2)	114.39(11)
C(7)-H(7A)	0.9900	O(1A)-C(1)-C(6)	122.0(5)
C(7)-H(7B)	0.9900	O(1)-C(1)-C(6)	112.28(18)
C(8)-H(8A)	0.9900	N(1)-C(1)-C(6)	113.76(11)
C(8)-H(8B)	0.9900	C(2)-C(1)-C(6)	93.93(10)
N(2A)-N(1)-N(2)	21.3(3)	N(1)-N(2)-C(9)	110.7(2)
N(2A)-N(1)-C(1)	111.4(4)	C(9)-O(1)-C(1)	109.0(3)
N(2)-N(1)-C(1)	110.80(16)	O(2)-C(9)-O(1)	111.6(2)
C(3)-C(2)-C(7)	111.98(11)	O(2)-C(9)-N(2)	110.89(19)

O(1)-C(9)-N(2)	103.8(2)	N(1)-N(2A)-C(9A)	110.5(6)
O(2)-C(9)-C(10)	108.19(19)	C(9A)-O(1A)-C(1)	108.5(7)
O(1)-C(9)-C(10)	112.4(2)	O(2A)-C(9A)-O(1A)	111.6(7)
N(2)-C(9)-C(10)	109.91(18)	O(2A)-C(9A)-N(2A)	109.2(5)
C(9)-O(2)-C(11)	113.45(18)	O(1A)-C(9A)-N(2A)	104.3(6)
O(2)-C(11)-H(11A)	109.5	C(2)-C(7)-C(8)	103.18(10)
O(2)-C(11)-H(11B)	109.5	C(2)-C(7)-H(7A)	111.1
H(11A)-C(11)-H(11B)	109.5	C(8)-C(7)-H(7A)	111.1
O(2)-C(11)-H(11C)	109.5	C(2)-C(7)-H(7B)	111.1
H(11A)-C(11)-H(11C)	109.5	C(8)-C(7)-H(7B)	111.1
H(11B)-C(11)-H(11C)	109.5	H(7A)-C(7)-H(7B)	109.1
C(9)-C(10)-H(10A)	109.5	C(6)-C(8)-C(7)	103.44(10)
C(9)-C(10)-H(10B)	109.5	C(6)-C(8)-H(8A)	111.1
H(10A)-C(10)-H(10B)	109.5	C(7)-C(8)-H(8A)	111.1
C(9)-C(10)-H(10C)	109.5	C(6)-C(8)-H(8B)	111.1
H(10A)-C(10)-H(10C)	109.5	C(7)-C(8)-H(8B)	111.1
H(10B)-C(10)-H(10C)	109.5	H(8A)-C(8)-H(8B)	109.0

Crystallographic data for *rel*-(1*R*,2*s*,2'*R*,4'*S*,5*R*,5'*S*)-5-methoxy-5-methylspiro[2,5-dihydro-1,3,4-oxadiazole-2,8'-tricyclo[3.2.1.0^{2,4}]octane] (29b)



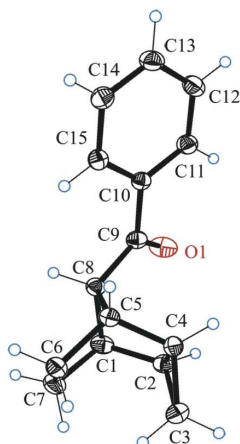
Empirical formula	C ₁₁ H ₁₆ N ₂ O ₂	
Formula weight	208.26	
Temperature	100(2) K	
Wavelength	0.71073 Å	
Crystal system, space group	monoclinic, P21/c	
Unit cell dimensions	a = 8.8383(8) Å	alpha = 90 deg.
	b = 12.6642(12) Å	beta = 93.092(5) deg.
	c = 9.5841(9) Å	gamma = 90 deg.
Volume	1071.19(17) Å ³	
Z, Calculated density	4, 1.291 Mg/m ³	
Absorption coefficient	0.090 mm ⁻¹	
F(000)	448	
Crystal size	0.60 x 0.40 x 0.30 mm	
Theta range for data collection	2.31 to 29.99 deg.	
Index ranges	-12 ≤ h ≤ 12, -17 ≤ k ≤ 17, -13 ≤ l ≤ 13	
Reflections collected / unique	73292 / 3114 [R(int) = 0.0646]	
Completeness to 2theta = 29.99	99.6%	
Max. and min. transmission	0.9735 and 0.9480	
Refinement method	Full-matrix least-squares on F ²	
Data / restraints / parameters	3114 / 5 / 149	
Goodness-of-fit on F ²	1.026	
Final R indices [I > 2sigma(I)]	R1 = 0.0542, wR2 = 0.1540	
R indices (all data)	R1 = 0.0746, wR2 = 0.1662	
Largest diff. peak and hole	0.405 and -0.509 e.Å ⁻³	

Bond Lengths (Å) and Angles (deg) for 29b

C(7)-C(2)	1.5476(18)	C(10X)-H(10F)	0.9560
C(7)-C(8)	1.558(2)	C(10X)-H(10L)	0.9600
C(7)-H(7A)	0.9900	C(10X)-H(10M)	0.9600
C(7)-H(7B)	0.9900	C(10X)-H(10N)	0.9600
C(2)-C(3)	1.5355(19)	C(2)-C(7)-C(8)	103.25(11)
C(2)-C(1)	1.5523(18)	C(2)-C(7)-H(7A)	111.1
C(2)-H(2)	1.0000	C(8)-C(7)-H(7A)	111.1
C(6)-C(5)	1.530(2)	C(2)-C(7)-H(7B)	111.1
C(6)-C(8)	1.5507(19)	C(8)-C(7)-H(7B)	111.1
C(6)-C(1)	1.5518(19)	H(7A)-C(7)-H(7B)	109.1
C(6)-H(6)	1.0000	C(3)-C(2)-C(7)	112.05(11)
C(5)-C(4)	1.512(2)	C(3)-C(2)-C(1)	99.99(10)
C(5)-C(3)	1.532(2)	C(7)-C(2)-C(1)	99.42(10)
C(5)-H(5)	1.0000	C(3)-C(2)-H(2)	114.5
C(3)-C(4)	1.509(2)	C(7)-C(2)-H(2)	114.5
C(3)-H(3)	1.0000	C(1)-C(2)-H(2)	114.5
C(8)-H(8A)	0.9900	C(5)-C(6)-C(8)	111.43(11)
C(8)-H(8B)	0.9900	C(5)-C(6)-C(1)	100.42(11)
C(4)-H(4A)	0.9900	C(8)-C(6)-C(1)	99.25(11)
C(4)-H(4B)	0.9900	C(5)-C(6)-H(6)	114.6
C(1)-O(1)	1.426(2)	C(8)-C(6)-H(6)	114.6
C(1)-O(1X)	1.427(7)	C(1)-C(6)-H(6)	114.6
C(1)-N(1)	1.4843(16)	C(4)-C(5)-C(6)	120.65(12)
N(1)-N(2X)	1.257(5)	C(4)-C(5)-C(3)	59.41(10)
N(1)-N(2)	1.263(2)	C(6)-C(5)-C(3)	104.08(11)
O(1)-C(9)	1.418(3)	C(4)-C(5)-H(5)	118.6
N(2)-C(9)	1.513(2)	C(6)-C(5)-H(5)	118.6
C(9)-O(2)	1.394(2)	C(3)-C(5)-H(5)	118.6
C(9)-C(10)	1.521(2)	C(4)-C(3)-C(5)	59.62(10)
O(2)-C(10X)	1.423(2)	C(4)-C(3)-C(2)	120.27(12)
O(1X)-C(9X)	1.424(7)	C(5)-C(3)-C(2)	104.13(11)
N(2X)-C(9X)	1.517(6)	C(4)-C(3)-H(3)	118.7
C(9X)-O(2X)	1.391(6)	C(5)-C(3)-H(3)	118.7
C(9X)-C(10X)	1.559(6)	C(2)-C(3)-H(3)	118.7
O(2X)-C(10)	1.390(4)	C(6)-C(8)-C(7)	103.69(11)
C(10)-H(10A)	0.9600	C(6)-C(8)-H(8A)	111.0
C(10)-H(10B)	0.9600	C(7)-C(8)-H(8A)	111.0
C(10)-H(10C)	0.9600	C(6)-C(8)-H(8B)	111.0
C(10)-H(10G)	0.9717	C(7)-C(8)-H(8B)	111.0
C(10)-H(10H)	0.9600	H(8A)-C(8)-H(8B)	109.0
C(10)-H(10I)	0.9575	C(3)-C(4)-C(5)	60.97(9)
C(10X)-H(10D)	0.9600	C(3)-C(4)-H(4A)	117.7
C(10X)-H(10E)	0.9720	C(5)-C(4)-H(4A)	117.7

C(3)-C(4)-H(4B)	117.7	C(9)-C(10)-H(10G)	151.9
C(5)-C(4)-H(4B)	117.7	H(10A)-C(10)-H(10G)	61.0
H(4A)-C(4)-H(4B)	114.8	H(10B)-C(10)-H(10G)	98.6
O(1)-C(1)-O(1X)	15.6(3)	H(10C)-C(10)-H(10G)	56.9
O(1)-C(1)-N(1)	105.74(13)	O(2X)-C(10)-H(10H)	110.2
O(1X)-C(1)-N(1)	103.2(3)	C(9)-C(10)-H(10H)	86.2
O(1)-C(1)-C(6)	111.23(12)	H(10A)-C(10)-H(10H)	62.2
O(1X)-C(1)-C(6)	124.9(3)	H(10B)-C(10)-H(10H)	64.5
N(1)-C(1)-C(6)	113.74(10)	H(10C)-C(10)-H(10H)	164.3
O(1)-C(1)-C(2)	117.78(12)	H(10G)-C(10)-H(10H)	108.5
O(1X)-C(1)-C(2)	106.5(3)	O(2X)-C(10)-H(10I)	110.0
N(1)-C(1)-C(2)	113.90(11)	C(9)-C(10)-H(10I)	87.4
C(6)-C(1)-C(2)	94.50(10)	H(10A)-C(10)-H(10I)	159.8
N(2X)-N(1)-N(2)	25.2(2)	H(10B)-C(10)-H(10I)	52.6
N(2X)-N(1)-C(1)	112.8(3)	H(10C)-C(10)-H(10I)	73.3
N(2)-N(1)-C(1)	109.94(12)	H(10G)-C(10)-H(10I)	108.7
C(9)-O(1)-C(1)	109.06(17)	H(10H)-C(10)-H(10I)	109.7
N(1)-N(2)-C(9)	111.19(14)	O(2)-C(10X)-C(9X)	40.26(18)
O(2)-C(9)-O(1)	112.32(14)	O(2)-C(10X)-H(10D)	90.9
O(2)-C(9)-N(2)	110.30(14)	C(9X)-C(10X)-H(10D)	109.8
O(1)-C(9)-N(2)	104.00(15)	O(2)-C(10X)-H(10E)	149.5
O(2)-C(9)-C(10)	107.73(13)	C(9X)-C(10X)-H(10E)	109.5
O(1)-C(9)-C(10)	113.00(15)	H(10D)-C(10X)-H(10E)	108.5
N(2)-C(9)-C(10)	109.45(14)	O(2)-C(10X)-H(10F)	85.2
C(9)-O(2)-C(10X)	114.71(13)	C(9X)-C(10X)-H(10F)	110.4
C(9X)-O(1X)-C(1)	110.1(5)	H(10D)-C(10X)-H(10F)	109.8
N(1)-N(2X)-C(9X)	109.2(4)	H(10E)-C(10X)-H(10F)	108.8
O(2X)-C(9X)-O(1X)	110.6(5)	O(2)-C(10X)-H(10L)	109.6
O(2X)-C(9X)-N(2X)	110.4(4)	C(9X)-C(10X)-H(10L)	149.6
O(1X)-C(9X)-N(2X)	103.9(5)	H(10D)-C(10X)-H(10L)	56.8
O(2X)-C(9X)-C(10X)	108.8(4)	H(10E)-C(10X)-H(10L)	100.8
O(1X)-C(9X)-C(10X)	112.1(4)	H(10F)-C(10X)-H(10L)	59.2
N(2X)-C(9X)-C(10X)	111.0(4)	O(2)-C(10X)-H(10M)	109.5
C(9X)-O(2X)-C(10)	113.7(3)	C(9X)-C(10X)-H(10M)	84.6
O(2X)-C(10)-C(9)	42.17(17)	H(10D)-C(10X)-H(10M)	66.4
O(2X)-C(10)-H(10A)	90.2	H(10E)-C(10X)-H(10M)	60.9
C(9)-C(10)-H(10A)	109.6	H(10F)-C(10X)-H(10M)	164.5
O(2X)-C(10)-H(10B)	151.0	H(10L)-C(10X)-H(10M)	109.5
C(9)-C(10)-H(10B)	109.4	O(2)-C(10X)-H(10N)	109.4
H(10A)-C(10)-H(10B)	109.5	C(9X)-C(10X)-H(10N)	89.6
O(2X)-C(10)-H(10C)	82.2	H(10D)-C(10X)-H(10N)	159.2
C(9)-C(10)-H(10C)	109.5	H(10E)-C(10X)-H(10N)	55.7
H(10A)-C(10)-H(10C)	109.5	H(10F)-C(10X)-H(10N)	68.4
H(10B)-C(10)-H(10C)	109.5	H(10L)-C(10X)-H(10N)	109.5
O(2X)-C(10)-H(10G)	109.8	H(10M)-C(10X)-H(10N)	109.5

Crystallographic data for phenyl((1*R*,2*R*,4*S*,5*S*,8*r*)-tricyclo[3.2.1.0^{2,4}]octan-8-yl)methanone (55)



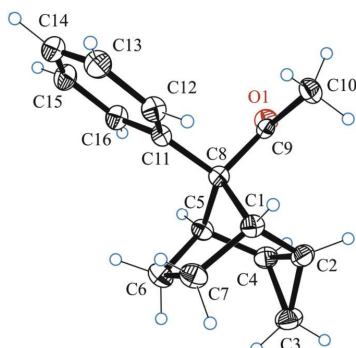
Empirical formula	C ₁₅ H ₁₆ O	
Formula weight	212.28	
Temperature	100(2) K	
Wavelength	0.71073 Å	
Crystal system, space group	orthorhombic, Pbcn	
Unit cell dimensions	a = 9.6760(4) Å	alpha = 90 deg.
	b = 13.6599(5) Å	beta = 90 deg.
	c = 16.9725(6) Å	gamma = 90 deg.
Volume	2243.31(15) Å ³	
Z, Calculated density	8, 1.257 Mg/m ³	
Absorption coefficient	0.077 mm ⁻¹	
F(000)	912	
Crystal size	0.30 x 0.20 x 0.10 mm	
Theta range for data collection	2.58 to 30.16 deg.	
Index ranges	-11 ≤ h ≤ 13, -19 ≤ k ≤ 18, -23 ≤ l ≤ 18	
Reflections collected / unique	44776 / 3317 [R(int) = 0.0572]	
Completeness to 2theta = 30.16	99.8%	
Max. and min. transmission	0.9924 and 0.9774	
Refinement method	Full-matrix least-squares on F ²	
Data / restraints / parameters	3317 / 0 / 145	
Goodness-of-fit on F ²	1.030	
Final R indices [I > 2sigma(I)]	R1 = 0.0462, wR2 = 0.1173	
R indices (all data)	R1 = 0.0701, wR2 = 0.1313	
Largest diff. peak and hole	0.392 and -0.236 e.Å ⁻³	

Bond Lengths (Å) and Angles (deg) for 55

O(1)-C(9)	1.2138(16)	C(4)-C(2)-C(1)	103.99(11)
C(1)-C(2)	1.532(2)	C(3)-C(2)-H(2)	118.4
C(1)-C(7)	1.533(2)	C(4)-C(2)-H(2)	118.4
C(1)-C(8)	1.5430(18)	C(1)-C(2)-H(2)	118.4
C(1)-H(1)	1.0000	C(2)-C(3)-C(4)	60.31(9)
C(2)-C(3)	1.5015(19)	C(2)-C(3)-H(3A)	117.7
C(2)-C(4)	1.5118(19)	C(4)-C(3)-H(3A)	117.7
C(2)-H(2)	1.0000	C(2)-C(3)-H(3B)	117.7
C(3)-C(4)	1.5080(19)	C(4)-C(3)-H(3B)	117.7
C(3)-H(3A)	0.9900	H(3A)-C(3)-H(3B)	114.9
C(3)-H(3B)	0.9900	C(3)-C(4)-C(2)	59.63(9)
C(4)-C(5)	1.5328(18)	C(3)-C(4)-C(5)	120.41(11)
C(4)-H(4)	1.0000	C(2)-C(4)-C(5)	103.87(10)
C(5)-C(6)	1.5320(18)	C(3)-C(4)-H(4)	118.7
C(5)-C(8)	1.5524(18)	C(2)-C(4)-H(4)	118.7
C(5)-H(5)	1.0000	C(5)-C(4)-H(4)	118.7
C(6)-C(7)	1.553(2)	C(6)-C(5)-C(4)	111.61(11)
C(6)-H(6A)	0.9900	C(6)-C(5)-C(8)	100.29(10)
C(6)-H(6B)	0.9900	C(4)-C(5)-C(8)	100.54(10)
C(7)-H(7A)	0.9900	C(6)-C(5)-H(5)	114.3
C(7)-H(7B)	0.9900	C(4)-C(5)-H(5)	114.3
C(8)-C(9)	1.5072(18)	C(8)-C(5)-H(5)	114.3
C(8)-H(8)	1.0000	C(5)-C(6)-C(7)	102.95(11)
C(9)-C(10)	1.4977(18)	C(5)-C(6)-H(6A)	111.2
C(10)-C(15)	1.3888(18)	C(7)-C(6)-H(6A)	111.2
C(10)-C(11)	1.3897(19)	C(5)-C(6)-H(6B)	111.2
C(11)-C(12)	1.380(2)	C(7)-C(6)-H(6B)	111.2
C(11)-H(11)	0.9500	H(6A)-C(6)-H(6B)	109.1
C(12)-C(13)	1.384(2)	C(1)-C(7)-C(6)	103.32(11)
C(12)-H(12)	0.9500	C(1)-C(7)-H(7A)	111.1
C(13)-C(14)	1.381(2)	C(6)-C(7)-H(7A)	111.1
C(13)-H(13)	0.9500	C(1)-C(7)-H(7B)	111.1
C(14)-C(15)	1.384(2)	C(6)-C(7)-H(7B)	111.1
C(14)-H(14)	0.9500	H(7A)-C(7)-H(7B)	109.1
C(15)-H(15)	0.9500	C(9)-C(8)-C(1)	114.41(11)
C(2)-C(1)-C(7)	111.19(11)	C(9)-C(8)-C(5)	116.84(11)
C(2)-C(1)-C(8)	100.90(10)	C(1)-C(8)-C(5)	93.23(10)
C(7)-C(1)-C(8)	100.22(11)	C(9)-C(8)-H(8)	110.4
C(2)-C(1)-H(1)	114.3	C(1)-C(8)-H(8)	110.4
C(7)-C(1)-H(1)	114.3	C(5)-C(8)-H(8)	110.4
C(8)-C(1)-H(1)	114.3	O(1)-C(9)-C(10)	119.43(12)
C(3)-C(2)-C(4)	60.06(9)	O(1)-C(9)-C(8)	121.29(12)
C(3)-C(2)-C(1)	120.95(12)	C(10)-C(9)-C(8)	119.25(11)

C(15)-C(10)-C(11)	119.19(12)	C(14)-C(13)-C(12)	120.21(13)
C(15)-C(10)-C(9)	122.59(12)	C(14)-C(13)-H(13)	119.9
C(11)-C(10)-C(9)	118.21(12)	C(12)-C(13)-H(13)	119.9
C(12)-C(11)-C(10)	120.51(13)	C(13)-C(14)-C(15)	119.90(13)
C(12)-C(11)-H(11)	119.7	C(13)-C(14)-H(14)	120.0
C(10)-C(11)-H(11)	119.7	C(15)-C(14)-H(14)	120.0
C(11)-C(12)-C(13)	119.83(13)	C(14)-C(15)-C(10)	120.34(13)
C(11)-C(12)-H(12)	120.1	C(14)-C(15)-H(15)	119.8
C(13)-C(12)-H(12)	120.1	C(10)-C(15)-H(15)	119.8

Crystallographic data for 1-((1*R*,2*R*,4*S*,5*S*,8*r*)-8-phenyltricyclo[3.2.1.0^{2,4}]octan-8-yl)ethan-1-one (56)



Empirical formula	$C_{16}H_{18}O$
Formula weight	226.30
Temperature	150(2) K
Wavelength	0.71073 Å
Crystal system, space group	orthorhombic, P212121
Unit cell dimensions	a = 6.1320(2) Å alpha = 90 deg. b = 10.6950(3) Å beta = 90 deg. c = 18.0264(5) Å gamma = 90 deg.
Volume	1182.20(6) Å ³
Z, Calculated density	4, 1.271 Mg/m ³
Absorption coefficient	0.077 mm ⁻¹
F(000)	488
Crystal size	0.25 x 0.03 x 0.03 mm
Theta range for data collection	2.21 to 30.12 deg.
Index ranges	-8 ≤ h ≤ 8, -15 ≤ k ≤ 14, -25 ≤ l ≤ 25
Reflections collected / unique	35201 / 3489 [R(int) = 0.0619]
Completeness to 2theta = 30.12	99.9%
Max. and min. transmission	0.9977 and 0.9810
Refinement method	Full-matrix least-squares on F ²
Data / restraints / parameters	3489 / 0 / 155
Goodness-of-fit on F ²	1.048
Final R indices [I > 2sigma(I)]	R1 = 0.0440, wR2 = 0.1008
R indices (all data)	R1 = 0.0610, wR2 = 0.1099
Absolute structure parameter	-0.2(15)
Largest diff. peak and hole	0.250 and -0.193 e.Å ⁻³

Bond Lengths (Å) and Angles (deg) for 56

O(1)-C(9)	1.2137(18)	C(8)-C(1)-H(1)	114.5
C(1)-C(7)	1.533(2)	C(3)-C(2)-C(4)	59.62(11)
C(1)-C(2)	1.536(2)	C(3)-C(2)-C(1)	120.13(14)
C(1)-C(8)	1.564(2)	C(4)-C(2)-C(1)	104.08(13)
C(1)-H(1)	1.0000	C(3)-C(2)-H(2)	118.8
C(2)-C(3)	1.506(2)	C(4)-C(2)-H(2)	118.8
C(2)-C(4)	1.524(2)	C(1)-C(2)-H(2)	118.8
C(2)-H(2)	1.0000	C(2)-C(3)-C(4)	60.76(11)
C(3)-C(4)	1.506(2)	C(2)-C(3)-H(3A)	117.7
C(3)-H(3A)	0.9900	C(4)-C(3)-H(3A)	117.7
C(3)-H(3B)	0.9900	C(2)-C(3)-H(3B)	117.7
C(4)-C(5)	1.525(2)	C(4)-C(3)-H(3B)	117.7
C(4)-H(4)	1.0000	H(3A)-C(3)-H(3B)	114.8
C(5)-C(6)	1.531(2)	C(3)-C(4)-C(2)	59.62(11)
C(5)-C(8)	1.5522(19)	C(3)-C(4)-C(5)	121.13(15)
C(5)-H(5)	1.0000	C(2)-C(4)-C(5)	103.67(13)
C(6)-C(7)	1.556(2)	C(3)-C(4)-H(4)	118.5
C(6)-H(6A)	0.9900	C(2)-C(4)-H(4)	118.5
C(6)-H(6B)	0.9900	C(5)-C(4)-H(4)	118.5
C(7)-H(7A)	0.9900	C(4)-C(5)-C(6)	111.40(13)
C(7)-H(7B)	0.9900	C(4)-C(5)-C(8)	101.12(12)
C(8)-C(11)	1.518(2)	C(6)-C(5)-C(8)	100.93(11)
C(8)-C(9)	1.525(2)	C(4)-C(5)-H(5)	114.0
C(9)-C(10)	1.502(2)	C(6)-C(5)-H(5)	114.0
C(10)-H(10A)	0.9800	C(8)-C(5)-H(5)	114.0
C(10)-H(10B)	0.9800	C(5)-C(6)-C(7)	102.88(12)
C(10)-H(10C)	0.9800	C(5)-C(6)-H(6A)	111.2
C(11)-C(12)	1.393(2)	C(7)-C(6)-H(6A)	111.2
C(11)-C(16)	1.396(2)	C(5)-C(6)-H(6B)	111.2
C(12)-C(13)	1.387(2)	C(7)-C(6)-H(6B)	111.2
C(12)-H(12)	0.9500	H(6A)-C(6)-H(6B)	109.1
C(13)-C(14)	1.379(3)	C(1)-C(7)-C(6)	103.60(12)
C(13)-H(13)	0.9500	C(1)-C(7)-H(7A)	111.0
C(14)-C(15)	1.382(3)	C(6)-C(7)-H(7A)	111.0
C(14)-H(14)	0.9500	C(1)-C(7)-H(7B)	111.0
C(15)-C(16)	1.379(2)	C(6)-C(7)-H(7B)	111.0
C(15)-H(15)	0.9500	H(7A)-C(7)-H(7B)	109.0
C(16)-H(16)	0.9500	C(11)-C(8)-C(9)	105.35(11)
C(7)-C(1)-C(2)	111.34(13)	C(11)-C(8)-C(5)	115.66(12)
C(7)-C(1)-C(8)	100.50(12)	C(9)-C(8)-C(5)	113.30(12)
C(2)-C(1)-C(8)	99.69(12)	C(11)-C(8)-C(1)	117.16(12)
C(7)-C(1)-H(1)	114.5	C(9)-C(8)-C(1)	112.59(12)
C(2)-C(1)-H(1)	114.5	C(5)-C(8)-C(1)	92.88(11)

O(1)-C(9)-C(10)	121.16(14)	C(11)-C(12)-H(12)	119.6
O(1)-C(9)-C(8)	121.65(14)	C(14)-C(13)-C(12)	120.22(16)
C(10)-C(9)-C(8)	117.17(13)	C(14)-C(13)-H(13)	119.9
C(9)-C(10)-H(10A)	109.5	C(12)-C(13)-H(13)	119.9
C(9)-C(10)-H(10B)	109.5	C(13)-C(14)-C(15)	119.65(16)
H(10A)-C(10)-H(10B)	109.5	C(13)-C(14)-H(14)	120.2
C(9)-C(10)-H(10C)	109.5	C(15)-C(14)-H(14)	120.2
H(10A)-C(10)-H(10C)	109.5	C(16)-C(15)-C(14)	120.45(16)
H(10B)-C(10)-H(10C)	109.5	C(16)-C(15)-H(15)	119.8
C(12)-C(11)-C(16)	118.23(14)	C(14)-C(15)-H(15)	119.8
C(12)-C(11)-C(8)	122.21(13)	C(15)-C(16)-C(11)	120.72(15)
C(16)-C(11)-C(8)	119.40(13)	C(15)-C(16)-H(16)	119.6
C(13)-C(12)-C(11)	120.74(15)	C(11)-C(16)-H(16)	119.6
C(13)-C(12)-H(12)	119.6		

Supplementary Data for Kinetic Measurements

Preparation of samples: 2.0 mg of oxadiazolines **29a** or **29b** in 2.0 mL decane.

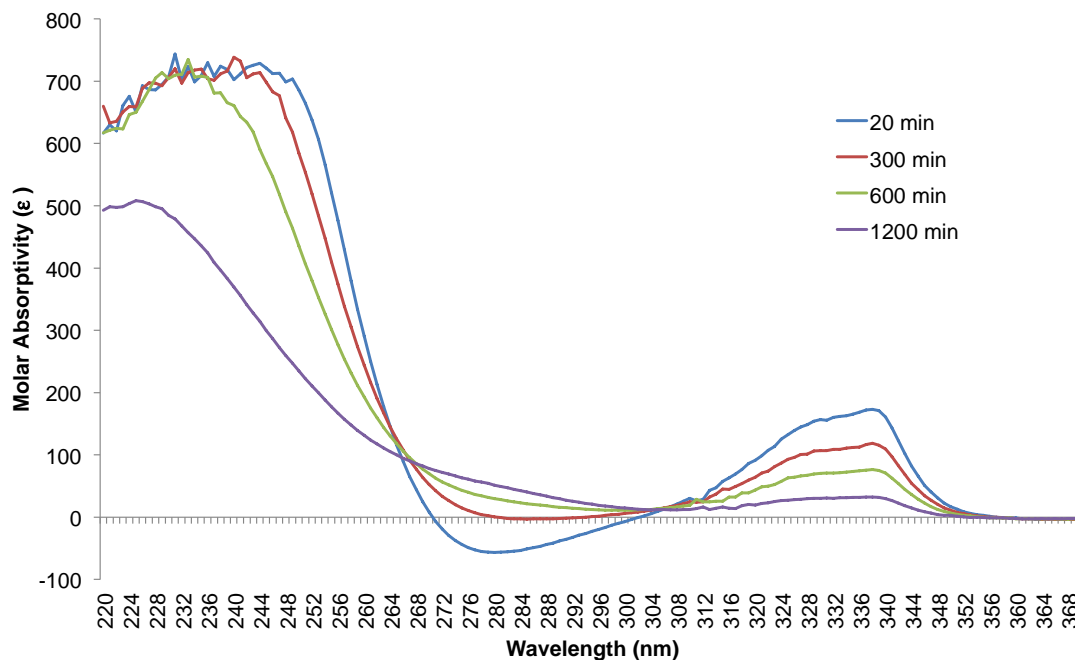


Figure A.1: UV spectra of oxadiazoline **29a** in decane (1 mg/mL) at 116 °C recorded after 20, 300, 600, and 1200 min, respectively.

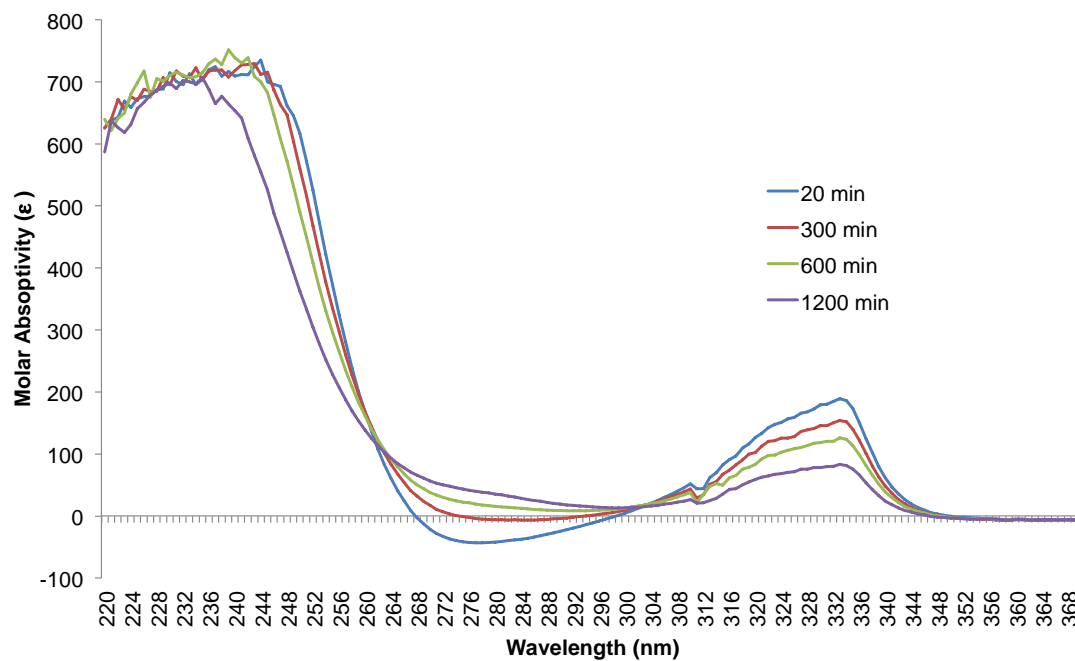


Figure A.2: UV spectra of oxadiazoline **29b** in decane (1 mg/mL) at 116 °C recorded after 20, 300, 600, and 1200 min, respectively.

Table A.1: UV Absorptions Measured for Oxadiazolines 29a and 29b at 333 and 338 nm at 116 °C

time (min)	absorption of 29a at 338 nm	absorption of 29a at 333 nm	absorption of 29b at 333 nm	absorption of 29b at 338 nm
0	0.9690	0.8490	1.0092	0.4860
20	0.8339	0.7798	0.9082	0.4880
40	0.8152	0.7624	0.8822	0.4682
60	0.7934	0.7246	0.8719	0.4630
120	0.7295	0.6769	0.8366	0.4368
180	0.6705	0.6222	0.8018	0.4170
240	0.6173	0.5736	0.7760	0.4006
300	0.5688	0.5224	0.7379	0.3840
360	0.5234	0.4846	0.7042	0.3736
420	0.4757	0.4440	0.6772	0.3541
480	0.4351	0.4086	0.6568	0.3427
540	0.4040	0.3751	0.6302	0.3263
600	0.3676	0.3431	0.6069	0.3154
660	0.3409	0.3200	0.5757	0.3054
720	0.3122	0.2914	0.5620	0.2890
780	0.2897	0.2690	0.5359	0.2783
840	0.2601	0.2445	0.5207	0.2665
900	0.2390	0.2303	0.4987	0.2564
960	0.2212	0.2117	0.4844	0.2467
1020	0.1979	0.1957	0.4548	0.2311
1080	0.1853	0.1784	0.4411	0.2228
1140	0.1704	0.1660	0.4198	0.2080
1200	0.1569	0.1508	0.4007	0.2046

NMR Spectra

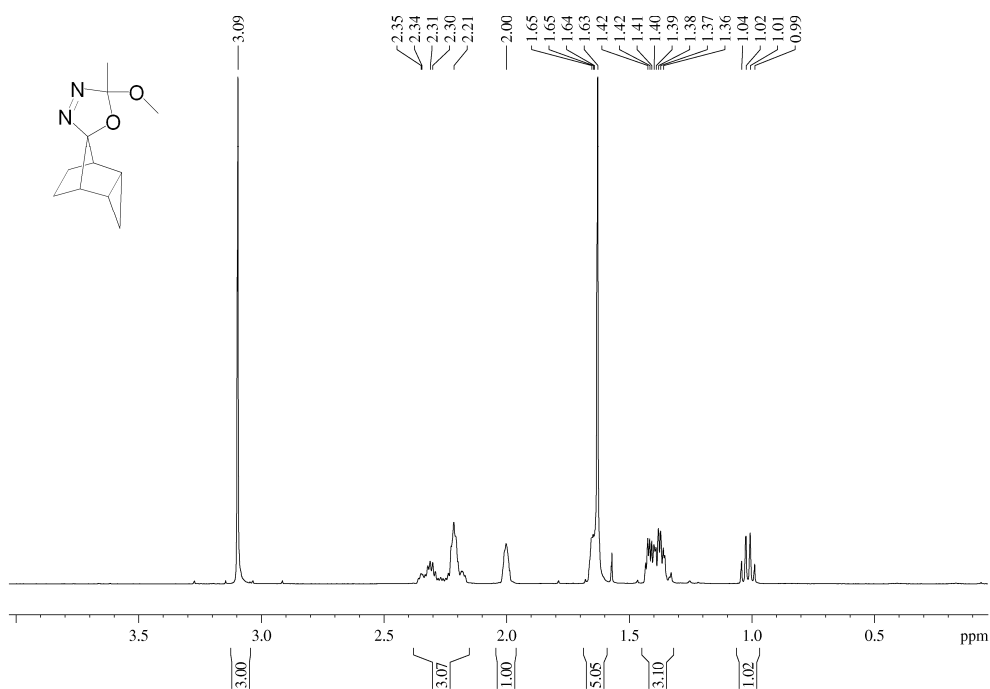


Figure A.3: ¹H NMR spectrum of *rel*-(1^{*R*},2^{*r*},2^{*R*},4^{*S*},5^{*R*},5^{*S*})-5-methoxy-5-methylspiro[2,5-dihydro-1,3,4-oxadiazole-2,8'-tricyclo[3.2.1.0^{2,4}]octane] (**29a**) (400.13 MHz, CDCl₃).

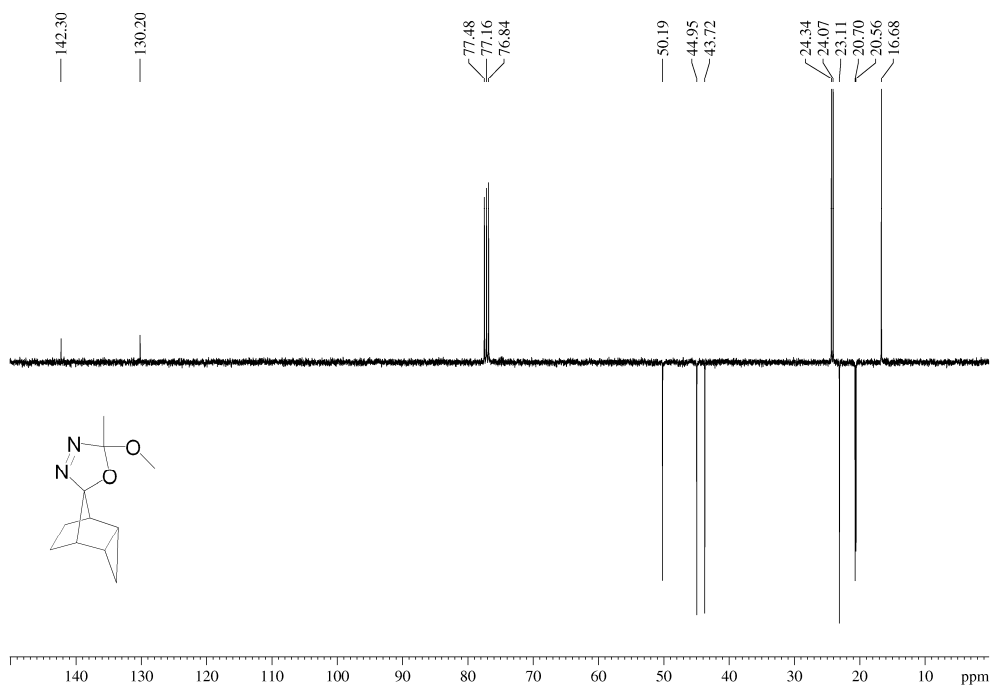


Figure A.4: ¹³C NMR spectrum of *rel*-(1^{*R*},2^{*r*},2^{*R*},4^{*S*},5^{*R*},5^{*S*})-5-methoxy-5-methylspiro[2,5-dihydro-1,3,4-oxadiazole-2,8'-tricyclo[3.2.1.0^{2,4}]octane] (**29a**) (100.62 MHz, CDCl₃).

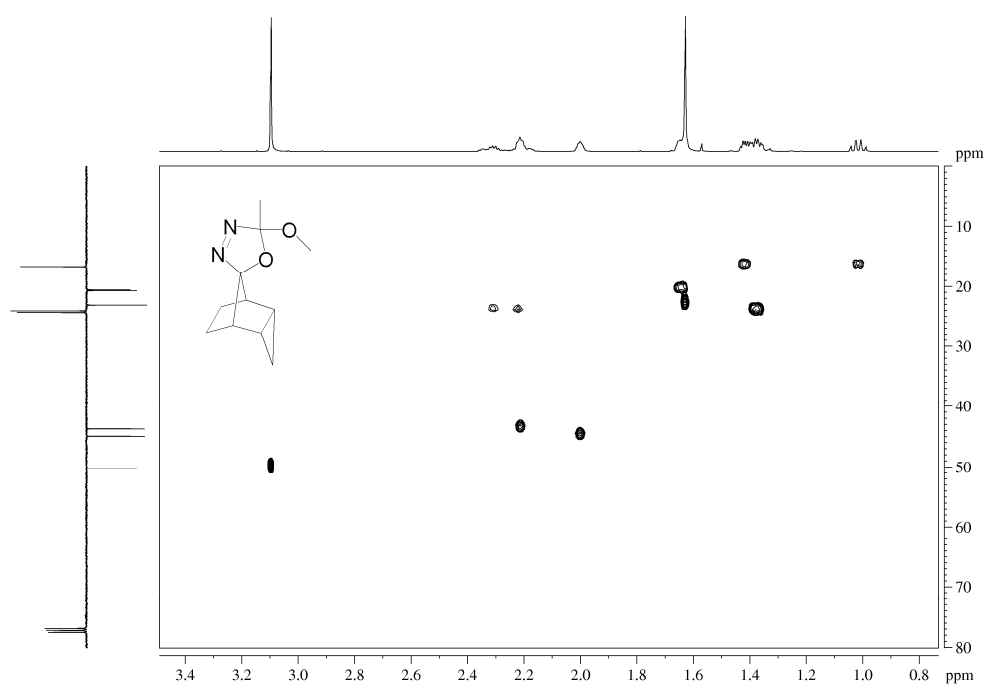


Figure A.5: HMQC spectrum of *rel*-(1'*R*,2*r*,2'*R*,4'*S*,5*R*,5'*S*)-5-methoxy-5-methylspiro[2,5-dihydro-1,3,4-oxadiazole-2,8'-tricyclo[3.2.1.0^{2,4}]octane] (**29a**) (400.13 and 100.62 MHz, CDCl₃).

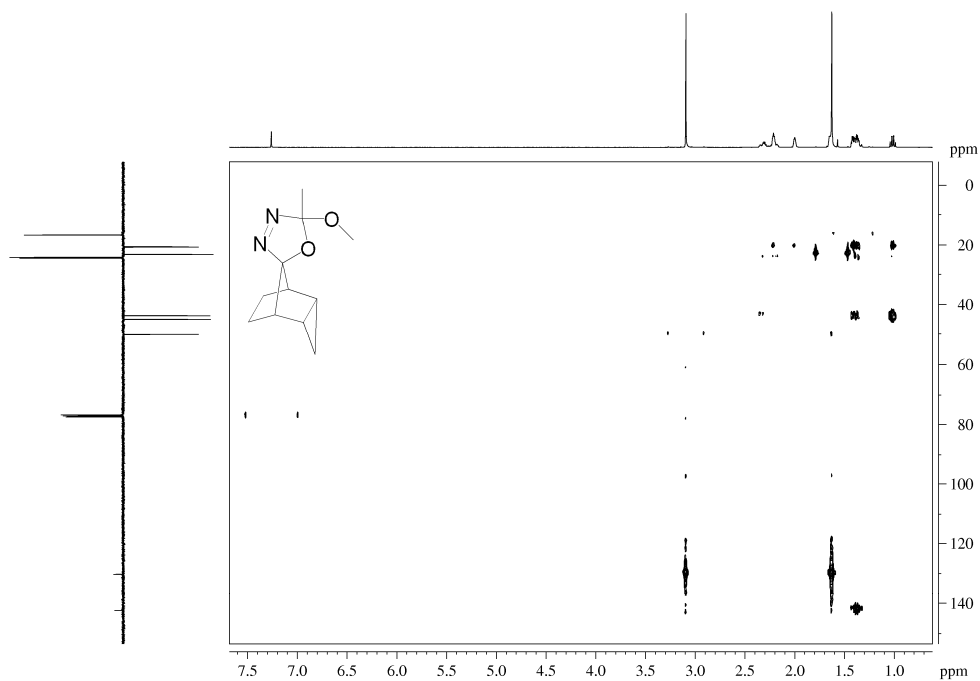


Figure A.6: HMBC (400.13 and 100.62 MHz, CDCl₃) of *rel*-(1'*R*,2*r*,2'*R*,4'*S*,5*R*,5'*S*)-5-methoxy-5-methylspiro[2,5-dihydro-1,3,4-oxadiazole-2,8'-tricyclo[3.2.1.0^{2,4}]octane] (**29a**).

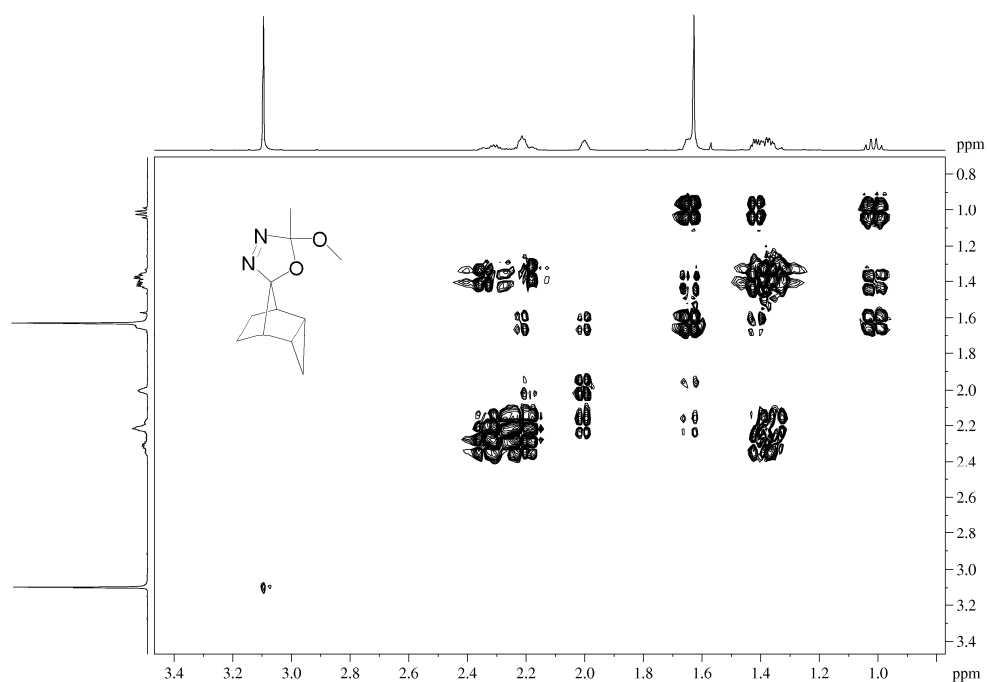


Figure A.7: COSY spectrum of *rel*-(1^R,2^r,2^R,4^S,5^R,5^S)-5-methoxy-5-methylspiro[2,5-dihydro-1,3,4-oxadiazole-2,8'-tricyclo[3.2.1.0^{2,4}]octane] (**29a**) (400.13 MHz, CDCl₃).

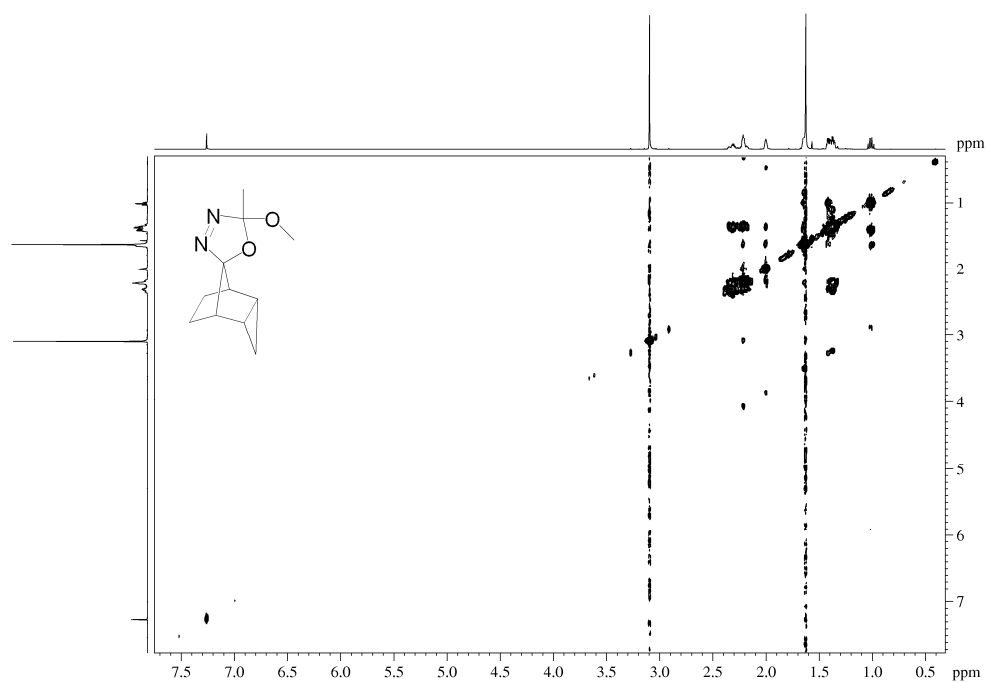


Figure A.8: NOESY spectrum of *rel*-(1^R,2^r,2^R,4^S,5^R,5^S)-5-methoxy-5-methylspiro[2,5-dihydro-1,3,4-oxadiazole-2,8'-tricyclo[3.2.1.0^{2,4}]octane] (**29a**) (400.13 MHz, CDCl₃).

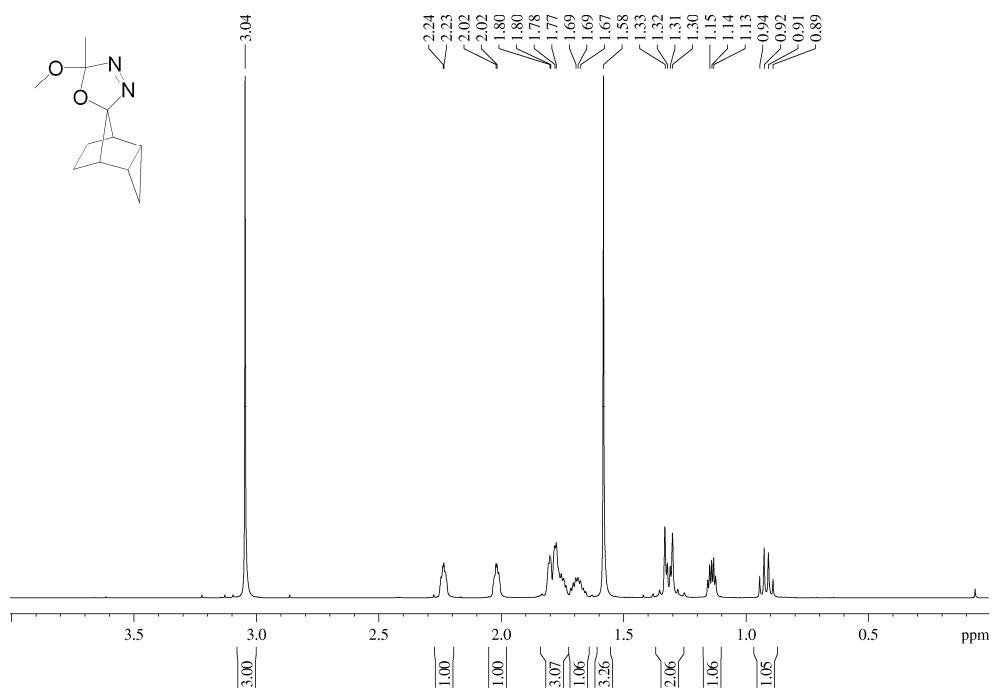


Figure A.9: ^1H NMR spectrum of *rel*-(1'*R*,2*s*,2'*R*,4'*S*,5*R*,5'*S*)-5-methoxy-5-methylspiro[2,5-dihydro-1,3,4-oxadiazole-2,8'-tricyclo[3.2.1.0^{2,4}]octane] (**29b**) (400.13 MHz, CDCl_3).

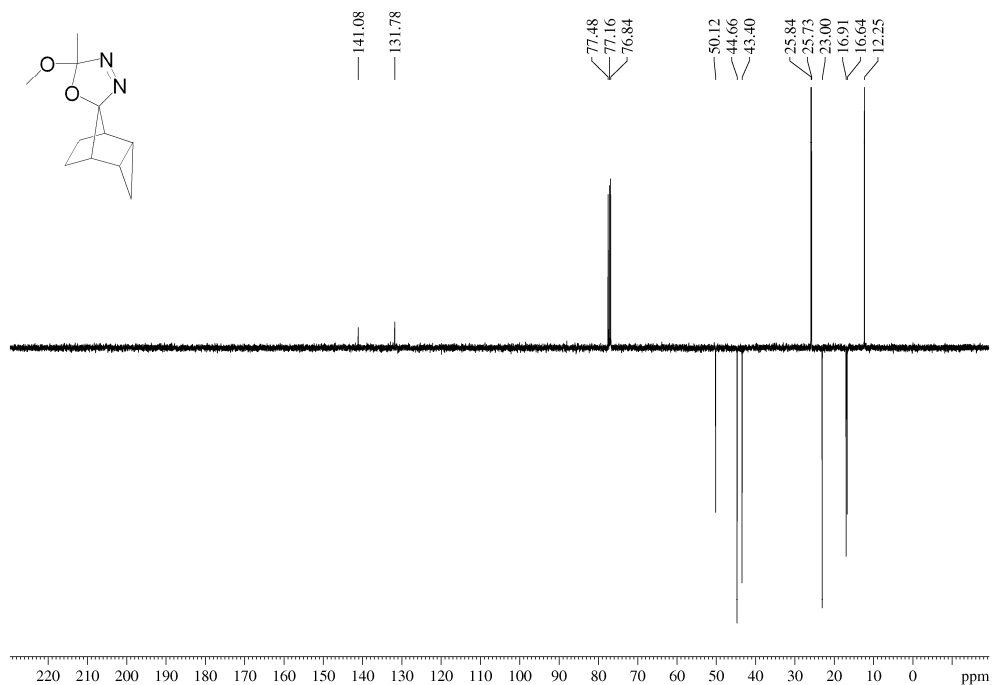


Figure A.10: ^{13}C NMR spectrum of *rel*-(1'*R*,2*s*,2'*R*,4'*S*,5*R*,5'*S*)-5-methoxy-5-methylspiro[2,5-dihydro-1,3,4-oxadiazole-2,8'-tricyclo[3.2.1.0^{2,4}]octane] (**29b**) (100.62 MHz, CDCl_3).

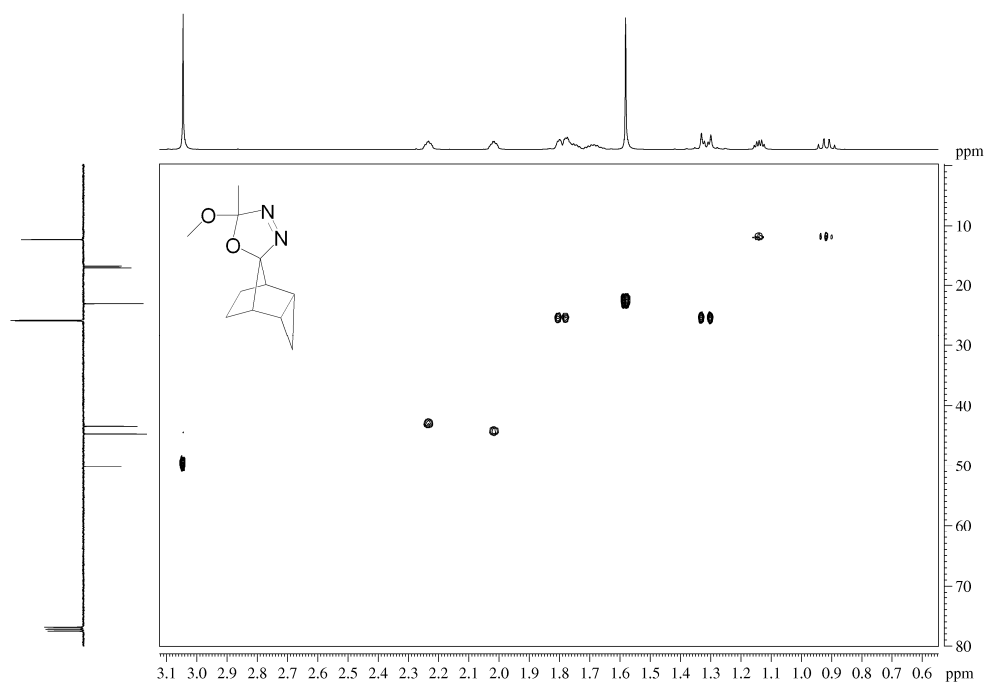


Figure A.11: HMQC spectrum of *rel*-(1^{*R*},2^{*s*},2^{*R*},4^{*S*},5^{*R*},5^{*S*})-5-methoxy-5-methylspiro[2,5-dihydro-1,3,4-oxadiazole-2,8'-tricyclo[3.2.1.0^{2,4}]octane] (**29b**) (400.13 and 100.62 MHz, CDCl₃).

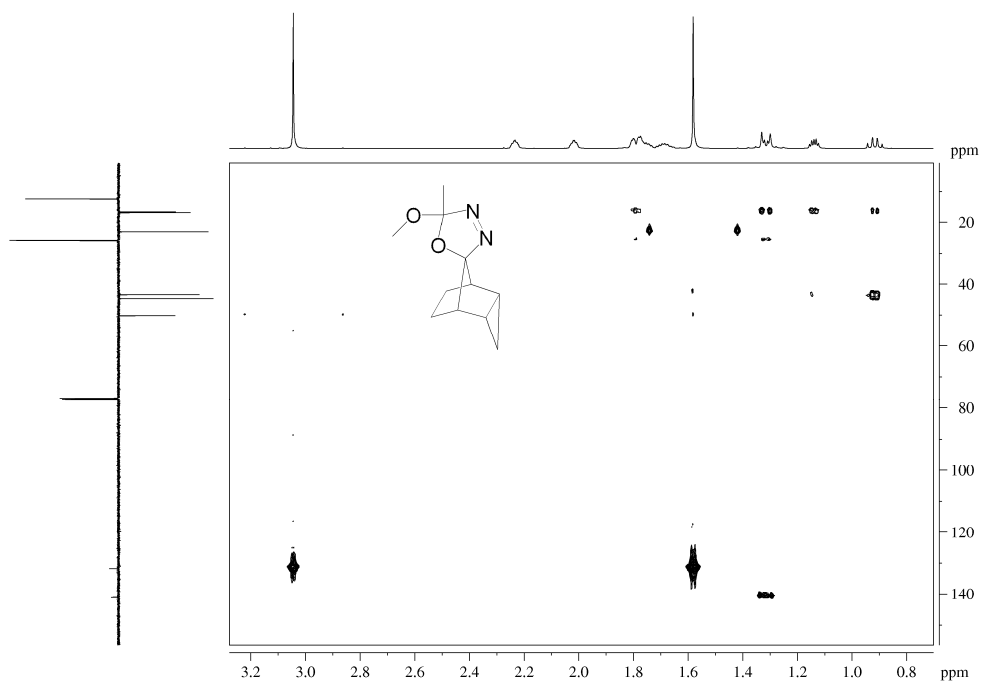


Figure A.12: HMBC spectrum of *rel*-(1^{*R*},2^{*s*},2^{*R*},4^{*S*},5^{*R*},5^{*S*})-5-methoxy-5-methylspiro[2,5-dihydro-1,3,4-oxadiazole-2,8'-tricyclo[3.2.1.0^{2,4}]octane] (**29b**) (400.13 and 100.62 MHz, CDCl₃).

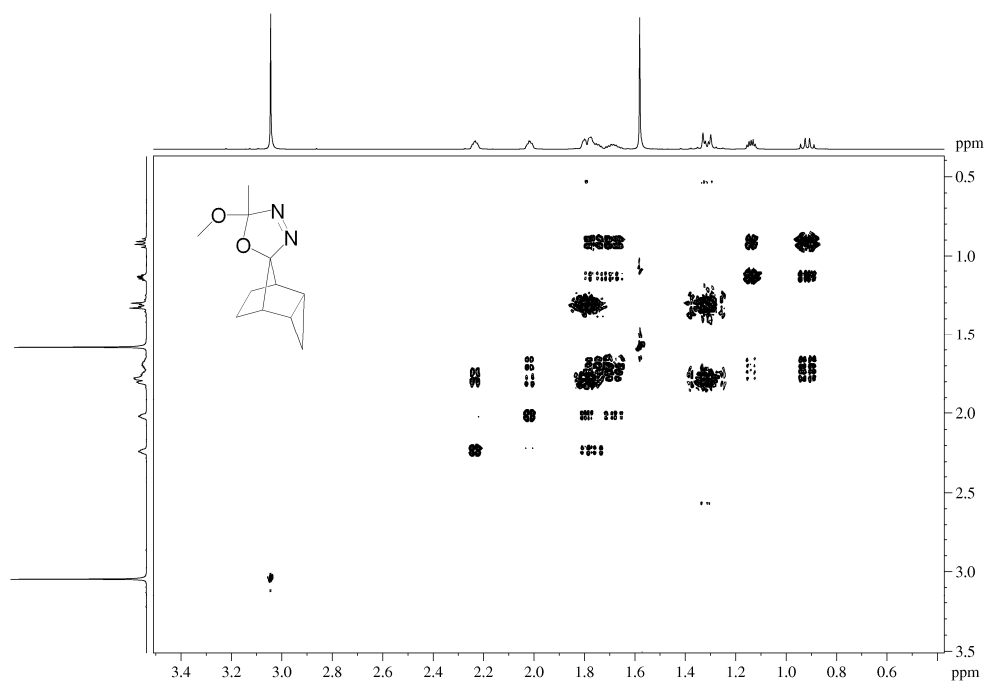


Figure A.13: COSY spectrum of *rel*-(1'*R*,2*s*,2'*R*,4'*S*,5*R*,5'*S*)-5-methoxy-5-methylspiro[2,5-dihydro-1,3,4-oxadiazole-2,8'-tricyclo[3.2.1.0^{2,4}]octane] (**29b**) (400.13 MHz, CDCl₃).

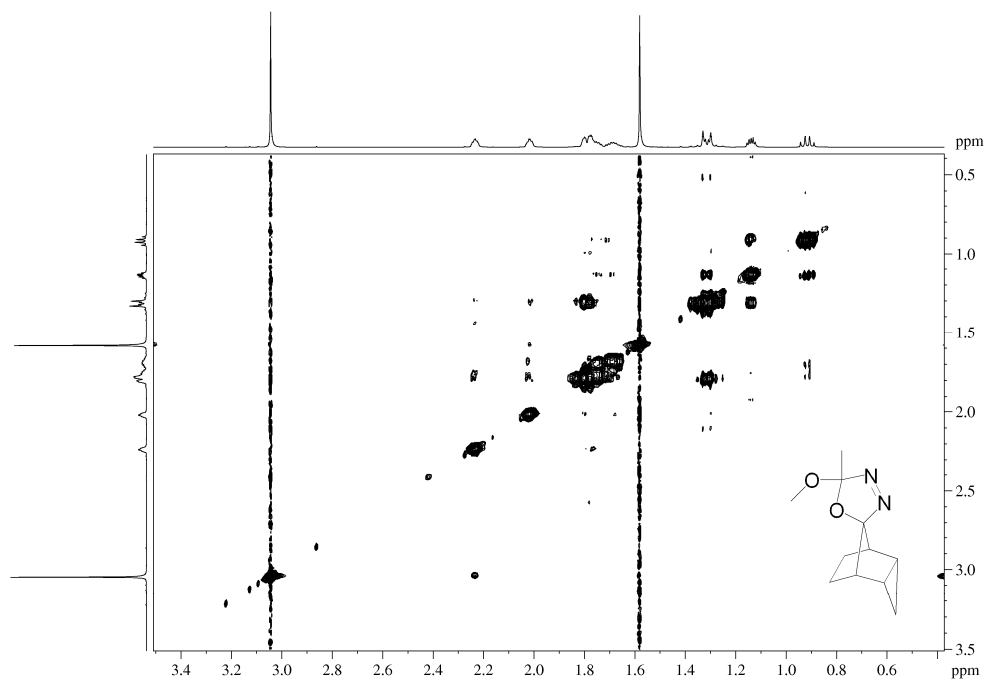


Figure A.14: NOESY spectrum of *rel*-(1'*R*,2*s*,2'*R*,4'*S*,5*R*,5'*S*)-5-methoxy-5-methylspiro[2,5-dihydro-1,3,4-oxadiazole-2,8'-tricyclo[3.2.1.0^{2,4}]octane] (**29b**) (400.13 MHz, CDCl₃).

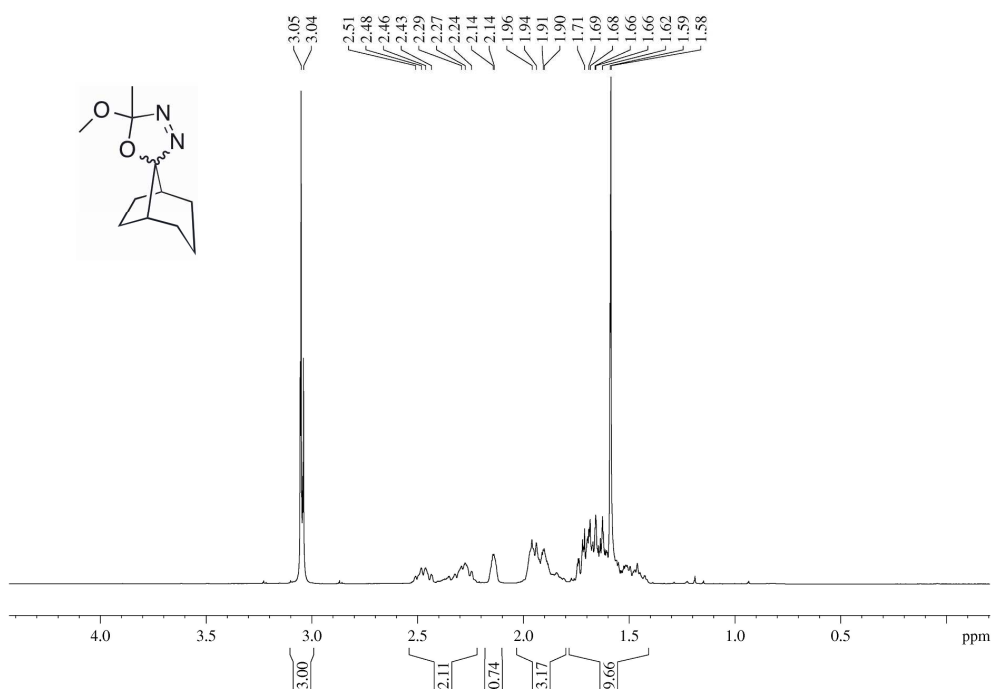


Figure A.15: ^1H NMR spectrum of *rac*-(1*R*,5*S*)-5'-methoxy-5'-methylspiro[bicyclo[3.2.1]octane-8,2'-2,5-dihydro-1,3,4-oxadiazole] (**39**) (400.13 MHz, CDCl_3).

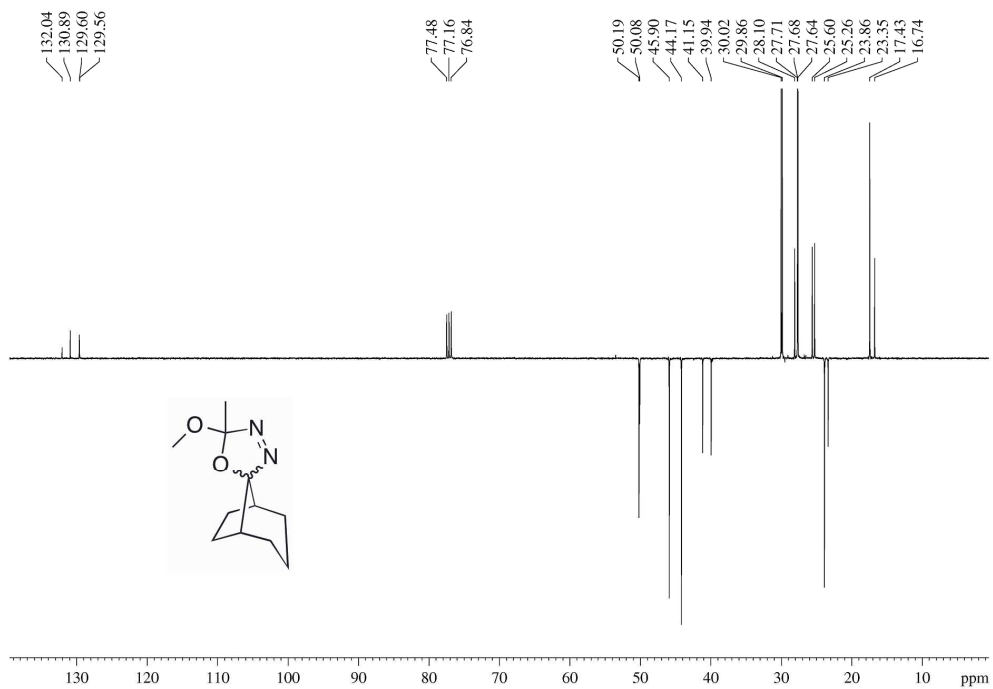


Figure A.16: ^{13}C NMR spectrum of *rac*-(1*R*,5*S*)-5'-methoxy-5'-methylspiro[bicyclo[3.2.1]octane-8,2'-2,5-dihydro-1,3,4-oxadiazole] (**39**) (100.62 MHz, CDCl_3).

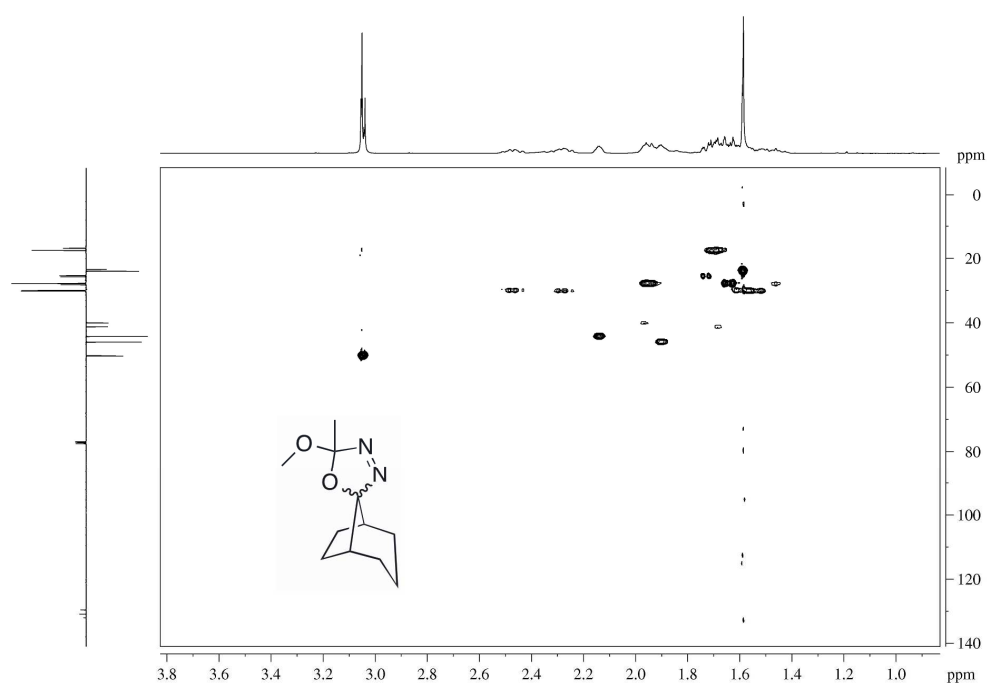


Figure A.17: HMQC spectrum of *rac*-(1*R*,5*S*)-5'-methoxy-5'-methylspiro[bicyclo[3.2.1]octane-8,2'-2,5-dihydro-1,3,4-oxadiazole] (**39**) (400.13 and 100.62, MHz, CDCl₃).

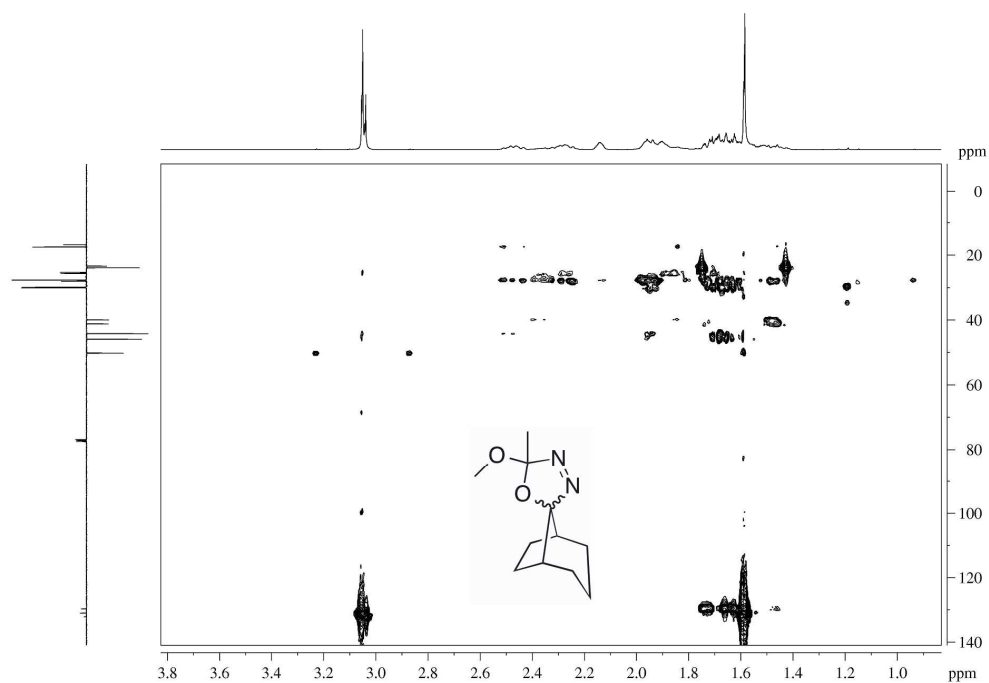


Figure A.18: HMBC spectrum of *rac*-(1*R*,5*S*)-5'-methoxy-5'-methylspiro[bicyclo[3.2.1]octane-8,2'-2,5-dihydro-1,3,4-oxadiazole] (**39**) (400.13 and 100.62, MHz CDCl₃).

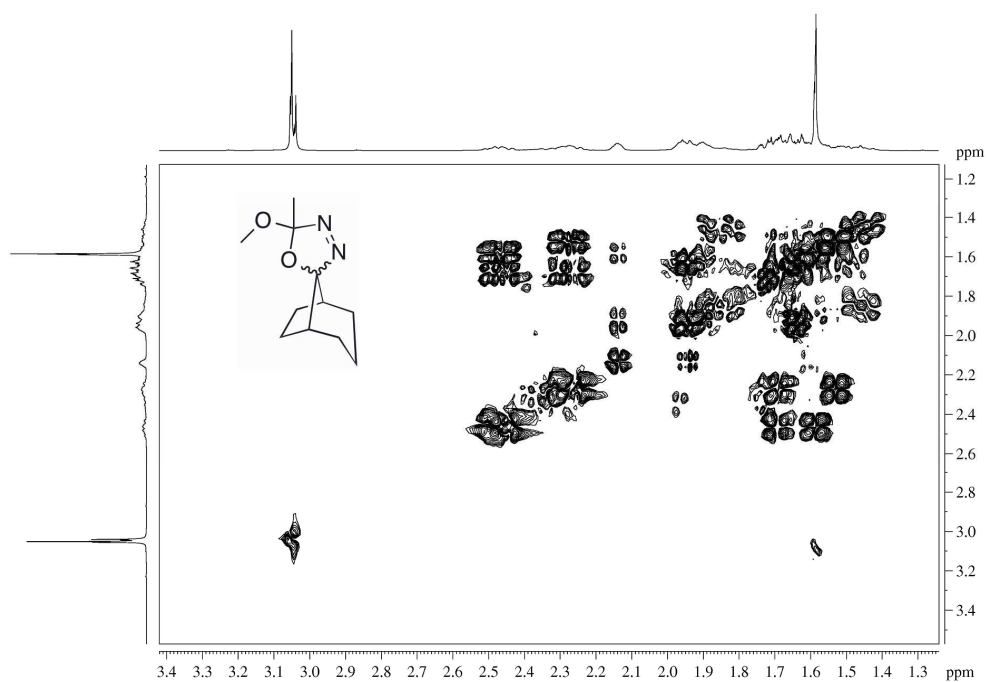


Figure A.19: COSY spectrum of *rac*-(1*R*,5*S*)-5'-methoxy-5'-methylspiro[bicyclo[3.2.1]octane-8,2'-2,5-dihydro-1,3,4-oxadiazole] (**39**) (400.13 MHz, CDCl₃).

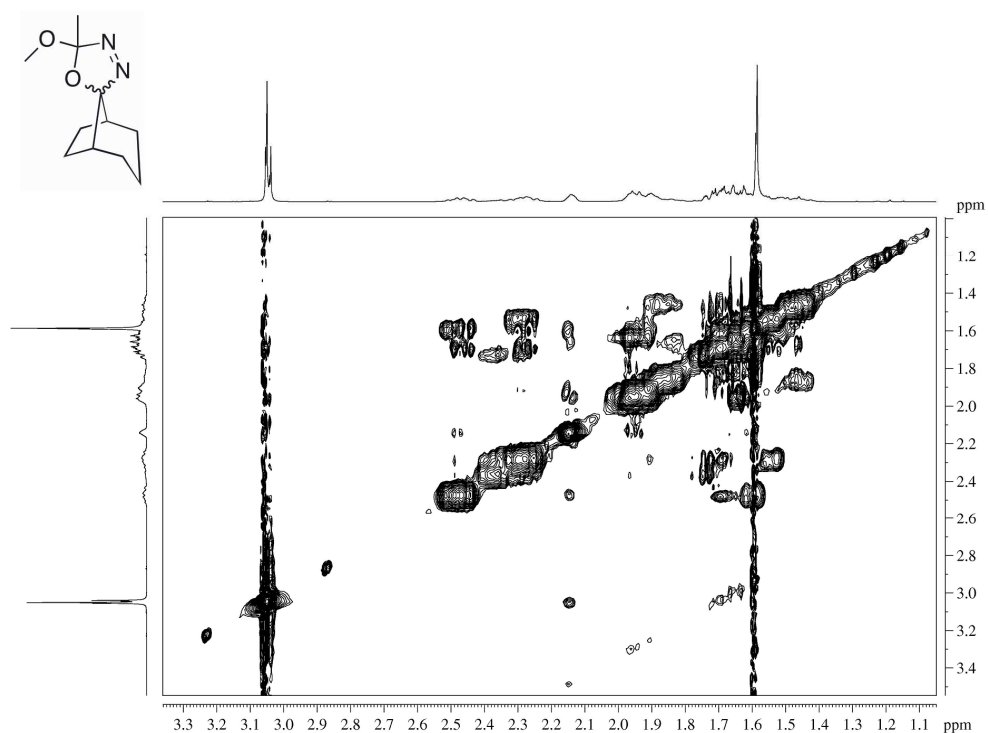


Figure A.20: NOESY spectrum of *rac*-(1*R*,5*S*)-5'-methoxy-5'-methylspiro[bicyclo[3.2.1]octane-8,2'-2,5-dihydro-1,3,4-oxadiazole] (**39**) (400.13 MHz, CDCl₃).

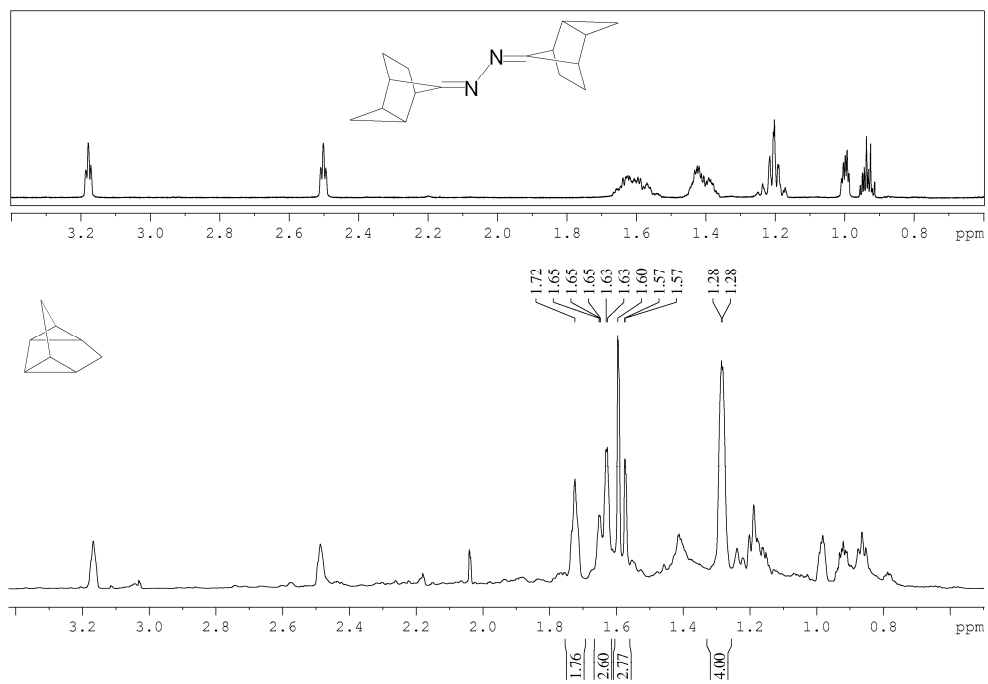


Figure A.21: ^1H NMR spectrum of tetracyclo[3.3.0.0. 2,8 0 4,6]octane (**41**) (600.13 MHz, CDCl_3).

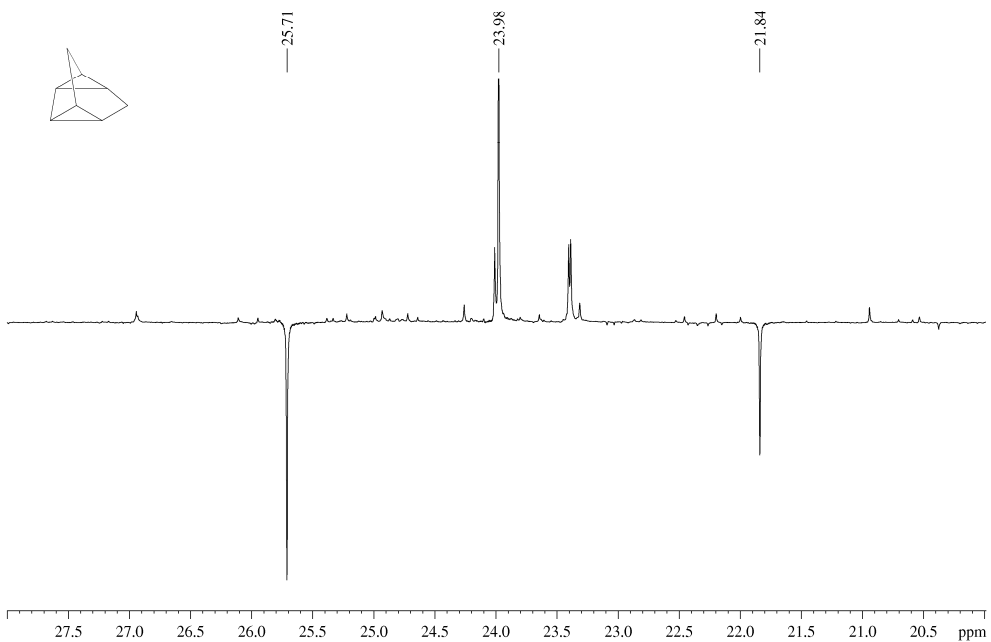


Figure A.22: ^{13}C NMR spectrum of tetracyclo[3.3.0.0. 2,8 0 4,6]octane (**41**) (150.92 MHz, CDCl_3).

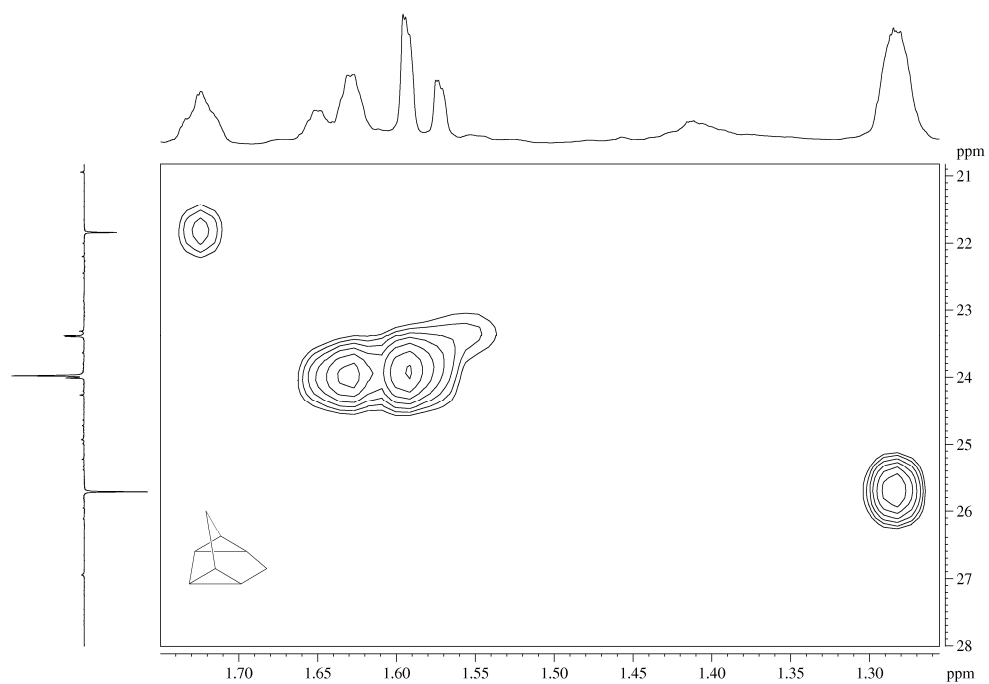


Figure A.23: HMBC spectrum of tetracyclo[3.3.0.0.^{2,8}0^{4,6}]octane (**41**) (600.13 and 150.92 MHz, CDCl₃).

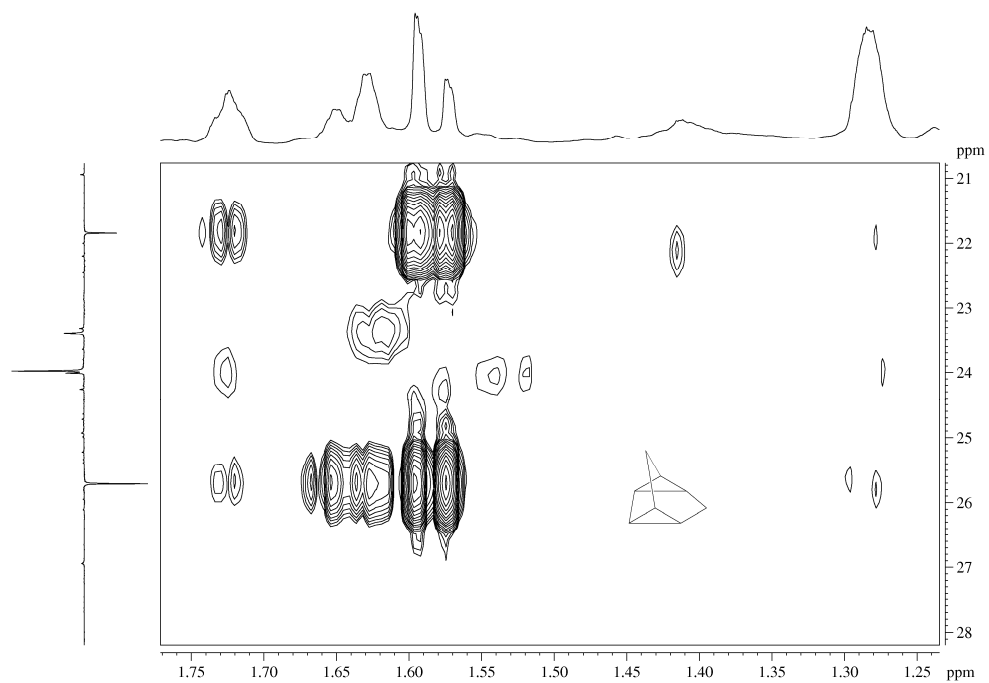


Figure A.24: HMBC spectrum of tetracyclo[3.3.0.0.^{2,8}0^{4,6}]octane (**41**) (600.13 and 150.92 MHz, CDCl₃).

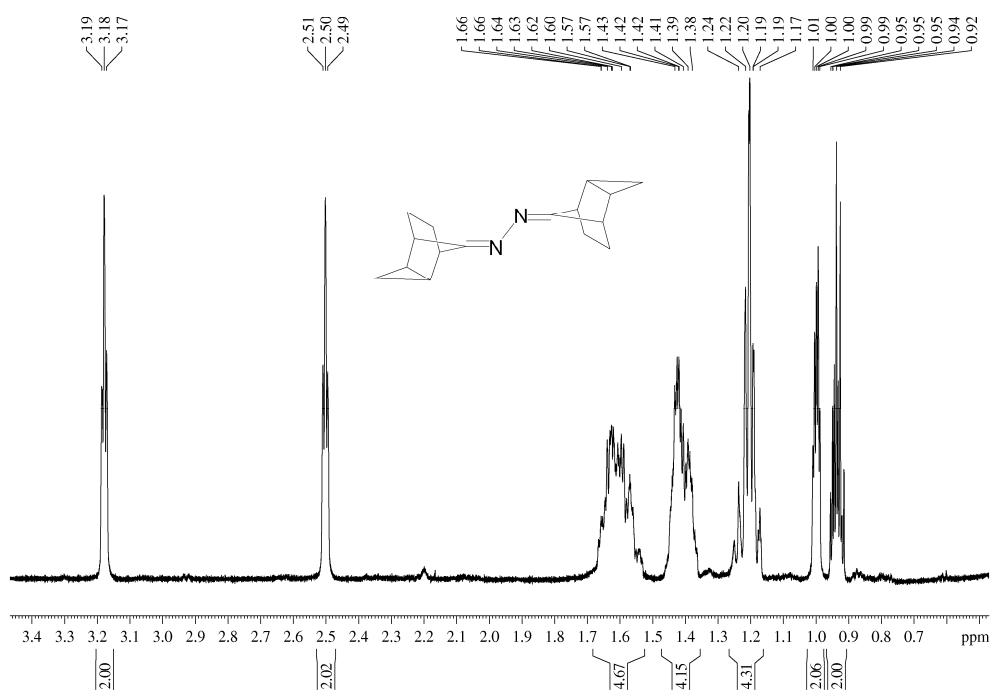


Figure A.25: ¹H NMR spectrum of *endo*-tricyclo[3.2.1.0^{2,4}]octan-8-one azine (**44**) (600.13 MHz, CDCl₃).

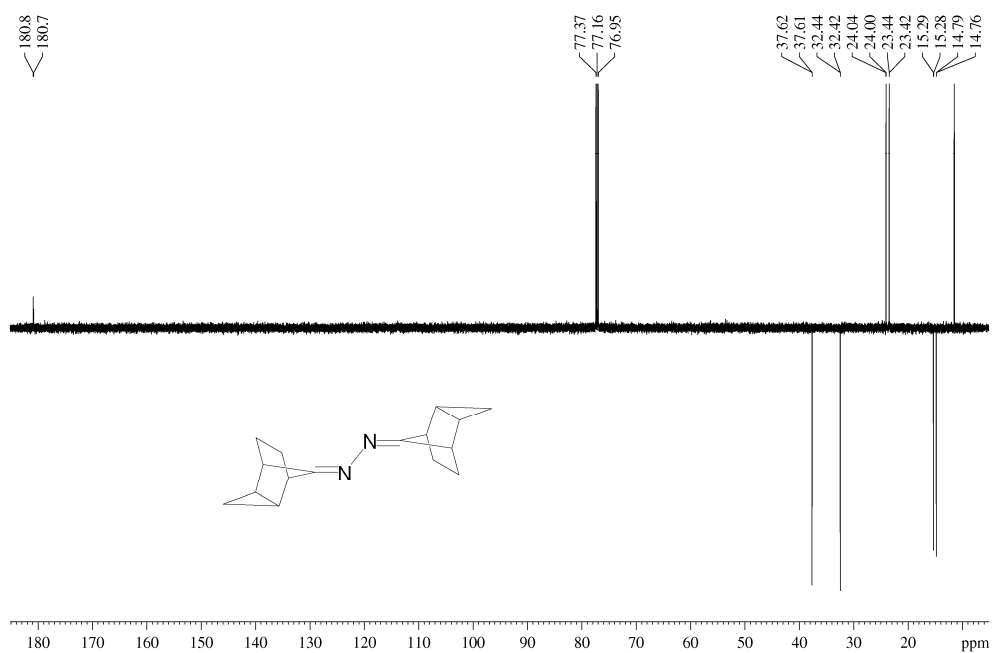


Figure A.26: ¹³C NMR spectrum of *endo*-tricyclo[3.2.1.0^{2,4}]octan-8-one azine (**44**) (150.92 MHz, CDCl₃).

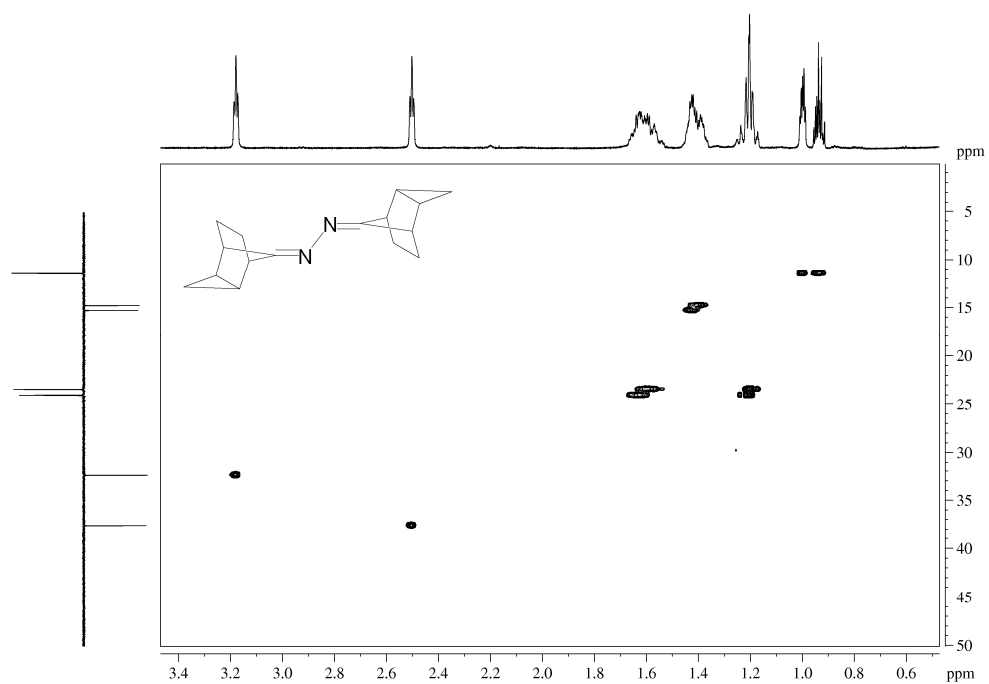


Figure A.27: HMQC spectrum of *endo*-tricyclo[3.2.1.0^{2,4}]octan-8-one azine (**44**) (600.13 and 150.92 MHz, CDCl₃).

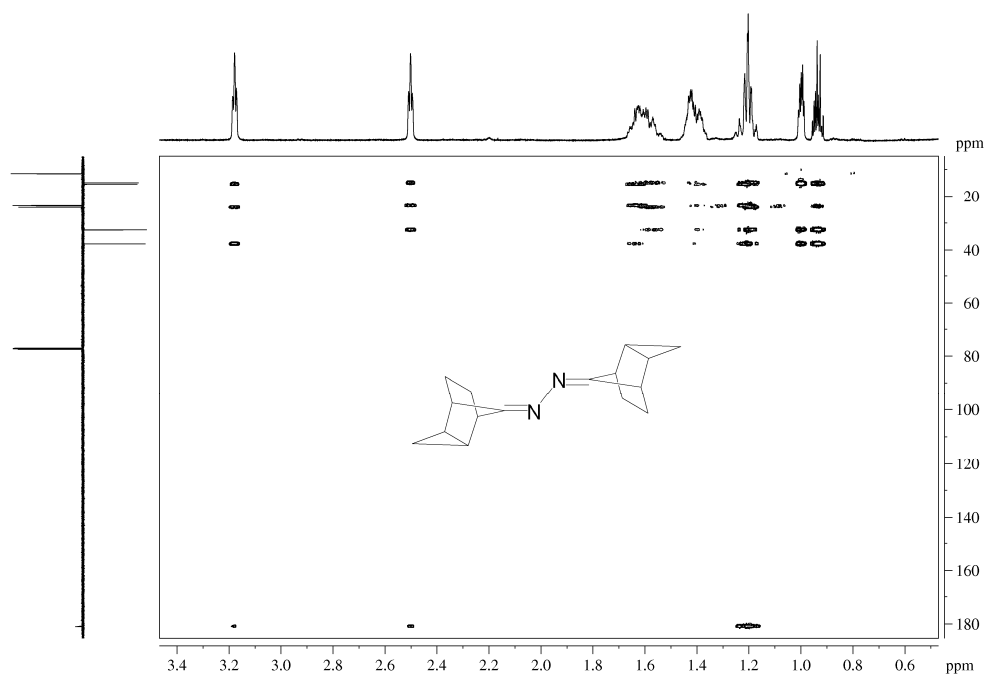


Figure A.28: HMBC spectrum of *endo*-tricyclo[3.2.1.0^{2,4}]octan-8-one azine (**44**) (600.13 and 150.92 MHz, CDCl₃).

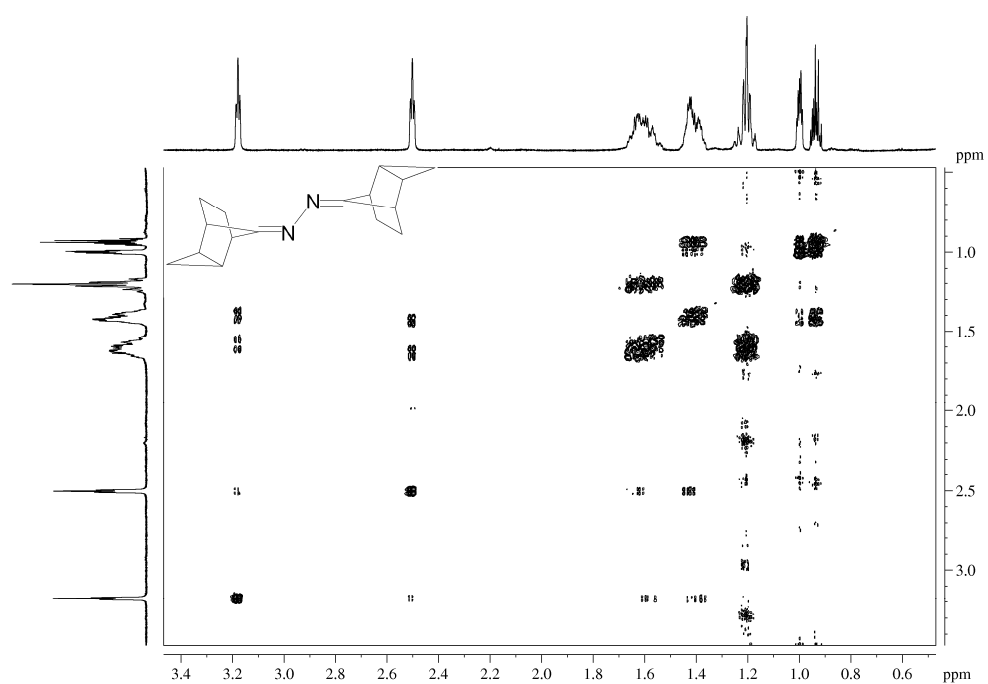


Figure A.29: COSY spectrum of *endo*-tricyclo[3.2.1.0^{2,4}]octan-8-one azine (**44**) (600.13 MHz, CDCl₃).

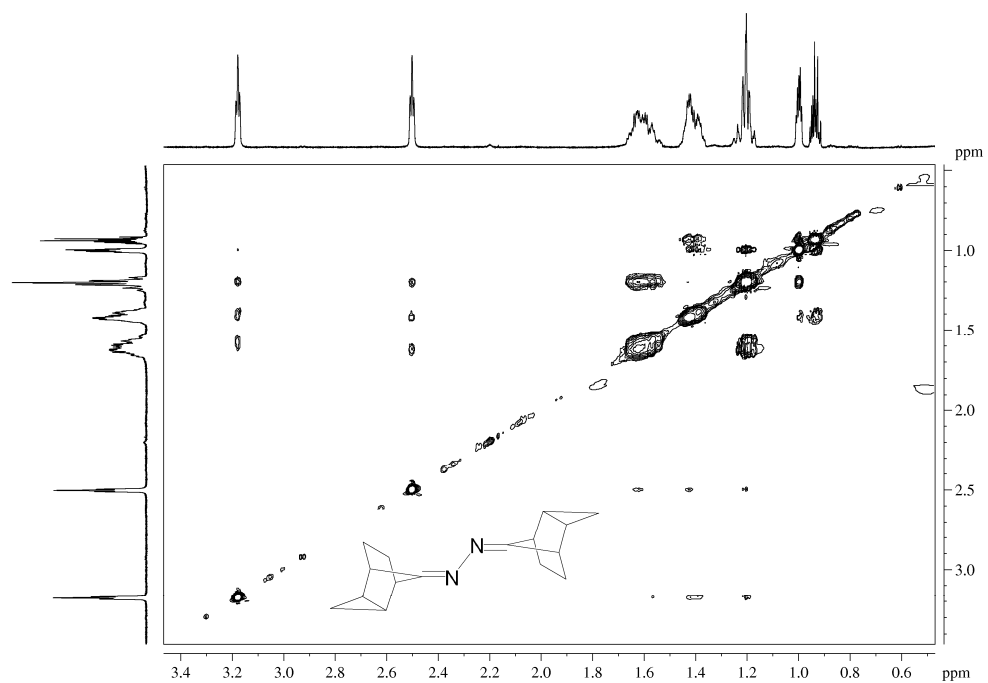


Figure A.30: NOESY spectrum of *endo*-tricyclo[3.2.1.0^{2,4}]octan-8-one azine (**44**) (600.13 MHz, CDCl₃).

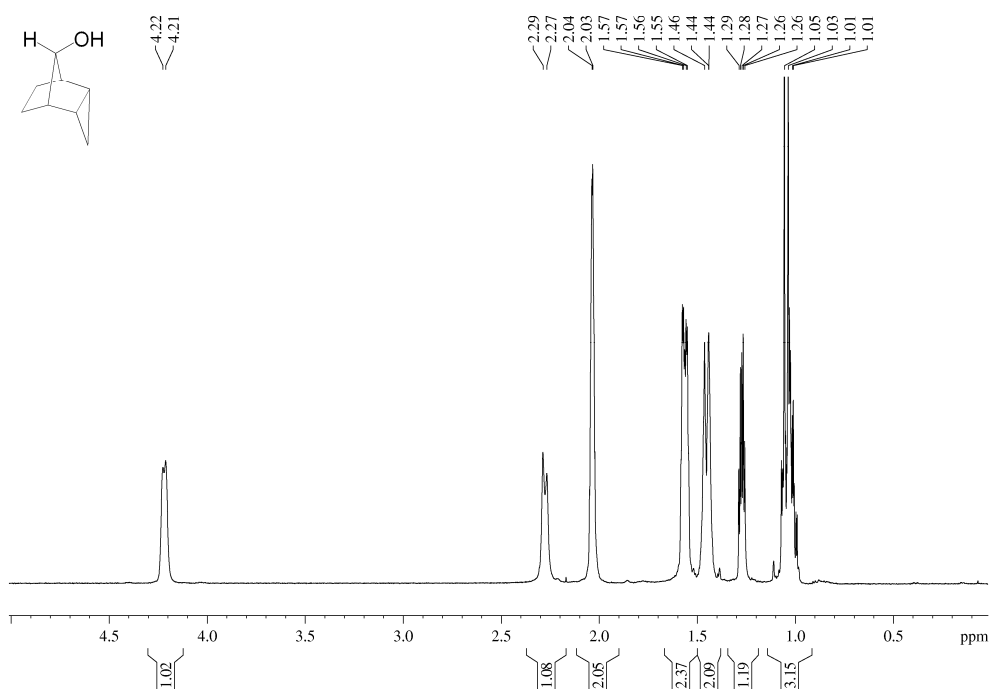


Figure A.31: ^1H NMR spectrum of *endo,syn*-tricyclo[3.2.1.0^{2,4}]octan-8-ol (**46**) (400.13 MHz, CDCl_3).

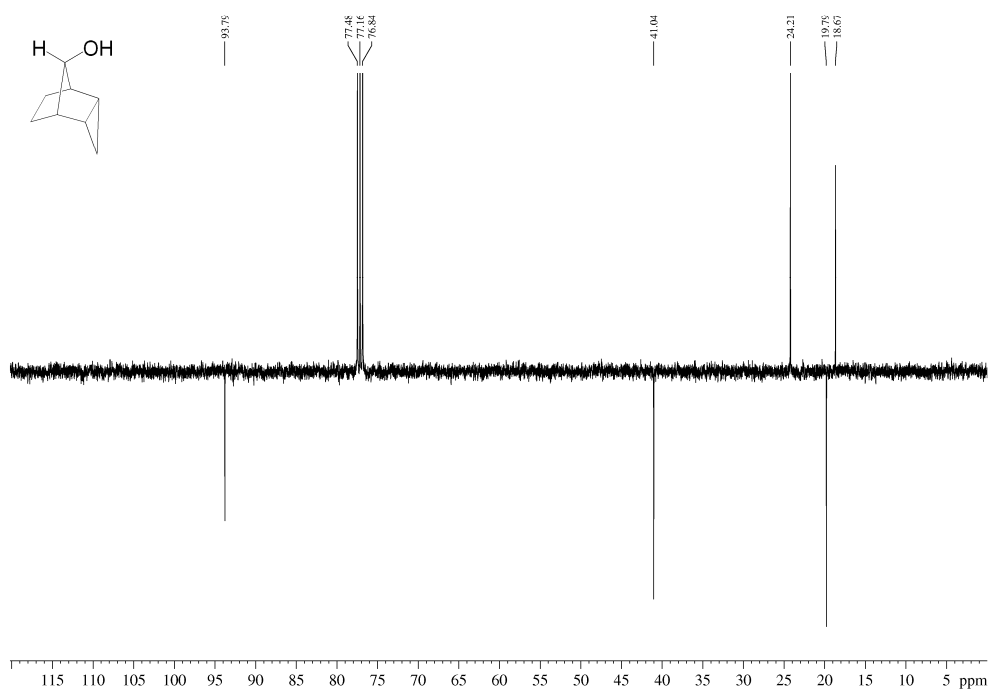


Figure A.32: ^{13}C NMR spectrum of *endo,syn*-tricyclo[3.2.1.0^{2,4}]octan-8-ol (**46**) (100.62 MHz, CDCl_3).

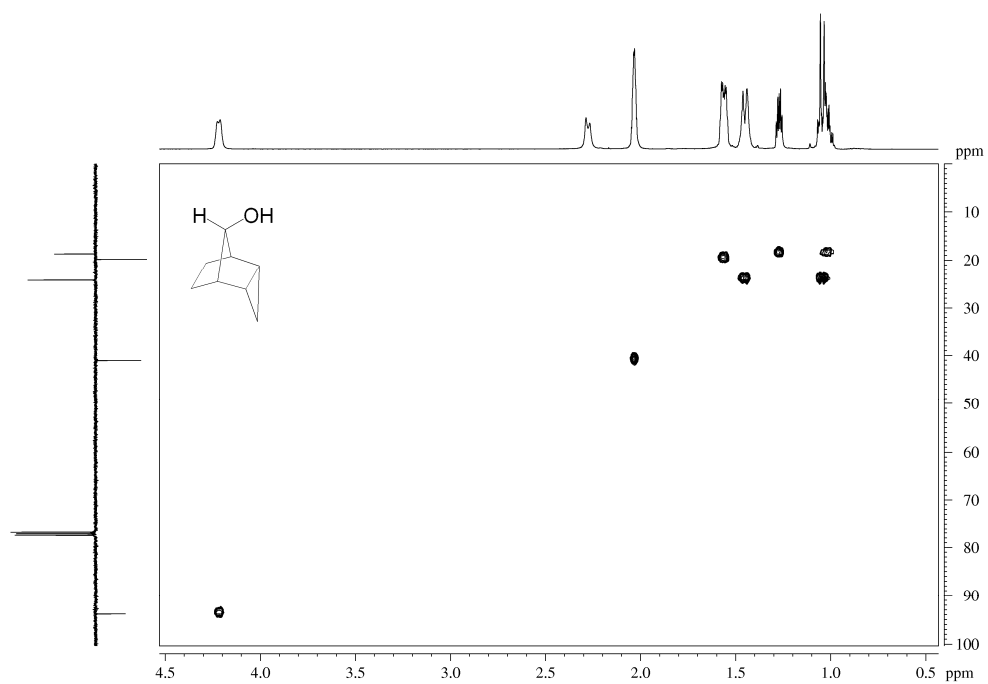


Figure A.33: HMQC spectrum of *endo,syn*-tricyclo[3.2.1.0^{2,4}]octan-8-ol (**46**) (400.13 and 100.62 MHz, CDCl₃).

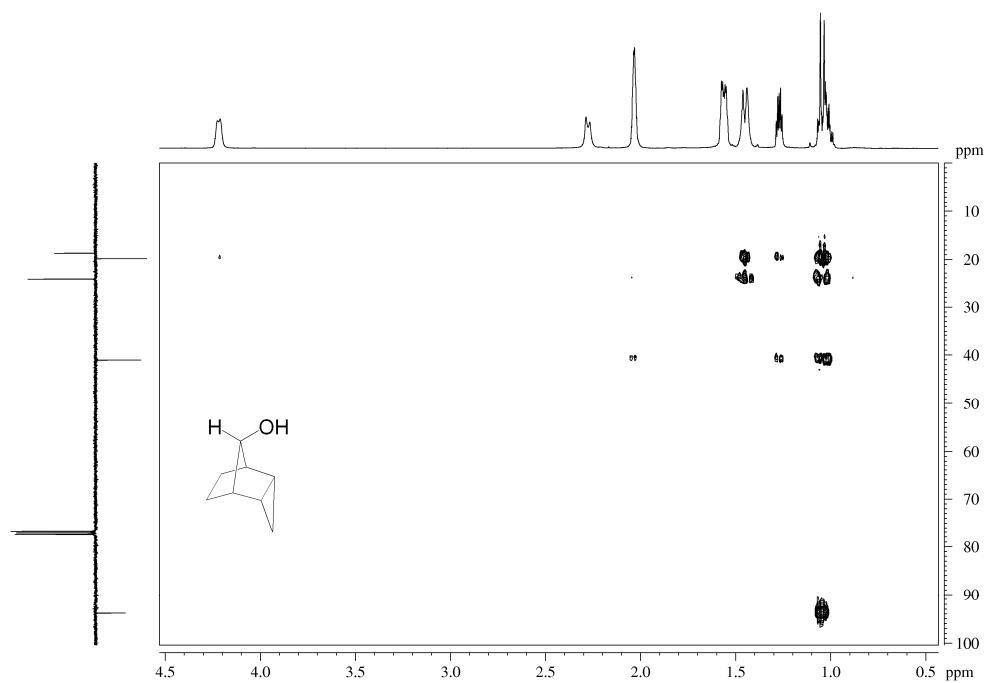


Figure A.34: HMBC spectrum of *endo,syn*-tricyclo[3.2.1.0^{2,4}]octan-8-ol (**46**) (400.13 and 100.62 MHz, CDCl₃).

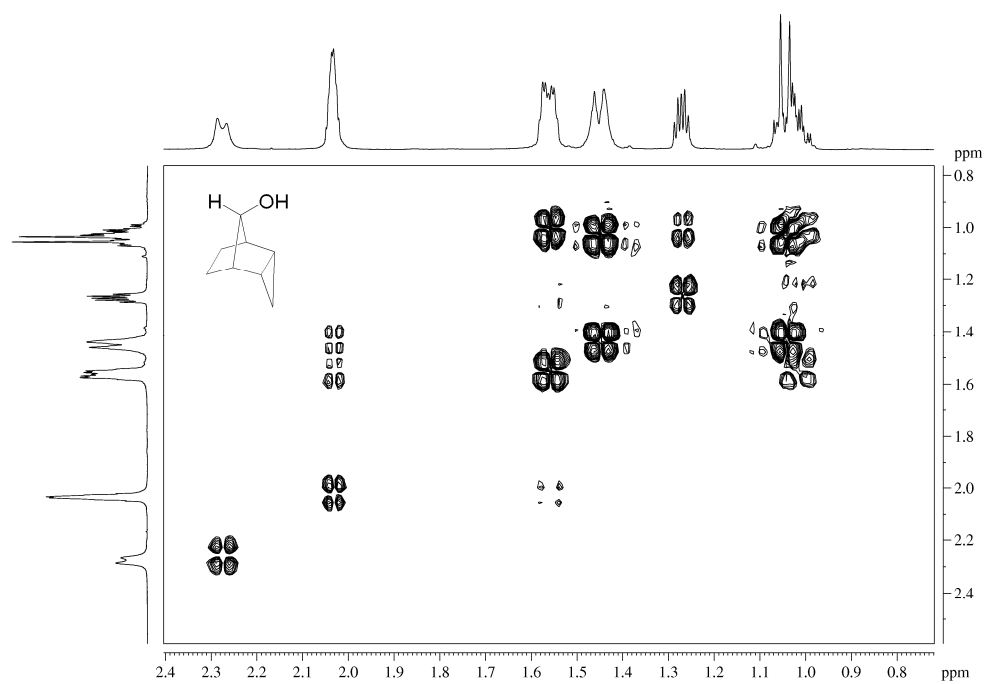


Figure A.35: COSY spectrum of *endo,syn*-tricyclo[3.2.1.0^{2,4}]octan-8-ol (**46**) (400.13 MHz, CDCl₃).

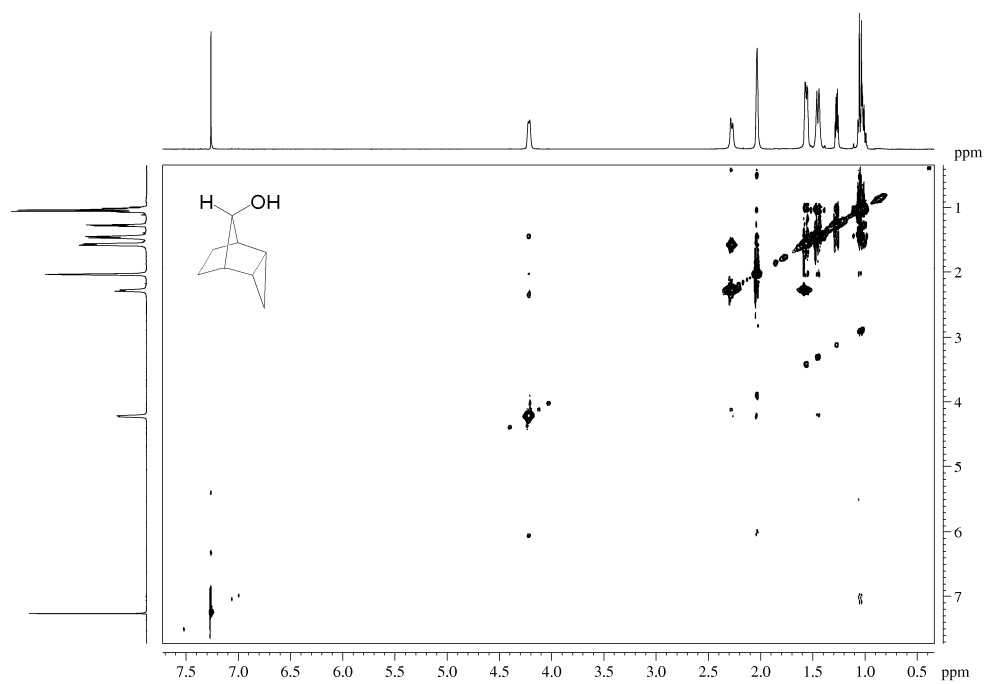


Figure A.36: NOESY spectrum of *endo,syn*-tricyclo[3.2.1.0^{2,4}]octan-8-ol (**46**) (400.13 MHz, CDCl₃).

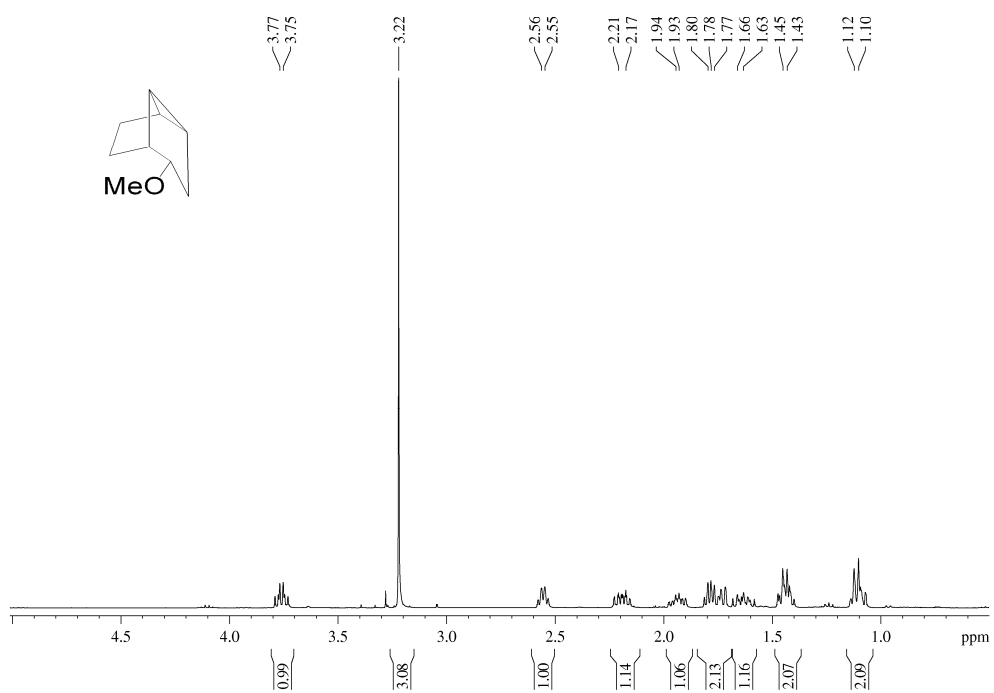


Figure A.37: ^1H NMR spectrum of *rac*-(1*R*,2*S*,4*S*,5*R*,6*R*)-2-methoxytricyclo[3.3.0.0^{4,6}]octane (**48**) (400.13 MHz, CDCl_3).

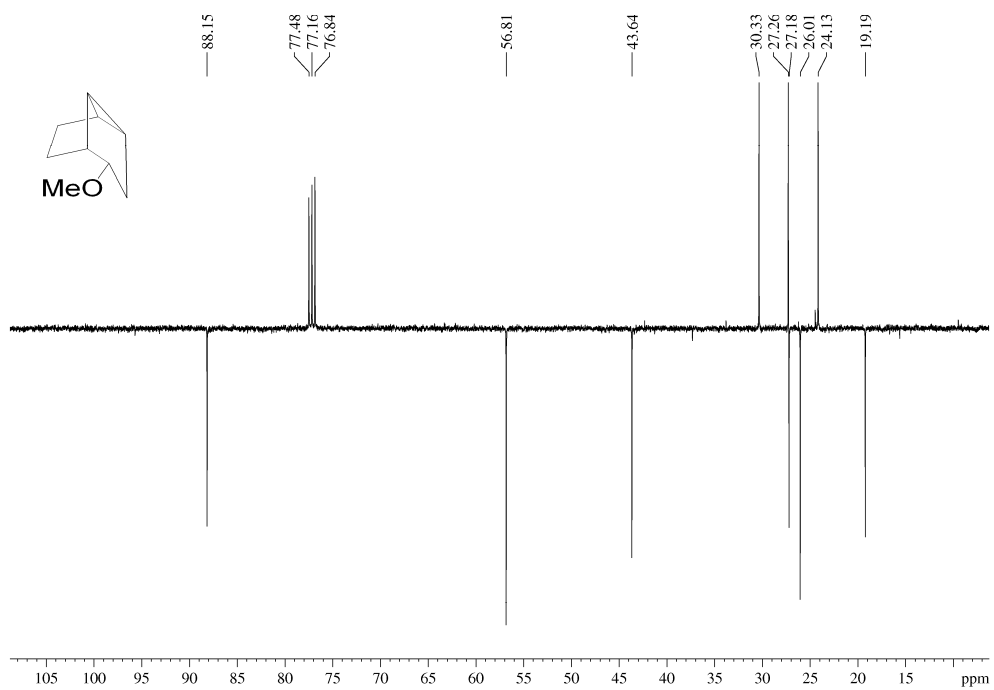


Figure A.38: ^{13}C NMR spectrum of *rac*-(1*R*,2*S*,4*S*,5*R*,6*R*)-2-methoxytricyclo[3.3.0.0^{4,6}]octane (**48**) (100.62 MHz, CDCl_3).

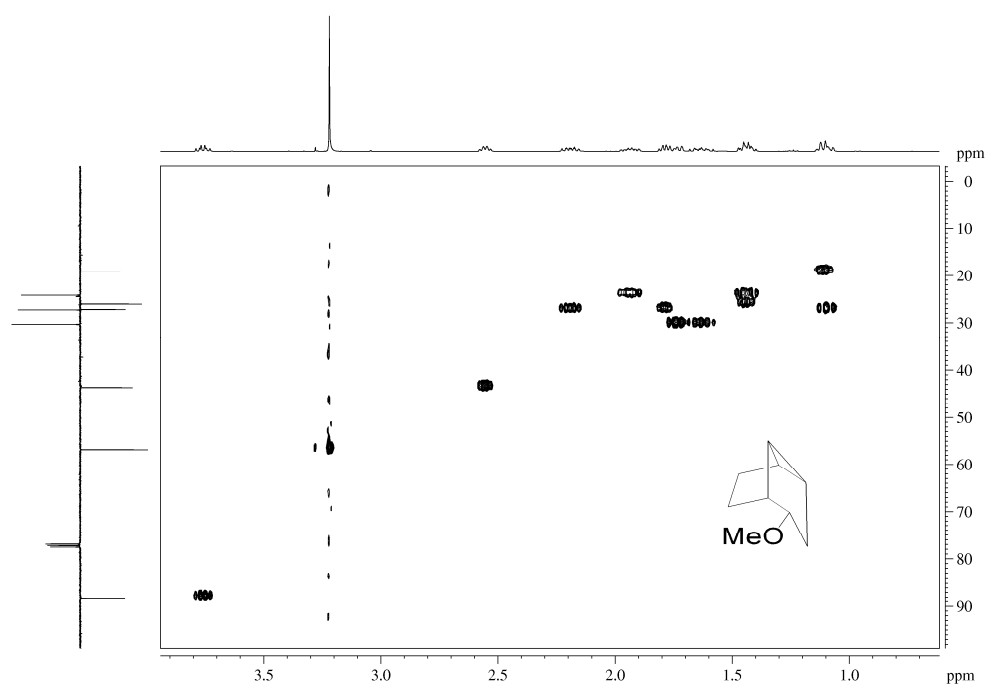


Figure A.39: HMBC spectrum of *rac*-(1*R*,2*S*,4*S*,5*R*,6*R*)-2-methoxytricyclo[3.3.0.0^{4,6}]octane (**48**) (400.13 and 100.62 MHz, CDCl₃).

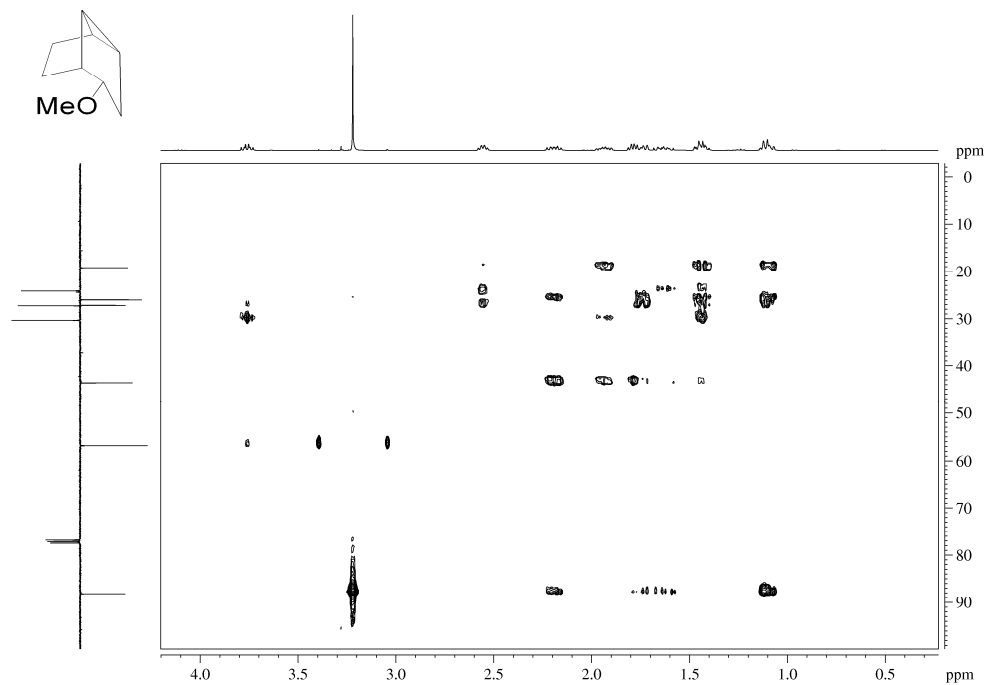


Figure A.40: HMBC spectrum of *rac*-(1*R*,2*S*,4*S*,5*R*,6*R*)-2-methoxytricyclo[3.3.0.0^{4,6}]octane (**48**) (400.13 and 100.62 MHz, CDCl₃).

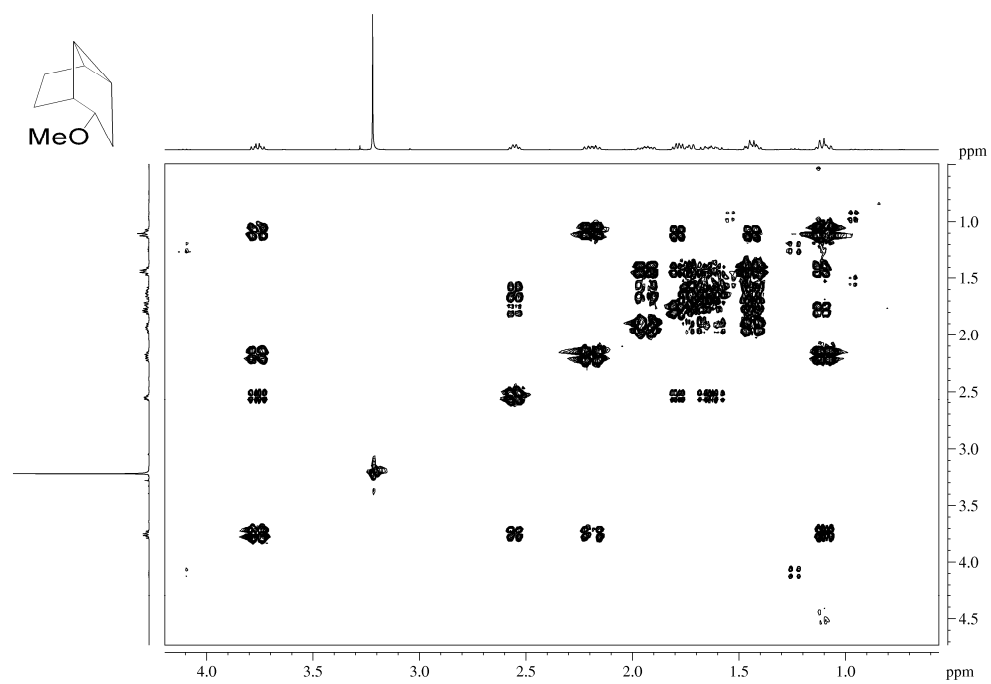


Figure A.41: COSY spectrum of *rac*-(1*R*,2*S*,4*S*,5*R*,6*R*)-2-methoxytricyclo[3.3.0.0^{4,6}]octane (**48**) (400.13 MHz, CDCl₃).

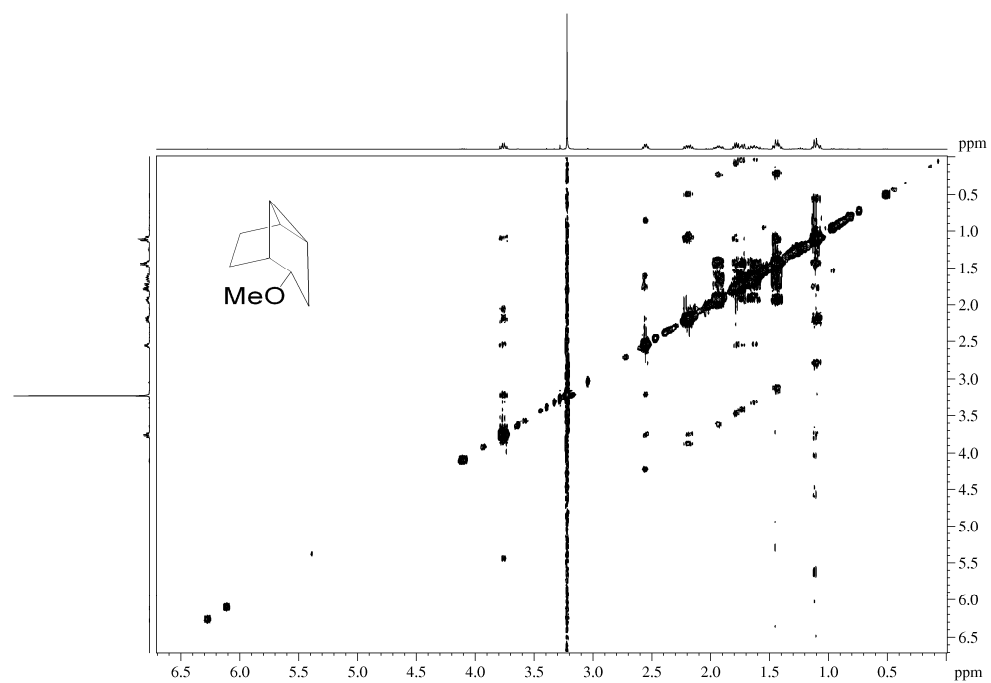


Figure A.42: NOESY spectrum of *rac*-(1*R*,2*S*,4*S*,5*R*,6*R*)-2-methoxytricyclo[3.3.0.0^{4,6}]octane (**48**) (400.13 MHz, CDCl₃).

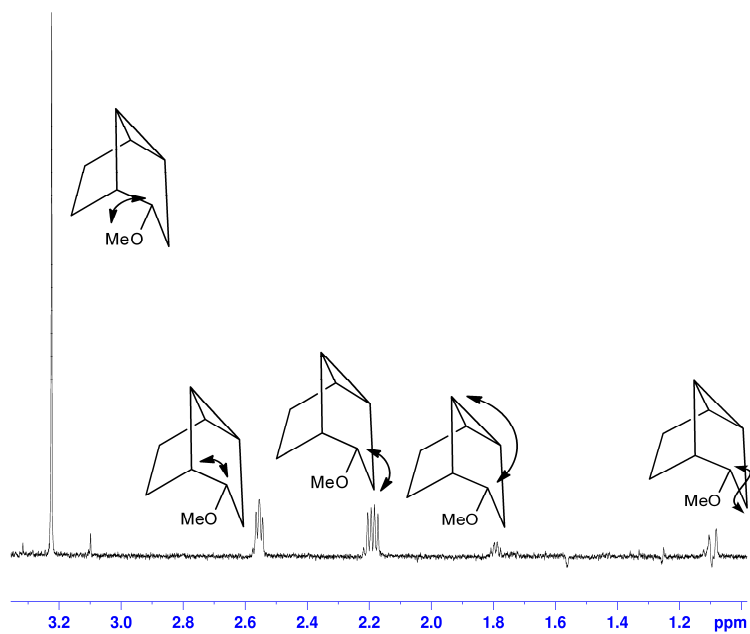


Figure A.43: 1D NOESY spectrum of *rac*-(1*R*,2*S*,4*S*,5*R*,6*R*)-2-methoxytricyclo[3.3.0.0^{4,6}]octane (**48**) (600.13 MHz, CDCl₃).

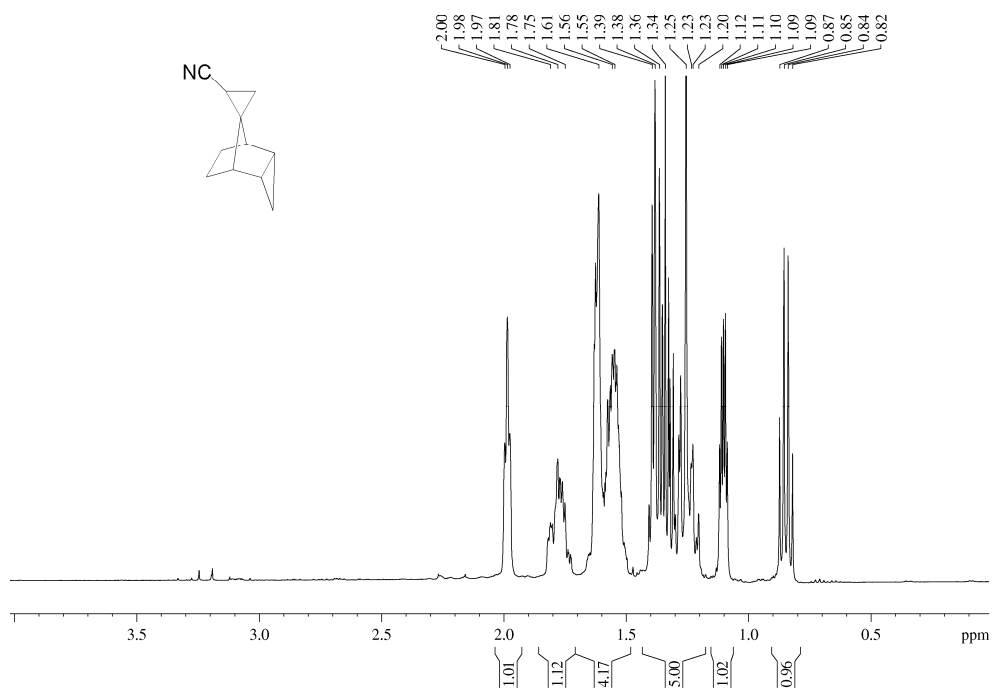


Figure A.44: ¹H NMR spectrum of *rel*-(1*s*,1'*R*,2*R*,2'*R*,4'*S*,5'*S*)-spiro[cyclopropane-1,8'-tricyclo[3.2.1.0^{2,4}]octane]-2-carbonitrile (**51**) (400.13 MHz, CDCl₃).

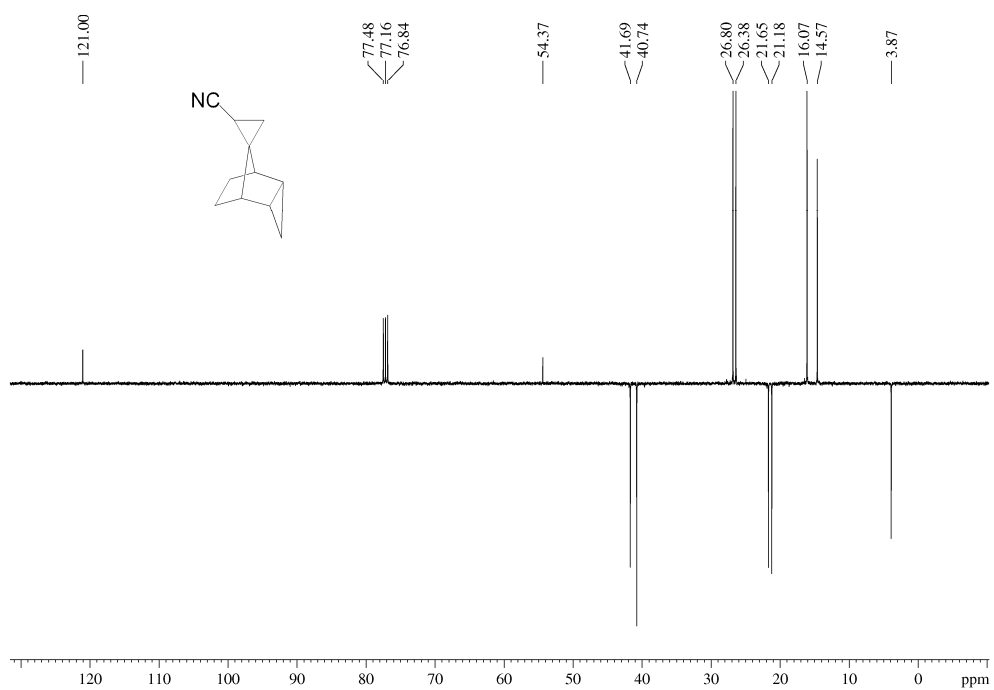


Figure A.45: ¹³C NMR spectrum of *rel*-(1*s*,1'*R*,2*R*,2'*R*,4'*S*,5'*S*)-spiro[cyclopropane-1,8'-tricyclo[3.2.1.0^{2,4}]octane]-2-carbonitrile (**51**) (100.62 MHz, CDCl₃).

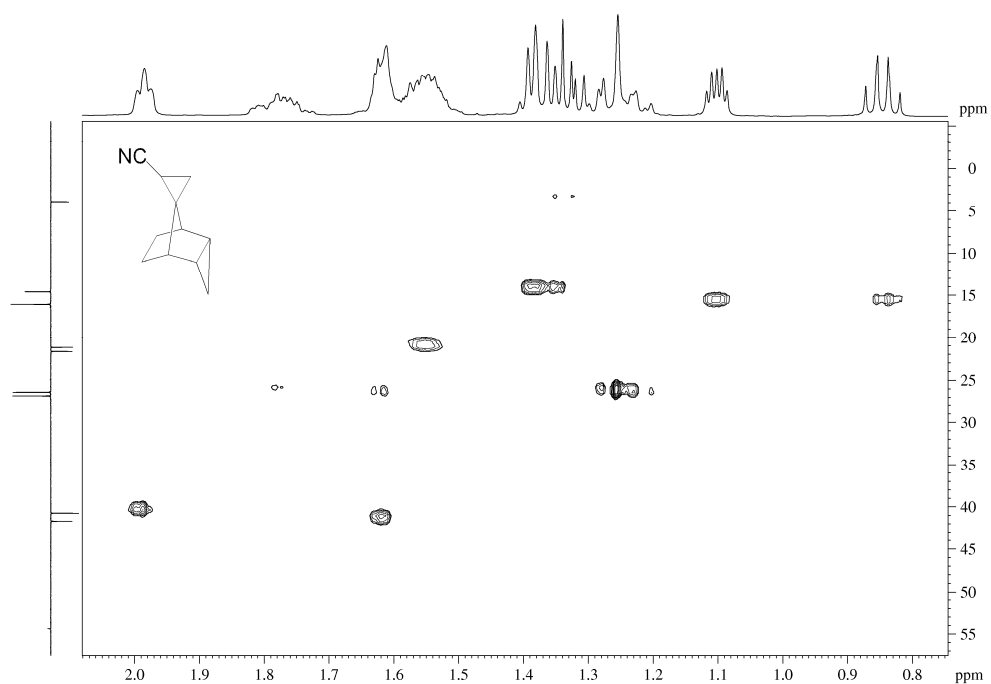


Figure A.46: HMQC spectrum of *rel*-(1*s*,1'*R*,2*R*,2'*R*,4'*S*,5'*S*)-spiro[cyclopropane-1,8'-tricyclo[3.2.1.0^{2,4}]octane]-2-carbonitrile (**51**) (400.13 and 100.62 MHz, CDCl₃).

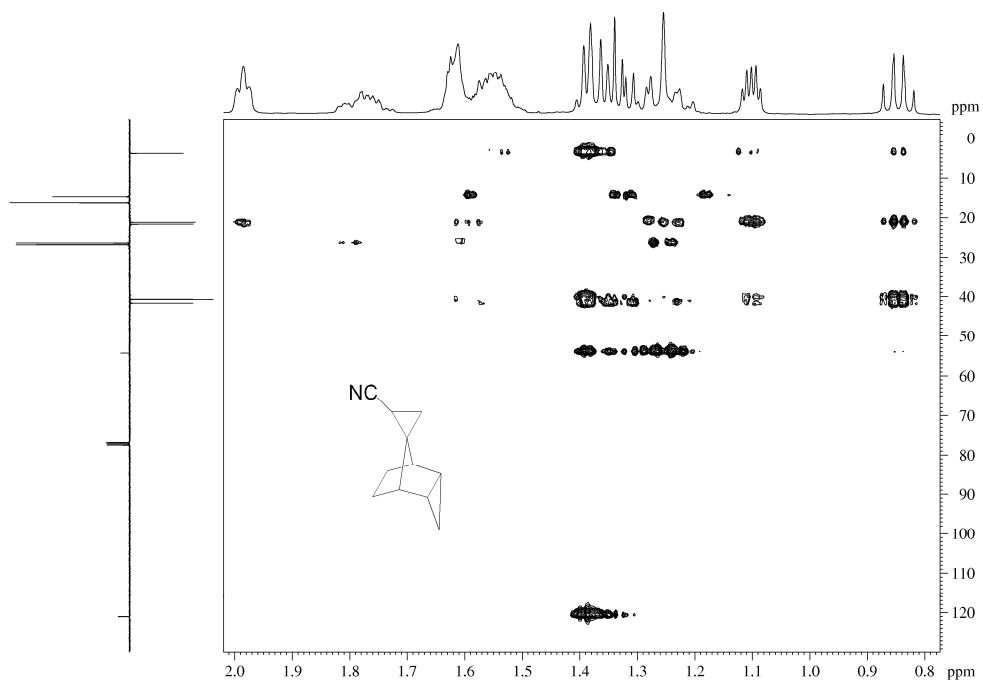


Figure A.47: HMBC spectrum of *rel*-(1*s*,1'*R*,2*R*,2'*R*,4'*S*,5'*S*)-spiro[cyclopropane-1,8'-tricyclo[3.2.1.0^{2,4}]octane]-2-carbonitrile (**51**) (400.13 and 100.62 MHz, CDCl₃).

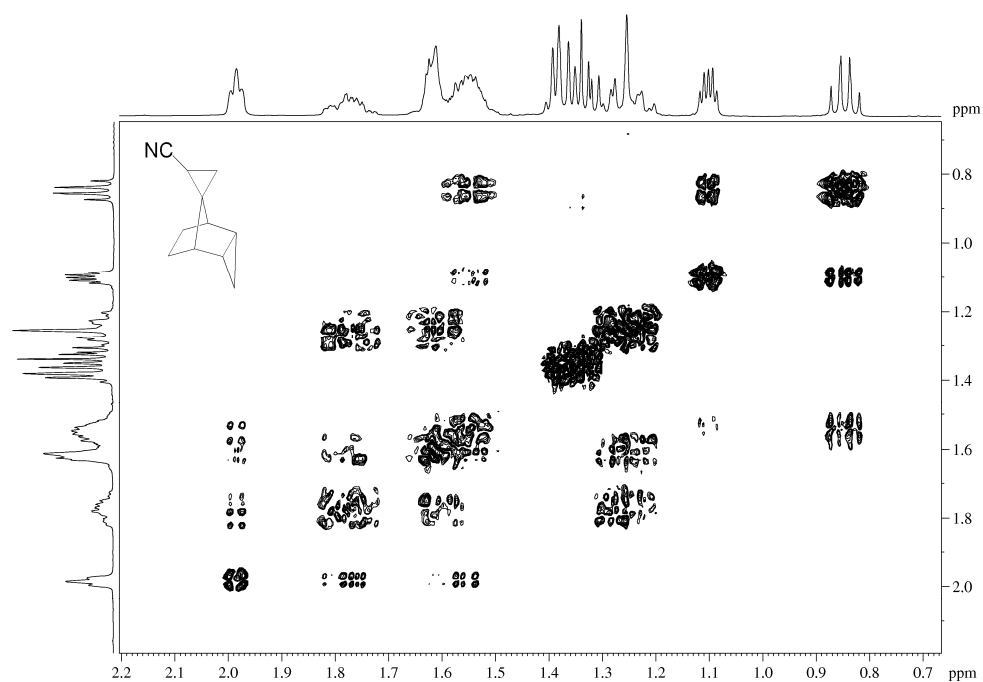


Figure A.48: COSY spectrum of *rel*-(1*s*,1'*R*,2*R*,2'*R*,4'*S*,5'*S*)-spiro[cyclopropane-1,8'-tricyclo[3.2.1.0^{2,4}]octane]-2-carbonitrile (**51**) (400.13 MHz, CDCl₃).

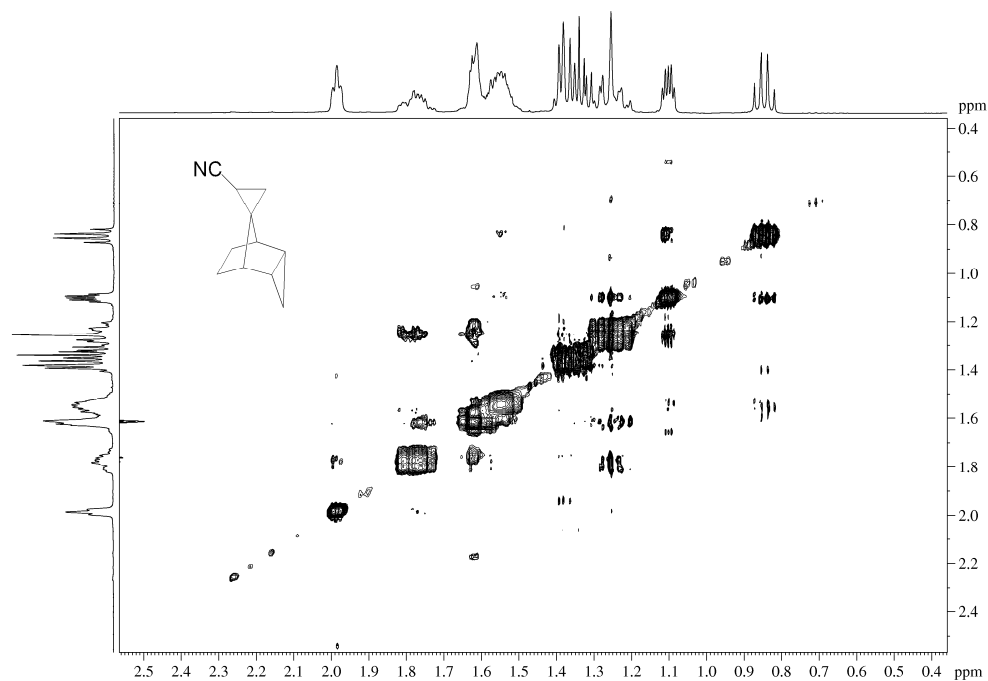


Figure A.49: NOESY spectrum of *rel*-(1*s*,1'*R*,2*R*,2'*R*,4'*S*,5'*S*)-spiro[cyclopropane-1,8'-tricyclo[3.2.1.0^{2,4}]octane]-2-carbonitrile (**51**) (400.13 MHz, CDCl₃).

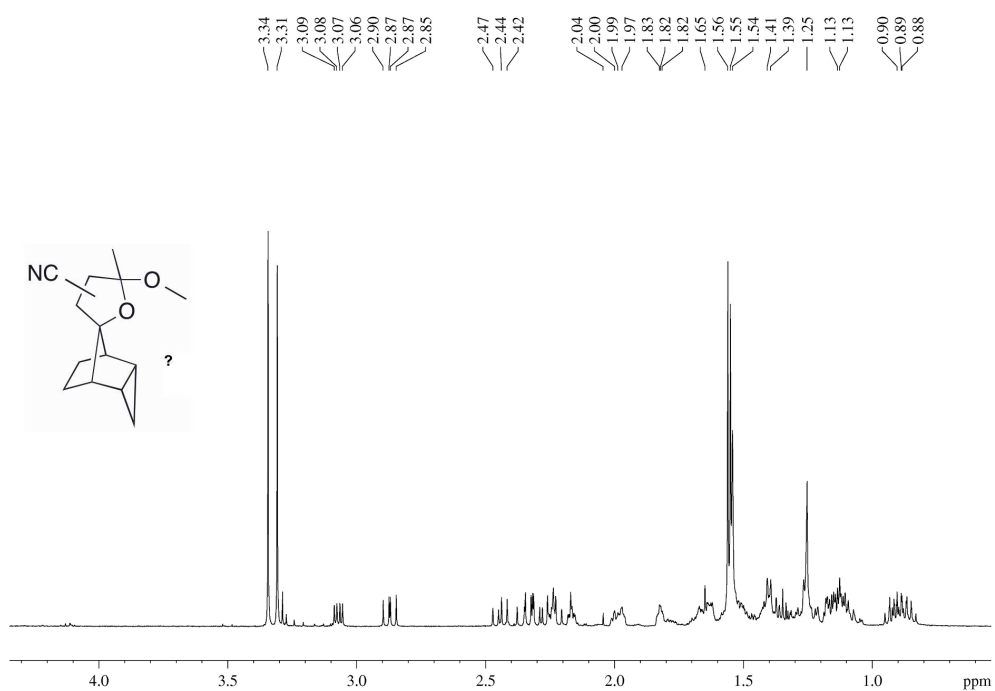


Figure A.50: ^1H NMR spectrum of some of the products possibly deriving from capture of *syn*-**32** with acrylonitrile (400.27 MHz, CDCl_3).

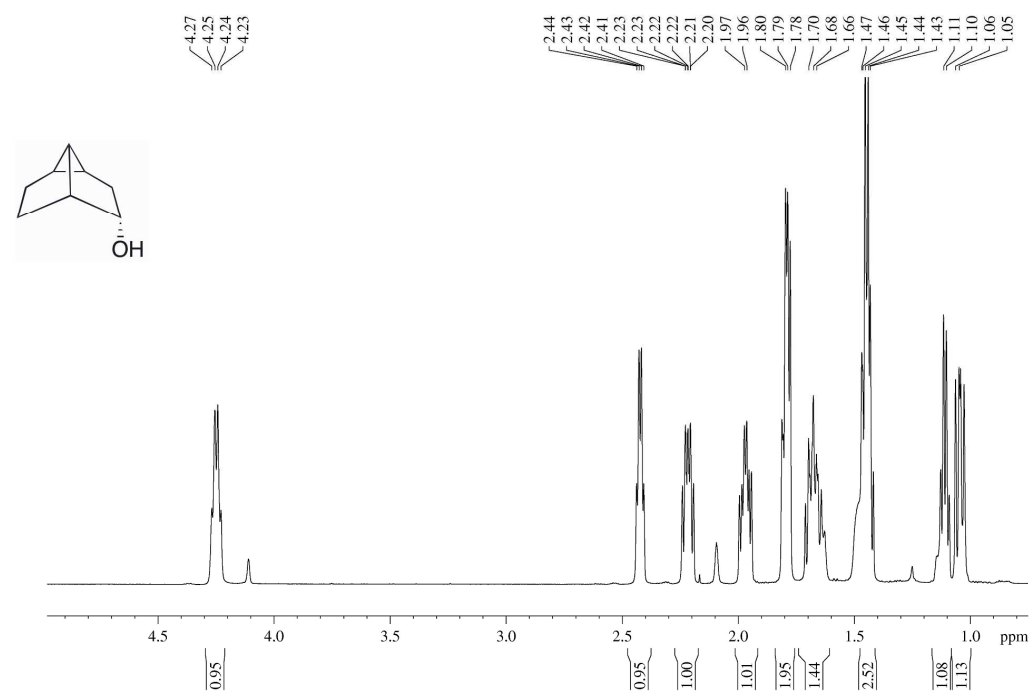


Figure A.51: ¹H NMR spectrum of *rac*-(1*R*,2*S*,4*S*,5*R*,6*R*)-2-hydroxytricyclo[3.3.0.0^{4,6}]octane (**52**) (600.13 MHz, CDCl₃).

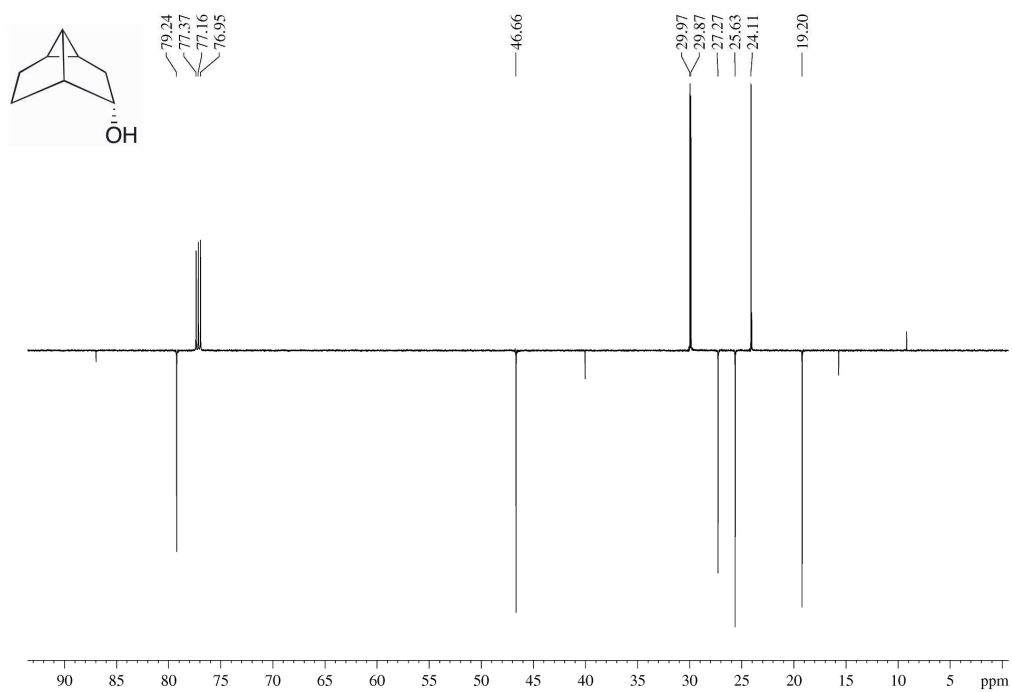


Figure A.52: ¹³C NMR spectrum of *rac*-(1*R*,2*S*,4*S*,5*R*,6*R*)-2-hydroxytricyclo[3.3.0.0^{4,6}]octane (**52**) (150.92 MHz, CDCl₃).

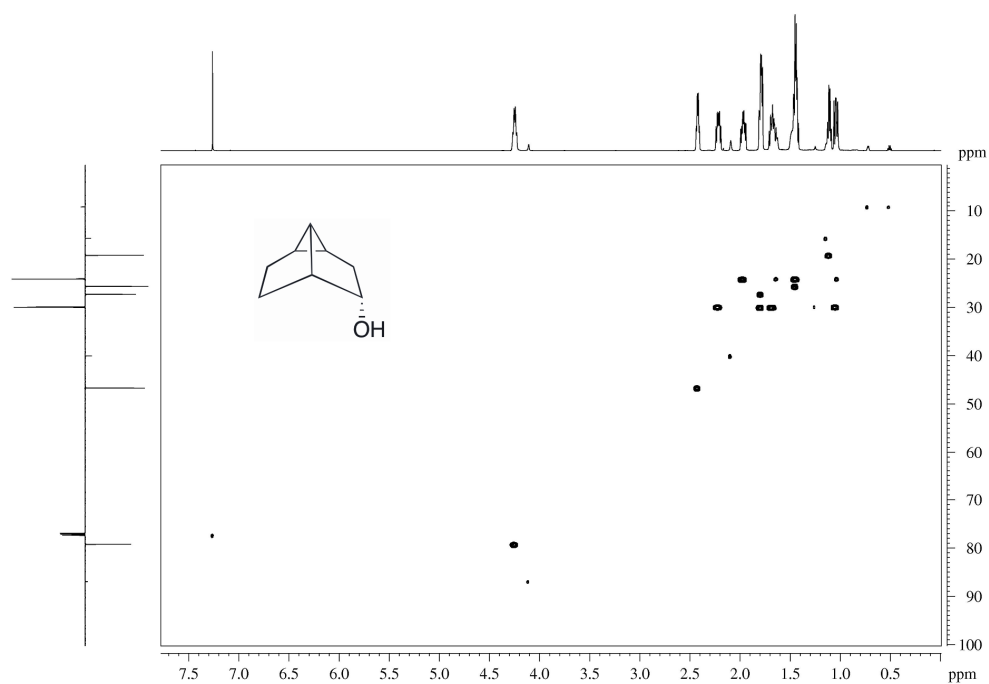


Figure A.53: HMQC spectrum of *rac*-(1*R*,2*S*,4*S*,5*R*,6*R*)-2-hydroxytricyclo[3.3.0.0^{4,6}]octane (**52**) (600.13 and 150.92 MHz, CDCl₃).

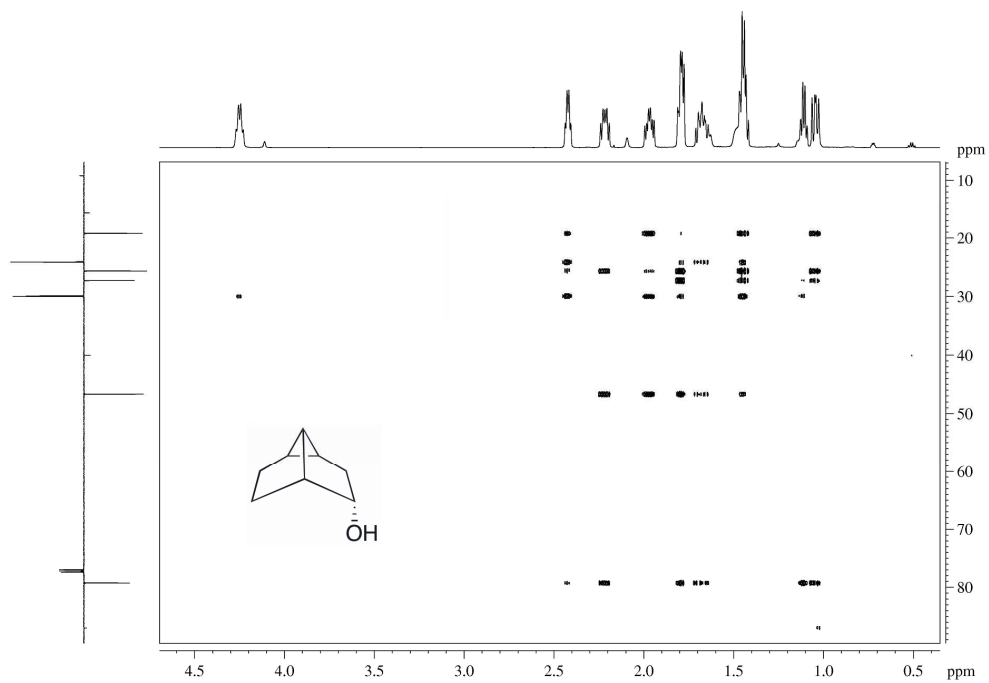


Figure A.54: HMBC spectrum of *rac*-(1*R*,2*S*,4*S*,5*R*,6*R*)-2-hydroxytricyclo[3.3.0.0^{4,6}]octane (**52**) (600.13 and 150.92 MHz, CDCl₃).

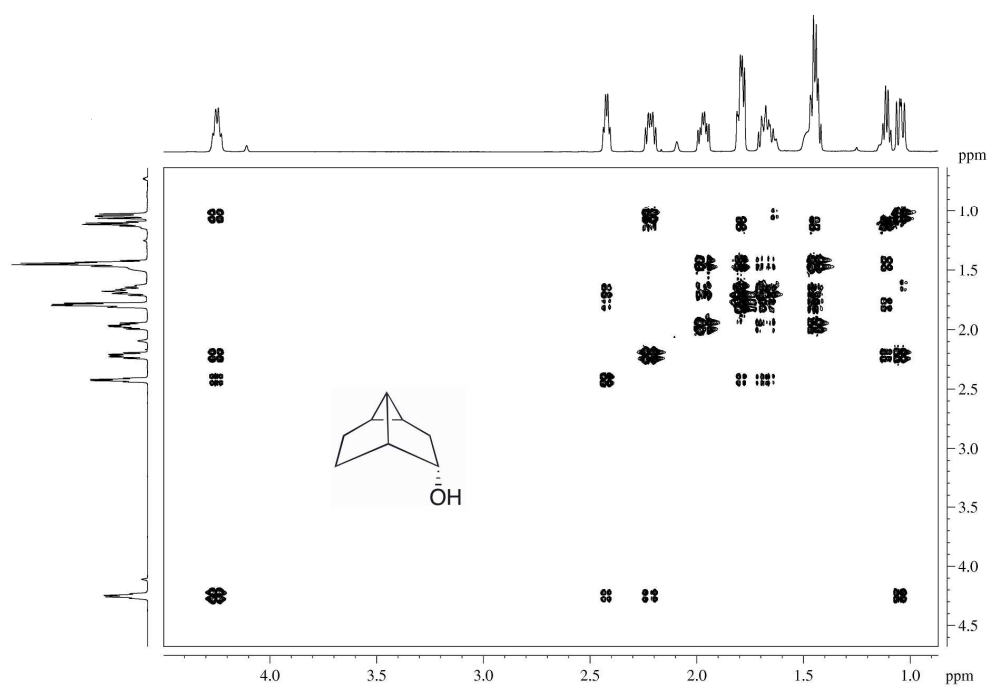


Figure A.55: COSY spectrum of *rac*-(1*R*,2*S*,4*S*,5*R*,6*R*)-2-hydroxytricyclo[3.3.0.0^{4,6}]octane (**52**) (600.13 MHz, CDCl₃).

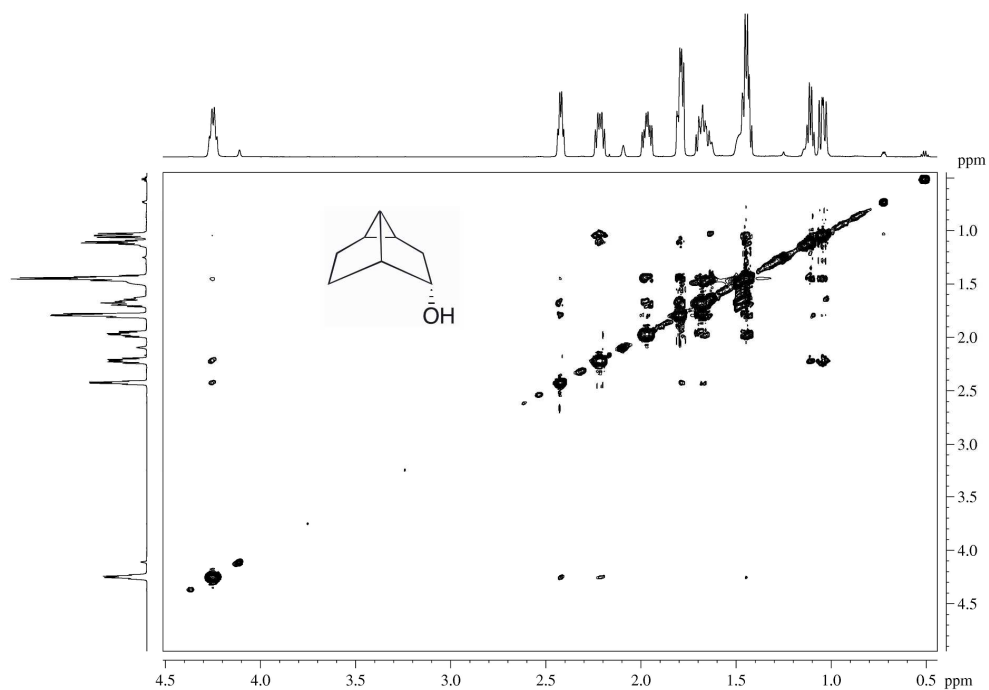


Figure A.56: NOESY spectrum of *rac*-(1*R*,2*S*,4*S*,5*R*,6*R*)-2-hydroxytricyclo[3.3.0.0^{4,6}]octane (**52**) (600.13 MHz, CDCl₃).

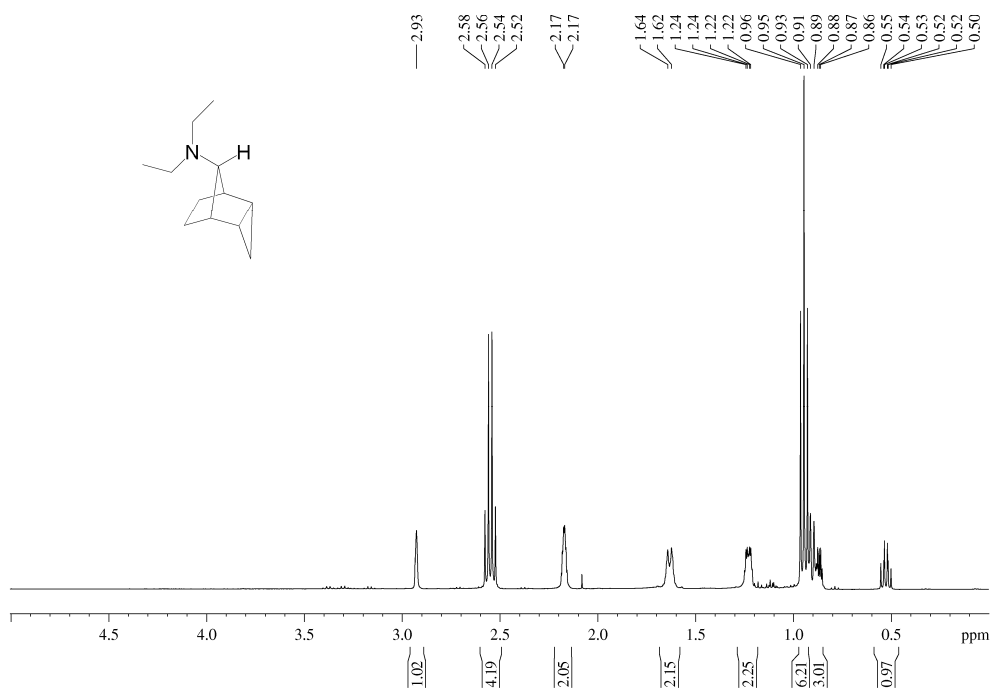


Figure A.57: ¹H NMR spectrum of *endo,anti*-*N,N*-diethyltricyclo[3.2.1.0^{2,4}]octan-8-amine (54) (400.13 MHz, CDCl₃).

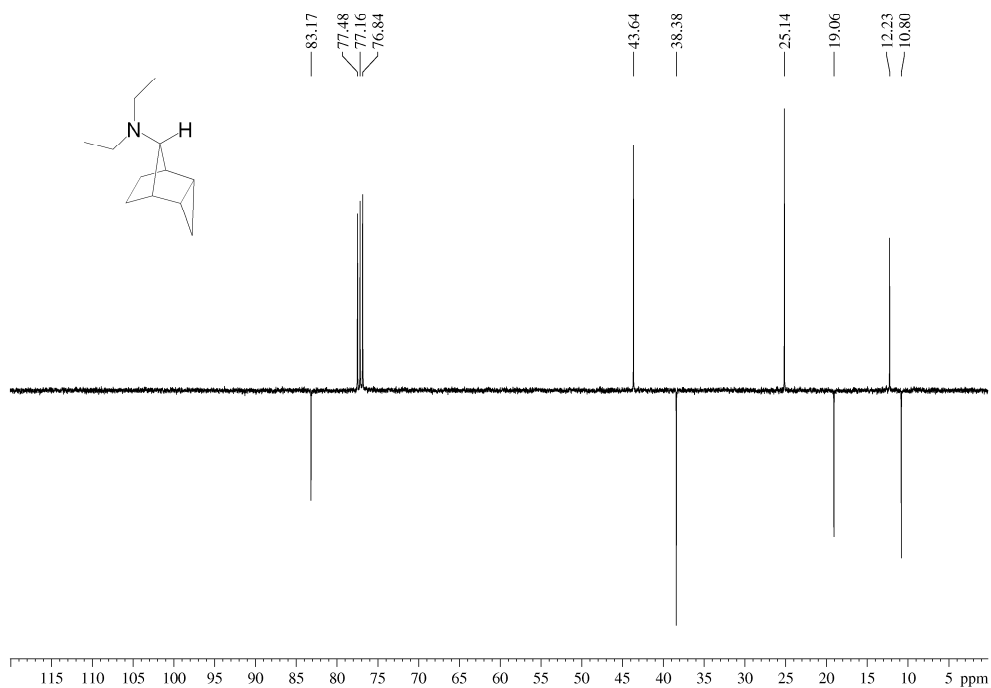


Figure A.58: ¹³C NMR spectrum of *endo,anti*-*N,N*-diethyltricyclo[3.2.1.0^{2,4}]octan-8-amine (54) (100.62 MHz, CDCl₃).

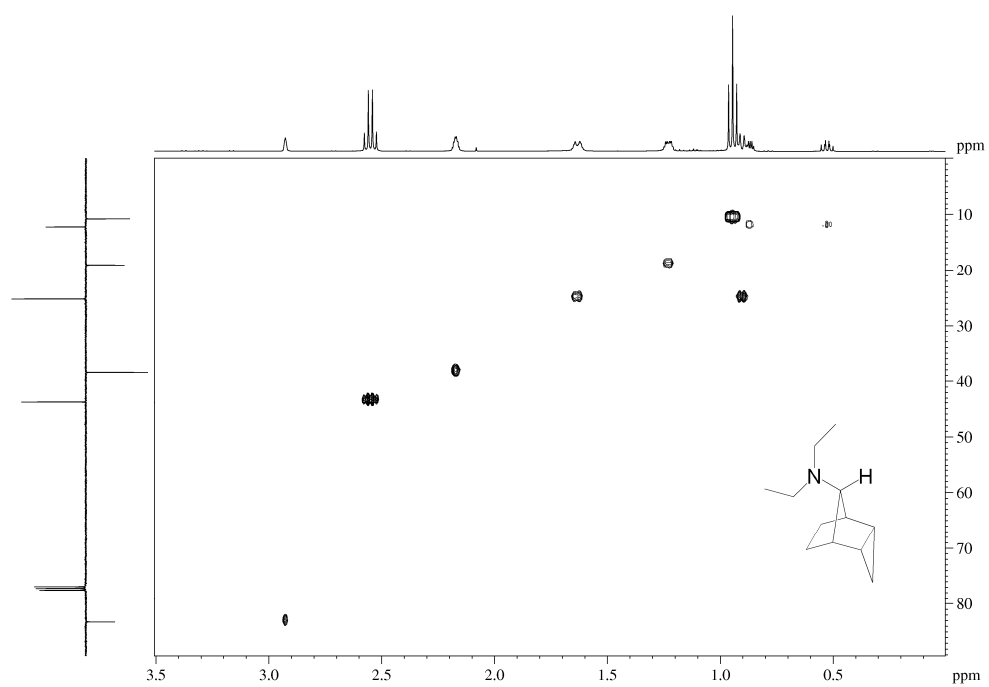


Figure A.59: HMQC spectrum of *endo,anti*-*N,N*-diethyltricyclo[3.2.1.0^{2,4}]octan-8-amine (**54**) (400.13 and 100.62 MHz, CDCl₃).

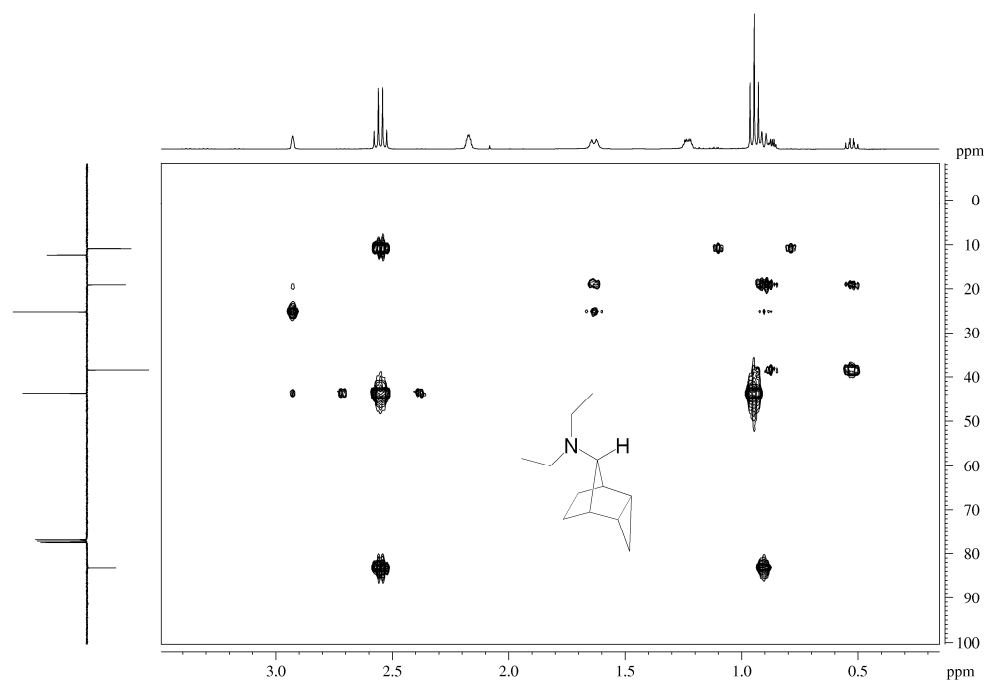


Figure A.60: HMBC spectrum of *endo,anti*-*N,N*-diethyltricyclo[3.2.1.0^{2,4}]octan-8-amine (**54**) (400.13 and 100.62 MHz, CDCl₃).

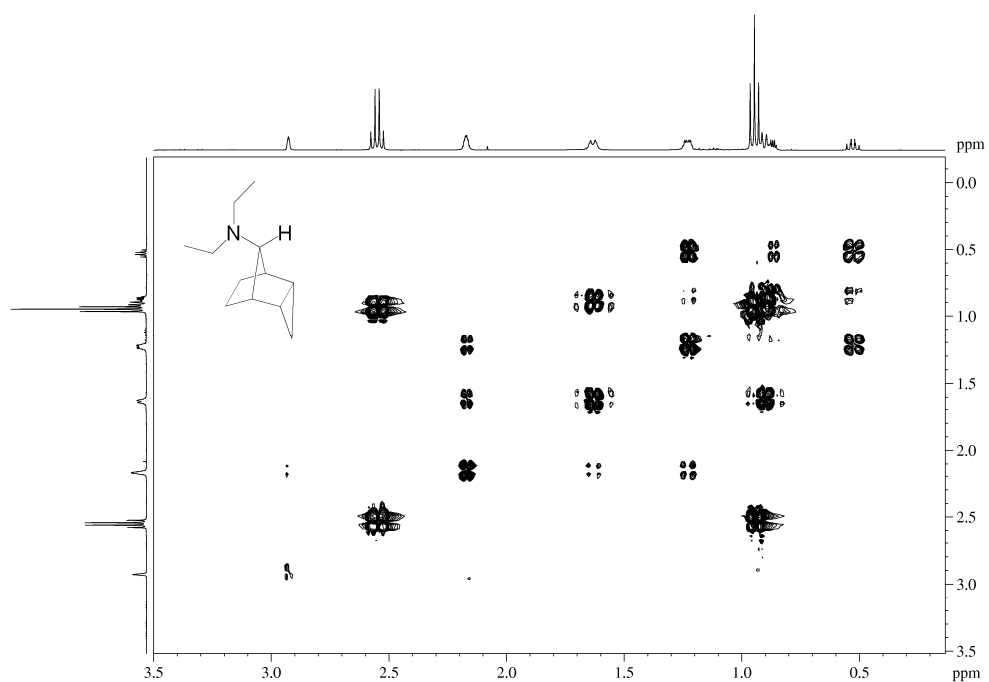


Figure A.61: COSY spectrum of *endo,anti*-*N,N*-diethyltricyclo[3.2.1.0^{2,4}]octan-8-amine (**54**) (400.13 MHz, CDCl₃).

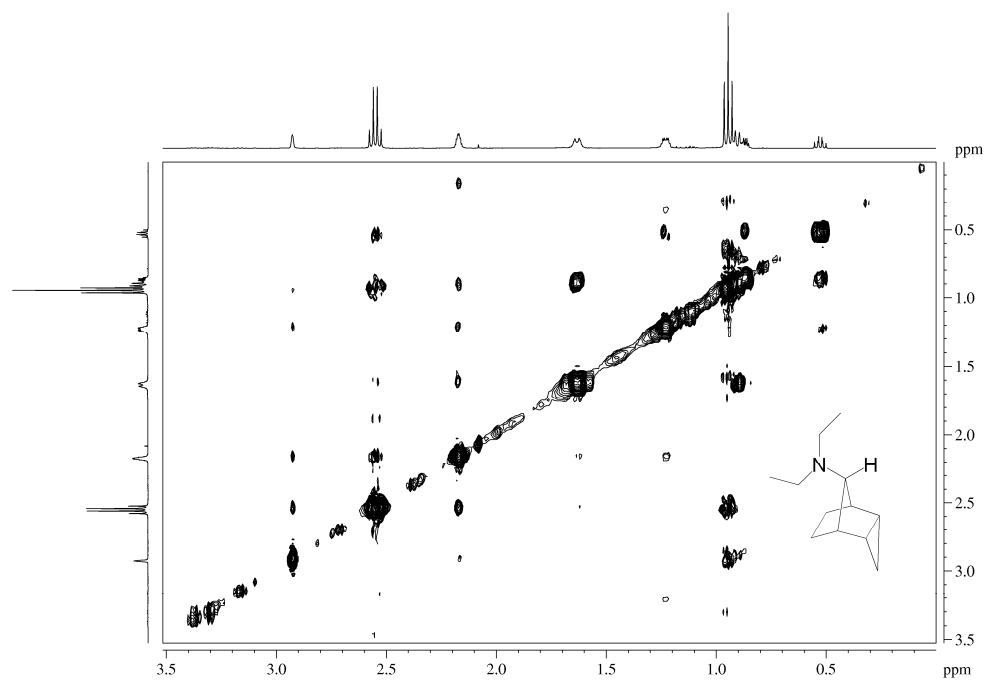


Figure A.62: NOESY spectrum of *endo,anti*-*N,N*-diethyltricyclo[3.2.1.0^{2,4}]octan-8-amine (**54**) (400.13 MHz, CDCl₃).

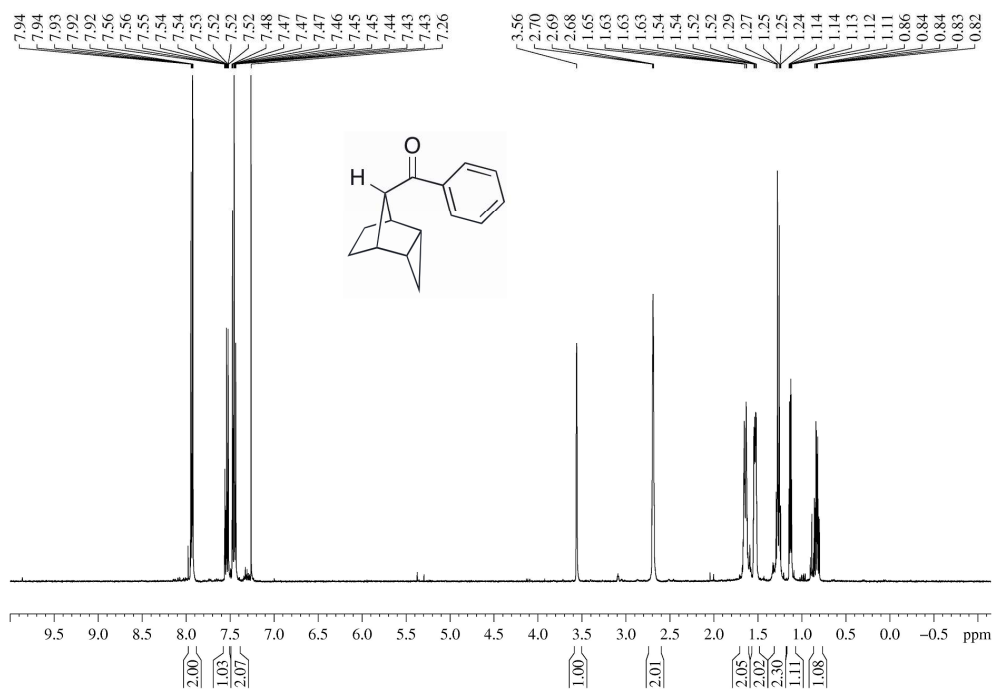


Figure A.63: ^1H NMR spectrum of phenyl((1R,2R,4S,5S,8r)-tricyclo[3.2.1.0^{2,4}]octan-8-yl)methanone (**55**) (400.13 MHz, CDCl_3).

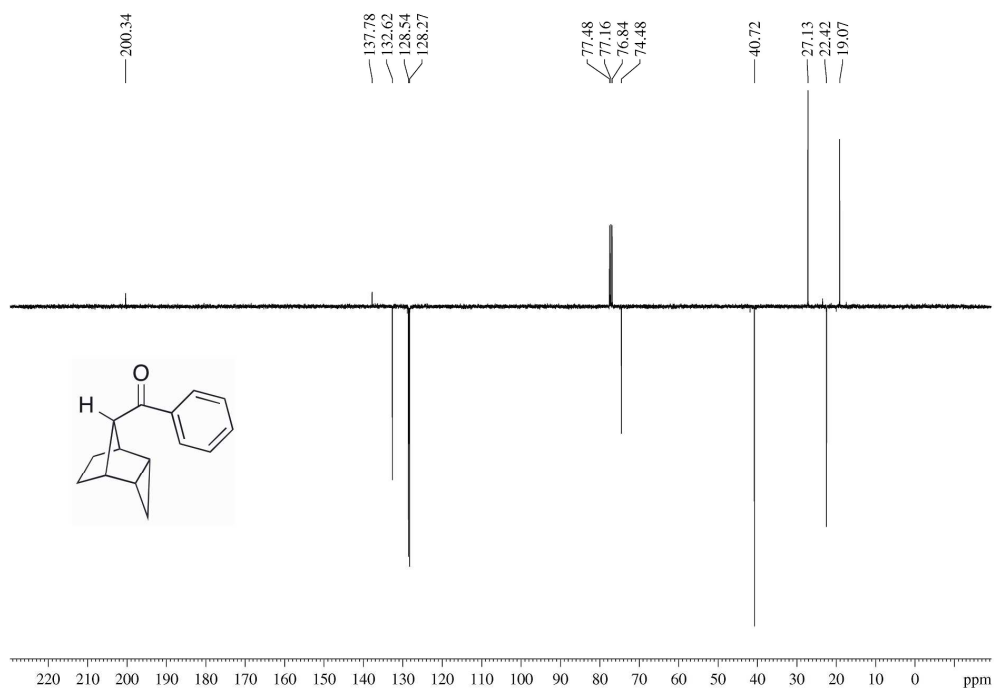


Figure A.64: ^{13}C NMR spectrum of phenyl((1R,2R,4S,5S,8r)-tricyclo[3.2.1.0^{2,4}]octan-8-yl)methanone (**55**) (100.62 MHz, CDCl_3).

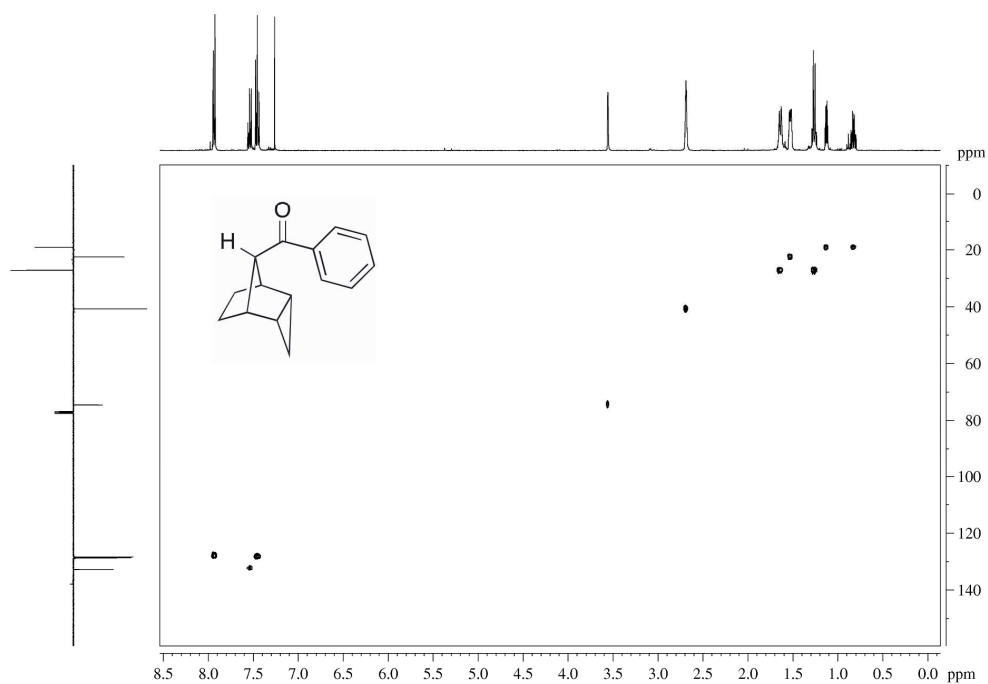


Figure A.65: HMQC spectrum of phenyl((1R,2R,4S,5S,8r)-tricyclo[3.2.1.0^{2,4}]octan-8-yl)methanone (**55**) (400.13 and 100.62 MHz, CDCl_3).

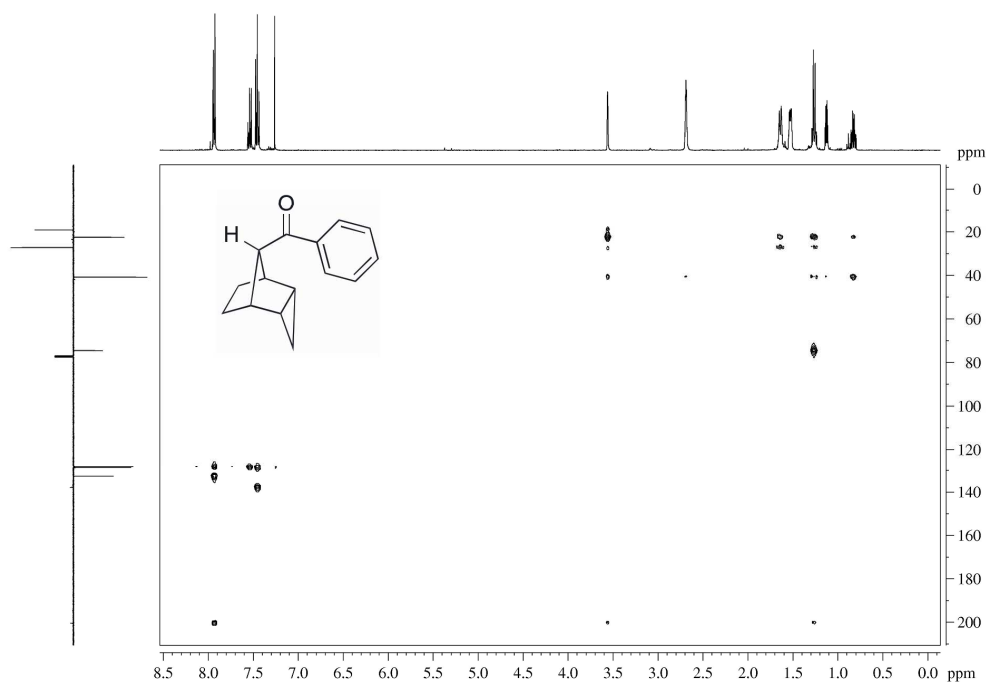


Figure A.66: HMBC spectrum of phenyl((1R,2R,4S,5S,8r)-tricyclo[3.2.1.0^{2,4}]octan-8-yl)methanone (**55**) (400.13 and 100.62 MHz, CDCl_3).

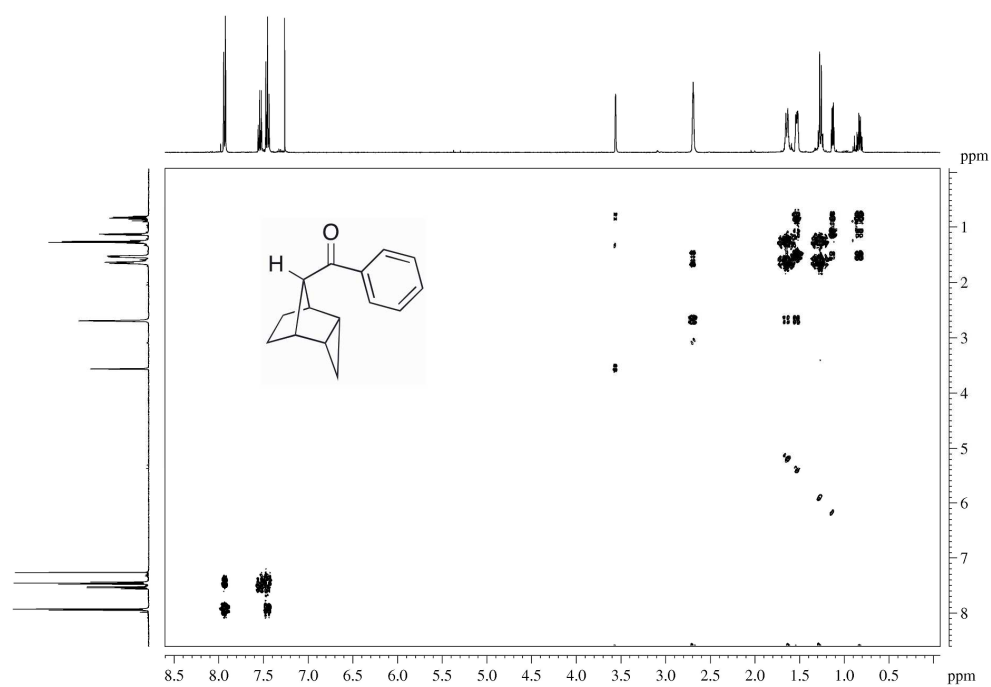


Figure A.67: COSY spectrum of phenyl((1*R*,2*R*,4*S*,5*S*,8*r*)-tricyclo[3.2.1.0^{2,4}]octan-8-yl)methanone (**55**) (400.13 MHz, CDCl₃).

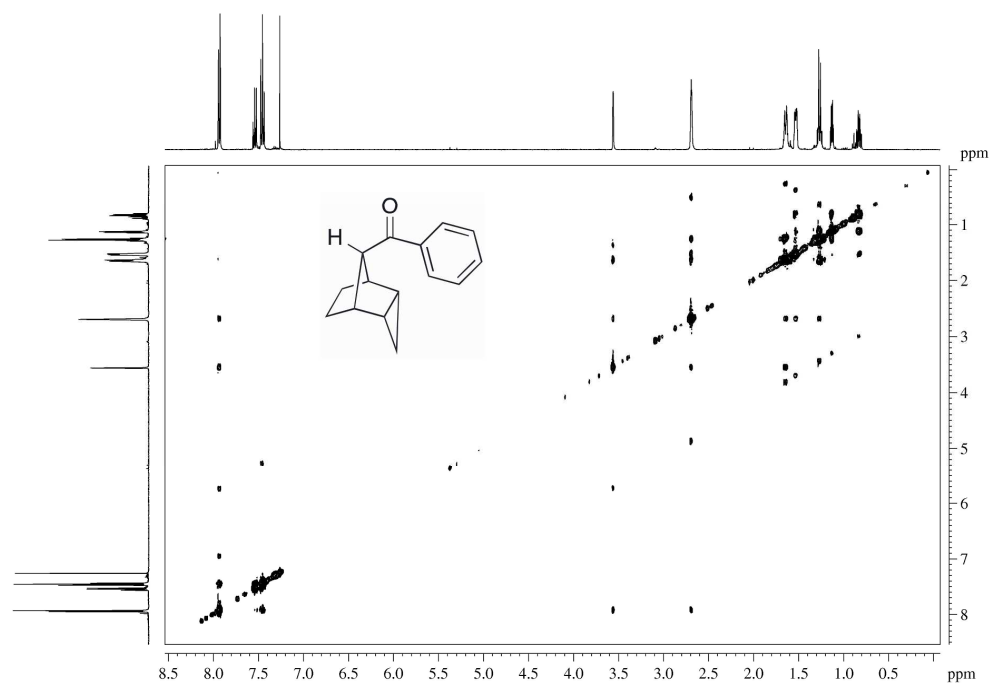


Figure A.68: NOESY spectrum of phenyl((1*R*,2*R*,4*S*,5*S*,8*r*)-tricyclo[3.2.1.0^{2,4}]octan-8-yl)methanone (**55**) (400.13 MHz, CDCl₃).

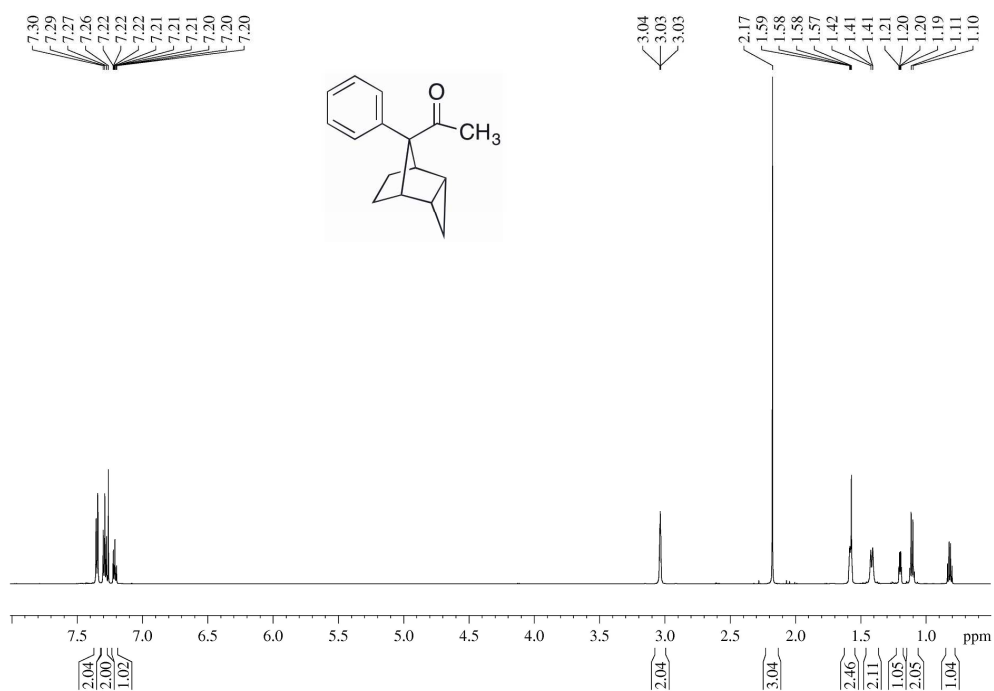


Figure A.69: ^1H NMR spectrum of 1-((1*R*,2*R*,4*S*,5*S*,8*r*)-8-phenyltricyclo[3.2.1.0^{2,4}]octan-8-yl)ethan-1-one (**56**) (600.13 MHz, CDCl_3).

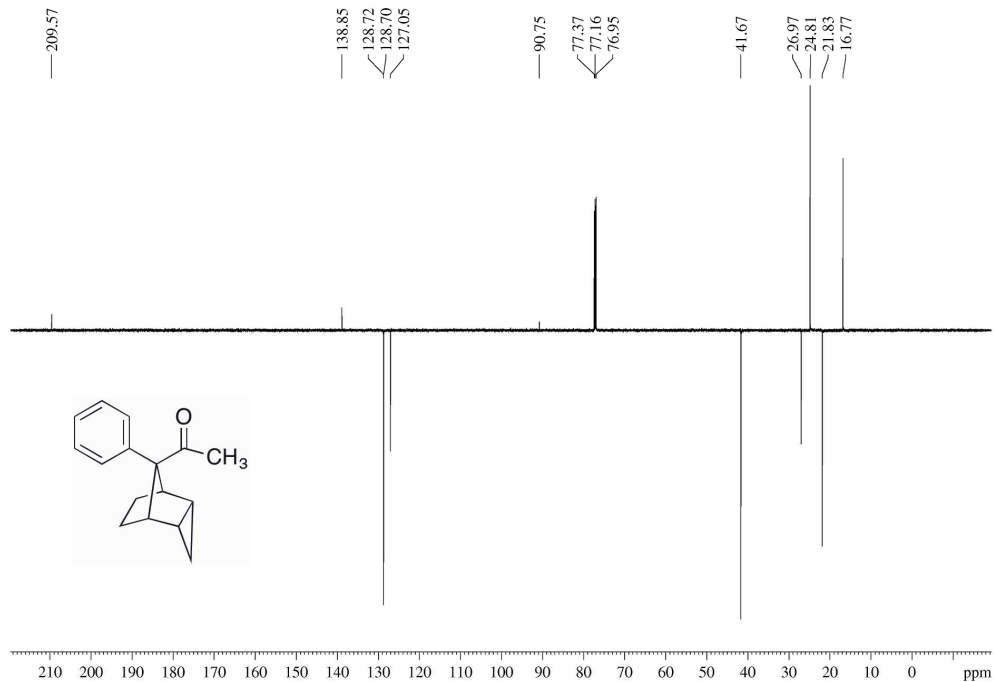


Figure A.70: ^{13}C NMR spectrum of 1-((1*R*,2*R*,4*S*,5*S*,8*r*)-8-phenyltricyclo[3.2.1.0^{2,4}]octan-8-yl)ethan-1-one (**56**) (150.92 MHz, CDCl_3).

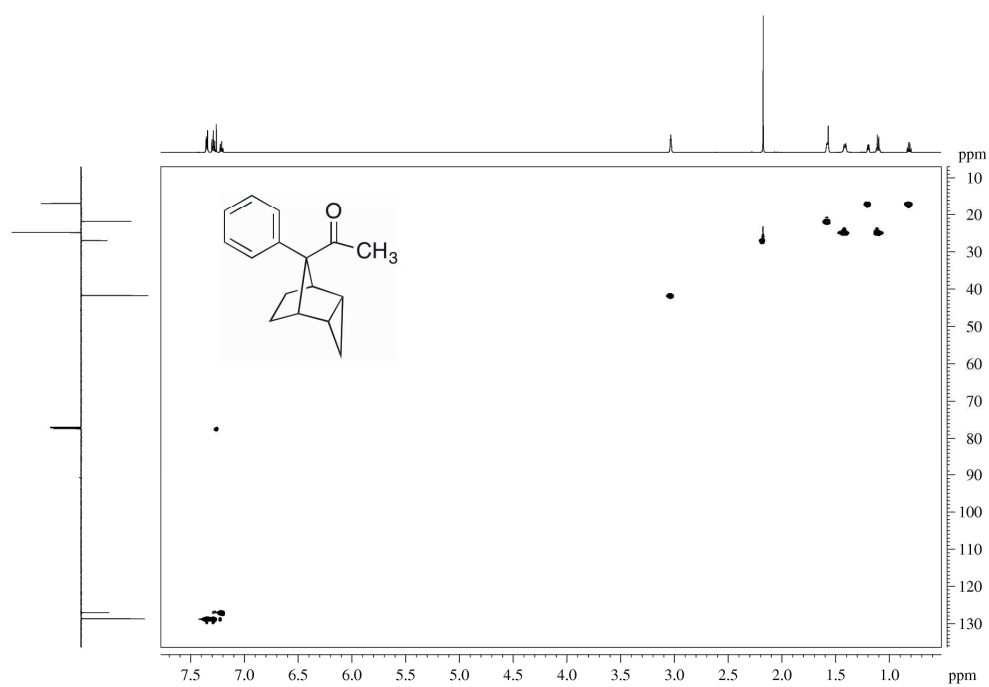


Figure A.71: HMBC spectrum of 1-((1*R*,2*R*,4*S*,5*S*,8*r*)-8-phenyltricyclo[3.2.1.0^{2,4}]octan-8-yl)ethan-1-one (**56**) (600.13 and 150.92 MHz, CDCl₃).

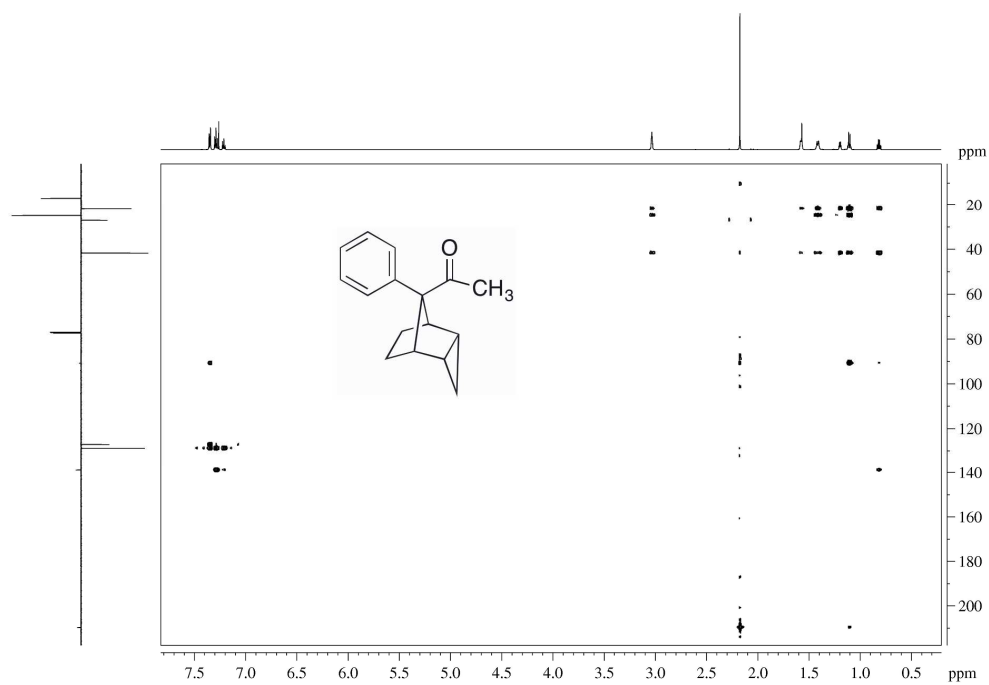


Figure A.72: HMBC spectrum of 1-((1*R*,2*R*,4*S*,5*S*,8*r*)-8-phenyltricyclo[3.2.1.0^{2,4}]octan-8-yl)ethan-1-one (**56**) (600.13 and 150.92 MHz, CDCl₃).

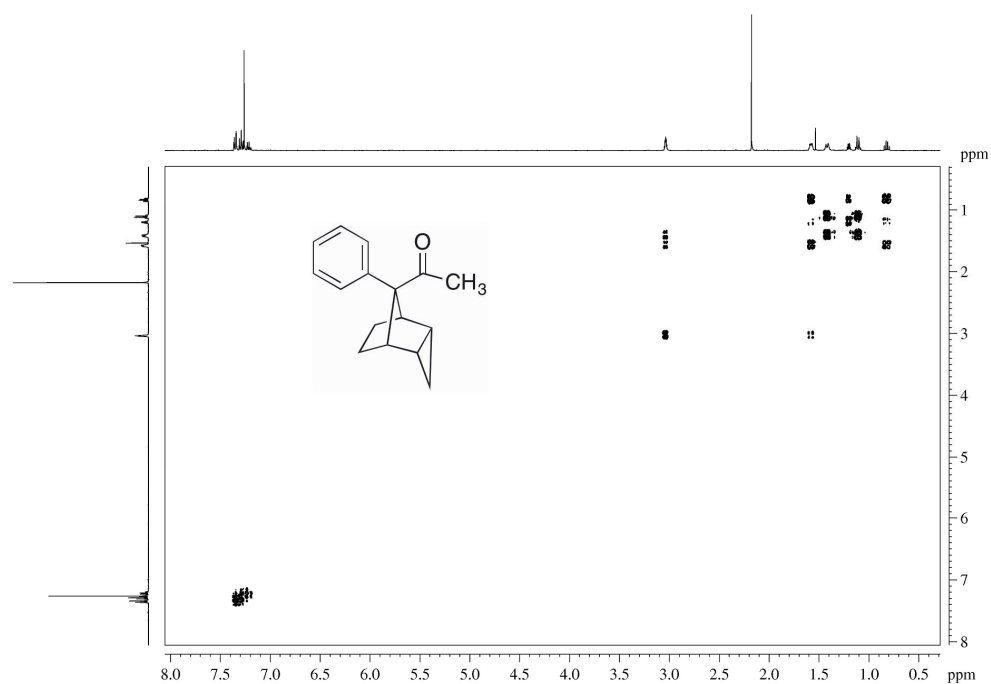


Figure A.73: COSY spectrum) of 1-((1*R*,2*R*,4*S*,5*S*,8*r*)-8-phenyltricyclo[3.2.1.0^{2,4}]octan-8-yl)ethan-1-one (**56**) (400.13 MHz, CDCl₃).

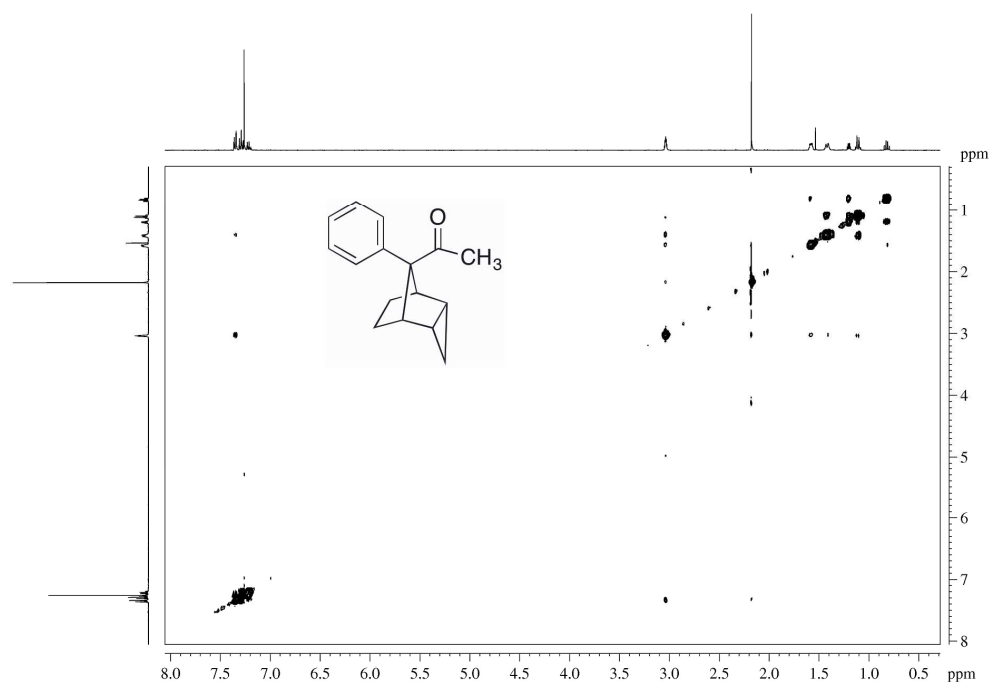


Figure A.74: NOESY spectrum of 1-((1*R*,2*R*,4*S*,5*S*,8*r*)-8-phenyltricyclo[3.2.1.0^{2,4}]octan-8-yl)ethan-1-one (**56**) (400.13 MHz, CDCl₃).

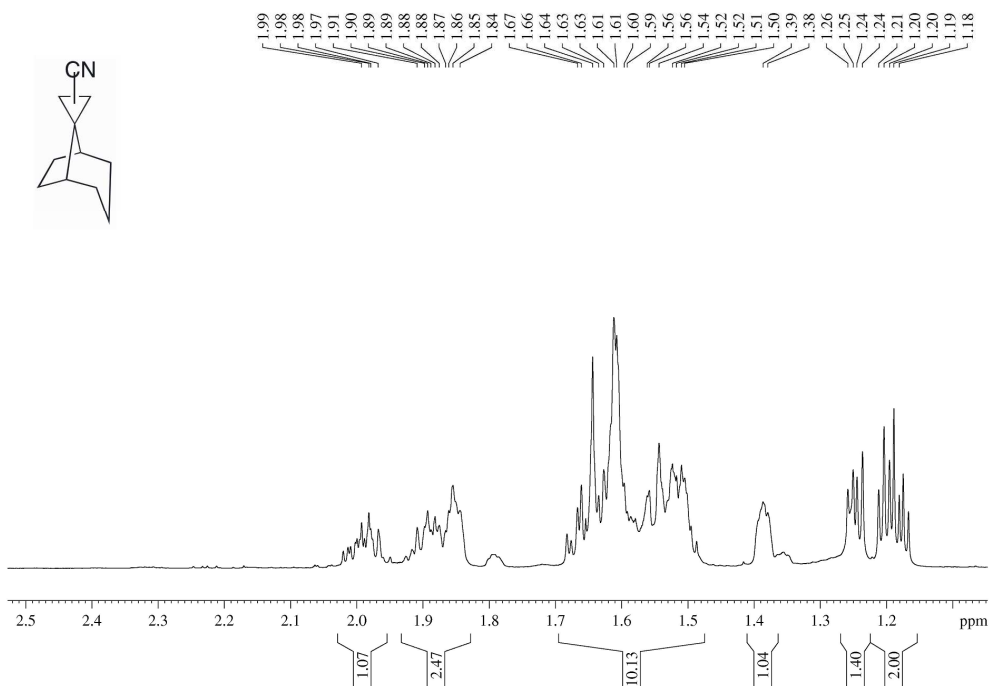


Figure A.75: ^1H NMR spectrum of spiro[bicyclo[3.2.1]octane-8,1'-cyclopropane]-2'-carbonitrile (**64**) (600.13 MHz, CDCl_3).

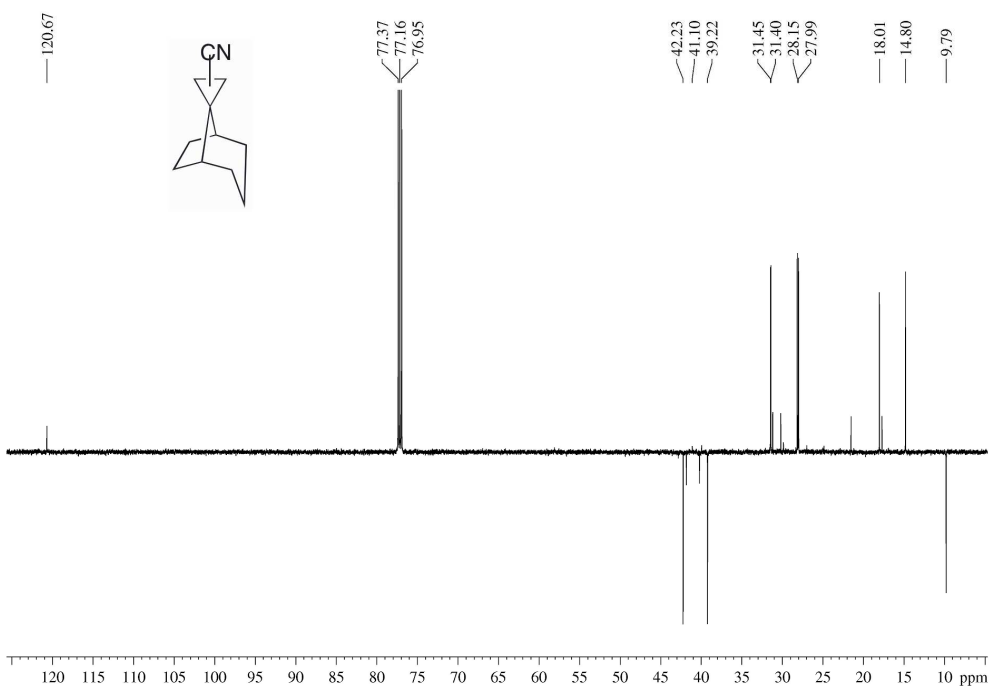


Figure A.76: ^{13}C NMR spectrum of spiro[bicyclo[3.2.1]octane-8,1'-cyclopropane]-2'-carbonitrile (**64**) (150.92 MHz, CDCl_3).

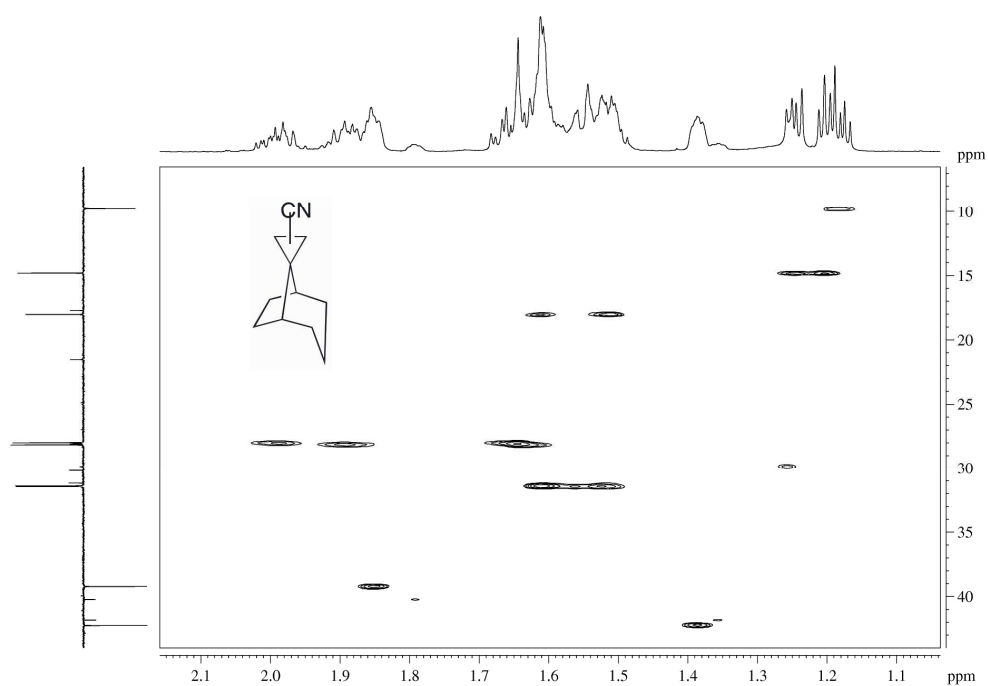


Figure A.77: HMQC spectrum spiro[bicyclo[3.2.1]octane-8,1'-cyclopropane]-2'-carbonitrile (**64**) (600.13 and 150.92 MHz, CDCl₃).

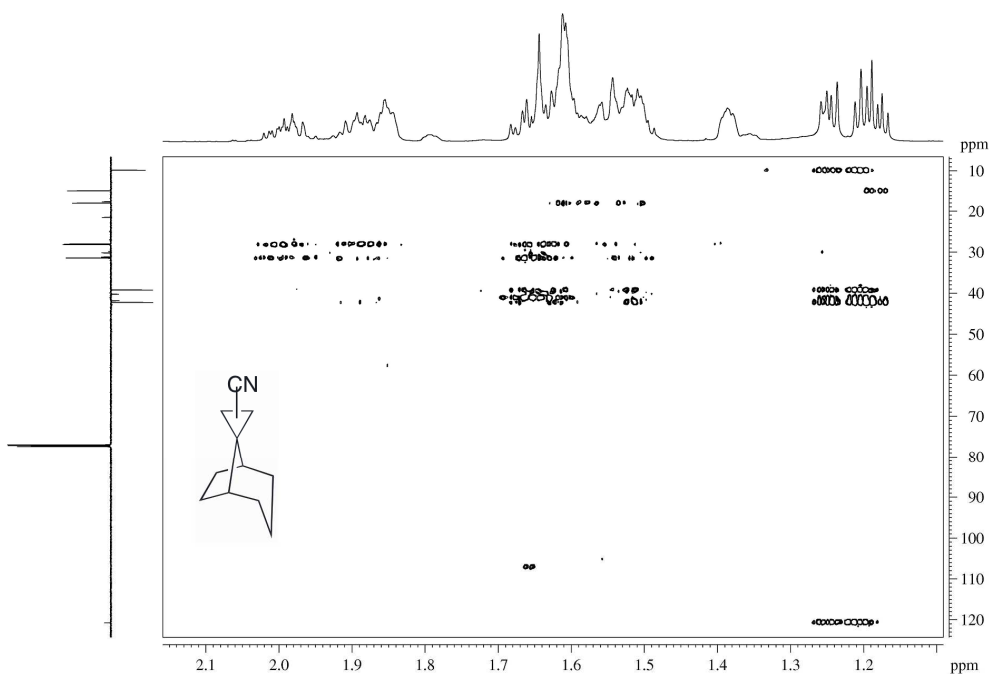


Figure A.78: HMBC spectrum of spiro[bicyclo[3.2.1]octane-8,1'-cyclopropane]-2'-carbonitrile (**64**) (600.13 and 150.92 MHz, CDCl₃).

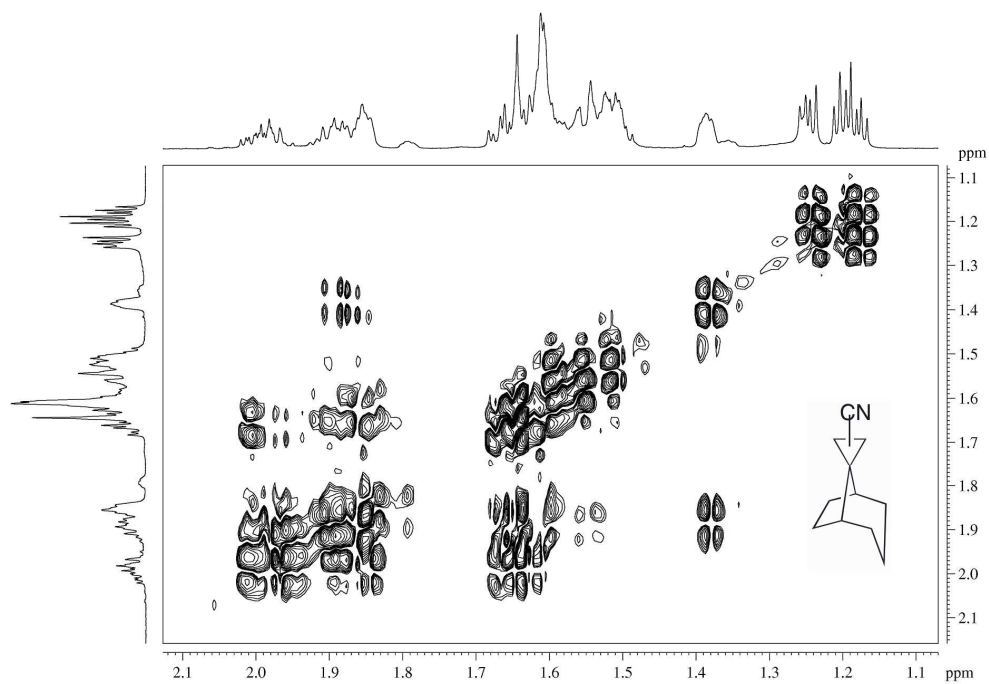


Figure A.79: COSY spectrum of spiro[bicyclo[3.2.1]octane-8,1'-cyclopropane]-2'-carbonitrile (**64**) (600.13 MHz, CDCl_3).

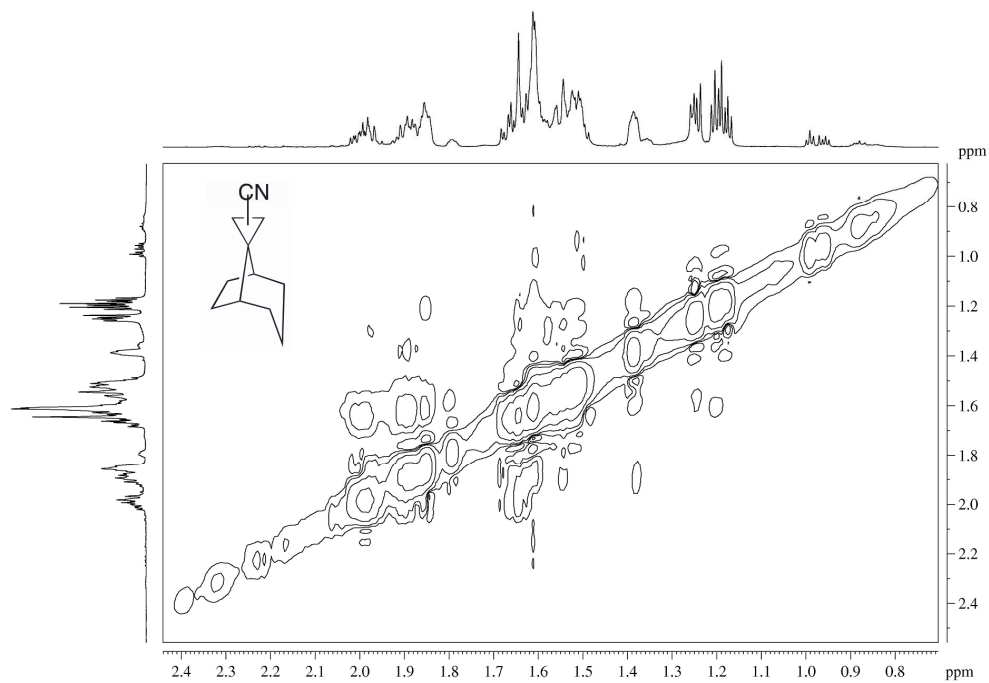


Figure A.80: NOESY spectrum of spiro[bicyclo[3.2.1]octane-8,1'-cyclopropane]-2'-carbonitrile (**64**) (600.13 MHz, CDCl_3).

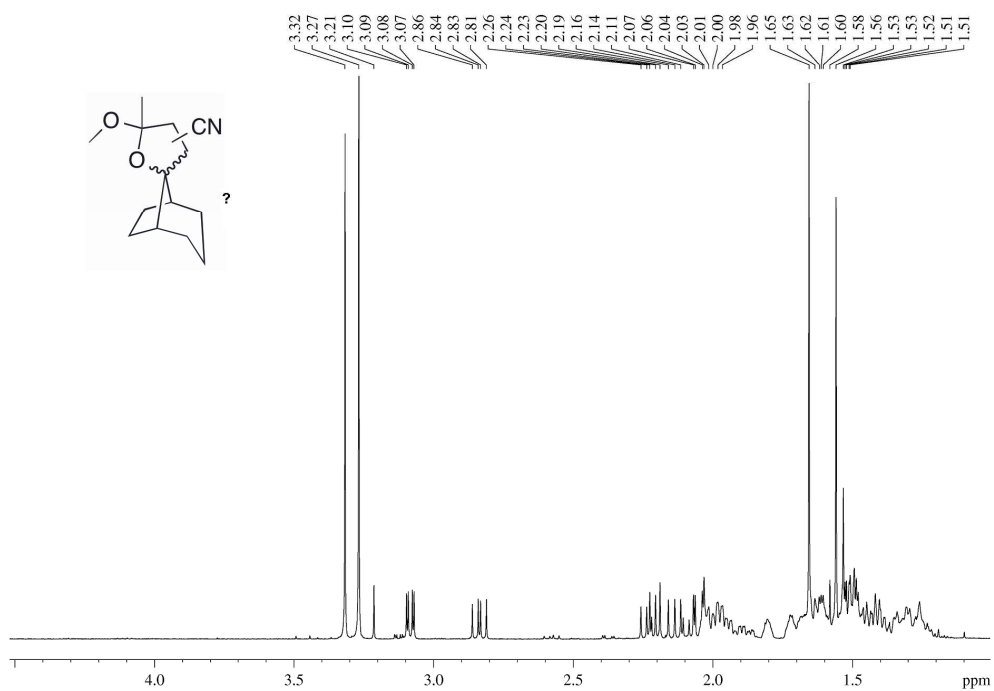


Figure A.81: ¹H NMR spectrum of some of the products possibly deriving from capture of carbonyl ylide **65** with acrylonitrile (400.27 MHz, CDCl₃).

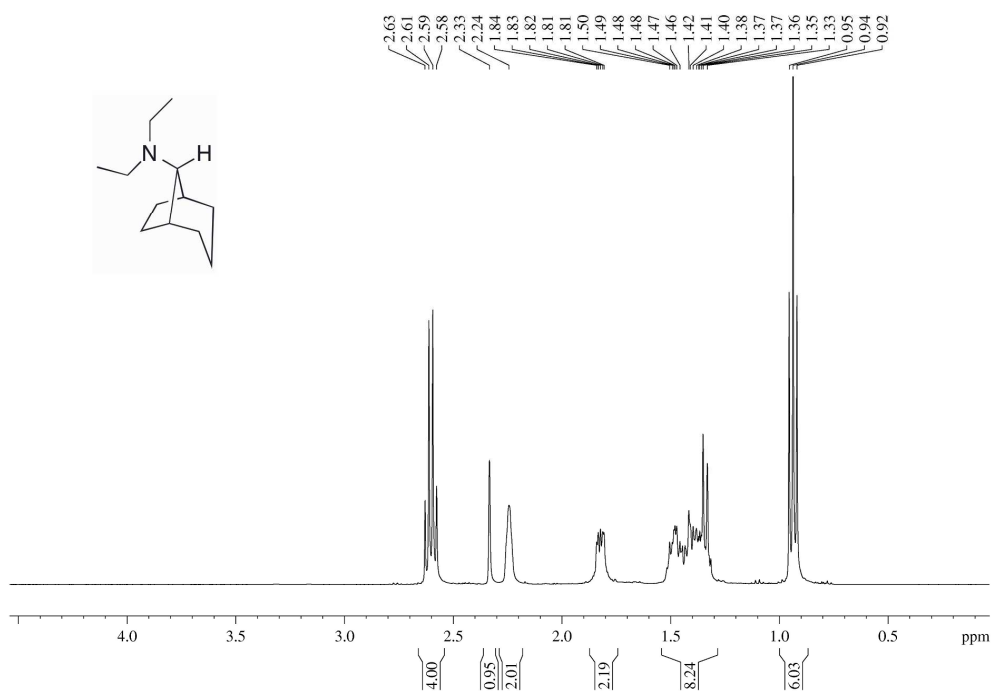


Figure A.82: ¹H NMR spectrum of *rel*-(1*R*,5*S*,8*r*)-*N,N*-diethylbicyclo[3.2.1]octan-8-amine (**67**) (400.13 MHz, CDCl₃).

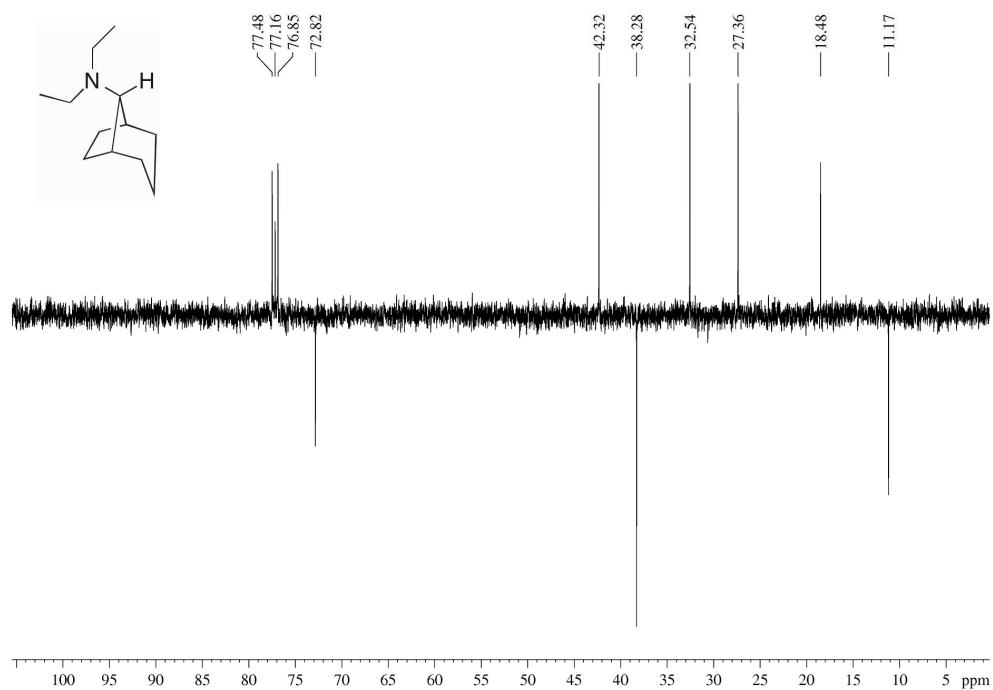


Figure A.83: ¹³C NMR spectrum of *rel*-(1*R*,5*S*,8*r*)-*N,N*-diethylbicyclo[3.2.1]octan-8-amine (**67**) (100.62 MHz, CDCl₃).

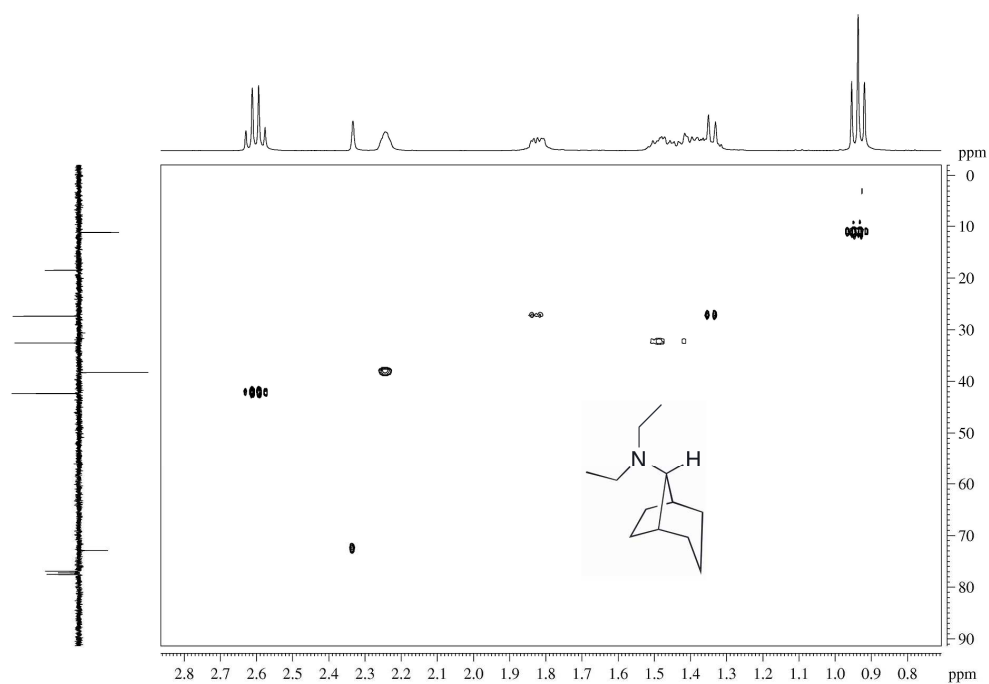


Figure A.84: HMBC spectrum *rel*-(1*R*,5*S*,8*r*)-*N,N*-diethylbicyclo[3.2.1]octan-8-amine (**67**) (400.13 and 100.62 MHz, CDCl₃).

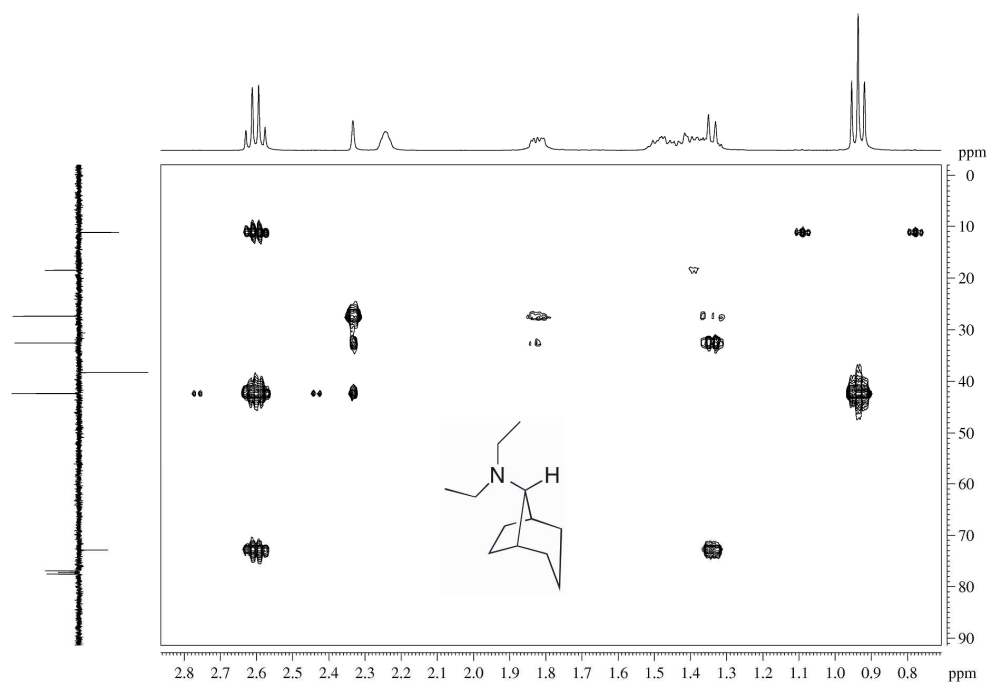


Figure A.85: HMBC spectrum of *rel*-(1*R*,5*S*,8*r*)-*N,N*-diethylbicyclo[3.2.1]octan-8-amine (**67**) (400.13 and 100.62 MHz, CDCl₃).

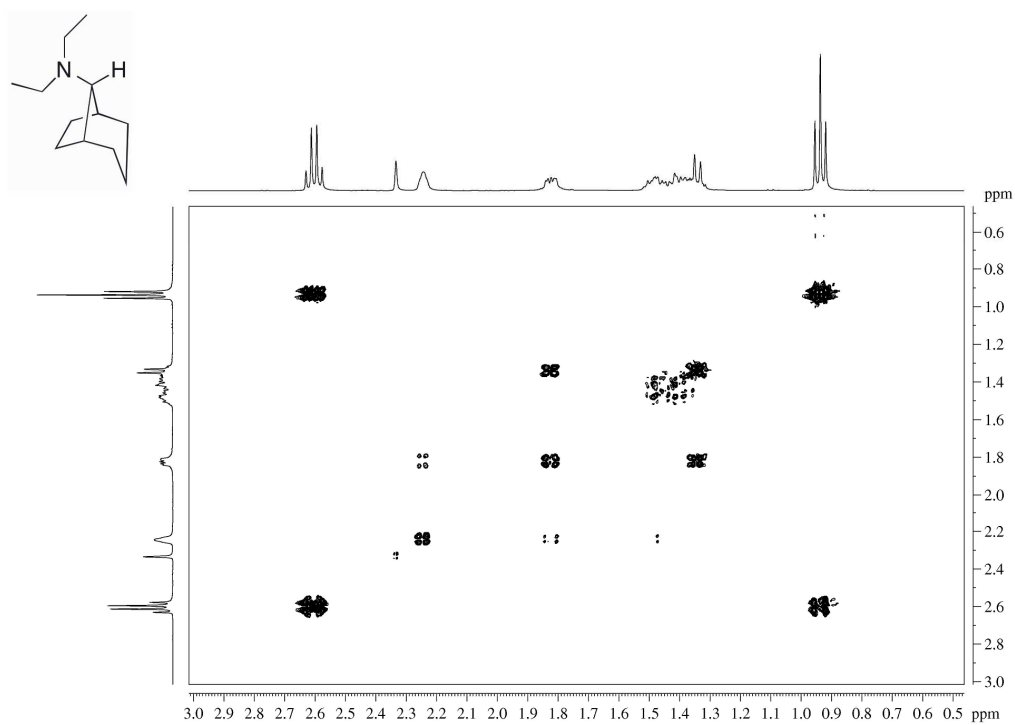


Figure A.86: COSY of *rel*-(1*R*,5*S*,8*r*)-*N,N*-diethylbicyclo[3.2.1]octan-8-amine (**67**) spectrum (400.13 MHz, CDCl₃).

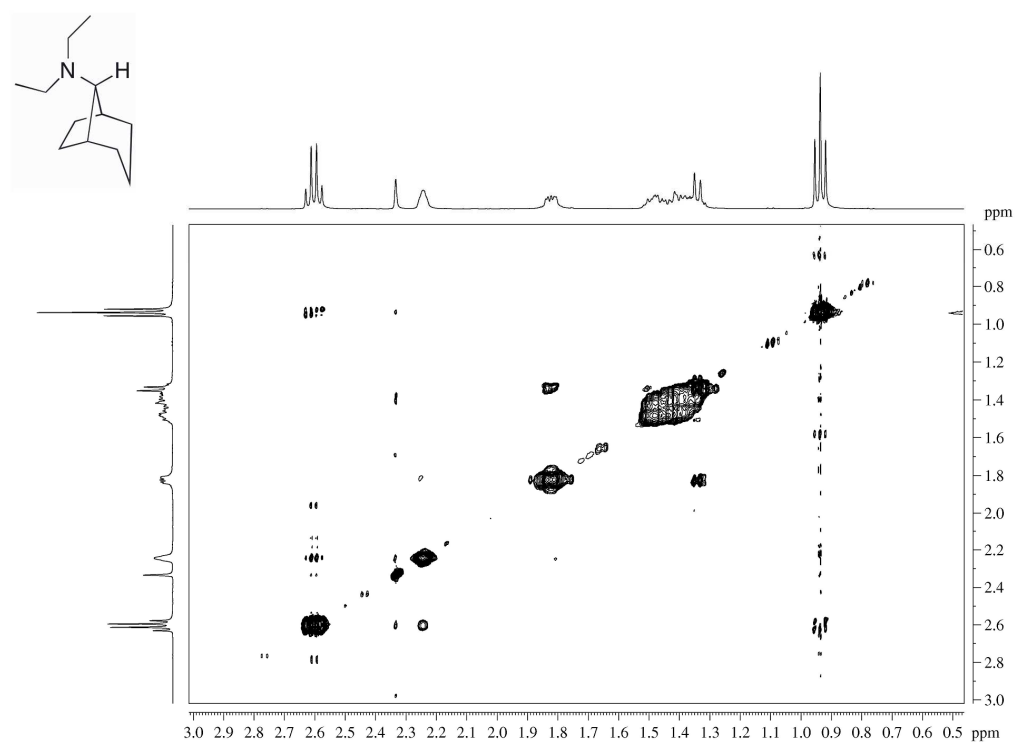


Figure A.87: NOESY spectrum of *rel*-(1*R*,5*S*,8*r*)-*N,N*-diethylbicyclo[3.2.1]octan-8-amine (**67**) (400.13 MHz, CDCl₃).

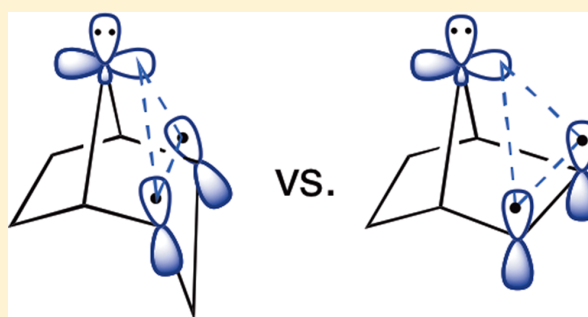
Probing the Nature and Extent of Stabilization within Foiled Carbenes: Homoallylic Participation by a Neighboring Cyclopropane Ring

Ingrid Malene Apeland, Hanspeter Kählig, Eberhard Lorbeer, and Udo H. Brinker*

Institute of Organic Chemistry, University of Vienna, Währinger Strasse 38, A-1090 Vienna, Austria

S Supporting Information

ABSTRACT: Oxadiazoline **6** was synthesized to generate *endo*-tricyclo[3.2.1.0^{2,4}]octan-8-ylidene (**3**) by either photolysis or thermolysis. Diastereomer **6a** thermally decomposed twice as fast as **6b**. Carbene **3** was trapped stereoselectively by acrylonitrile and diethylamine in high yields. It behaved as a nucleophilic carbene with electron-poor alkenes, like acrylonitrile, but as an electrophile with very electron-rich species, such as diethylamine. However, when the reactions were performed in cyclohexane and cyclohexene, isomerization of **3** was favored. Replacement of the double bond in 7-norbornenyldene (**1**) by the single bond in the *endo*-fused cyclopropane unit of carbene **3** led to similar outcomes. Carbene **3** rightfully belongs to the family of foiled carbenes.



INTRODUCTION

In 1968, Gleiter and Hoffmann coined the term “foiled carbenes” for a special class of singlet carbenes.^{1,2} These reactive species are stabilized to some degree by electron donation from an intramolecular π -bond into the empty p-orbital of the divalent carbon atom (Figure 1). This results in

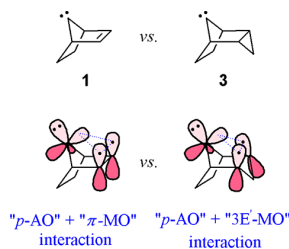
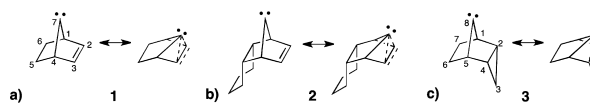


Figure 1. Interaction of the single bond Walsh orbital in carbene **3** mimics that of the double bond π -MO in carbene **1**, thereby establishing a two-electron, three-center bond with each carbene's p-AO.

the formation of a two-electron, three-center bond, a charge-delocalized arrangement found in certain analogous (non-classical) carbonium ions.³ Addition of the divalent carbon to the double bond is foiled because it would lead to an impossibly strained product featuring an inverted carbon atom with all four bonds pointed in one hemisphere.

The classic example of a foiled carbene is norbornen-7-ylidene (**1**) (Scheme 1a).⁴ Computations indicate that the bridge containing the divalent carbon leans toward the double

Scheme 1. Stabilization of Foiled Carbenes by Electron Donation to the Divalent Carbon Atom



bond by $\omega = 37^\circ$ when compared with norbornene.⁵ Early on, it was suggested that such bending should be reflected in the stereoselectivity of intermolecular reactions; a reactant should approach the divalent carbon more easily from the face *anti* to the double bond because more space is available.¹ Indeed, a substantial bias was observed for the addition of **1** with 3,3-dimethylbutene.⁶ Pyrolysis of the corresponding tosylhydrazone carbene precursor (i.e., Bamford–Stevens reagent) in the presence of the alkene gave two adducts wherein the *tert*-butyl group was oriented *syn* or *anti* to the double bond in a ratio of 7:1. However, the combined yield of the two products amounted to only 0.1%. The stereoselectivity was also investigated using density functional theory (DFT).⁷ The most stable transition state was obtained when 3,3-dimethylbutene approached the divalent carbon of **1** *anti* to the double bond with the bulky *tert*-butyl group directed head-on to avoid a steric interaction with the *exo* hydrogens at C-5 and C-6 of **1**. This course would lead to the *syn* product, which was indeed the “major” product obtained experimentally.⁶

Received: March 3, 2013

Published: April 16, 2013

In order to achieve reasonable yields of intermolecular products from foiled carbenes, one must recognize their predominantly nucleophilic behavior.^{8,9} The introduction of reactants that can behave as electron-pair acceptors is warranted. For example, tricyclo[6.2.1.0^{2,7}]undec-9-en-11-ylidene (**2**) comprises **1** as a subunit (Scheme 1b). It was generated by thermal decomposition of an oxadiazoline precursor. Carbene **2** reacted stereoselectively, via *anti* approach, with each of the following reactants: diethylamine (77% yield),¹⁰ acrylonitrile (42% yield),⁷ and malononitrile (29% yield).¹¹

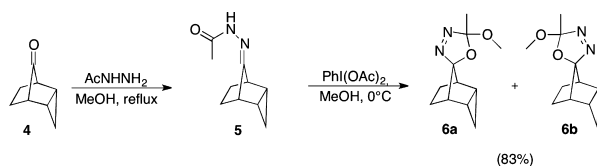
Cyclopropanes sometimes demonstrate a reactivity resembling that of alkenes. DFT calculations indicate that the three-membered ring of *endo*-tricyclo[3.2.1.0^{2,4}]octan-8-ylidene (**3**) stabilizes the divalent carbon in a way similar to that of a double bond (Figure 1 and Scheme 1c).¹² Computations also suggest the singlet electronic state of **3** to be lower in energy than the triplet.¹² Thus far, few experiments have been conducted to support the existence of an interaction between the divalent carbon atom and the cyclopropane ring.¹³ Although rearrangements of **3** have been studied,¹³ its potential classification as a foiled carbene could be more thoroughly assessed by examining its intermolecular reactions. Herein, the results of such experiments are presented. For these studies, oxadiazolines were employed as carbene precursors. Their syntheses and kinetics of decomposition are described as well.

RESULTS AND DISCUSSION

Synthesis of Oxadiazolines as Carbene Precursors.

Oxadiazolines are quite versatile compounds and popular carbene precursors.^{10,14} Depending on their substituents, they decompose by different pathways to give a variety of products. (1'*R*,2'*R*,4'*S*,5'*S*)-5-Methoxy-5-methylspiro[2,5-dihydro-1,3,4-oxadiazole-2,8'-tricyclo[3.2.1.0^{2,4}]octane] (**6**) is expected to generate the requisite carbene **3** by either photolysis or thermolysis. Carbene **3**, however, is not produced directly from **6**, but through either a carbonyl ylide or a diazo intermediate (*vide infra*). The necessary oxadiazoline **6** was synthesized from ketone **4** (Scheme 2).¹⁵ Two diastereomers were produced (dr

Scheme 2. Synthesis of the Oxadiazoline (**6**) Used To Generate Carbene **3**



= 1:1.7) in a combined yield of 83%. Isomers **6a** and **6b** were separated by column chromatography, and the absolute configuration of each pseudoasymmetric spirocyclic C atom (i.e., *r/syn* vs *s/anti*) was determined by X-ray crystallography (Figure 2).

Kinetics Measurements. The rate of thermolysis of **6a** and **6b** was measured at 116 °C (1 mg/mL in decane) by monitoring the decay of the UV absorption maxima of their oxadiazoline groups at $\lambda_{\text{max}} = 338$ and 333 nm, respectively. The decay of both **6a** and **6b** follows a first-order rate law with rate constants $k = 2.3 \times 10^{-5} \text{ s}^{-1}$ and $k = 1.2 \times 10^{-5} \text{ s}^{-1}$, respectively. These values are typical for the decomposition of oxadiazolines (Figure 3),^{14e,k} which normally thermolyze by

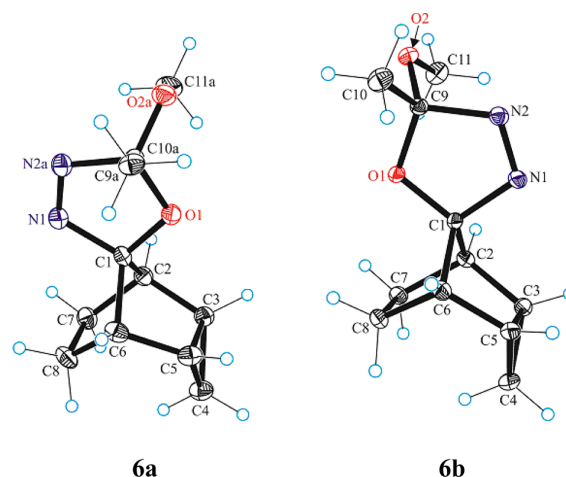


Figure 2. Single-crystal X-ray diffraction was used to elucidate the structures of the *rel*-(1'*R*,2'*r*,2'*R*,4'*S*,5'*R*,5'*S*)-5-methoxy-5-methylspiro[2,5-dihydro-1,3,4-oxadiazole-2,8'-tricyclo[3.2.1.0^{2,4}]octane] (**6a**) and *rel*-(1'*R*,2'*s*,2'*R*,4'*S*,5'*R*,5'*S*)-5-methoxy-5-methylspiro[2,5-dihydro-1,3,4-oxadiazole-2,8'-tricyclo[3.2.1.0^{2,4}]octane] (**6b**).

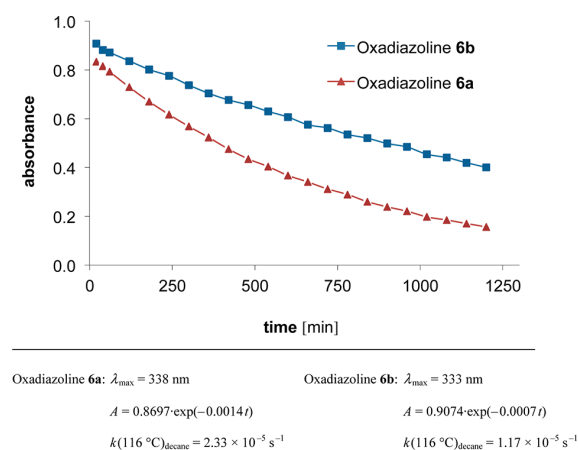


Figure 3. Decay of oxadiazolines **6a** and **6b** at 116 °C monitored using their UV absorbance maxima and found to be first-order.

first expelling molecular nitrogen.^{14b,c} Diastereomer **6a** decomposes about twice as fast as **6b**, ostensibly because its configuration allows the cyclopropane ring to anchimerically assist with the expulsion of N₂. Such an interpretation is supported by results from solvolysis experiments with tricyclo[3.2.1.0^{2,4}]octan-8-yl derivatives, which have shown that the relative orientation of the cyclopropyl subunit and the leaving group at C-8 are decisive when considering the rates of solvolysis.¹⁶ The order of observed reactivity is *endo,anti* \gg *exo,syn* > *endo,syn* > *exo,anti*.¹⁷ Thus, it is not surprising that the *endo,anti* relationship between the nitrogen and cyclopropyl group of **6a** accelerates its decomposition when compared with that of **6b**, which exhibits an *endo,syn* relationship. Among other factors, the modest 2-fold rate increase may arise from anchimeric assistance by the filled Walsh orbital of the cyclopropane moiety of **6a** into an antibonding MO, resulting in the loss of N₂.

Reactions of *endo*-Tricyclo[3.2.1.0^{2,4}]octan-8-ylidene (3**).** All thermolysis (165 °C) and photolysis ($\lambda > 200$ nm,

Table 1. GC–MS Analysis of Product Distribution Obtained from Thermolysis and Photolysis of Oxadiazolines **6a** and **6b** in Cyclohexane and Cyclohexene

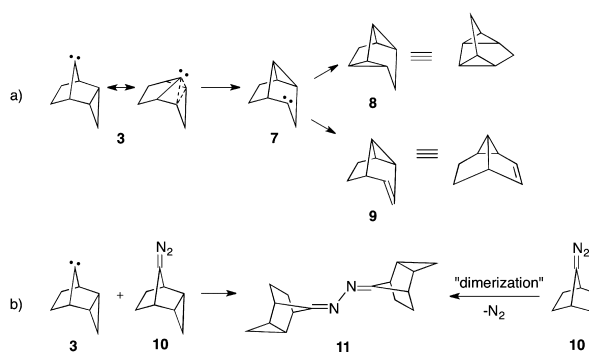
precursor	substrate	concn (mg/mL)	conditions	intermol. product yield (%)	intramol. product 8 yield (%)	intramol. product 9 yield (%)	azine 11 yield (%)
6a	cyclohexane	10	Δ	3	55	3	—
6b		10	Δ	4	17	1	31
6a		10	$h\nu$	—	27	2	47
6a		6	$h\nu$	—	23	2	31
6b		11	$h\nu$	—	44	3	31
6b		5	$h\nu$	—	20	1	38
6a	cyclohexene	10	Δ	5	71	10	—
6b		10	Δ	4	71	10	—
6a		10	$h\nu$	6	15	1	40
6a		6	$h\nu$	8	20	2	35
6b		12	$h\nu$	2	12	1	25
6b		5	$h\nu$	3	25	2	17

water bath, room temperature) experiments were conducted by dissolving precursors **6a** and **6b**, respectively, in the solvent under investigation. First, the chemistry of **3** in cyclohexane and cyclohexene was studied under the conditions listed in Table 1. The resulting solutions were subjected to GC–MS analysis, and yields were determined using camphor as an internal standard.

As presented in Table 1, there were some cases in which small peaks were detected in the chromatograms that might derive from compounds formed by intermolecular reactions of carbene **3** with cyclohexane (M^+ ; $m/z = 190$) or cyclohexene (M^+ ; $m/z = 188$). However, the estimated yields were low (ca. 2–8%). This lack of reactivity indicates a stabilization of carbene **3**, but it could also mean that intramolecular reactions are faster. Moreover, the *slow* addition to the electron-rich double bond of cyclohexene suggests that **3** acts as a nucleophilic carbene as gauged by the “philicity” scale of carbenes in carbene–alkene addition reactions.¹⁸

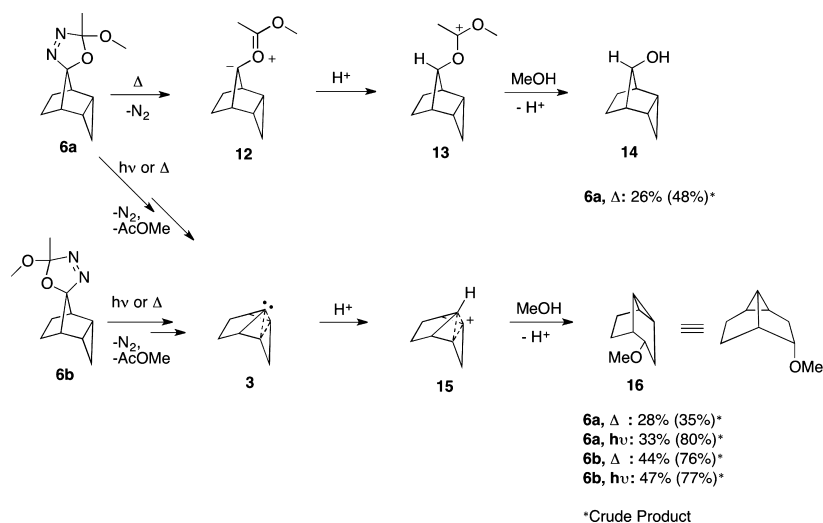
In all experiments, significant formation of a product (M^+ ; $m/z = 106$) was observed. This presumably results from an isomerization of **3**. In order to identify this compound, thermolysis of **6b** was carried out in cyclohexane- d_{12} , and the reaction mixture was analyzed by NMR spectroscopy. Additionally, **6b** was thermolyzed in pentane, and after concentration, the resulting product mixture was subjected to diffusion-edited NMR.¹⁹ Two spectra with attenuated signals were obtained after conducting two pulsed-field gradient spin echo experiments in which one had a very low gradient amplitude and the other had a much higher one. A pure trace for compound **8** was computed by subtracting these spectra from each other after the vertical scale was adjusted to the peak of the undesired background (Figure S13 in the Supporting Information). The ¹H NMR and ¹³C NMR signals were in accordance with tetracyclo[3.3.0.0^{2,8}.0^{4,6}]octane (**8**) (Scheme 3a).²⁰ In addition, a minor product with the same mass was formed. It is thought to be tricyclo[3.3.0.0^{4,6}]oct-2-ene (dihydrosemibullvalene) (**9**) (Scheme 3a), based on characteristic ¹H NMR patterns of the alkenyl hydrogens.^{14k,21} Compounds **8** and **9** have also been obtained from carbene **3** under different conditions (vide infra).^{13a,b} A mechanism for the formation of **8** and **9** was proposed involving a conversion of **3** into **7**,^{13b,22} as shown in Scheme 3a.

Under nearly all reaction conditions (Table 1), *endo*-tricyclo[3.2.1.0^{2,4}]octan-8-one azine (**11**) (Scheme 3b) was formed. The compound was identified by scaling up the reaction of the thermolysis of **6b** in pentane, which gave **11** in

Scheme 3. Products Formed by Thermolysis or Photolysis of Oxadiazoline **6a** or **6b** in Cyclohexane or Cyclohexene

an isolated yield of 11%. The azine can derive either from the reaction of carbene **3** with diazo compound **10**, which is formed by the loss of methyl acetate from oxadiazoline **6**, or from a bimolecular reaction of **10** with itself followed by the loss of N_2 (Scheme 3b).²³ These processes can occur simultaneously wherein the dominating one depends on the solution's concentration. As an additional possibility, carbene **3** might attack the remote N atom of precursor **6**, which would subsequently lose methyl acetate to afford **11**. The GC–MS results indicate that **11** is formed more frequently during photolysis than thermolysis. Alternatively, oxadiazolines **6a** and **6b** can decompose by an initial loss of N_2 , yielding a carbonyl ylide, which further collapses to carbene **3**.¹⁴ The ¹³C NMR spectrum of **11** revealed two sets of signals in a 1:1 ratio. After evaporation of the solvent, the sample was redissolved and allowed to stand for 3 h before another analysis. Subsequently, the spectrum revealed one major and one minor set of signals. However, the 1:1 ratio was reestablished over time as the two species equilibrated (Figure S25 in the Supporting Information).

In previous experiments,^{13a,b} the corresponding tosylhydrazone precursor of carbene **3** was thermolyzed in diglyme (i.e., 2,5,8-trioxanonane) in the presence of 5.74 equiv of sodium methoxide. In addition to products **8** and **9**, three methyl ethers were obtained, resulting from intermolecular reactions of carbene **3** with methanol. These compounds are believed to form through a carbenium ion pathway in which the carbene is protonated. Either the carbenium ion or the carbene route can be favored by varying the reaction conditions. Here, a different

Scheme 4. Thermolysis and Photolysis of Oxadiazolines **6a** and **6b** in the Presence of Methanol

carbene precursor was used (i.e., an oxadiazoline) that was directly dissolved in methanol. This could lead to a different outcome. In addition, the reactions were carried out under both thermolytic and photolytic conditions.

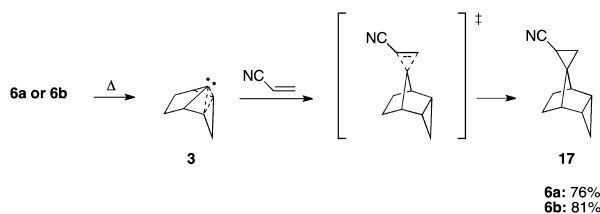
In all experiments, only methyl ethers were formed. In each case, GC–MS of the crude sample showed one main product, which was isolated by column chromatography and identified as *rac*-(1*R*,2*S*,4*S*,5*R*,6*R*)-2-methoxytricyclo[3.3.0.0^{4,6}]octane (**16**) (Scheme 4). Compound **16** is identical to the main methyl ether obtained by the reported Bamford–Stevens reaction.^{13a,b} The isolated yields were considerably lower after chromatography (Scheme 4). It is possible that **16** decomposes on silica adsorbent because the crude products were quite pure according to ¹H NMR analysis.

In addition to **16**, *endo*,*syn*-tricyclo[3.2.1.0^{2,4}]octan-8-ol (**14**) was formed in 26% yield during the thermolysis of **6a** in methanol (Scheme 4). The production of alcohol **14** is best explained by protonation of the proximal ylide intermediate **12** with methanol to afford **13**, which locks in the stereo-configuration at C-8. Subsequent methanolysis of **13** gives **14**. A similar reaction sequence was observed for the oxadiazoline precursor of **2**.²⁴ In contrast, the distal ylide intermediate formed from **6b** (not shown) might be destabilized by electron donation from the three-membered ring because of the aforementioned *endo*,*anti* relationship. This may lead to its collapse before being trapped by a proton. However, proton transfer rates to a negatively charged C atom are extremely fast. The experiments with methanol therefore stand as the single example where **6a** and **6b** reacted differently. Because **14** is not formed during photolysis, it can be assumed that the oxadiazoline decomposes through diazo intermediate **10** rather than ylide **12**.

The formal insertion reaction of foiled carbenes into methanol has been shown to occur through initial protonation of the carbene to give a carbenium ion.²⁵ The positive charge in **15** is delocalized among C-2, C-4, and C-8. Product **16** is formed by an attack of methanol at C-2 or C-4. This indicates that the charge is concentrated largely at these identical carbon atoms. In addition, the delocalized charge in **15** shields it from an attack by methanol at the *exo* positions of C-4 and C-2. Thus, formation of the corresponding *exo*-methyl ether of **16** is

prevented.^{16b,c} The stereochemistry of product **16** is determined by **15** originating from protonation of carbene **3**.²⁶

Next, conditions were needed where carbene **3** would react directly with an added substrate. Because foiled carbenes in general are nucleophilic, trapping them with an electron-deficient alkene has proven to be successful.⁷ Thus, when **6a** or **6b** was thermolyzed in acrylonitrile, *rel*-(1*s*,1'*R*,2*R*,2'*R*,4'*S*,5'*S*)-spiro[cyclopropane-1,8'-tricyclo[3.2.1.0^{2,4}]octane]-2-carbonitrile (**17**) (Scheme 5) was formed exclusively in a yield of 76%

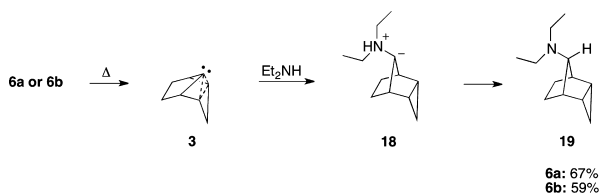
Scheme 5. Thermolysis of Oxadiazolines **6a** and **6b** in the Presence of Acrylonitrile

or 81%, respectively. These values are considerably higher than those obtained for carbene **2**. The stereochemistry of **17** was assigned with the help of two-dimensional NMR experiments. Because the reaction occurs stereoselectively (i.e., the cyano group is always found to be *anti* to the cyclopropane), it can be assumed that the product is formed through a concerted mechanism, which is expected for a singlet carbene.^{2c} The assumed transition state is shown in Scheme 5. Previous DFT calculations suggest that the *anti* product is formed with electron-poor alkenes, whereas the *syn* product is preferred with electron-rich alkenes.⁷ In both cases, the alkene approaches the divalent carbon *anti* to the stabilizing moiety (i.e., double bond or cyclopropane ring), but subsequent stereoelectronic effects determine how the alkene's substituents are orientated in the product. Both the nucleophilic behavior and the diastereoselectivity in this reaction provide strong evidence for a foiled carbene **3**.

Foiled carbenes can also exhibit ambiphilicity. For example, carbene **2** was successfully trapped by highly nucleophilic diethylamine.¹⁰ Therefore, thermolyses were carried out for

both **6a** and **6b** in the neat amine. One main product was obtained from both reactions: *endo,anti-N,N*-diethyltricyclo[3.2.1.0^{2,4}]octan-8-amine (**19**) (Scheme 6), in yields of 67%

Scheme 6. Thermolysis of Oxadiazolines **6a and **6b** in the Presence of Diethylamine**



and 59% from **6a** and **6b**, respectively. The GC–MS chromatograms showed a small amount of an additional compound with the same molar mass as **19** in ratios of 30:1 and 58:1, respectively. This minor product could be the *syn* analog of **19**, or it could result from a reaction of diethylamine with carbene **7**. The reaction **6** → **19** is assumed to proceed through ylide intermediate **18** (Scheme 6),^{10,27} thereby preserving the diastereoselectivity of step **3** → **18**.²⁸ The stereochemistry of product **19** suggests an *anti* approach of diethylamine. In any case, however, an *anti* approach is necessary to obtain **19** even if the mechanism involves a concerted insertion of carbene **3** into the N–H bond. Thus, this reaction also suggests a foiled carbene **3** as an intermediate.

CONCLUSION

The experiments described above support that *endo*-tricyclo[3.2.1.0^{2,4}]octan-8-ylidene (**3**) is a stabilized carbene. The occupied Walsh orbitals of the three-membered ring donate electron density into the empty p-orbital of the divalent carbon (Figure 1), causing the main bridge to bend toward the cyclopropane ring as is the case with alkenylidene **1**. This is reflected in intermolecular reactions with acrylonitrile and diethylamine, which both approach the divalent carbon *anti* to the cyclopropane unit. Oxadiazolines **6a** and **6b** are useful precursors of **3**. The two diastereomers show almost identical reactivities, although **6a** thermally decomposes about twice as fast as **6b**. Azine **11** was isolated in nearly all reactions (Table 1). It is formed more frequently during photolysis than thermolysis. In the thermolysis of **6a**, ylide intermediate **12** was trapped with methanol to give the tricyclic alcohol **14**. Carbene **3** is added as a nucleophile to acrylonitrile and as an electrophile to diethylamine in high yields. The reactions are stereoselective. Replacing the CH=CH unit in 7-norbornenylidene (**1**) with an *endo*-fused cyclopropane ring, as in carbene **3**, leads to comparable reactive behavior. Thus, on the basis of the experiments outlined in this study, carbene **3** rightfully belongs to the family of foiled carbenes.

EXPERIMENTAL SECTION

Equipment. Melting points were measured on a melting point microscope and are uncorrected. The NMR spectra were obtained on either a DRX 400 WB instrument, operating at a frequency of 400.13 MHz for ¹H and 100.62 MHz for ¹³C, or a DRX 600 at a frequency of 600.13 MHz for ¹H and 150.95 MHz for ¹³C. The chemical shifts are given in parts per million with respect to TMS. For the ¹H NMR spectra, the residual peak of CDCl₃ ($\delta_{\text{H}} = 7.26$ ppm) or cyclohexane-*d*₁₂ ($\delta_{\text{H}} = 1.38$ ppm) was used as an internal standard. For the ¹³C NMR spectra, the central peak of the CDCl₃ triplet ($\delta_{\text{C}} = 77.16$ ppm) was used as an internal standard. Conventional gradient-enhanced

two-dimensional COSY, NOESY, HMBC, and HMQC spectra were used to derive proton and carbon assignments. The diffusion edited NMR experiments were done on the DRX 600, where a longitudinal eddy current delay sequence with 1 ms smoothed square bipolar gradient pulse pairs²⁹ was used, with a diffusion delay set to 100 ms. Two spectra were recorded, one with 3% and the second with 73% gradient amplitude. The resulting ¹H NMR spectra were subtracted by scaling the signal intensity of the background signals to equal heights, giving a trace with only compound **8** (Figure S13 in the Supporting Information). Infrared spectra were measured with an ATR attachment, and the absorptions are given in wavenumbers (cm⁻¹). HRMS was performed on a mass spectrometer outfitted with a TOF analyzer using ESI techniques, or a double-focusing sector field analyzer using EI (70 eV) techniques. Single-crystal X-ray analyses were performed on a diffractometer. Photolysis experiments were carried out using a medium pressure mercury lamp doped with FeI₂ ($\lambda_{\text{max}} = 370$ nm), which was placed in a water-cooled jacket made of quartz. GC–MS data were obtained using an instrument equipped with a mass selective detector (70 eV) on a 30 m × 0.25 mm HP-5MS poly-(methylphenylsiloxane) (95% dimethyl and 5% diphenyl, 0.25 μ m film thickness) capillary column using helium as the carrier gas.

General Settings for GC–MS Analysis. Pressure: 0.416 bar. Flow: 0.7 mL/min. Average velocity: 32 cm/s. Injection volume: 1.0 μ L. Split ratio: 1:25. Injection temperature: 270 °C. Starting temperature: 80 °C for 2 min. Ramp: 5 °C/min up to 145 °C. Ramp: 15 °C/min up to 220 °C. Isotherm: 220 °C for 3 min. Ramp: 15 °C/min up to 270 °C. Isotherm: 270 °C for 3 min.

Materials. Dry pentane was obtained by distillation from calcium hydride. Cyclohexane, cyclohexene, acrylonitrile, diethylamine, and methanol were distilled and dried over molecular sieves (3 Å or 4 Å) before use. Commercially available compounds were used without further purification. Ketone **4** was synthesized according to the literature.^{16b,30} Analytical TLC was performed on aluminum plates with silica gel 60 F₂₅₄, and detection was obtained with an iodine chamber or a UV lamp at $\lambda = 254$ nm. Flash chromatography was conducted using silica gel 60 (230–400 mesh) as the stationary phase with hexane, ethyl acetate, and dichloromethane in different ratios as the mobile phase.

rac-(1'*R*,2'*R*,4'*S*,5'*S*)-5-Methoxy-5-methylspiro[2,5-dihydro-1,3,4-oxadiazole-2,8'-tricyclo[3.2.1.0^{2,4}]octane] (**6**). Ketone **4** (1.830 g, 14.98 mmol) and acetyl hydrazide (1.225 g, 16.54 mmol) were dissolved in methanol (100 mL) and refluxed for 3 h. The reaction mixture was cooled to 0 °C, and PhI(OAc)₂ (5.308 g, 16.48 mmol) was added over a period of 5 min. The mixture was stirred overnight as the ice bath melted. The solvent was removed on a rotary evaporator, and the product was isolated as a diastereomeric mixture (**6a**:**6b** = 1:1.7) by column chromatography using hexane/ethyl acetate (4:1) as eluant to give **6** (2.594 g, 83%). The two diastereomers were separated by column chromatography using hexane/dichloromethane (2:3) as eluant, affording **6a** and **6b** as white solids.

rel-(1'*R*,2'*R*,4'*S*,5'*S*)-5-Methoxy-5-methylspiro[2,5-dihydro-1,3,4-oxadiazole-2,8'-tricyclo[3.2.1.0^{2,4}]octane] (**6a**). mp: 35–39 °C. ¹H NMR (400.13 MHz, CDCl₃): δ 3.09 (s, 3H), 2.38–2.16 (m, 3H), 2.03–1.97 (m, 1H), 1.68–1.59 (m, 2H), 1.63 (s, 3H), 1.44–1.34 (m, 3H), 1.06–1.01 (dt, *J* = 7.4 Hz (t), 6.5 Hz (d), 1H). ¹³C NMR (100.62 MHz, CDCl₃): δ 142.3 (C), 130.2 (C), 50.2 (CH₃), 45.0 (CH), 43.7 (CH), 24.3 (CH₂), 24.1 (CH₂), 23.1 (CH₃), 20.7 (CH), 20.6 (CH), 16.7 (CH₂). IR: ν 3069 (w), 2964 (m), 2880 (w), 1568 (w), 1477 (w), 1446 (w), 1377 (m), 1309 (w), 1240 (m), 1203 (s), 1131 (s), 1081 (m), 1045 (s), 987 (w), 927 (s), 907 (s), 872 (s), 787 (w), 760 (m) cm⁻¹. MS (EI, 70 eV): *m/z* 208 [M]⁺ (<1), 177 (7), 153 (4), 115 (6), 105 (38), 91 (100), 78 (48), 65 (10), 51 (7). HRMS (ESI): *m/z* [M + H]⁺ calcd for C₁₁H₁₇N₂O₂ 209.1290; found 209.1289. Anal. Calcd for C₁₁H₁₆N₂O₂: C, 63.44; H, 7.74; N, 13.45; O, 15.37. Found: C, 63.76; H, 7.61; N, 13.34; O, 15.21.

rel-(1'*R*,2'*S*,2'*R*,4'*S*,5'*S*)-5-Methoxy-5-methylspiro[2,5-dihydro-1,3,4-oxadiazole-2,8'-tricyclo[3.2.1.0^{2,4}]octane] (**6b**). mp: 54–58 °C. ¹H NMR (400.13 MHz, CDCl₃): δ 3.05 (s, 3H), 2.26–2.21 (m, 1H), 2.05–1.99 (m, 1H), 1.83–1.73 (m, 3H), 1.72–1.64 (m, 1H), 1.58 (s, 3H), 1.39–1.24 (m, 2H), 1.17–1.11 (m, 1H), 0.95–0.88 (m, 1H). ¹³C

NMR (100.62 MHz, CDCl₃): δ 141.1 (C), 131.8 (C), 50.1 (CH₃), 44.7 (CH), 43.4 (CH), 25.8 (CH₂), 25.7 (CH₂), 23.0 (CH₃), 16.9 (CH), 16.6 (CH), 12.2 (CH₂). IR: ν 3042 (w), 2966 (m), 2877 (w), 1560 (w), 1472 (w), 1448 (w), 1376 (m), 1313 (w), 1238 (m), 1201 (s), 1138 (s), 1083 (m), 1051 (s), 977 (w), 913 (s), 869 (m), 791 (m), 761 (m) cm⁻¹. MS (EI, 70 eV): m/z 208 [M]⁺ (<1), 177 (9), 153 (5), 115 (6), 105 (38), 91 (100), 78 (45), 65 (8), 51 (6). HRMS (EI, 70 eV): m/z [M]⁺ calcd for C₁₁H₁₆N₂O₂ 208.1212; found 208.1215. Anal. Calcd for C₁₁H₁₆N₂O₂: C, 63.44; H, 7.74; N, 13.45; O, 15.37. Found: C, 63.65; H, 7.63; N, 13.31; O, 14.93.

General Procedure for GC–MS Analysis of Thermolysis and Photolysis of Oxadiazolines 6a and 6b in Cyclohexane and Cyclohexene. For thermolysis, the oxadiazoline was dissolved in either cyclohexane or cyclohexene and stirred in a pressure tube at 165 °C for 3–6 h. For photolysis, the oxadiazoline was dissolved in either cyclohexane or cyclohexene in a round-bottomed flask equipped with a rubber septum. The solution was degassed with argon and subjected to photolysis for 6–15 h. The temperature was controlled with a water bath. Camphor was added as an internal standard to the resultant reaction mixtures before GC–MS analysis.

Tetracyclo[3.3.0.0^{2,8}.0^{4,6}]octane (8). A solution of oxadiazoline **6b** (0.319 g, 1.53 mmol) in pentane (20 mL) was stirred in a pressure tube for 4 h at 165 °C. Pentane was carefully removed by Kugelrohr distillation, and the residue was subjected to gradient NMR analysis. Spectroscopic data were in agreement with the literature.²⁰

¹H NMR (600.13 MHz, CDCl₃): δ 1.74–1.69 (m, 2H), 1.65–1.55 (m, 4H), 1.29–1.25 (m, 4H). ¹³C NMR (150.95 MHz, CDCl₃): δ 25.7 (CH), 24.0 (CH₂), 21.8 (CH).

Thermolysis of 6b in Cyclohexane-*d*₁₂. A solution of oxadiazoline **6b** (0.030 g, 0.14 mmol) in cyclohexane-*d*₁₂ (1 mL) was stirred in a pressure tube for 3 h at 165 °C. The reaction mixture was subjected to NMR analysis (see Figure S18 in the Supporting Information for ¹H NMR spectrum of the mixture).

endo-Tricyclo[3.2.1.0^{2,4}]octan-8-one Azine (11). A solution of oxadiazoline **6b** (0.254 g, 1.22 mmol) in pentane (3 mL) was stirred in a pressure tube for 4 h at 165 °C. The reaction mixture was filtered and concentrated. The product was isolated by column chromatography using hexane/ethyl acetate (1:1) as eluant, giving **11** (0.016 g, 11%) as a sticky white solid.

mp: 130–143 °C. ¹H NMR (600.13 MHz, CDCl₃): δ 3.21–3.14 (m, 2H), 2.54–2.46 (m, 2H), 1.69–1.51 (m, 4H), 1.47–1.36 (m, 4H), 1.28–1.16 (m, 4H), 1.03–0.97 (m, 2H), 0.97–0.90 (m, 2H). ¹³C NMR (150.95 MHz, CDCl₃): δ 180.88 and 180.79 (C), 37.62 and 37.61 (CH), 32.44 and 32.42 (CH), 24.04 and 24.00 (CH₂), 23.44 and 23.42 (CH₂), 15.29 and 15.28 (CH), 14.79 and 14.76 (CH), 11.48 and 11.44 (CH₂). IR: ν 3029 (m), 2950 (m), 2873 (m), 1682 (s), 1523 (m), 1473 (m), 1311 (m), 1301 (m), 1180 (w), 1147 (m), 1108 (m), 1047 (m), 1030 (m), 928 (m), 789 (m), 757 (s), 719 (m) cm⁻¹. MS (EI, 70 eV): m/z 240 [M]⁺ (12), 174 (3), 120 (36), 93 (100), 77 (27), 65 (13), 54 (7). HRMS (ESI): m/z [M + H]⁺ calcd for C₁₆H₂₁N₂ 241.1705; found 241.1696.

endo,syn-Tricyclo[3.2.1.0^{2,4}]octan-8-ol (14). See the procedure below for thermolysis of **6a** in methanol. **14** was isolated (0.022 g, 26%) as a white solid. Spectroscopic data were in agreement with the literature.^{16b,31}

¹H NMR (400.13 MHz, CDCl₃): δ 4.27–4.16 (m, 1H), 2.32–2.24 (m, 1H), 2.07–1.99 (m, 2H), 1.61–1.51 (m, 2H), 1.50–1.40 (m, 2H), 1.31–1.23 (m, 1H), 1.10–0.97 (m, 3H). ¹³C NMR (100.62 MHz, CDCl₃): δ 93.8 (CH), 41.0 (CH), 24.2 (CH₂), 19.8 (CH), 18.7 (CH₂).

rac-(1R,2S,4S,5R,6R)-2-Methoxytricyclo[3.3.0.0^{4,6}]octane (16). From thermolysis of **6a**: A solution of oxadiazoline **6a** (0.141 g, 0.677 mmol) in methanol (7.5 mL) was stirred in a pressure tube for 4 h at 165 °C. The reaction mixture was filtered and concentrated in vacuo. The crude product was subjected to column chromatography using hexane/ethyl acetate (9:1) as eluant, giving **16** (0.026 g, 28%) as a yellow liquid.

From thermolysis of **6b**: A solution of oxadiazoline **6b** (0.143 g, 0.687 mmol) in methanol (7.5 mL) was stirred in a pressure tube for 4 h at 165 °C. The reaction mixture was filtered and concentrated in

vacuo. The crude product was subjected to column chromatography using hexane/ethyl acetate (9:1) as eluant, giving **16** (0.042 g, 44%) as a yellow liquid.

From photolysis of **6a**: A solution of oxadiazoline **6a** (0.100 g, 0.480 mmol) in methanol (5 mL) was degassed with argon and photolyzed for 7 h, using a water bath for cooling. The reaction mixture was filtered and concentrated in vacuo. The crude product was subjected to column chromatography using hexane/ethyl acetate (9:1) as eluant, giving **16** (0.022 g, 33%) as a yellow liquid.

From photolysis of **6b**: A solution of oxadiazoline **6b** (0.100 g, 0.480 mmol) in methanol (5 mL) was degassed with argon and photolyzed for 7 h, using a water bath for cooling. The reaction mixture was filtered and concentrated in vacuo. The crude product was subjected to column chromatography using hexane/ethyl acetate (9:1), giving **16** (0.031 g, 47%) as a yellow liquid. Spectroscopic data were in agreement with the literature.^{13b}

¹H NMR (400.13 MHz, CDCl₃): δ 3.80–3.72 (m, 1H), 3.22 (s, 3H), 2.60–2.51 (m, 1H), 2.25–2.12 (m, 1H), 1.99–1.88 (m, 1H), 1.83–1.69 (m, 2H), 1.69–1.57 (m, 1H), 1.49–1.39 (m, 2H), 1.16–1.05 (m, 2H). ¹³C NMR (100.62 MHz, CDCl₃): δ 88.1 (CH), 56.8 (CH₃), 43.6 (CH), 30.3 (CH₂), 27.3 (CH₂), 27.2 (CH), 26.0 (CH), 24.1 (CH₂), 19.2 (CH). IR: ν 3029 (m), 2943 (m), 2867 (m), 1736 (m), 1471 (m), 1450 (m), 1367 (m), 1349 (m), 1212 (m), 1177 (m), 1117 (s), 1098 (s), 975 (m) cm⁻¹. MS (EI, 70 eV): m/z 138 [M]⁺ (4), 123 (3), 106 (28), 91 (21), 84 (10), 79 (45), 71 (100), 67 (17), 53 (2). HRMS (EI, 70 eV): m/z [M]⁺ calcd for C₉H₁₄O 138.1045; found 138.1044.

rel-(1*S*,1'*R*,2*R*,2'*R*,4'*S*,5'*S*)-Spiro[cyclopropane-1,8'-tricyclo[3.2.1.0^{2,4}]octane]-2-carbonitrile (17). From thermolysis of **6a**: A solution of oxadiazoline **6a** (0.122 g, 0.586 mmol) in acrylonitrile (6 mL) was stirred in a pressure tube for 4 h at 165 °C. The reaction mixture was filtered and concentrated in vacuo. The product was isolated by column chromatography using hexane/ethyl acetate (4:1) as eluant, giving **17** (0.071 g, 76%) as a white solid.

From thermolysis of **6b**: A solution of oxadiazoline **6b** (0.125 g, 0.600 mmol) in acrylonitrile (6 mL) was stirred in a pressure tube for 4 h at 165 °C. The reaction mixture was filtered and concentrated in vacuo. The product was isolated by column chromatography using hexane/ethyl acetate (4:1) as eluant, giving **17** (0.077 g, 81%) as a white solid.

mp: 34–36 °C. ¹H NMR (400.13 MHz, CDCl₃): δ 2.02–1.94 (m, 1H), 1.84–1.70 (m, 1H), 1.68–1.48 (m, 4H), 1.42–1.19 (m, 5H), 1.14–1.08 (m, 1H), 0.88–0.83 (dt, J = 7.4 Hz (t), 6.3 Hz (d), 1H). ¹³C NMR (100.62 MHz, CDCl₃): δ 121.0 (C), 54.4 (C), 41.7 (CH), 40.7 (CH), 26.8 (CH₂), 26.4 (CH₂), 21.7 (CH), 21.2 (CH), 16.1 (CH₂), 14.6 (CH₂), 3.9 (CH). IR: ν 3028 (m), 2959 (s), 2877 (m), 2228 (s), 1474 (m), 1442 (m), 1386 (w), 1317 (m), 1302 (m), 1205 (w), 1173 (m), 1113 (m), 1097 (m), 1037 (m), 1010 (s), 963 (m), 928 (s), 837 (m), 786 (s), 732 (s) cm⁻¹. MS (EI, 70 eV): m/z 159 [M]⁺ (<1), 144 (4), 130 (15), 117 (15), 104 (21), 91 (50), 78 (100), 65 (10), 51 (9). HRMS (ESI): m/z [M + Na]⁺ calcd for C₁₁H₁₃NNa 182.0946; found 182.0947.

endo,anti-N,N-Diethyltricyclo[3.2.1.0^{2,4}]octan-8-amine (19). From thermolysis of **6a**: A solution of oxadiazoline **6a** (0.122 g, 0.586 mmol) in diethylamine (6 mL) was stirred in a pressure tube for 4 h at 165 °C. The reaction mixture was filtered and concentrated in vacuo. The product was isolated by column chromatography using ethyl acetate as eluant, giving **19** (0.070 g, 67%) as a yellow liquid.

From thermolysis of **6b**: A solution of oxadiazoline **6b** (0.120 g, 0.576 mmol) in diethylamine (6 mL) was stirred in a pressure tube for 4 h at 165 °C. The reaction mixture was filtered and concentrated in vacuo. The product was isolated by column chromatography using ethyl acetate as eluant, giving **19** (0.061 g, 59%) as a yellow liquid.

¹H NMR (400.13 MHz, CDCl₃): δ 2.94–2.91 (m, 1H), 2.59–2.50 (q, J = 7.1 Hz, 4H), 2.20–2.14 (m, 2H), 1.68–1.58 (m, 2H), 1.28–1.19 (m, 2H), 0.97–0.92 (t, J = 7.1 Hz, 6H), 0.92–0.85 (m, 3H), 0.56–0.49 (dt, J = 7.4 Hz (t), 6.0 Hz (d), 1H). ¹³C NMR (100.62 MHz, CDCl₃): δ 83.2 (CH), 43.6 (CH₂), 38.4 (CH), 25.1 (CH₂), 19.1 (CH), 12.2 (CH₂), 10.8 (CH₂). IR: ν 3022 (m), 2964 (s), 2816 (m), 1469 (m), 1369 (m), 1209 (m), 1180 (m), 1121 (m), 1070 (m), 1038

(m), 988 (w), 791 (m), 740 (m) cm^{-1} . MS (EI, 70 eV): m/z 179 [M]⁺ (2), 164 (4), 125 (5), 112 (100), 99 (13), 79 (11), 56 (15). HRMS (ESI): m/z [M + H]⁺ calcd for C₁₂H₂₂N 180.1752; found 180.1746.

■ ASSOCIATED CONTENT

Supporting Information

NMR spectra for all new compounds and CIFs for crystallographic data of **6a** and **6b**. This material is available free of charge via the Internet at <http://pubs.acs.org>.

■ AUTHOR INFORMATION

Corresponding Author

*Udo.Brinker@univie.ac.at

Notes

The authors declare no competing financial interest.

■ ACKNOWLEDGMENTS

We thank Prof. V. B. Arion, A. Roller (Institute of Inorganic Chemistry, University of Vienna), and Dr. J. Graf (Incoatec, Geesthacht, Germany) for single-crystal X-ray analyses; Prof. L. Brecker (Institute of Organic Chemistry, University of Vienna) for NMR interpretation; and Prof. D. Krois (Institute of Organic Chemistry, University of Vienna) and Dr. M. G. Rosenberg (The State University of New York at Binghamton) for helpful discussions. We thank the reviewers for their valuable suggestions.

■ REFERENCES

- Gleiter, R.; Hoffmann, R. *J. Am. Chem. Soc.* **1968**, *90*, 5457–5460.
- (a) Kirmse, W. *Carbene Chemistry*; Academic: New York, 1971. (b) Jones, W. M.; Brinker, U. H. In *Pericyclic Reactions*; Marchand, A. P., Lehr, R. E., Eds.; Academic: New York, 1977; Vol. 1, pp 109–198. (c) Moss, R. A.; Platz, M. S.; Jones, M., Jr. *Reactive Intermediate Chemistry*; Wiley: Hoboken, NJ, 2005; pp 273–461.
- (a) Winstein, S.; Trifan, D. S. *J. Am. Chem. Soc.* **1949**, *71*, 2953–2953. (b) Winstein, S.; Shatavsky, M.; Norton, C.; Woodward, R. B. *J. Am. Chem. Soc.* **1955**, *77*, 4183–4184. (c) Brookhart, M.; Diaz, A.; Winstein, S. *J. Am. Chem. Soc.* **1966**, *88*, 3135–3136. (d) Rzepa, H. S.; Allan, C. S. M. *J. Chem. Educ.* **2010**, *87*, 221–228. (e) Bartlett, P. D. *Nonclassical Carbonium Ions*; W. A. Benjamin: Menlo Park, CA, 1965.
- Moss, R. A.; Dolling, U.-H.; Whittle, J. R. *Tetrahedron Lett.* **1971**, 931–934.
- Mieusset, J.-L.; Brinker, U. H. *J. Am. Chem. Soc.* **2006**, *128*, 15843–15850.
- Moss, R. A.; Ho, C.-T. *Tetrahedron Lett.* **1976**, 1651–1654.
- Mieusset, J.-L.; Abraham, M.; Brinker, U. H. *J. Am. Chem. Soc.* **2008**, *130*, 14634–14639.
- Moss, R. A.; Dolling, U.-H. *Tetrahedron Lett.* **1972**, 5117–5120.
- Mieusset, J.-L.; Brinker, U. H. *J. Org. Chem.* **2008**, *73*, 1553–1558.
- Mieusset, J.-L.; Bespokoiev, A.; Pačar, M.; Abraham, M.; Arion, V. B.; Brinker, U. H. *J. Org. Chem.* **2008**, *73*, 6551–6558.
- Mieusset, J.-L.; Schrems, A.; Abraham, M.; Arion, V. B.; Brinker, U. H. *Tetrahedron* **2009**, *65*, 765–770.
- (a) Freeman, P. K. *J. Am. Chem. Soc.* **1998**, *120*, 1619–1620. (b) Freeman, P. K.; Pugh, J. K. *J. Org. Chem.* **2000**, *65*, 6107–6111. (c) Freeman, P. K.; Dacres, J. E. *J. Org. Chem.* **2003**, *68*, 1386–1393.
- (a) Freeman, P. K.; Raghavan, R. S.; Kuper, D. G. *J. Am. Chem. Soc.* **1971**, *93*, 5288–5290. (b) Freeman, P. K.; Hardy, T. A.; Raghavan, R. S.; Kuper, D. G. *J. Org. Chem.* **1977**, *42*, 3882–3892. (c) Murahashi, S.-I.; Okumura, K.; Kubota, T.; Moritani, I. *Tetrahedron Lett.* **1973**, 4197–4200. (d) Murahashi, S.-I.; Okumura, K.; Maeda, Y.; Sonoda, A.; Moritani, I. *Bull. Chem. Soc. Jpn.* **1974**, *47*, 2420–2425. (e) Okumura, K.; Murahashi, S.-I. *Tetrahedron Lett.* **1977**, 3281–3284.
- (a) Hoffmann, R. W.; Luthardt, H. *J. Chem. Ber.* **1968**, *101*, 3861–3871. (b) Békhazi, M.; Warkentin, J. *J. Am. Chem. Soc.* **1981**, *103*, 2473–2474. (c) Békhazi, M.; Warkentin, J. *J. Am. Chem. Soc.* **1983**, *105*, 1289–1292. (d) Majchrzak, M. W.; Békhazi, M.; Tse-Sheepy, I.; Warkentin, J. *J. Org. Chem.* **1989**, *54*, 1842–1845. (e) El-Saidi, M.; Kassam, K.; Pole, D. L.; Tadey, T.; Warkentin, J. *J. Am. Chem. Soc.* **1992**, *114*, 8751–8752. (f) Jefferson, E. A.; Warkentin, J. *J. Org. Chem.* **1994**, *59*, 455–462. (g) Kassam, K.; Warkentin, J. *J. Org. Chem.* **1994**, *59*, 5071–5075. (h) Tae, E. L.; Zhu, Z.; Platz, M. S. *J. Phys. Chem. A* **1999**, *103*, 5336–5342. (i) Warkentin, J. *J. Chem. Soc., Perkin Trans. 1* **2000**, 2161–2169. (j) Snoonian, J. R.; Platz, M. S. *J. Phys. Chem. A* **2001**, *105*, 2106–2111. (k) Brinker, U. H.; Bespokoiev, A. A.; Reisenauer, H. P.; Schreiner, P. R. *J. Org. Chem.* **2012**, *77*, 3800–3807.
- Yang, R.-Y.; Dai, L.-X. *J. Org. Chem.* **1993**, *58*, 3381–3383.
- (a) Battiste, M. A.; Deyrup, C. L.; Pincock, R. E.; Haywood-Farmer, J. *J. Am. Chem. Soc.* **1967**, *89*, 1954–1955. (b) Haywood-Farmer, J. S.; Pincock, R. E. *J. Am. Chem. Soc.* **1969**, *91*, 3020–3028. (c) Haywood-Farmer, J. *Chem. Rev.* **1974**, *74*, 315–350.
- Here, the position of the cyclopropane ring is expressed as *endo* or *exo*, and the substituent at the bridgehead is *anti*- or *syn*-positioned relative to the cyclopropane ring.
- (a) Schoeller, W. W.; Brinker, U. H. *Z. Naturforsch.* **1980**, *35B*, 475–476. (b) Moss, R. A. *Acc. Chem. Res.* **1980**, *13*, 58–64. (c) Moss, R. A. *Acc. Chem. Res.* **1989**, *22*, 15–21.
- Kählig, H.; Dietrich, K.; Dorner, S. *Monatsh. Chem.* **2002**, *133*, 589–598.
- (a) LeBel, N. A.; Liesemer, R. N. *J. Am. Chem. Soc.* **1965**, *87*, 4301–4309. (b) Jefford, C. W.; De los Heros, V. *Bull. Soc. Chim. Belg.* **1979**, *88*, 969–972.
- (a) Chapman, O. L.; Borden, G. W.; King, R. W.; Winkler, B. J. *Am. Chem. Soc.* **1964**, *86*, 2660–2664. (b) Christl, M.; Herzog, C.; Kemmer, P. *Chem. Ber.* **1986**, *119*, 3045–3058.
- According to ref 13b, the conversion **3** → **7** actually proceeds intermolecularly. It was noted by a reviewer that carbenes **3** and **7** are nearly isoenergetic, and the intramolecular rearrangement **3** → **7** is expected to have a prohibitively high activation barrier.
- (a) Regitz, M.; Maas, G. *Diazo Compounds: Properties and Synthesis*; Academic: New York, 1986. (b) Pezacki, J. P.; Couture, P.; Dunn, J. A.; Warkentin, J.; Wood, P. D.; Luszytky, J.; Ford, F.; Platz, M. S. *J. Org. Chem.* **1999**, *64*, 4456–4464. (c) Merkle, N.; El-Saidi, M.; Warkentin, J. *Can. J. Chem.* **2000**, *78*, 356–361.
- Mieusset, J.-L.; Billing, P.; Abraham, M.; Arion, V. B.; Brecker, L.; Brinker, U. H. *Eur. J. Org. Chem.* **2008**, 5336–5345.
- (a) Kirmse, W.; Meinert, T. *J. Chem. Soc., Chem. Commun.* **1994**, 1065–1066. (b) Kirmse, W. In *Advances in Carbene Chemistry*; Brinker, U. H., Ed.; Elsevier: Amsterdam, 2001; Vol. 3, pp 1–51. (c) Kirmse, W. In *Advances in Carbene Chemistry*; Brinker, U. H., Ed.; JAI: Greenwich, CT, 1994; Vol. 1, pp 1–57.
- One reviewer's calculations show that the direct protonation **3** → **15** is endothermic even when solvent effects are taken into account. Therefore, an alternative mechanism might be operating (e.g., **3** → **7** → **15**).
- Kirmse, W. *Eur. J. Org. Chem.* **2005**, 237–260.
- One reviewer's calculations (B3LYP/6-31G(d)) found ylide **18** to be 9 kcal/mol more stable than the separated reactants. Moreover, solvation should further increase its stability.
- Wu, D.; Chen, A.; Johnson, C. S., Jr. *J. Magn. Reson., Ser. A* **1995**, *115*, 260–264.
- (a) Wannagat, U.; Niederprüm, H. *Chem. Ber.* **1961**, *94*, 1540–1547. (b) Hoch, P. E. *J. Org. Chem.* **1961**, *26*, 2066–2072. (c) Binger, P.; Wedemann, P.; Goddard, R.; Brinker, U. H. *J. Org. Chem.* **1996**, *61*, 6462–6464. (d) Binger, P.; Wedemann, P.; Brinker, U. H. *Org. Synth.* **2000**, *77*, 254–259.
- Haywood-Farmer, J.; Pincock, R. E.; Wells, J. I. *Tetrahedron* **1966**, *22*, 2007–2014.

Curriculum Vitae

Name: MSc Ingrid Malene Apeland

Primary School

1992 – 1998 Sunde Skole

Lower Secondary School

1998 – 2001 Revheim Skole

Upper Secondary School

2001 – 2004 Stavanger Katedralskole

Higher Education

2004 – 2007 Bachelor's degree in Chemistry

University of Bergen

2006 Erasmus Exchange, included in the Bachelor's degree

University of Strathclyde, Glasgow

2007 – 2009 Master's degree in Chemistry – Organic Chemistry

University of Bergen

Title of thesis: "Synthesis of Some Substituted Dihydrofuran-3-(2*H*)-ones from 3,3,4,4-Tetraethoxybut-1-yne (TEB)"

Supervisor: Prof. Leiv K. Sydnes

2009 – 2013 Doctoral Studies

University of Vienna, Institute of Organic Chemistry